Global soil respiration: interaction with macroscale environmental variables and response to climate change

Jinshi Jian

Dissertation submitted to the faculty of the Virginia Polytechnic Institute and State University in partial fulfillment of the requirements for the degree of

Doctor of Philosophy
In
Crop and Soil Environmental Sciences

Meredith K. Steele (Chair)
James B. Campbell
R. Quinn Thomas
Steven C. Hodges
Susan D. Day

December 6, 2017
Blacksburg, VA

Keywords: Soil respiration, macro-scale, modeling, benchmark, spatio-temporal variation, surrogates, acclimation, DNDC

Global soil respiration: interaction with macroscale environmental variables and response to climate change

ACADEMIC ABSTRACT

The response of global soil respiration (Rs) to climate change determines how long the land can continue acting as a carbon sink in the future. This dissertation research identifies how temporal and spatial variation in environmental factors affects global scale Rs modeling and predictions of future Rs under global warming. Chapter 1 describes the recommend time range for measuring Rs across differing climates, biomes, and seasons and found that the best time for measuring the daily mean Rs is 10:00 am in almost all climates and biomes. Chapter 2 describes commonly used surrogates in Rs modeling and shows that air temperature and soil temperature are highly correlated and that they explain similar amounts of Rs variation; however, average monthly precipitation between 1961 and 2014, rather than monthly precipitation for a specific year, is a better predictor in global Rs modeling. Chapter 3 quantifies the uncertainty generated by four different assumptions of global Rs models. Results demonstrate that the time-scale of the data, among other sources, creates a substantial difference in global estimates, where the estimate of global annual Rs based on monthly Rs data (70.85 to 80.99 Pg C yr^{-1}) is substantially lower than the current benchmark for land models (98 Pg C yr^{-1}). Chapter 4 simulates future global Rs rates based on two temperature scenarios and demonstrates that temperature sensitivity of Rs will decline in warm climates where the level of global warming will reach 3ºC by 2100 relative to current air temperature; however, these regional decelerations will be offset by large Rs accelerations in the boreal and polar regions. Chapter 5 compares CO_2 fluxes from turfgrass and wooded areas of five parks in Blacksburg, VA and tests the ability of the Denitrification-Decomposition model to estimate soil temperature, moisture and CO_2 flux across the seasons.

Cumulatively, this work provides new insights into the current and future spatial and temporal heterogeneity of Rs and its relationship with environmental factors, as well as key insights in upscaling methodology that will help to constrain global Rs estimates and predict how global Rs will respond to global warming in the future.

Global soil respiration: interaction with macroscale environmental variables and response to climate change

GENERAL ABSTRACT

CO_2 flux emitted from global soil is the second largest carbon exchange between the land and atmosphere. Accurately estimating global soil CO_2 flux and how it responds to climate change is critical to predict terrestrial carbon stocks. The objectives of this dissertation are to evaluate how time-scale affects our ability to estimate global soil CO_2 flux. In Chapter 1, we show that the best time period for measuring daily mean soil CO_2 flux is at around 10:00 am in almost all climate regions and vegetation types. The previously recommended time range (09:00 am and 12:00 pm) reasonably captures the daily mean soil CO_2 flux. The results from Chapter 2 indicate that air temperature is a good proxy for soil temperature in modeling global soil CO_2 flux. However, monthly precipitation is a uniformly poor proxy for soil water content; instead, average monthly precipitation is a better predictor for global soil CO_2 flux modeling. Chapter 3 demonstrates that the time-scale used in parameterizing models strongly affects the prediction of global CO_2 flux. When using monthly time-scale soil CO_2 flux and air temperature data, soil CO_2 flux increases as air temperature increases at air temperatures below 27 ℃, but soil CO_2 flux begins to decrease when air temperature is over 27 ℃. However, when using annual time-scale data, this response to temperature is masked, soil CO_2 flux increases as air temperature increases in all temperature conditions. As a result, the estimate of global annual soil CO_2 flux, based on monthly soil respiration data (70.85 to 80.99 Pg C yr^{-1}), is lower than the estimate based on the annual soil respiration data (98 Pg C yr^{-1}). Chapter 4 shows that if the level of global warming maintains its current rate (3ºC by the year 2100), then the annual soil CO_2 flux will either decrease or remains the same in arid, winter-dry temperate and tropical climate regions.

However, these regional decelerations were offset by large soil CO_2 flux accelerations in the boreal and polar regions. Chapter 5 shows a significant difference in CO_2 flux among the five selected parks in Blacksburg, VA. The Denitrification-Decomposition model, despite having been developed for agriculture and undeveloped lands, closely estimates soil temperature, moisture and CO_2 flux across the seasons and therefore can be used to estimate and understand CO_2 fluxes from urban ecosystems in future studies.

This study highlights that the relationship between soil CO_2 fluxes and environmental factors such as air temperature and precipitation differs from region to region. The study also demonstrates that daily and monthly time-scale soil CO_2 fluxes and environmental data help constrain global soil CO_2 flux estimates and help to predict how global soil CO_2 fluxes will respond to global warming in the future.

ACKNOWLEDGEMENTS

First I want to thank my wife Xuan Du and my three-year old son Joshua Jian, this research would not happen without their support. I would also like to thank my parents, whose love and guidance are with me in whatever I pursue.

My PhD research experience would not have been so great without the guidance and support of my advisor, Dr. Meredith K. Steele, who provided me a wide range of research opportunities, encourages me to develop new skills, helps me overcome challenges, and shares her wisdom in every aspect of life with me. I would also like to give all my acknowledgments to my committee members, Dr. James B. Campbell, Dr. R. Quinn Thomas, Dr. Steven C. Hodges, and Dr. Susan D. Day for their service in my committee and valuable advice on my research.

I sincerely appreciate Mr. Dean Crane, the director of parks and recreation in Blacksburg, VA, for allowing me conduct my experiment in selected parks in Blacksburg. I am grateful to Steve Nagle and Julia Burger for helping me prepare experiment equipment and performing soil physical and chemical property analyses. I also sincerely appreciate Dr. Benjamin F. Tracy and Dr. Ryan Stewart for letting me use their equipment and analyze soil texture at their lab. Many thanks to Xiaojin Li and Oluwatosin Ogunmayowa for helping me measure soil CO_2 flux during the middle of the night.

I would like to thank the financial support of the Hatch Grant from the Crop and Soil Environmental Sciences and the Graduate Research Development Program (GRDP) from Virginia Tech.

Last but not least, I would like to extend thanks to many unspecifiable people such as the statistical collaborators from Virginia Tech's Laboratory for Interdisciplinary Statistical Analysis (LISA) who offered great help on statistical analyses and contributed to the work presented in my dissertation.

Table of Contents

OVERVIEW

Despite being a major flux, global soil respiration (Rs) and the feedback mechanisms remain the least well understood component of the terrestrial carbon cycle (Davidson and Janssens 2006; Janssens et al. 2001; Trumbore 2006). Global soil respiration cannot be measured directly. To capture the global soil respiration pattern and its controlling factors, many chamber measurements of soil CO_2 emissions have been made across the world for many decades. To estimate the global scale Rs, researchers have aggregated these field Rs measurements, and then modeled the relationship between Rs and environmental factors such as air temperature and precipitation (Ben Bond-Lamberty and Thomson 2010; Hashimoto et al. 2015; Raich and Potter 1995; Raich, Potter, and Bhagawati 2002; Raich and Schlesinger 1992) (Figure 1). These empirical or semi-empirical models play an important role in estimating global soil respiration (B. Bond-Lamberty and Thomson 2010; Hashimoto et al. 2015; Raich et al. 2002; Raich and Schlesinger 1992); however, a big gap exists between different estimates even based on similar approaches (Hashimoto et al. 2015). We argue that time-scale and spatial-scale play an important role on constraining these uncertainties. The current method of modeling and estimating Rs ignores the heterogeneity and controlling factors at both very small scales and intermediate scales that might influence Rs and introduce measurement error and model structure error into global scale estimates. Currently, however, we know little about the variation of Rs and the controlling factors of these alternative scales and how they affect global carbon cycling estimates (Figure 1).

At very fine temporal scales, Rs varies within a day due to the diurnal patterns; however, this heterogeneity is typically ignored. Due to expense and labor requirements, researchers commonly measure soil respiration once per week, once per month, or even once per season,

then upscale to estimate annual soil respiration (Chen et al. 2014; Davidson, Belk, and Boone 1998; Sheng et al. 2010a). These measurements are typically only measured at a specific time of day (e.g., at 10:00 am), and then scaled to the weekly, monthly, and annual Rs. However, there is no protocol for guiding when to measure soil respiration; many researchers measured their Rs from 09:00 to 12:00 based on the results from Davidson et al (1998). However, whether Rs measured at this time period can capture soil respiration daily means across the globe is unknown. Rs diurnal fluctuation varies across different climate regions and biomes. Therefore, it is hard to determine whether measured Rs captures the diurnal mean. When field Rs are upscaled to larger time-scale and spatial-scale Rs, we do not know how much bias may be introduced as a result of not accurately accounting for sub-daily variation in Rs caused by diurnal fluctuation.

The most important factors affecting soil respiration are soil temperature and soil water content; however, we do not have high spatiotemporal resolution soil temperature and soil water content data. Air temperature and precipitation are used as surrogates of soil temperature and soil water content. The validity of those proxies on sub-global scales has not been tested. Another issue of using precipitation to predict soil respiration from the model is that the predicted Rs will be zero if the monthly precipitation is zero; this does not match with the real world (Raich and Potter 1995). Since drought will become more common in the future, improving our ability to predict soil respiration under extreme drought becomes more and more important.

Variation across intermediate spatial (regional to continental, aka “macro”, scales) and temporal (monthly or seasonal) scales is also currently ignored by current methods of estimating global and annual Rs (Figure 1). One of the most important assumptions in scaling from site to global Rs is the application of the first order exponential relationships to describe Rs and temperature (blue dashed line of Rs model at left bottom panel, Figure 1). First order exponential

models are widely used in global Rs models and assumed to describe all climates and vegetation types (Exbrayat, Pitman, and Abramowitz 2014). These models describe a continuous acceleration of Rs as temperatures increase and have been supported by annually aggregated data (Ben Bond-Lamberty and Thomson 2010; Hashimoto et al. 2015). Alternatively, second order exponential have been observed in site scale and incubation data (Hamdi *et al.*, 2013; O'Connell, 1990). Second order exponential models predict that at some temperatures, Rs would begin to decline with increasing temperatures. The lack of observed second order trends in global scale data might be the result of the coarse time-scale (annual) used in the models, which tends to compress the range of observed temperatures and Rs. Using the appropriate model (first vs second order) to describe Rs is extremely important because it dictates how the soil carbon pool will respond to increasing global temperatures, particularly at higher temperature regions such as tropical.

Under a first order exponential model, warming temperatures cause more CO_2 to be emitted from soil and accelerate global warming (positive feedback). The IPCC assessment report estimated the carbon climate feedback overland will lead to the terrestrial biosphere loss 58-79 Pg C when the planetary temperature increases 1 ℃. The positive feedback coupled model indicated that terrestrial ecosystems may transition from carbon sinks to carbon sources by 2050 (Friedlingstein et al. 2006). Global Rs models estimate an approximately 0.1 Pg C yr^{-1} increase in Rs rate caused by current global warming (Ben Bond-Lamberty and Thomson 2010; Hashimoto et al. 2015). Considering terrestrial ecosystems take up around 1.7 Pg C per year (IPCC 2007), if Rs keep increasing at a rate of 0.1 Pg C yr^{-1}, the increased global annual Rs will surpass the current magnitude of carbon sink within 17 (1.7/0.1) years.

Second-order models predict a different scenario for carbon cycling under warmer temperatures. Some on site experiments found that microbial communities could adapt to the temperature change (acclimation), which challenges the positive feedback between global warming and Rs. For instance, in a tall grass prairie in Oklahoma, a 2.0 ℃ increase in temperature does not lead to an increase in soil respiration (Luo et al. 2001). Similar acclimation was also detected in other places (Bradford et al. 2008; Eliasson et al. 2005; Kirschbaum 2004; Melillo et al. 2002; Sistla et al. 2013); therefore, acclimation may also occur at macro- and global- scales. Large scale acclimation to warming may restrict Rs (Figure 1 - negative relationship between Rs and temperature when over the threshold, purple line of Rs model) and change soil carbon's fate under global warming. This scenario is very different than the one predicted by first-order models, and thus it is critical we identify if, and where, each model should be applied.

Lastly, another source of macroscale variation in Rs is changing land cover and land use, specifically urbanization. Cities are expanding globally, while soil respiration in urban ecosystems has received much less study compared with nature ecosystems and agriculture ecosystems. Urban ecosystems are highly affected by human activities such as clearing, top soil removal, and compaction (Chen et al. 2013). Thus urban vegetation coverage, bulk density, and soil carbon content can be very different in nature or agriculture ecosystems. More research needs be conducted to 1) better understand how urbanization affects soil carbon and soil respiration and 2) to explore the mechanisms that control urban ecosystem's soil respiration spatial and temporal variation.

This dissertation describes five experiments that focus on four themes related to Rs: 1) scaling up from small to large spatial and temporal scales; 2) quantifying sources of uncertainty;

3) macroscale variation; and 4) response to warming temperatures. Chapter 1 analyzed the diurnal and seasonal fluctuations of Rs and tested the accuracy of typical measurement practices under different climates and biomes. In Chapter 2 we used 13482 Rs measurements from a monthly global Rs database and climate data from Fluxnet to characterize the relationships between air and soil temperature, precipitation and soil water content to explore whether air temperature and precipitation are good surrogates of soil temperature and soil water content in global Rs modeling. In Chapter 3, we developed four climate-driven models (first-order exponential, second-order exponential, and second-order exponential with a hyperbolic precipitation function), and used two time-scales (monthly and annual) of climate and Rs data to predict global annual Rs. From the resulting global annual Rs estimates, we calculated uncertainty associated with constant and variable Q_{10}, mixed-time-scale climate data, different time-scales, and the precipitation function. In Chapter 4, using monthly global Rs data, we modeled the relationship between Rs and temperature for the globe and eight climate regions. We then estimated annual Rs for two time periods (1961-2014 and 2015-2100) using historical temperature data and two future temperature warming scenarios (RCP 2.6: the most conservative global warming scenario where greenhouse gas emission will be significantly controlled, and RCP 8.5: the gravest global warming scenario where greenhouse gas emission will not be controlled) to identify whether differences in the sensitivity of Rs to temperature change may alter the regional acceleration rates of Rs. In the last chapter, we investigated the temporal variations in CO_2 flux from turfgrass and wooded areas of five parks in Blacksburg, Virginia, USA, between June 2016 and July 2017. We investigated the environmental factors affecting CO_2 flux and tested the effectiveness of the Denitrification-Decomposition (DNDC) model to predict CO_2 flux.

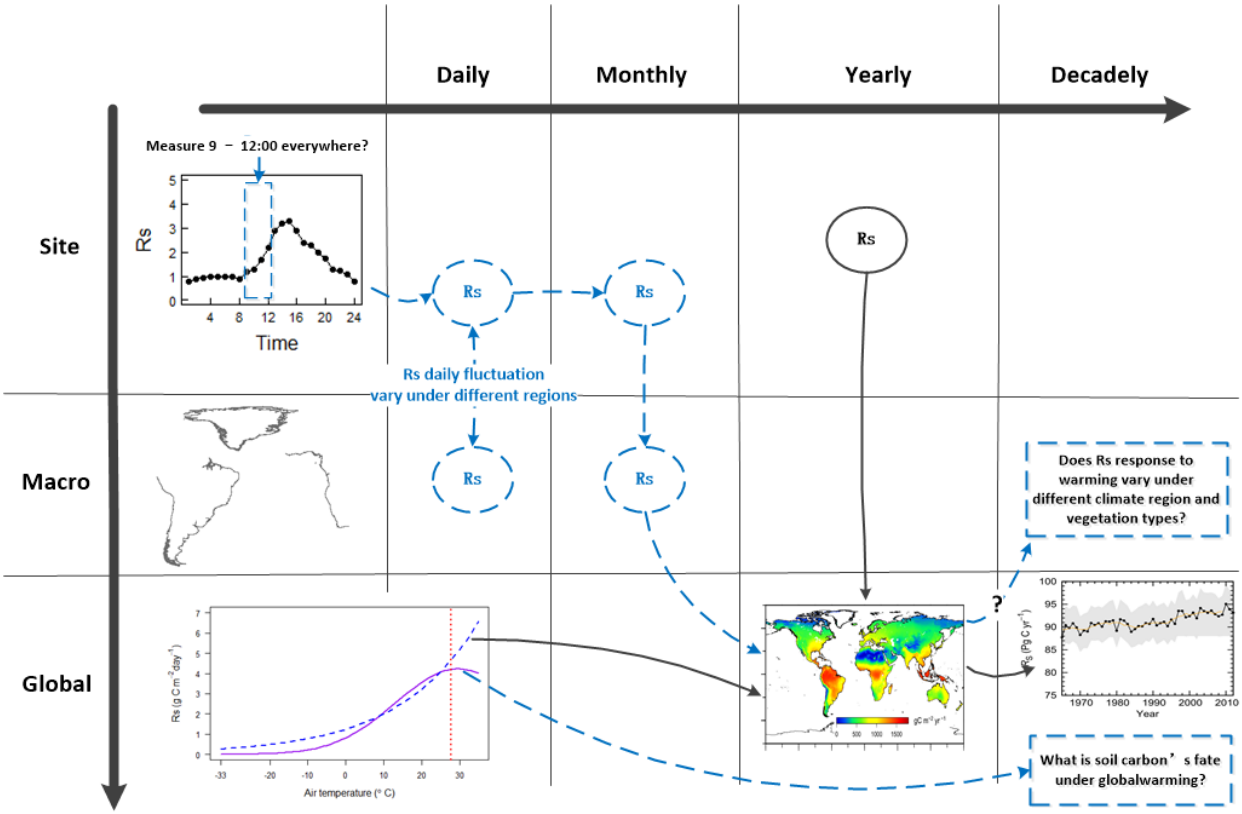

Figure 1. A conceptual diagram exploring scaling from site scale measured Rs to global Rs, from diurnal time-scales to decadal scales, and the interactions between them. Solid black arrows indicate upscaling approach by current research, which using a first order exponential model, scaling from site scale soil respiration (Rs) measurements directly to yearly global Rs. Dashed blue arrows indicate upscaling in this dissertation.

REFERENCES

Arora, Vivek K. et al. 2013. “Carbon-Concentration and Carbon-Climate Feedbacks in CMIP5 Earth System Models.” *Journal of Climate* 26(15):5289–5314.

Bond-Lamberty, B. and A. Thomson. 2010. “A Global Database of Soil Respiration Data.” *Biogeosciences* 7(6):1915–26.

Bond-Lamberty, Ben and Allison Thomson. 2010. “Temperature-Associated Increases in the Global Soil Respiration Record.” *Nature* 464(7288):579–82.

Bradford, Mark A. et al. 2008. “Thermal Adaptation of Soil Microbial Respiration to Elevated Temperature.” *Ecology Letters* 11(12):1316–27.

Chen, Yujuan et al. 2013. “Changes in Soil Carbon Pools and Microbial Biomass from Urban Land Development and Subsequent Post-Development Soil Rehabilitation.” *Soil Biology and Biochemistry* 66:38–44.

Chen, Yujuan et al. 2014. “Influence of Urban Land Development and Soil Rehabilitation on Soil–atmosphere Greenhouse Gas Fluxes.” *Geoderma* 226–227:348–53.

Davidson, E. A. and Ivan A. Janssens. 2006. “Temperature Sensitivity of Soil Carbon Decomposition and Feedbacks to Climate Change.” *Nature* 440(7081):165–73.

Davidson, Eric A., Elizabeth Belk, and Richard D. Boone. 1998. “Soil Water Content and Temperature as Independent or Confounded Factors Controlling Soil Respiration in a Temperate Mixed Hardwood Forest.” *Global Change Biology* 4(2):217–27.

Eliasson, Peter E. et al. 2005. “The Response of Heterotrophic CO_2 Flux to Soil Warming.” *Global Change Biology* 11(1):167–81.

Exbrayat, J. F., A. J. Pitman, and G. Abramowitz. 2014. “Response of Microbial Decomposition to Spin-up Explains CMIP5 Soil Carbon Range until 2100.” *Geoscientific Model Development* 7(6):2683–92.

Friedlingstein, P. et al. 2006. “Climate–Carbon Cycle Feedback Analysis: Results from the C^4 MIP Model Intercomparison.” *Journal of Climate* 19(14):3337–53.

Hamdi, Salwa, Fernando Moyano, Saidou Sall, Martial Bernoux, and Tiphaine Chevallier. 2013. “Synthesis Analysis of the Temperature Sensitivity of Soil Respiration from Laboratory Studies in Relation to Incubation Methods and Soil Conditions.” *Soil Biology and Biochemistry* 58:115–26.

Hashimoto, S. et al. 2015. “Global Spatiotemporal Distribution of Soil Respiration Modeled Using a Global Database.” *Biogeosciences Discussions* 12(5):433–64.

Janssens, I. A. et al. 2001. “Productivity Overshadows Temperature in Determining Soil and Ecosystem Respiration across European Forests.” *Global Change Biology* 7(3):269–78.

Kirschbaum, M. U. F. 2004. “Soil Respiration under Prolonged Soil Warming: Are Rate Reductions Caused by Acclimation or Substrate Loss?” *Global Change Biology* 10(11):1870–77.

Luo, Y., S. Wan, D. Hui, and L. L. Wallace. 2001. “Acclimatization of Soil Respiration to Warming in a Tall Grass Prairie.” *Nature* 413(6856):622–25.

Melillo, J. M. et al. 2002. “Soil Warming and Carbon-Cycle Feedbacks to the Climate System.” *Science* 298(5601):2173–76.

O’Connell, A. M. 1990. “Microbial Decomposition (Respiration) of Litter in Eucalypt Forests of South-Western Australia: An Empirical Model Based on Laboratory Incubations.” *Soil Biology and Biochemistry* 22(2):153–60.

Raich, J. W. and W. H. Schlesinger. 1992. “The Global Carbon Dioxide Flux in Soil Respiration and Its Relationship to Vegetation and Climate.” *Tellus B* 44(2):81–99.

Raich, James W. and Christopher S. Potter. 1995. “Global Patterns of Carbon Dioxide Emissions from Soils.” *Global Biogeochemical Cycles* 9(1):23–36.

Raich, James W., Christopher S. Potter, and Dwipen Bhagawati. 2002. “Interannual Variability in Global Soil Respiration, 1980–94.” *Global Change Biology* 8(8):800–812.

Sheng, Hao et al. 2010. “The Dynamic Response of Soil Respiration to Land-Use Changes in Subtropical China.” *Global Change Biology* 16(3):1107–21.

Sistla, Seeta A et al. 2013. “Long-Term Warming Restructures Arctic Tundra without Changing Net Soil Carbon Storage.” *Nature* 497(7451):615–18.

Trumbore, Susan. 2006. “Carbon Respired by Terrestrial Ecosystems–recent Progress and Challenges.” *Global Change Biology* 12(2):141–53.

Zhao, Maosheng and Steven W. Running. 2010. “Drought-Induced Reduction in Global Terrestrial Net Primary Production from 2000 Through 2009.” *Science* 329(6046):940–43.

CHAPTER 1. Measurement strategies to account for temporal heterogeneity in soil respiration across diverse regions

ABSTRACT

Soil respiration (Rs) rates fluctuate daily and seasonally; therefore, timing of measurements is critical when estimating the daily mean and scaling up to annual Rs rates. Temporal fluctuations also vary with climate and biome, yet the current recommendation for when to measure Rs (e.g., 09:00 to 12:00) has not been evaluated for different climates, biomes, and seasons. To provide more refined recommendations for measuring Rs, we: 1) analyzed diurnal and seasonal fluctuations of Rs and tested the accuracy of typical measurement practices under different climates and biomes, and 2) identified the measurement frequency necessary for different climates and biomes to achieve certain levels of accuracy in estimating annual Rs. Across biomes, diurnal variation in Rs is considerable in spring and summer, moderate in autumn, and minimal in winter, and closely related with soil temperature and gross primary production. Based on these diurnal patterns, the best measurement time for estimating the daily mean Rs was 10:00 in almost all climates and biomes, within the recommend range (09:00 and 12:00) previously identified for temperate forests. Measurements made between 20:00 and 23:00 also accurately estimated the daily mean Rs. Regions with average high plant coverage over the year have lower seasonal variation and require less frequent measurements. For global scale estimates, Rs needs to be measured once per day to attain an accuracy of ±10% of the Rs population mean with 95% confidence, and once per month to achieve ±30% with a confidence of 80%. Results from this study provide guidelines that reduce measurement frequency while retaining reasonable accuracy for better Rs estimates using manual chamber systems.

1.1 INTRODUCTION

Climate change has driven considerable interest in soil respiration (Rs) field measurements, which have been intergrated into a global Rs dataset and to parameterize model and quantify interactions between terrestrial and atmospheric carbon pools (Kicklighter et al. 1994). Understanding dynamics of Rs is critical to predicting how soil carbon pools will respond to climate change. With the advancement of the infrared gas analyzer (IRGA) in the 1970s, measurement accuracy was significantly improved, and now IRGA is widely used in dynamic chamber techniques for measuring Rs (Luo and Zhou 2006). Chamber-based Rs measurements taken in the field are widely used to explore how Rs varies spatially and responds to environmental conditions (e.g., Campoe *et al.*, 2012; Chen *et al.*, 2013; Matteucci *et al.*, 2015). Within a recent global soil respiration database, the number of Rs records generated by IRGA measurements were more than triple the Rs records from all other equipment (B. Bond-Lamberty and Thomson 2010). Automatic dynamic chamber equipment is recognized as the best technique for capturing the substantial temporal heterogeneity of Rs (Luo and Zhou 2006); however, automatic Rs measurements are too expensive and labor intensive for use over large areas and long periods (Luo and Zhou 2006). Instead of measuring Rs continuously, many Rs measurements are taken at discrete times, typically no more than several minutes per measurement, by manual chamber systems (Cueva et al. 2017). Manual chamber system takes just a few minutes to measure Rs, making it very flexible for spatial sampling of Rs (Luo and Zhou 2006). Consequently, due to their commercial availability and ease of use, manual chamber systems are now the most widely used equipment to measure Rs (Luo and Zhou 2006). One

disadvantage of manual chamber systems, however, is their difficulty in evaluating temporal variation of Rs. Manual chamber systems usually rely on single Rs measurements made within a few minutes to stand for daily mean Rs; most of these single Rs measurements are made during daytime. Thus these discrete measurements neglect diurnal and seasonal fluctuations of Rs, which can bias estimates of the daily mean Rs (Parkin and Kaspar 2004) and create uncertainty when used to extrapolate weekly or monthly measurements to an annual carbon budget (Tang and Baldocchi 2005).

It is difficult to quantify the heterogeneity of Rs diurnal variation across different climates and biomes, making it difficult to evaluate the best time period to take Rs measurements under a specific climate and biome (Dore, Fry, and Stephens 2014). The timing of Rs measurements within a day and year varies substantially among studies. For example, Chen *et al*. (2014) conducted their measurements from 13:00 to 15:00, Saiz *et al*. (2006) measured Rs from 10:00 to 16:00, and Savage *et al*. (2008) measured from 09:00 to 15:00 to represent daily mean Rs. To estimate annual Rs at a site, Rs measurements have been taken once per week, once per month, or even once per season (Chen et al. 2014; Davidson, Belk, and Boone 1998; Sheng et al. 2010b) in different studies. Though multiple studies quantified fine-scale Rs temporal dynamics in ecosystems all over the world, researchers lack a consensus protocol to help make decisions regarding Rs measurement timing and frequency because Rs temporal dynamics among climates and biomes has not been synthesized with respect to measurement timing (Akinremi, Mcginn, and Mclean 1999; Goulden et al. 1996, 1998; Kutsch and Kappen 1997; Lee et al. 2004; Nakadai et al. 2002; Riveros-Iregui et al. 2007; Shen, Li, and Fu 2015; Tedeschi et al. 2006; Valentini et al. 2000; Wan and Luo 2003; Wang et al. 2005; Xu and Qi 2001). In order to provide basic data supporting future Rs field measure protocol, we synthesize available information using high

quality data to anzlyze the optimum time period to capture daily mean Rs for different climates and biomes.

Numerous studies have described Rs diurnal and seasonal fluctuations in different climates and biomes (Chen et al. 2014; Davidson et al. 1998; Parkin and Kaspar 2004; Savage and Davidson 2003; Sheng et al. 2010b; Xu and Qi 2001). Daily fluctuations in Rs are usually driven by changes in soil temperature (Rixon, 1968; Medina & Zelwer, 1972; Larionova *et al.*, 1989), humidity (Medina and Zelwer 1972), and precipitation (Rochette et al. 1991). Davidson *et al*. (1998) reported that Rs measured from 09:00 to 12:00 most accurately represented the daily mean of Rs in a temperate mixed-hardwood forest. Many subsequent experiments thus measured Rs during a similar period to represent Rs daily means (Chen et al. 2014; Parkin and Kaspar 2004; Savage and Davidson 2003; Sheng et al. 2010b; Xu and Qi 2001; Zhang 2011). However, Davidson *et al*. (1998) reached their conclusion based on Rs measured on August 6 & 7, 1994, in a temperate mixed hardwood forest, no study of applicability to other climates or biomes. Whether the 09:00 to 12:00 window (local time) is appropriate in other climates, biomes, and seasons is uncertain. Environmental factors such as soil moisture and canopy photosynthesis affect diurnal variation in Rs and complicate measurement timing. For example, by quantifying a soil temperature-independent component of Rs in a forest system, Liu *et al*. (2006) found that diurnal variations in photosynthetically active radiation (PAR) and affected the soil temperature-independent component of Rs, which varies in much the same matnner as temperature. Likewise, Tang *et al*. (2005) found that diurnal variation of Rs in an open area was driven by soil temperature, while diurnal patterns of Rs under trees were controlled by both photosynthesis and air temperature. Their Rs peak lagged 7–12 hours behind photosynthesis peak. Rs diurnal pattern was also closely related to soil water content and thus show more complicated patterns. For

instance, Li and Dong (2003) found that Rs diurnal patterns were affected by soil temperature and soil moisture, and two Rs peaks appeared separately at 07:00–08:00 and at 14:00. In a semiarid shrubland in Baja California, México, Cueva *et al.* (2017) found that optimum times to capture the daily mean were at night (17:00 to 19:00 in the shrub treatment, and 20:00 to 21:00 in the trench treatment). Given the substantial heterogeneity in the diurnal pattern observed in past studies, the timing of Rs measurements should be carefully considered when those measurements are used to estimate the daily mean.

Measurements made exclusively at night may also bias up-scaled estimates; however, there is no analysis of how much Rs measured at nighttime affects the daily mean in global and eco-region scales. Recent developments of eddy covariance technique have provided the opportunity for continuous long-term monitoring of ecosystem respiration (eddy covariance can measure Rs if gas flux measurement equipment were set up under canopy or landscape without vegetation) at the ecosystem level (Griffis et al. 2004). One disadvantage of eddy covariance is that it is very difficult to measure carbon released by respiration in the daytime because part of carbon consumed by photosynthesis and, thus, a common practice is to use loss of CO_2 during nighttime to represent the respiration rate for Rs and for Q_{10} estimation (Liu et al. 2006; Wohlfahrt et al. 2005). However, many site scale studies have demonstrated that Rs measured at nighttime was less than daily Rs rate (Griffis et al. 2004; Rambal et al. 2004). As eddy covariance becomes more commonly used worldwide as a measurement of CO_2 flux, it is essential to quantify how much Rs measured at night biases the daily mean Rs, and to test whether using Rs from a certain nighttime period rather than using Rs over the whole night to represent the daily mean can reduce bias.

In addition to diurnal variation, quantification of annual Rs can be affected by seasonal Rs. Seasonal effects influence Rs in almost all ecosystems (Luo and Zhou 2006), driven largely by changes in temperature or moisture (especially in dry climates), where Rs rates are usually higher in warm periods and lower during colder periods. Soil moisture is usually another main limiting factor of Rs in arid and semiarid ecosystems (Davidson et al. 2000). Within a certain climate region, the controlling factors of Rs variation may change from season to season. For instance, in the Great Plains of the USA, neither temperature nor moisture is a limiting factor for Rs in the spring, but moisture becomes a limiting factor in the summer and temperature becomes a limiting factor in the winter (Wan et al. 2005). In Mediterranean climates, water usually constrains Rs during the hot, dry summers, but temperature limits Rs in cold, wet winters (Xu and Qi 2001). Thus, different biomes exist different spatial and seasonal Rs variation. . Plant phenology, such as differential timing of root growth, root turnover, and litterfall, are important influences on Rs seasonal variation (Curiel Yuste et al. 2004). In young *Pinus radiata* tree sites in Christchurch, New Zealand, seasonal increases in Rs were closely related to increases in root production and biomass (Thomas et al. 2000). On a global scale, Raich and Potter (1995) found Rs positively correlated with annual gross primary productivity. Seasonal changes in leaf area index were also positively correlated with seasonal changes in Rs (Ben Bond-Lamberty and Thomson 2010). High measurement frequency (e.g., once per day for at least one year) is required to avoid uncertainty caused by Rs seasonal variation when measuring annual Rs rates. However, manual chamber systems usually do not take Rs measurements everyday during measurement period. Measurements may be taken once per week, once per month, or even once per season, and then scaled up to estimate the annual Rs rate (Chen et al. 2014; Davidson et al.

1998; Sheng et al. 2010b). When sampling is infrequent, seasonal variation of Rs can introduce errors to scaled up estimates if seasonal variation of Rs is not considered in the sampling design.

Whether or not the time period within which Rs measurements are taken and the frequency with which they are taken biases global Rs estimates must be carefully considered. Therefore, in this study, we collected and digitized all available studies that reported hourly Rs measurements to summarize and interpret Rs diurnal and annual patterns at a global level. Specifically, we explored: (1) the best time to capture daily mean Rs in different climates and biomes, (2) the Rs diurnal variation and how it relates to temperature and SWC, (3) the difference between Rs measured at daytime or nighttime versus daily mean Rs, and (4) the measurement frequency necessary for different climates and biomes to achieve specific levels of accuracy in estimating annual Rs. Our goal was to reduce Rs measurement frequency but ascertain a certain level of accuracy by selecting an appropriate measurement periods during the day and by deciding an appropriate measurement frequency within a year for a specific climate or biome.

1.2 MATERIALS AND METHODS

1.2.1 Data collection

Rs diurnal variation analysis requires hourly time-scale data that we obtained by developing an hourly global Rs database (HGRsD) from digitized published articles. We used the key words "soil respiration," "soil CO_2 flux", "soil carbon emission", and "soil respiration diurnal pattern" in the ISI Web of Science and the China National Knowledge Infrastructure (CNKI) to search published papers. We used the following criteria to determine whether the publication would be included in our hourly global Rs database. Inclusion of publication criteria

were: (1) Rs measurements were conducted in the field; (2) the publications included either diurnal Rs measurements or allow diurnal Rs to be calculated with no or few assumptions; and (3) all continuous diurnal Rs records were included, irrespective of the measurement method used. Within these constraints, 9748 Rs data points were digitized from 148 sites across the globe (Figure 1-1); the data has been shared at VTechData (https://data.lib.vt.edu/collections/ns0646000). Most of the Rs measurements were digitized from figures, using Data Thief III (http://datathief.org/). The units of all digitized data were converted to standard units of g C m^{-2} day^{-1} before analyzing. A variety of ancillary data, including measurement time (year, day of year, and hour), latitude and longitude of measured sites, Rs measurement methods, land use type, and biomes were also collected, if available. If no biome was recorded in the original paper, the biome of the sites was entered based on the International Geosphere-Biosphere Programme (IGBP) classification system (Loveland et al. 2000) according to the latitude and longitude of the sites. Measurements in the hourly global Rs database were distributed from 1971 to 2013, from 30 countries, and included 20 records from Antarctica. The countries most frequently represented include China (4992 records) and the USA (3199). A substantial number of Rs measurements were collected in Japan (1212), Canada (520), and Germany (484). Little information was available for the remaining countries, but all together, there were 1302 additional reported records. Most measurements were measured using an infrared gas analyzer (IRGA, 6541) and gradient (1690), while others were collected by gas chromatography (GC, 453) and alkali absorption (AA, 358) methods. The remaining 2667 records' measurement methods were not reported in the papers. The climatic properties of each measurement site were entered based on Köppen Climate Classification (http://koeppen-geiger.vu-wien.ac.at/) according to the latitude and longitude of sites.

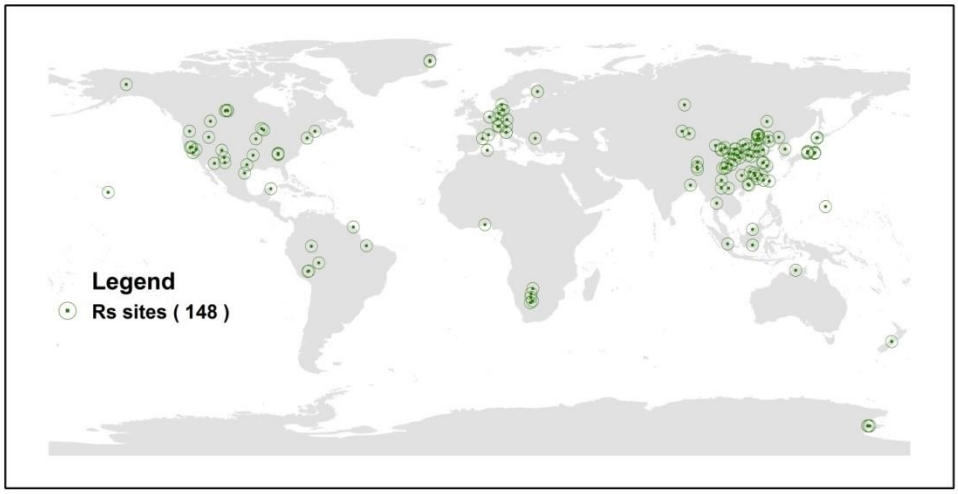

Figure 1-1. The spatial distribution of sites in the hourly global soil respiration database (HGRsD). Sites labeled as "Rs sites" indicate 148 sites collected from 148 publications.

1.2.2 Data analysis

Rs data in HGRsD evenly distributed within 24 time periods (from 1 to 24) in a day (data not shown), each time period covers one hour (e.g., 1:00 means from 1:00 to 2:00, same for all 24 time periods expression hereafter if without explanation). First, we tested how close Rs measurements at a specific time period of day were to the daily mean Rs. Because the Rs measurements were not normally distributed, measurements were highly variable, and some biomes had small samples sizes (data not shown), we used a bootstrapping method to resample differences between Rs measured during a specific time and daily mean Rs in every climate and biome. In the bootstrapping method, subsamples of the difference between Rs measured at a specific period versus daily mean Rs were randomly taken 10,000 times, and the mean of the 10,000 subsamples followed a normal distribution. The confidence interval of the subsampling include zero, indicating no difference between Rs measured during a specific time period and daily mean Rs. If the confidence interval was greater than zero, the mean of Rs measured during

a time period was consistently greater than the daily mean Rs. A confidence interval less than zero indicated that Rs measured at a time period was consistently smaller than the daily mean Rs.

For logistical reasons, it usually takes several hours rather than a single hour or less to finish Rs sampling at multiple sites and collars. Therefore, we used the bootstrapping approach to test how close Rs measurements made during several different time periods were to the daily mean Rs [between 08:00 and 12:00, 09:00 and 11:00, 20:00 and 21:00, 19:00 and 22:00, measuring between 7:00 and 18:00 (day time), or measuring between 19:00 and 6:00 (night time)]. We first calculated average Rs rates between 08:00 and 12:00, and then differences between daily mean Rs and the Rs mean from 08:00 to 12:00 were calculated. Boostrapping methods were used to test differences between daily mean Rs and Rs measured between 08:00 and 12:00. Similar approachs were applied to the other five time periods.

To assess the optimum measurement frequency needed to capture the seasonal variability for Rs in each climate and biome, we quantified the number of days needed to predict a yearly Rs mean ±10%, ±20%, or ±30%, and with 95%, 90%, or 80% confidence intervals (CI), respectively. We used the equation (1-1) developed by Davidson *et al*. (2002) to calculate number of days needed to measure Rs within a year,

$$n = \left[\frac{t \cdot s}{range/2}\right]^2 \qquad (1\text{-}1)$$

where *n* is the number of days needed to measure Rs within a year; *t* is the two-way statistical *t* value for a given confidence level (95%, 90%, and 80% were used in this study) and degrees of freedom (depending on sample sizes in different climates and biomes); *s* is the standard deviation of the all Rs measurements from the HGRsD within a specific climate or biome; and *range* is the width of the population mean ×10%, 20%, or 30%.

When measurement frequency and confidence intervals are fixed, a relevant cut off level should be chosen to determine that the detected Rs seasonal variation was not caused by measurement error, and this cut off value should be greater than the measurement error of the instrument used to measure the Rs rate. The minimum detectable difference (δ) was thus suggested as the cut off level (Bruynesteyn et al. 2005). According to Dore *et al*. (2014), when the number of days and confidence intervals are fixed, the minimum detectable Rs difference (δ) from the measured mean can be calculated by equation (1-2),

$$\delta = \sqrt{\frac{s^2 \cdot t}{n}} \qquad (1\text{-}2)$$

where *s*, *t*, and *n* are the same as in equation (1). The minimum detectable Rs difference (δ) evaluates the detectable annual variation within a specific climate and biome under a certain measurement frequency and confidence interval. All of the above statistical analyses were performed using R, version 3.1.1 (R Core Team, 2014).

1.3 RESULTS

1.3.1 Rs measurement temporal and spatial distribution in the HGRsD

Rs measurements from the HGRsD were temporally unevenly distributed, with more measurements taken during warm periods (Figure 1-2 panel a). This is also true when measurements were scaled down to climates and biomes (data not shown). Within a day, however, Rs measurements were evenly distributed from 01:00 to 24:00 in different climates and biomes (Figure 1-2 panel b). Averaging the 9,748 hourly Rs records from the HGRsD produces 596 daily Rs records. The daily measurement frequency in the HGRsD differs from publication to publication, with most Rs data measured once per hour (178 days), once per two hours (131

days), less than once per hour but more than once per two hours (79 days), and less than once per two hours but more than (or equal to) once per six hours (208 days, Figure 1-2 panel c). In other words, there were 208 daily mean Rs were created by averaging fewer than 12 Rs measurements within a day. We compared the Rs diurnal pattern from those 208 low frequency measurements versus Rs diurnal patterns from other high frequency Rs measurements. We found a similar pattern as the other high frequency Rs measurements (results not shown), thus we included those 208 low measure frequency Rs data in this study.

Based on the Köppen Climate classification (the Köppen Climate classification has a three-stage classification, we used the second stage classification at this study) (Kottek et al. 2006), Rs measurements in the hourly global Rs database (HGRsD) were unevenly distributed in eight different climate regions (Figure 1-2 panel d). The climates that were most frequently represented include: arid (B, 15.01% of total, 1463 measurements), temperate humid (Cf, 24.69%, 2407 measurements), boreal humid (Df, 17.07%, 1664 measurements), and boreal summer dry or winter dry (Dw, 11.93%, 1163 measurements). A substantial number of Rs measurements were collected from vegetative regions: temperate summer dry (Cs, 12.77%, 1245 measurements) and temperate winter dry (Cw, 11.17%, 1089 measurements). Little information was available for tropical (A, 4.95%, 483 measurements) and polar (E, 2.4%, 234 measurements) regions (Figure 1-2 panel e). Based on biomes reported in the papers, a substantial number of measurements were collected from cropland (CRO, 11.82%, 1152 measurements), deciduous forests (DF, 19.07%, 1859 measurements), evergreen forests (EF, 19.48%, 1899 measurements), grasslands (GRA, 19.48%, 1916 measurements), mixed forests (MF, 10.61%, 1034 measurements), and scrublands (SH, 10.42%, 1016 measurements). Few data were reported from

barren or sparsely vegetated (BSV, 5.91%, 576 measurements) and wetland (WET, 3.04%, 296 measurements) (Figure 1-2 panel e) biomes.

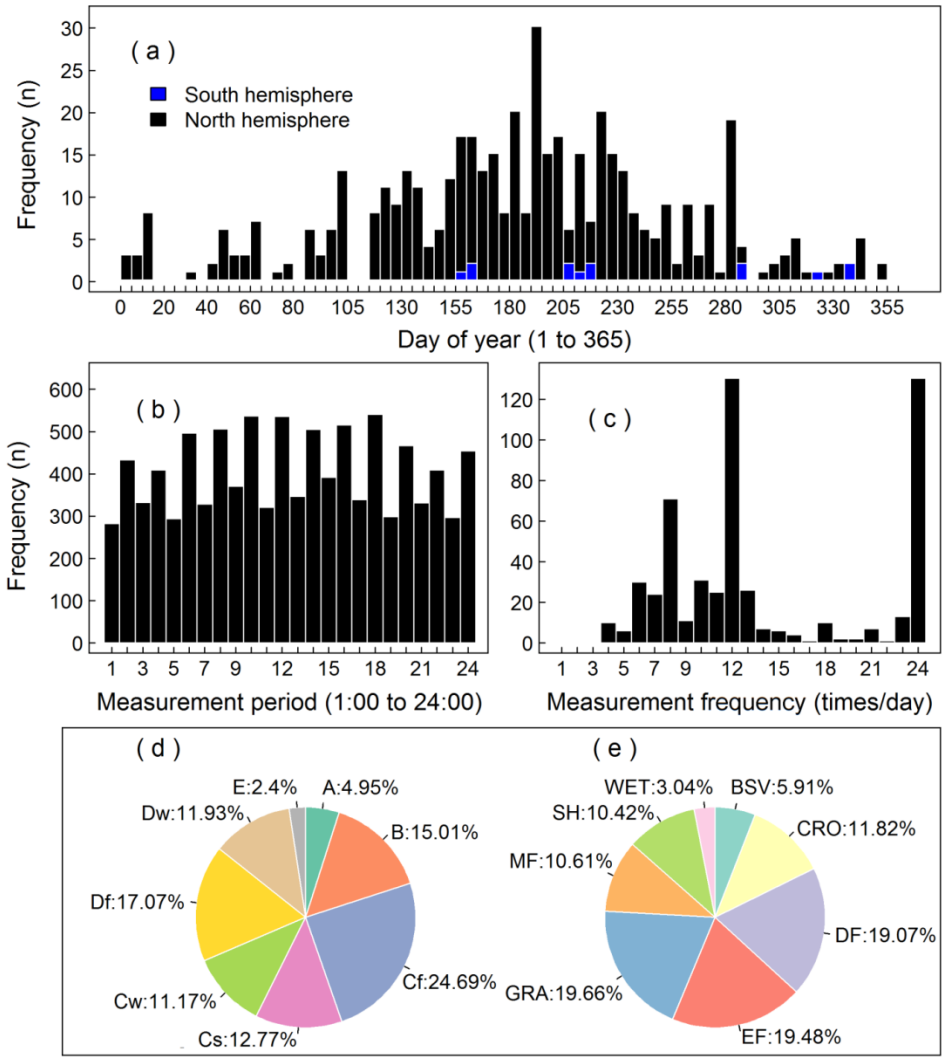

Figure 1-2. Soil respiration (Rs) temporal and spatial distribution in the hourly global Rs database (HGRsD). (a) Rs measurements frequency in HGRsD across 365 days of a year; (b) Rs measurements distributed from 1:00 to 24:00 in HGRsD. (c) Daily Rs measure frequency (times per day) in HGRsD. (d): Rs measurements distribution across eight climates, including: tropical (A), arid region (B), temperate humid (Cf), temperate summer dry (Cs), temperate winter dry (Cw), boreal humid (Df), boreal summer dry or winter dry (Dsw), polar (E); (e): Rs measurements distribution across eight biomes, including: barren or sparsely vegetated (BSV), crop land (CRO), deciduous forest (DF), evergreen forest (EF), grass land (GRA), mixed forest (MF), shrub land (SH) and wet land (WET).

1.3.2 Measuring time to estimate the daily mean

For all the Rs records from HGRsD, bootstrap sampling found that the 95% CI include zero at 10:00, 20:00, and 21:00, which means that Rs rates measured during these periods do not significantly differ from daily mean Rs rates (Figure 1-3). From 22:00 to 09:00, the 95% CI was below zero, indicating that Rs measured before 10:00 was less than the daily mean Rs rate. From 11:00 to 19:00, the 95% CI was above zero, indicating that Rs measured at this period was greater than daily mean Rs. The Rs diurnal variation in the spring, summer, and autumn was similar to the whole year (Figure 1-3). In winter, however, Rs measured during any period did not significantly differ from the daily mean Rs (Figure 1-3).

It worth noting that the results were based on local time, Rs measured at a specific time period (e.g., 10:00) does not significantly differ from Rs measured one or two hours before or after (e.g., 9:00 or 11:00, Table 1-1), When comparing the local time versus standard world map of time zone (http://www.fgienr.net/time-zone/), we found that the local time in most sites in HGRsD match with the standard world time zone except for some sites in China. China has a vast territory, which covers approximately three world time zones but the entire Nation China uses a single time zone. The largest time difference between local time and standard world time is two hours. As a result, it is likely that the effect of time zone could be ignored in terms of determining the time period to measure the Rs which can represent the daily mean Rs. We converted the local time zone into standard world time zone by changing the local time back two hours (e.g., 24:00 changes to 22:00, same for all 24 time periods) for sites within China between longitude east 82.5° and 97.5°. We changed the local time back one hour (e.g., 24:00 changes to 23:00, same for all 24 time periods) for sites located in China between east 97.5° and 112.5°. The time remains the same for all other sites in China. We then applied bootstrapping to test the

difference between daily mean Rs and Rs measured at specific time period under the standard time zone and detected very similar results (results not shown) as the results from the local time (Figure 1-3). We thus use local time zones in this study.

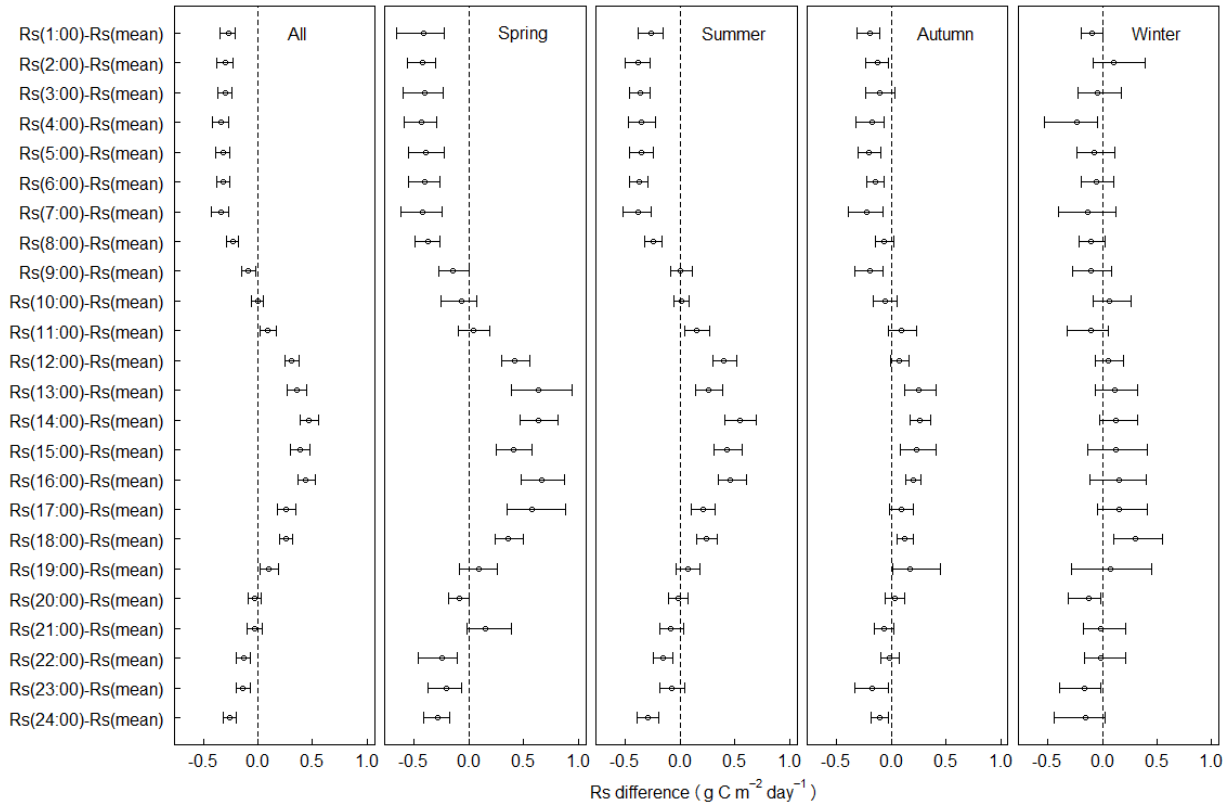

Figure 1-3. Bootstrapping sampling for the difference between Rs measured at specific time points (01:00–24:00) and Rs daily mean for all data from the hourly global soil respiration database (HGRsD), and separated into spring, summer, autumn and winter. The circles indicate the 10,000 measurements mean, and the error bars indicate the 95% confidence interval, CI include zero indicates no significant difference, CI above zero indicates overestimate, and CI below zero indicates significant underestimate.

Diurnal variation of Rs closely followed soil temperature changes in different season, climates and biomes (Figure 1-4 and 1-5). Rs usually increased in the morning, reached a peak at noon, and then decreased from afternoon throughout the night, which coincides with daily variation of soil temperature, as hourly soil temperature also reached the daily mean at around 9:00, and again at 20:00 (vertical dashed line in Figure 1-4 and 1-5). However, no clear diurnal

variation of SWC was detected at any climate or biome (Figure 1-4), indicating diurnal variation in SWC has little effect on Rs diurnal variation.

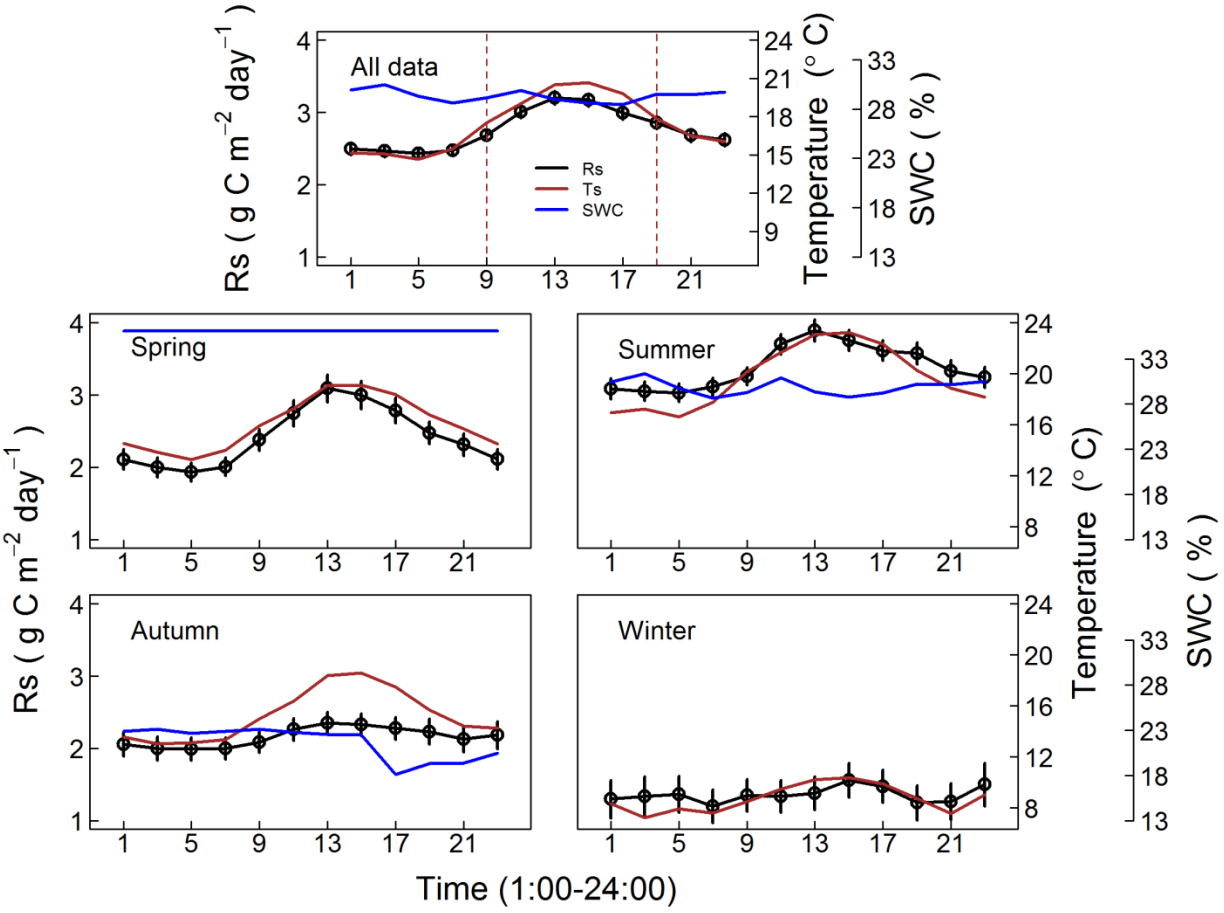

Figure 1-4. Soil respiration, soil temperature, and soil water content (SWC) diurnal patterns for all data, across spring, summer, autumn, and winter. The dash lines in all data indicate the time points when soil temperature most close to daily mean temperature.

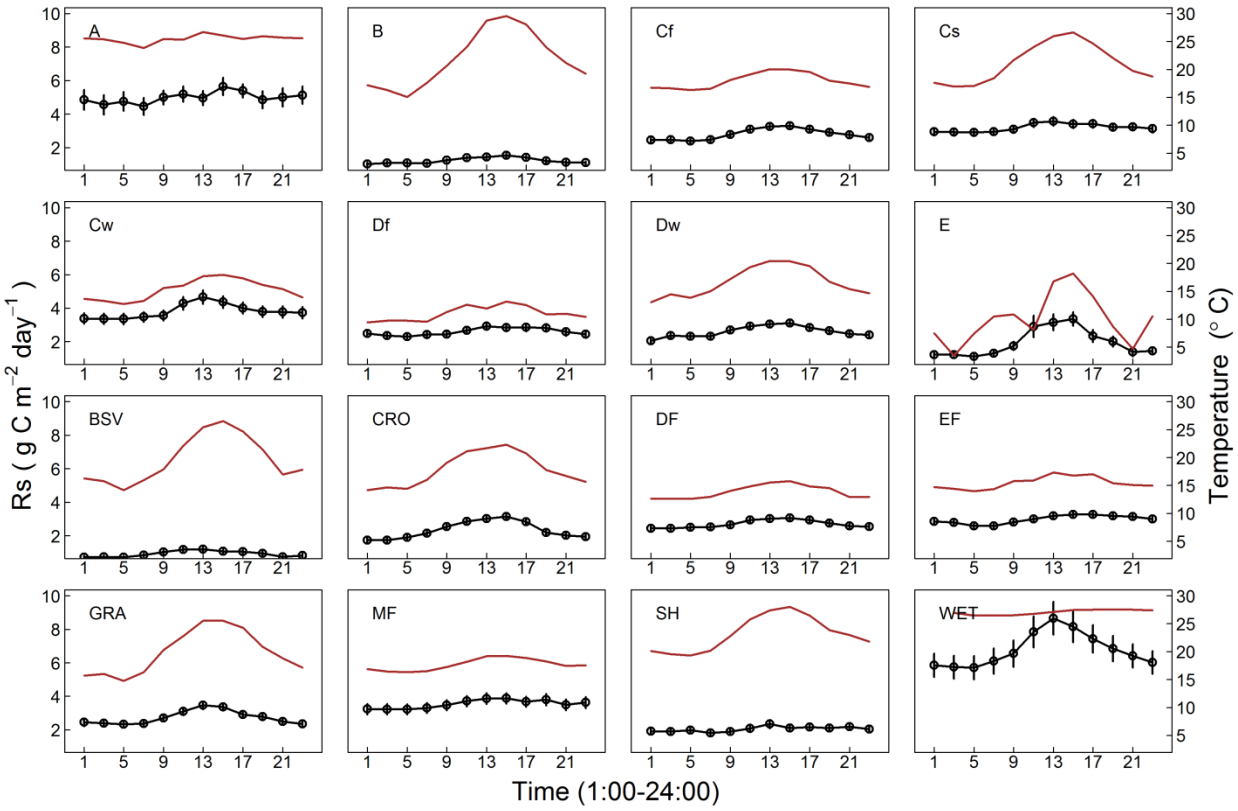

Figure 1-5. Soil respiration and soil temperature diurnal pattern across tropical (A), arid region (B), temperate humid (Cf), temperate summer dry (Cs), temperate winter dry (Cw), boreal humid (Df), boreal summer dry or winter dry (Dsw), polar (E), Barren or sparsely vegetated (BSV), Crop land (CRO), Deciduous forest (DF), Evergreen forest (EF), Grass land (GRA), Mixed forest (MF), Shrubs land (SH) and wet land (WET).

The bootstrapping sampling showed that daytime Rs was greater than daily mean Rs by 0.17 g C m^{-2} day^{-1} (Figure 1-6 panel a), or approximately 6% (0.17/2.71) of the daily mean Rs (2.71 g C m^{-2} day^{-1}). Suppose that the entire set of discrete field Rs measurements from across the globe were randomly distributed over the daytime, our results indicate that the bias caused by Rs diurnal variation is approximately 6% (Figure 1-6 panel a). However, Rs measured from 08:00 to 12:00 (Figure 1-6 panel b) and from 09:00 to 11:00 (Figure 1-6 panel c) did not significantly differ from daily mean Rs, which suggests that in order to neutralize the bias caused by measurement time, it is important to measure Rs at around 10:00 and broaden on both sides

evenly if necessary (e.g., measured from 09:00 to 11:00). Given the fact that a majority of Rs measurements were taken between 09:00 and 12:00, it is likely that the bias caused by Rs diurnal variation is smaller than 6% in global Rs data.

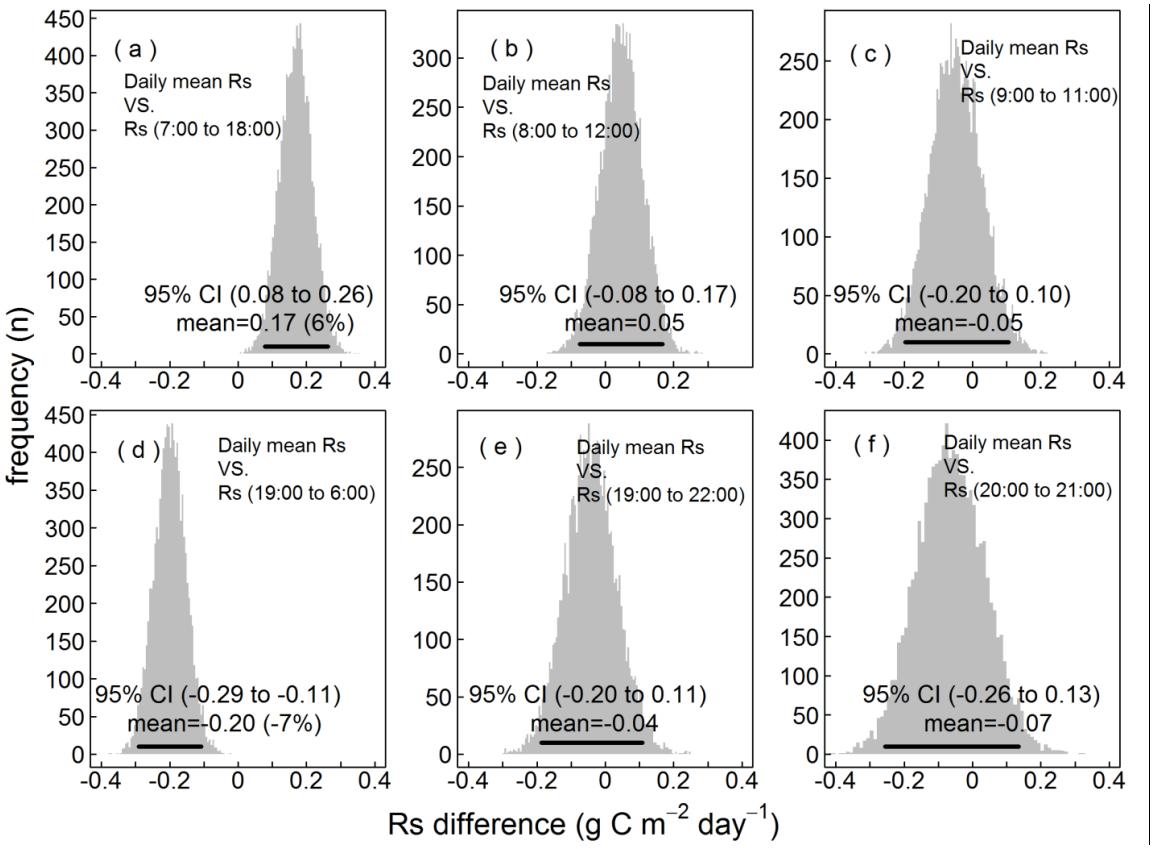

Figure 1-6. The difference between Rs measured at time windows and 24 hours Rs mean. (a) Rs measured during the daytime (from 7:00 to 18:00) was significantly greater than daily mean Rs; (b) Soil respiration measured from 8:00 to 12:00 did not significantly differ from Rs measured from all 24 hours; (c) Rs measured from 9:00 to 11:00 did not significantly differ from daily mean Rs; (d) Rs measured at night time (from 19:00 to 6:00) significantly smaller than daily mean Rs; (e) Rs measured between 19:00 and 22:00 did not significantly differ from daily mean Rs; (f) Rs measured between 20:00 and 21:00 does not significantly differ from daily mean Rs. The black lines labeled the 95% confidence interval (CI), CI covers zero indicates no significant difference, CI above zero indicates overestimate, and CI below zero indicates significant underestimate.

Eddy covariance technique provides convenience new method of capturing ecosystem respiration temporal variation at the ecosystem level (Griffis et al. 2004). However, eddy covariance has to use nighttime loss of CO_2 to represent the respiration variation because the

CO_2 flux during daytime is mixed with carbon consumed by photosynthesis (Liu et al. 2006; Wohlfahrt et al. 2005). It is thus important to test whether nighttime respiration rate represents the 24-hour respiration rate mean at the global scale. Based on the hourly Rs collected across globe at this study, our results showed that the nighttime respiration rate was smaller than the daily mean respiration rate by 0.20 g C m^{-2} day^{-1}, or, in other words, approximately 7% (0.20/2.71) of the daily mean respiration rate (Figure 1-6 panel d). However, respiration rates measured between 19:00 and 22:00 (Figure 1-6 panel e) or between 20:00 and 21:00 (Figure 1-6 panel f) did not significantly differ from the daily mean respiration rate. Therefore, respiration rates measured between 20:00 and 21:00, or between 19:00 and 22:00 represent the daily mean respiration rate in the eddy covariance data is a plausible strategy to resolve the problem of nighttime respiration rates being smaller than daily mean respiration rates.

1.3.3 Rs diurnal variation across climates and biomes

The above analysis of the global hourly Rs dataset suggests that the best daytime period to capture the daily mean of Rs is at around 10:00, which supports the conclusion by Davidson *et al*. (1998) that morning measurements are reasonable estimates of the daily mean of Rs. When we tested the difference between Rs measured at specific time points and daily mean Rs in different climates and biomes, the results showed that Rs measured at around 10:00 also captured daily mean Rs in all regions. Wetlands had insufficient data available at 10:00; there, the 95% CI of nearby periods, 09:00 or 11:00, were used (Figure 1-7). The results showed that some climates and biomes showed more significant Rs diurnal fluctuation than others. In tropical, arid, temperate summer dry, boreal humid, barren or sparsely vegetated, forest and shrub-land regions, the difference between Rs measured at specific time points and daily mean Rs did not

significantly differ for most periods, indicating that within those regions, time period is less important in terms of capturing daily mean Rs (Figure 1-7). For instance, in tropical, Rs measured at any time except 4:00, 7:00 16:00 are close to daily mean Rs, but in temperate humid region, only Rs measured at 9:00, 19:00-21:00 represent the daily mean Rs (Table 1-1).

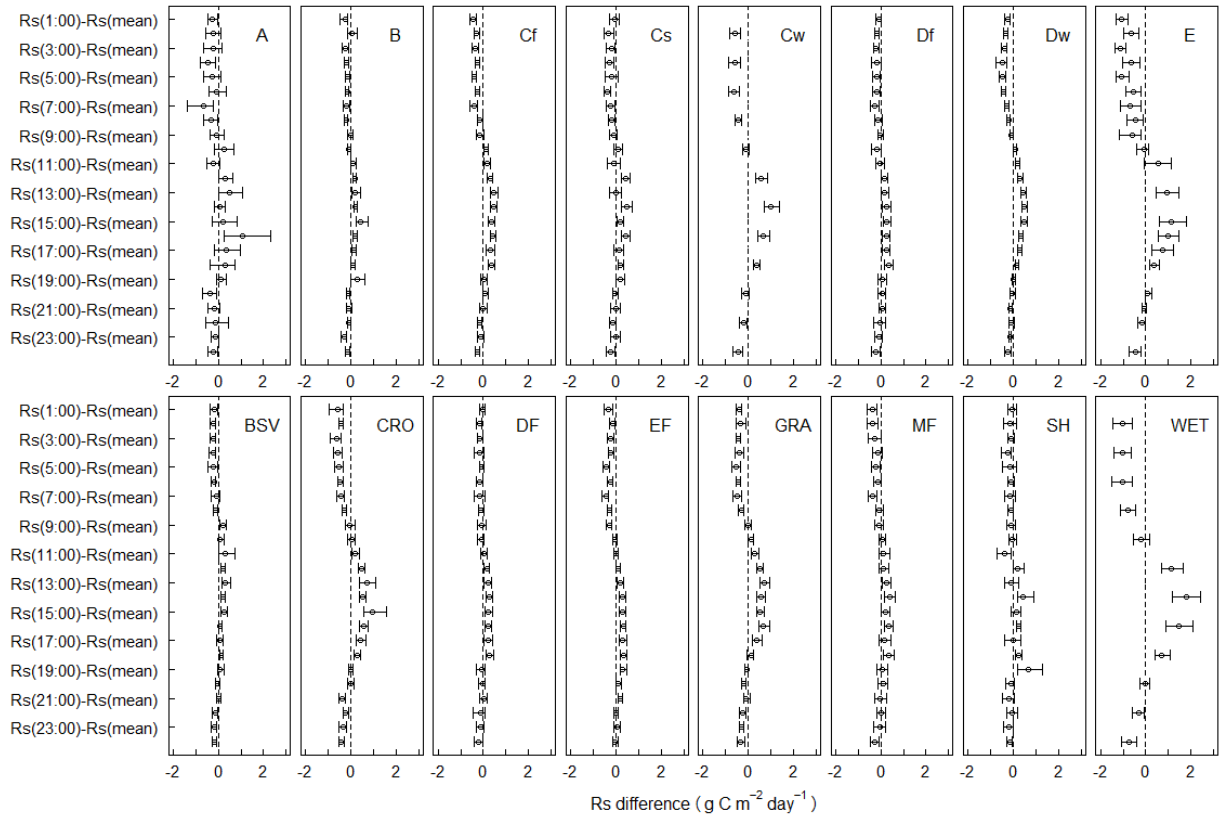

Figure 1-7. Bootstrapping to test the difference between Rs measured at specific time points (01:00–24:00) and Rs daily mean in different climates and biomes. The circles indicate the 10,000 measurements mean, and the error bars indicate the 95% confidence interval, CI covers zero indicates no significant difference, CI above zero indicates significant overestimate, and CI below zero indicates significant underestimate. Acronym: tropical (A), arid region (B), temperate humid (Cf), temperate summer dry (Cs), temperate winter dry (Cw), boreal humid (Df), boreal summer dry or winter dry (Dsw), polar (E), Barren or sparsely vegetated (BSV), Crop land (CRO), Deciduous forest (DF), Evergreen forest (EF), Grass land (GRA), Mixed forest (MF), Shrub land (SH) and wet land (WET).

1.3.4 Soil respiration annual variation and measurement frequency

We next used the global hourly Rs dataset to determine the relationship between sampling frequency and the probability of capturing the annual mean. Firstly, by analyzing seasonal Rs variation in different climates and biomes, we identified the measurement frequency required to capture a certain range of Rs with a certain confidence (equation 1-1). We then identified the minimum detectable Rs difference (equation 1-2) associated with each biome, with fixed desired accuracy and probability values. The seasonal Rs variability in different climates and biomes directly affected ability to measure Rs (Figure 1-8 panels a and Table 1-1), and affected the minimum detection of differences among climates or biomes (Figure 1-8 panel b). Overall, the number of days necessary to obtain Rs mean±10% from all Rs measurements ranged from 131 days (80% CI, Figure 1-8 panel a and Table 1-1) to 308 days (95% CI, Figure 1-8 panel a and Table 1-1), indicating that if the purpose was to capture annual daily mean within ±10% of the population mean with a 95% CI, it requires measurement of Rs almost once per day. The measurement frequency can be decreased to once per two days when the confidence interval decreases to 80%. When down-scaled to climates and biomes, the tropical, temperate humid, boreal dry, polar, cropland, forest, and wetland biomes required fewer days to obtain the same mean range with the same CI than arid, temperate summer dry, temperate winter dry, boreal humid, barren or sparsely vegetated, grassland, mixed forest, and shrubland biomes (Figure 1-8 panel a and Table 1-1). Widening the desired accuracy to ±30% of the population mean, the required measurement days decreased to 15 days (80% CI, Figure 1-8 panel a) or to 34 days (95% CI, Figure 1-8 panel a) for all data in the global scale , indicating that slightly higher than once per month measurement frequency allows 80% confidence to capture daily means within

±30% of the population mean. The measurement frequency needed to be increased to approximately three times per month to obtain a confidence of 95%.

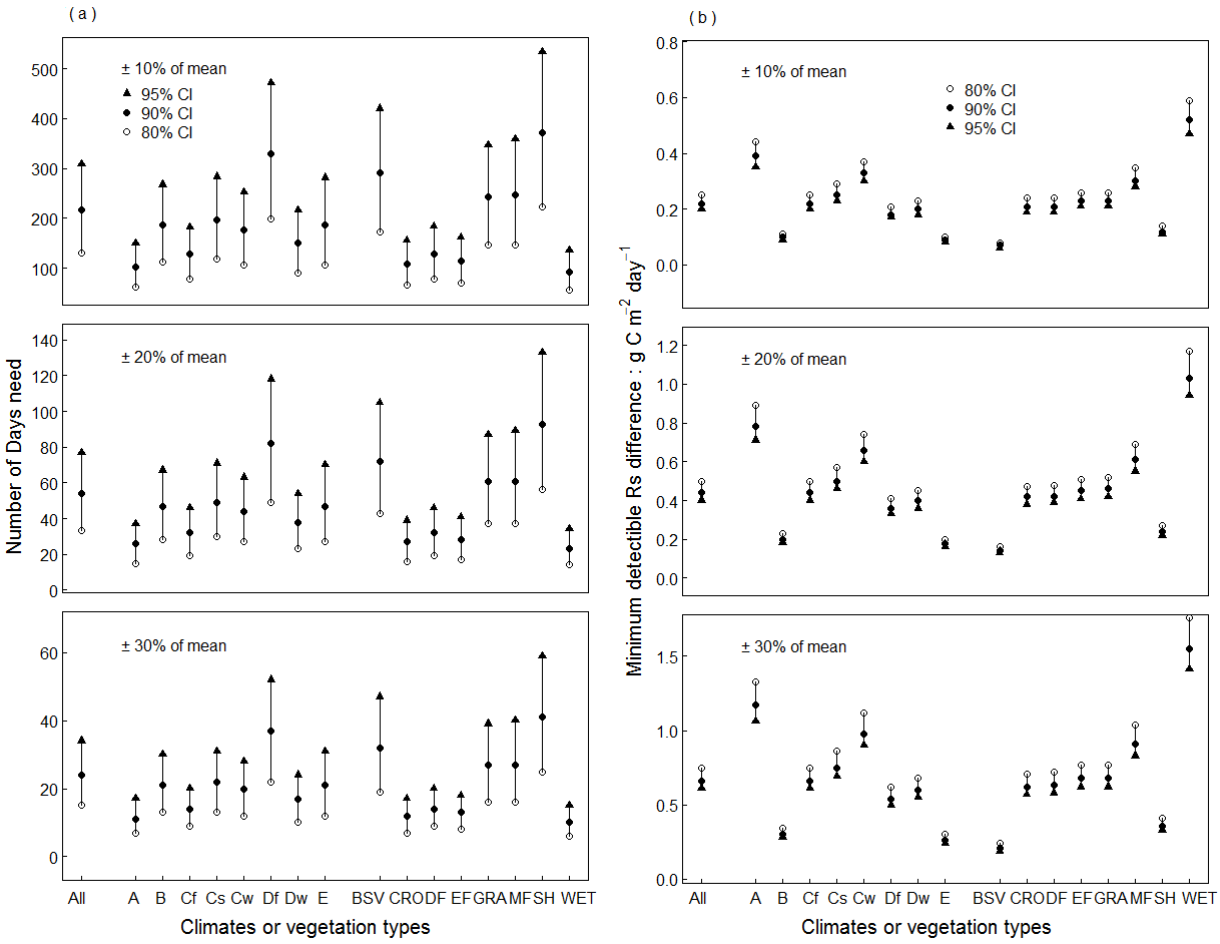

Figure 1-8. Number of days required to measure ±10, ±20, and ±30% of the annual mean at the 95%, 90%, and 80% confidence levels and minimum detectible Rs difference (δ, units: g C m^{-2} day^{-1}) from the measured soil respiration mean at 95%, 90% and 80% confidence interval at different climates and biomes. Acronym: tropical (A), arid region (B), temperate humid (Cf), temperate summer dry (Cs), temperate winter dry (Cw), boreal humid (Df), boreal summer dry or winter dry (Dsw), polar (E), Barren or sparsely vegetated (BSV), Crop land (CRO), Deciduous forest (DF), Evergreen forest (EF), Grass land (GRA), Mixed forest (MF), Shrub land (SH) and wet land (WET).

Table 1-1. Measurement windows (note that usually there are more than one window to capture the daily mean Rs, and time window including 10am were labeled as bold) for measuring Rs to capture daily mean Rs and measure frequency required to capture Rs seasonal variation within ±10, ±20 and ±30% of the Rs annual mean at the 95%, 90% and 80% confidence level in global and in each climate and biome. Acronym: tropical (A), arid region (B), temperate humid (Cf), temperate summer dry (Cs), temperate winter dry (Cw), boreal humid (Df), boreal summer dry or winter dry (Dsw), polar (E), Barren or sparsely vegetated (BSV), Crop land (CRO), Deciduous forest (DF), Evergreen forest (EF), Grass land (GRA), Mixed forest (MF), Shrub land (SH) and wet land (WET). Note that 1:00 means the time period from 1:00 to 2:00, same for all 24 time periods.

	Measurement Windows	Measurement frequency (times per year)								
		CI=80%			CI=90%			CI=95%		
		±10%	±20%	±30%	±10%	±20%	±30%	±10%	±20%	±30%
Global										
All	10:00, 20:00, 21:00	131	33	15	217	24	54	308	77	34
By climates										
A	1:00-3:00, 5:00-15:00, 16:00-24:00	61	15	7	103	11	26	149	37	17
B	2:00, 9:00, 11:00,18:00-22:00	113	28	13	187	21	47	267	67	30
Cf	9:00, 19:00-21:00	77	19	9	128	14	32	182	46	20
Cs	1:00, 5:00, 9:00-11:00, 13:00, 19:00-23:00	119	30	13	197	22	49	283	71	31
Cw	10:00, 20:00	106	27	12	176	20	44	252	63	28
Df	1:00, 4:00, 8:00-11:00, 13:00, 19:00-23:00	198	49	22	329	37	82	471	118	52
Dw	9:00, 19:00, 22:00	91	23	10	151	17	38	216	54	24
E	10:00-12:00, 20:00-22:00	107	27	12	186	21	47	281	70	31
By biomes										
BSV	7:00, 10:00, 17:00, 19:00-21:00	173	43	19	290	32	72	420	105	47
CRO	9:00-11:00, 19:00	66	16	7	109	12	27	156	39	17
DF	1:00, 4:00, 7:00-11:00, 19:00-23:00	77	19	9	128	14	32	183	46	20
EF	10:00-12:00, 20:00, 22:00-24:00	69	17	8	114	13	28	162	41	18
GRA	9:00, 18:00, 21:00	147	37	16	243	27	61	347	87	39
MF	3:00-6:00, 8:00-12:00, 15:00, 17:00, 19:00-23:00	146	37	16	246	27	61	358	89	40
SH	1:00-3:00, 5:00-10:00, 12:00, 15:00, 17:00, 20:00-23:00	223	56	25	371	41	93	533	133	59
WET	10:00, 20:00	55	14	6	93	10	23	136	34	15

Seasonal Rs variation, defined as the minimum detectible difference from the measured mean Rs (δ), affects ability to capture seasonal Rs fluctuations (Figure 1-8 panel b), and the regions showed higher detectible variability requiring fewer measurement days. In the global scale (all data), if the required accuracy is ±10% of the population mean and the measured frequency is 308, meeting a 95% CI requires a minimum detectible difference of 0.20 g C m^{-2} day^{-1}; meeting a 80% CI requires the minimum detectible difference to be 0.25 g C m^{-2} day^{-1} (Figure 1-8). In another words, when the Rs seasonal variation is greater than 0.20 g C m^{-2} day^{-1} (95% CI), or 0.25 g C m^{-2} day^{-1} (80% CI), detected Rs seasonal variation exceeded measurement error. The results from different climates and biomes indicated that the minimum detectible difference from the measured mean (δ) ranged from 0.24 (95% CI) to 1.76 (80% CI) g C m^{-2} day^{-1}, if the required accuracy is ±30% of the population mean (Figure 1-8 panel b). The minimum detectible difference from the measured mean (δ) ranged from 0.06 (95% CI) to 0.59 (80% CI) g C m^{-2} day^{-1}, if the required accuracy is ±10% of the population mean.

1.4 DISCUSSION

Diurnal variations in Rs make daily average Rs estimates problematic. Identifying accurate measurement windows to capture daily mean Rs is critical for developing protocols for measuring gas exchange between soil and the atmosphere using manual chamber systems. Our results showed that temperature is a major factor that affects Rs diurnal variation; however, Rs measured at 10:00, 20:00, 23:00 or evenly broadened from those time periods in either earlier or later hours (e.g., 08:00–12:00) did not significantly differ from the Rs daily mean. Rs diurnal patterns were very different across different biomes (Figure 1-7), where the Rs diurnal pattern in

biomes, including forest and scrubland, showed much smaller fluctuations compared with cropland, grassland, and wetland. Yet, despite this variability, the measurement windows above are relatively consistent across biomes.

The results indicated that plant coverage is an important factor that affects Rs diurnal fluctuation in both site scale and eco-region scale. Vegetation could affect micro-scale climate (soil temperature and soil moisture) and thus impact Rs. In Fazenda Vitória, Brazil, comparing relationships between Rs and SWC in primary forests, secondary forests, active cattle pastures, and degraded cattle pastures, Davidson *et al*. (2000) found that all land-uses showed lower Rs during the dry season (June to December); however, the primary and secondary forests were less stressed by the dry conditions. Diurnal variation in Rs was detected in the active pasture but not in the primary forest and degraded pasture, possibly due to pasture soils experienced greater diurnal soil temperature variation (24 to 28.5 ℃) than forest soil (22 to 24.5 ℃). Moreover, roots of grass and crop plants could be shallower in the profile than in the forest and shrub soils (Nepstad et al. 1994); thus, Rs in forest and shrub land were less likely to be limited by SWC as deep roots can absorb water from deep soil layer.

Our results showed that Rs measured from 20:00 to 23:00 does not significantly differ from daily mean Rs (Figure 1-3), similar as the conclusion from Cueva *et al.* (2017). It is possible that Rs decreasing more slowly in afternoon because soil temperature decay much slower at afternoon than in the morning, which is clear at winter and autumn (Figure 1-4). Soil temperature decay slow at afternoon may related with the lag between soil temperature and air temperature. Based on soil temperature and air temperature measured in 13 sites in the Swiss Alps, Gehrig-Fasel *et al.* (2008) found a one to two days of lag in the thermal response of a soil temperature relative to air temperature change. Mackiewicz (2012) found that snow act as an

insulation barrier that creates an observable lag between soil temperature and air temperature. Rs decreasing more slowly in afternoon likely also because vegetation can affect root respiration mainly through its aboveground canopy photosynthesis, which is the source of root exudates (Hogberg et al. 2001; Tang and Baldocchi 2005). It is plausible that the effects of carbohydrates can explain why Rs does not differ from the daily mean for around three hours after 23:00, yet only display a clear pattern during the summer and autumn. In spring, the GPP diurnal pattern is clear, but the lag effect on Rs is not as significant as in summer and autumn. One possibility is more carbohydrates are being directed to above-ground growth in spring rather than root growth. Since leaf area index and photosynthesis usually reach a peak in summer and autumn, the lag phenomenon only appears in the summer and autumn (Figure 1-3). It should be noted that in winter, Rs after 20:00 also did not significantly differ from daily mean, but that is because the daily variation of Rs in winter is very small rather than the effect of GPP.

Many previous studies also reported that photosynthesis closely affect Rs, for instance, in a natural Scots pine forest at northern Sweden, tree-girdling reduced the Rs by 54% comparing with the control, likely due to girdling stopping the supply of current photosynthates to roots (Hogberg et al. 2001). In a temperate deciduous forest, Liu *et al*. (2006) found that temperature-independent component of Rs (Ri) could be best explained by PAR in the growing season with a time lag of 1h, but Ri was not correlate with PAR in dormant-season. The results from Tang *et al*. (2005) showed that Rs significantly correlated with photosynthesis, with a 7-12 hours lag time. The time lag between Rs and photosynthesis may be due to the time needed to transport photosynthetic products from leaves to roots via phloem. However, the short-time lag (1h to 12h) only reflects the effect of photosynthetic products on Rs at the diurnal time-scale. Larger time lags between Rs and photosynthesis have been detected on day-to-day and week-to-week Rs

variation. In a boreal mixed coniferous forest, Ekblad & Högberg (2001) found photosynthesis products took one to four days to transport from leaves to roots from 20-25 meter high trees. In western Oregon, USA, five to ten days' time lags of Rs to photosynthesis were found for different tree species (Bowling et al. 2002). The wide range of lag time between Rs and photosynthesis suggests that photosynthesis may modulate respiration in multiple pathways.

Soil water content is another important environmental condition that affects Rs; however, the results from this study have shown that SWC did not show significant diurnal variation in any season, climate or vegetation type, and plays a negligible role on affecting Rs diurnal variation (Figure 1-4). SWC plays a more important role in Rs seasonal variation rather than diurnal variation, which was also supported by some site scale studies (Davidson et al. 1998; Savage and Davidson 2003; Sheng et al. 2010b). How SWC affects Rs diurnal fluctuation varies from site to site. For instance, in a grassland in Inner Mongolia, China, Li and Dong (2003) reported a bimodal Rs diurnal pattern, with one peak at 07:00–08:00 and another peak at 14:00 (Figure 1-9), the first Rs peak was derived by the presence of dew in the early morning, and the second peak was derived by the temperature variation. It may be true that the presence of dew will increase the soil moisture in the early morning in grassland in some sites; however, by averaging all 2,237 Rs (from HGRsD) observations in grasslands, the diurnal variation of Rs in grassland showed no co-variation as diurnal SWC (Figure 1-9), indicated that a double peak Rs diurnal dynamic in grassland is likely not a common phenomenon.

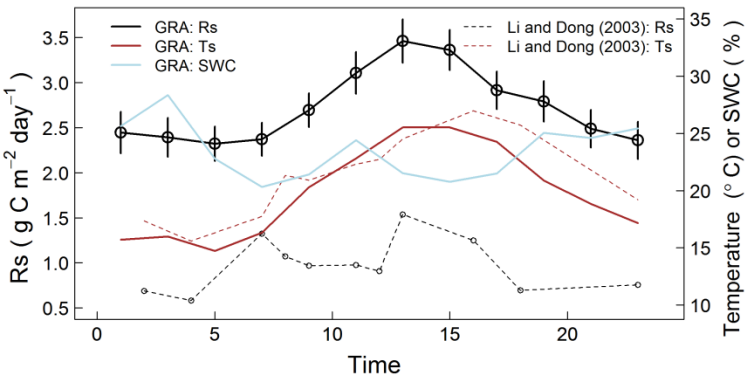

Figure 1-9. Soil respiration, soil temperature and soil water content diurnal patterns for all grassland sites from HGRsD (solid bold lines) and for the site from Li and Dong (2003) (dashed lines).

It is important to explore whether Rs at daytime differs from daily mean Rs, because discrete Rs measurements by manual chamber systems usually were taken on daytime. Our results showed that daytime Rs was greater than daily mean by 6%. If the global Rs database provides Rs measurement time information, it is possible to quantify the magnitude of Rs error caused by using discrete Rs measurements representing daily mean Rs. Unfortunately, the measurement time information was rarely reported in publications, thus the measured period is not available from the global soil respiration database [e.g., the yearly time-scale global Rs database developed by (B. Bond-Lamberty and Thomson 2010)]. However, most chamber measurements were conducted in the daytime, and the most conservative estimate of bias caused by Rs diurnal variation is when all measurements were randomly distributed across the daytime, which was greater than daily mean Rs by approximately 6% (Figure 1-6 panel a). Davidson *et al*. (1998) suggested 09:00–12:00 as the most ideal period to measure daily mean Rs, and many following field measurements followed their suggestion (Chen et al. 2014; Parkin and Kaspar 2004; Savage and Davidson 2003; Sheng et al. 2010b; Xu and Qi 2001; Zhang 2011). Thus, Rs diurnal variation-related bias in the global Rs database should be smaller than 6%.

It is also important to explore whether respiration rate at nighttime differ from daily mean respiration rate because eddy covariance uses nighttime CO_2 flux to represent daily mean respiration rate (Griffis et al. 2004). Using a synthesis of chamber measurements, our results demonstrated that nighttime respiration rate was smaller than daily mean respiration rate by 7% (Figure 1-6 panel d), indicating that either a different period of CO_2 efflux from the eddy covariance data (e.g., from 20:00 to 21:00 or from 19:00 to 22:00, Figure 1-6 panel e and f) should be chosen to represent daily mean respiration rate.

Understanding variation of Rs at fine time-scales is essential to explore the impact of climate variations and management practices on Rs (Delogu et al. 2017). Many Earth system models have now been successfully adapted to a day-time or even 30 minute time-scale (Delogu et al. 2017). However, a fine time-scale soil respiration database is still missing, and the yearly time-scale global soil respiration database has been used as the benchmark. The daily time-scale of the HGRsD developed in this study can fill this time-scale gap and better serve fine time-scale process land models.

1.5 CONCLUSION

This study suggests that the Rs diurnal pattern is closely related to soil temperature. Generally, the best time to measure Rs is at 10:00, and Rs measured at 10:00 captures the daily Rs mean in almost all climates or biomes. When a chamber method was applied to measure Rs, the common practice of measuring Rs from 09:00 to 12:00 to estimate the Rs reasonably captured the daily mean. Rs annual variation is more important in less plant-shaded areas, such as BSV, GRA, and SH land types. Overall, a minimum of one Rs measurement per day is required to estimate an annual Rs rate ±10% from the mean of all Rs measurements with a 95% confidence interval, and if the desired accuracy is decreased to ±30% of the population mean, the confidence interval decreases to 80% and the required measurement frequency decreases to slightly higher than once per month (15 measurements per year). This study analyzed global temporal Rs variation across different climates and biomes. Results from this study can provide theory and data for future Rs chamber method measurements to decrease measurement frequency and still provide a certain level of accuracy.

REFERENCES

Akinremi, O. O., S. M. Mcginn, and H. D. J. Mclean. 1999. “Effects of Soil Temperature and Moisture on Soil Respiration in Barley and Fallow Plots.” *Canadian Journal of Soil Science* 79(1):5–13.

Bond-Lamberty, B. and A. Thomson. 2010. “A Global Database of Soil Respiration Data.” *Biogeosciences* 7(6):1915–26.

Bond-Lamberty, Ben and Allison Thomson. 2010. “Temperature-Associated Increases in the Global Soil Respiration Record.” *Nature* 464(7288):579–82.

Bowling, David et al. Ehleringer. 2002. “C 13 Content of Ecosystem Respiration Is Linked to Precipitation and Vapor Pressure Deficit.” *Oecologia* 131(1):113–24.

Bruynesteyn, K. et al. 2005. “Deciding on Progression of Joint Damage in Paired Films of Individual Patients: Smallest Detectable Difference or Change.” *Annals of the Rheumatic Diseases* 64(2):179–82.

Campoe, Otavio C. et al. 2012. “Stand-Level Patterns of Carbon Fluxes and Partitioning in a Eucalyptus Grandis Plantation across a Gradient of Productivity, in Sao Paulo State, Brazil.” *Tree Physiology* 32(6):696–706.

Chen, Yujuan et al. 2013. “Changes in Soil Carbon Pools and Microbial Biomass from Urban Land Development and Subsequent Post-Development Soil Rehabilitation.” *Soil Biology and Biochemistry* 66:38–44.

Chen, Yujuan et al. 2014. “Influence of Urban Land Development and Soil Rehabilitation on Soil–atmosphere Greenhouse Gas Fluxes.” *Geoderma* 226–227:348–53.

Cueva, Alejandro et al. 2017. “Potential Bias of Daily Soil CO_2 Efflux Estimates due to Sampling Time.” *Scientific Reports* 7(1):11925.

Curiel Yuste, J., I. A. Janssens, A. Carrara, and R. Ceulemans. 2004. “Annual Q10 of Soil Respiration Reflects Plant Phenological Patterns as Well as Temperature Sensitivity.” *Global Change Biology* 10(2):161–69.

Davidson, E. A., K. Savage, L. V. Verchot, and R. Navarro. 2002. “Minimising Artifacts and Biases in 20 Chamber-Based Measurements of Soil Respiration.” *Agriculture and Ecosystems Meteorology* 113(1):21–37.

Davidson, Eric. A., Elizabeth Belk, and Richard D. Boone. 1998. “Soil Water Content and Temperature as Independent or Confounded Factors Controlling Soil Respiration in a Temperate Mixed Hardwood Forest.” *Global Change Biology* 4(2):217–27.

Davidson, Eric A. et al. 2000. “Effects of Soil Water Content on Soil Respiration in Forests and Cattle Pastures of Eastern Amazonia.” *Biogeochemistry* 48(1):53–69.

Delogu, Emilie et al. 2017. “Improved Methodology to Quantify the Temperature Sensitivity of the Soil Heterotrophic Respiration in Croplands.” *Geoderma* 296:18–29.

Dore, Sabina, Danny L. Fry, and Scott L. Stephens. 2014. “Spatial Heterogeneity of Soil CO_2 Efflux after Harvest and Prescribed Fire in a California Mixed Conifer Forest.” *Forest Ecology and Management* 319:150–60.

Ekblad, A. and P. Högberg. 2001. “Natural Abundance of 13C in CO_2 Respired from Forest Soils Reveals Speed of Link between Tree Photosynthesis and Root Respiration.” *Oecologia* 127(3):305–8.

Gehrig-Fasel, Jacqueline, Antoine Guisan, and Niklaus E. Zimmermann. 2008. “Evaluating Thermal Treeline Indicators Based on Air and Soil Temperature Using an Air-to-Soil Temperature Transfer Model.” *Ecological Modelling* 213(3):345–55.

Goulden, M. L. et al. 1998. “Sensitivity of Boreal Forest Carbon Balance to Soil Thaw.” *Science* 279(5348), 214–217.

Goulden, Michael L. et al. 1996. “Measurements of Carbon Sequestration by Long-Term Eddy Covariance: Methods and a Critical Evaluation of Accuracy.” *Global Change Biology* 2(3):169–82.

Griffis, T. J. et al. 2004. “Seasonal Variation and Partitioning of Ecosystem Respiration in a Southern Boreal Aspen Forest.” *Agricultural and Forest Meteorology* 125(3):207–23.

Hogberg, P. et al. 2001. “Large-Scale Forest Girdling Shows That Current Photosynthesis Drives Soil Respiration.” *Nature* 411(6839):789–92.

Kicklighter, David W. et al. 1994. “Aspects of Spatial and Temporal Aggregation in Estimatingregional Carbon Dioxide Fluxes from Temperate Forest Soils.” *Journal of Geophysycal Research* 99(93):1303–15.

Kottek, Markus, Jürgen Grieser, Christoph Beck, Bruno Rudolf, and Franz Rubel. 2006. “World Map of the Köppen-Geiger Climate Classification Updated.” Meteorologische Zeitschrift 15(3):259–63.

Kutsch, Werner L. and Ludger Kappen. 1997. “Aspects of Carbon and Nitrogen Cycling in Soils of the Bornh ¨ Oved Lake District II. Modelling the Influence of Temperature Increase on Soil Respiration and Organic Carbon Content in Arable Soils under Different Managements.” *Biogeochemistry* 39(2):207–24.

Larionova, A. A., L. N. Rozonova, and T. I. Samoylov. 1989. “Dynamics of Gas Exchange in the Profile of a Gray Forest Soil.” *Soviet Soil Science (USA).*

Lee, Xuhui, Huiju Wu, Jeffrey Sigler, Christopher Oishi, and Thomas Siccama. 2004. “Rapid and Transient Response of Soil Respiration to Rain.” *Global Change Biology* 10(6):1017–26.

Li, Mingfeng and Yunshe Dong. 2003. “The Analysis of Diurnal Variation of CO_2 Flux in Leymus Chinensis Grassland of Xilin River.” *Grassland of China* 25(3):9–14.

Liu, Q. et al. 2006. “Temperature-Independent Diel Variation in Soil Respiration Observed from a Temperate Deciduous Forest.” *Global Change Biology* 12(11):2136–45.

Loveland, T. R. et al. 2000. “Development of a Global Land Cover Characteristics Database and IGBP DISCover from 1 Km AVHRR Data.” *International Journal of Remote Sensing* 21(6-7):1303–30.

Luo, Yiqi and Xuhui Zhou. 2006. *Soil Respiration and the Environment*. San Diego, California, Elsevier Academic Press.

Mackiewicz, Michael C. 2012. “A New Approach to Quantifying Soil Temperature Responses to Changing Air Temperature and Snow Cover.” *Polar Science* 6(3–4):226–36.

Matteucci, Marco, Carsten Gruening, Ignacio Goded Ballarin, Guenther Seufert, and Alessandro Cescatti. 2015. “Components, Drivers and Temporal Dynamics of Ecosystem Respiration in a Mediterranean Pine Forest.” *Soil Biology and Biochemistry* 88:224–35.

Medina, Ernesto and Manuelita Zelwer. 1972. *Soil Respiration in Tropical Plant Communities.”* Tropical Ecology with an Emphasis on Organic Production. Athens, GA: University of Georgia 245–69.

Nakadai, Toshie, Masayuki Yokozawa, Hiroaki Ikeda, and Hiroshi Koizumi. 2002. “Diurnal Changes of Carbon Dioxide Flux from Bare Soil in Agricultural Field in Japan.” *Applied Soil Ecology* 19(2):161–71.

Nepstad, Daniel C. et al. 1994. “The Role of Deep Roots in the Hydrological and Carbon Cycles of Amazonian Forests and Pastures.” *Nature* 372(6507):666–69.

Parkin, T. B. and T. C. Kaspar. 2004. “Temporal Variability of Soil Carbon Dioxide Flux. Effect of Sampling Frequency on Cumulative Carbon Loss Estimation.” *Soil Science Society of the America Journal* 68(4):1234–41.

R Core Team. 2014. *R: A Language and Environment for Statistical Computing. R Foundation for Statistical Computing*. Vienna, Austria.

Raich, James W. and Christopher S. Potter. 1995. “Global Patterns of Carbon Dioxide Emissions from Soils.” *Global Biogeochemical Cycles* 9(1):23–36.

Rambal, S., R. Joffre, J. M. Ourcival, J. Cavender-Bares, and A. Rocheteau. 2004. “The Growth Respiration Component in Eddy CO_2 Flux from a Quercus Ilex Mediterranean Forest.” *Global Change Biology* 10(9):1460–69.

Riveros-Iregui, Diego A. et al. 2007. “Diurnal Hysteresis between Soil CO_2 and Soil Temperature Is Controlled by Soil Water Content.” *Geophysical Research Letters* 34(17):L17404.

Rixon, A. J. 1968. “Oxygen Uptake and Nitrification at Various Moisture Levels by Soils and Mats from Irrigated Pastures.” *European Journal of Soil Science* 19(1):56–66.

Rochette, P., R. L. Desjardins, and E. Pattey. 1991. “Spatial and Temporal Variability of Soil Respiration in Agricultural Fields.” *Canadian Journal of Soil Science* 71(2):189–96.

Saiz, Gustavo et al. 2006. “Stand Age-Related Effects on Soil Respiration in a First Rotation Sitka Spruce Chronosequence in Central Ireland.pdf.” *Global Change Biology* 12(6):1007–20.

Savage, K., E. A. Davidson, and A. D. Richardson. 2008. “A Conceptual and Practical Approach to Data Quality and Analysis Procedures for High-Frequency Soil Respiration Measurements.” *Functional Ecology* 22(6):1000–1007.

Savage, Kathleen E. and Eric A. Davidson. 2003. “A Comparison of Manual and Automated Systems for Soil CO_2 Flux Measurements: Trade-Offs between Spatial and Temporal Resolution.” *Journal of Experimental Botany* 54(384):891–99.

Shen, ZhenXi, YunLong Li, and Gang Fu. 2015. “Response of Soil Respiration to Short-Term Experimental Warming and Precipitation Pulses over the Growing Season in an Alpine Meadow on the Northern Tibet.” *Applied Soil Ecology* 90(June 2013):35–40.

Sheng, Hao et al. 2010. “The Dynamic Response of Soil Respiration to Land-Use Changes in Subtropical China.” *Global Change Biology* 16(3):1107–21.

Tang, Jianwu and Dennis D. Baldocchi. 2005. “Spatial–temporal Variation in Soil Respiration in an Oak–grass Savanna Ecosystem in California and Its Partitioning into Autotrophic and Heterotrophic Components.” *Biogeochemistry* 73(1):183–207.

Tang, Jianwu, Dennis D. Baldocchi, and Liukang Xu. 2005. “Tree Photosynthesis Modulates Soil Respiration on a Diurnal Timescale.” *Global Change Biology* 11(8):1298–1304.

Tedeschi, Vanessa et al. 2006. “Soil Respiration in a Mediterranean Oak Forest at Different Developmental Stages after Coppicing.” *Global Change Biology* 12(1):110–21.

Thomas, Stephen M., Freeman J. Cook, David Whitehead, and John A. Adams. 2000. “Seasonal Soil-Surface Carbon Fluxes from the Root Systems of Young Pinus Radiata Trees Growing at Ambient and Elevated CO_2 Concentration.” *Global Change Biology* 6(4):393–406.

Valentini, R. et al. 2000. “Respiration as the Main Determinant of Carbon Balance in European Forests.” *Nature* 404(6780):861–65.

Wan, Shiqiang, Dafeng Hui, Linda Wallace, and Yiqi Luo. 2005. “Direct and Indirect Effects of Experimental Warming on Ecosystem Carbon Processes in a Tallgrass Prairie.” *Global Biogeochemical Cycles* 19(2):1–13.

Wan, Shiqiang and Yiqi Luo. 2003. “Substrate Regulation of Soil Respiration in a Tallgrass Prairie: Results of a Clipping and Shading Experiment.” *Global Biogeochemical Cycles* 17(2):1054.

Wang, Wei, Kenji Ohse, Jianjun Liu, Wenhong Mo, and Takehisa Oikawa. 2005. “Contribution of Root Respiration to Soil Respiration in a C 3 / C 4 Mixed Grassland.” *India Academy of Sciences* 30(4):507–14.

Wohlfahrt, Georg et al. 2005. “Quantifying Nighttime Ecosystem Respiration of a Meadow Using Eddy Covariance, Chambers and Modelling.” *Agricultural and Forest Meteorology* 128(3–4):141–62.

Xu, Ming and Ye Qi. 2001. “Soil Surface CO_2 Efflux and Its Spatial and Temporal Variations in a Young Ponderosa Pine Plantation in Northern California.” *Global Change Biology* 7:667–77.

Zhang, Gexiang. 2011. “The Variations of Soil Respiration and Microbial Biomass Carbon at the Different Vegetation Types of Urban Green Spaces.” PhD Dissertation, Nanjing forestry University.

CHAPTER 2. Air temperature and precipitation as surrogates of soil temperature and soil water content: implications for global soil respiration modeling

ABSTRACT

Soil respiration (Rs) is a major flux in the global carbon cycle, which is strongly influenced by temperature and moisture. Because of lack of data, current approaches to global Rs modeling use air temperature (Ta) and monthly precipitation (Pm) as surrogates for soil temperature (Ts) and soil water content (SWC). Despite their common use, accuracy of Ta and Pm as surrogates across varying climate regions has not been tested. Here, we used 13482 Rs measurements from a monthly global Rs database and climate data from Fluxnet to characterize the relationships between (1) Ta and Ts, (2) Pm and SWC, and (3) Rs and Ta, Ts, Pm and SWC. Results indicated that Ta and Ts are highly correlated, explaining similar amounts of Rs variation; however, the Rs response to Ta is less sensitive than Rs response to Ts. Pm, however, was a uniformly poor indicator of SWC. To test for a better predictor for Rs, we evaluated several alternative measurements of precipitation (annual precipitation, mean annual precipitation between 1961 and 2014, average monthly precipitation and previous month's precipitation) and found that (1) average monthly precipitation is the best single parameter, and (2) average monthly precipitation plus previous month's precipitation are the best combined factors to predict Rs and resolve the "Zero precipitation, zero respiration" problem because the average is never zero. This study highlights the heterogeneity of relationships between Ts and Ta, Rs and temperature, Pm, and SWC in different climate regions. The modified Rs model helps improve the accuracy of Rs simulation, thus helping to evaluate future soil carbon dynamics under global climate change in the future.

2.1 INTRODUCTION

Global soil respiration (Rs, sometimes called belowground respiration or soil CO_2 efflux) plays a critical role in regulating atmospheric CO_2 concentration and climate dynamics in the earth system. Rs is estimated to range from 68 to 98 Pg C yr^{-1} (Raich, Potter, and Bhagawati, 2002; Raich and Potter, 1995; Bond-Lamberty and Thomson, 2010), making it the second largest flux in the global terrestrial carbon cycle, after gross primary productivity (GPP), which ranges from 97 to 153.48 Pg C yr^{-1} (Schimel et al. 2001; Yebra et al. 2015; Zhao and Running 2010). As a part of the carbon cycle, Rs is related to multiple environmental conditions, including temperature and moisture (Luo and Zhou 2006). At the site scale, soil temperature (Ts) and soil water content (SWC refers to volumetric soil water content in this paper) are key factors that control Rs, because they influence the rate of evaporation, the rates of chemical and biological processes (Davidson et al. 1998; Fang et al. 1998; Jensen et al. 1996; Luo and Zhou 2006), and microbial activities occurring in the soil (Awe, Reichert, and Wendroth 2015; Gehrig-Fasel et al. 2008; Mackiewicz 2012; Yazaki et al. 2013). At the global scale, however, there are insufficient long-term, high-frequency Ts and SWC data available to support Rs modeling. Thus, global climate-based Rs models used air temperature (Ta) and precipitation as Rs predictors to explore how Rs will react to global climate change (Ben Bond-Lamberty and Thomson 2010; Chen et al. 2010; Raich and Potter 1995; Raich et al. 2002; Raich and Schlesinger 1992; Wang, Chen, and Wang 2010; Wang and Fang 2009). These surrogates are assumed to be closely related to the parameters they replace, yet to date no studies have examined the nature of these relationships by eco-region.

Many studies have used empirical models that estimate Ts based on Ta and other factors (Kang, Kim, and Lee 2000; Mariko et al. 2000; Thunholm 1990; Zhang, Chen, and Cihlar 2003;

Zheng, Hunt, and Running 1993). Using data from six climates across the United States, Zheng *et al.*, (1993) found that daily Ta and precipitation can explain 85% to 96% daily Ts variation. In Switzerland, a study showed that daily Ts at the treeline can be accurately simulated from Ta using a soil-to-air transfer model (Gehrig-Fasel et al. 2008). Another study demonstrated that annual mean, seasonal, and monthly Ts can be simulated based on only Ta with reasonable accuracy by a simple linear model (Toy, Kuhaida, and Munson 1978). Using a physically based numerical model, Thunholm (1990) found soil surface temperature can be estimated from the Ta and the soil surface energy balance. The close relationship between Ts and Ta indicates that Ta could be a good surrogate for Ts in soil respiration modeling, at least in site scale and at shorter time-scales. However, researchers have also found that the very strong relationship between Ts and Ta observed at the site scale usually becomes weak at watershed, continental, or global scales (Kang et al. 2000; Liang et al. 2014). For instance, at the watershed scale, a number of environmental conditions, including surface global radiation, albedo of surface, water content and soil texture, elevation, slope and aspect, leaf area index (LAI) and ground litter stores, in addition to Ta, were related to Ts variation (Kang et al. 2000; Liang et al. 2014).

Other factors, such as the presence of snowpack, significantly affects the co-variation of Ts with Ta during the winter (Wang et al. 2006; Rango and Martinec 1995; Mariko et al. 2000; Brooks et al. 2005). A process-based model demonstrated that, at the ecosystem scale, the integrated climate conditions, vegetation and ground features, and hydrological conditions used to simulate permafrost thermal regimes in Canada, better explained Ts variability rather than by Ta alone (Zhang et al. 2003). Another study found that two-meter-deep snowpack interrupted gas emissions, while a snowpack of less than a one-meter acted as a thermal insulator (Mariko et al. 2000). A study of four Greenland sites demonstrated that under the snowpack, the Ts only

changed by 0.12 to 0.23 ℃ in response to a 1 ℃ change in Ta (Mackiewicz 2012). A study from Japan revealed that differences between Ta and Ts positively related to the cumulative freezing degree-days (Yazaki et al. 2013). Current use of Ta as a surrogate for Ts neglects effects of biotic and abiotic factors on Rs, while lack of agreement suggests that when using Ta as surrogate for Ts, other biotic or abiotic factors should be considered.

SWC is another key property that controls belowground ecological and biogeochemical processes and affects terrestrial carbon budgets. Climate conditions, such as Ta and precipitation, are factors that cause variation in SWC (Holsten et al. 2009). Previous studies found that SWC at the regional scales is strongly coupled with precipitation, and feedback between precipitation and SWC is predominantly positive (Hohenegger et al. 2009; Koster et al. 2004). Due to the limited availability of high-resolution and long-term SWC data, Rs studies have heavily relied on SWC simulations from indirect measurements such as precipitation. Many land surface models simulate SWC based on climate and soil properties inputs (Hongxiang Yan 2016; Sun et al. 2016). However, many studies found that variation of SWC is a complex result of multiple climatic factors and their interactions; no single factor can fully explain SWC variation (Gaur and Mohanty 2013; Holsten et al. 2009; Wohl et al. 2012). For instance, *Sterling et al.* (2012) and *Yang et al.* (2012) found that land cover is the most important factor influence SWC. Several other studies reported that the relationships between SWC and precipitation varies with land cover conditions (Haddeland et al. 2014; Li et al. 2009). A study in the Poyang Lake Basin demonstrated that SWC responds positively with precipitation, but responds negatively to Ta change, and that Ta explained more SWC variation than did precipitation (Feng and Liu 2015). Although using precipitation as proxy of SWC in the global scale Rs modeling causes substantial uncertainty, no studies have investigated the validity of the proxy. It is thus very important to

analyze whether air temperature and monthly precipitation are good surrogates of soil temperature and soil water content in global Rs modeling.

In global Rs modeling, a hyperbolic precipitation function has been widely used to describe relationships between precipitation and Rs (Hashimoto et al., 2015 ; Raich and Potter, 1995; Raich et al., 2002). A common problem when using the hyperbolic function to explain how Rs responds to monthly precipitation is the "zero precipitation, zero respiration" problem. To resolve this issue, Reichstein *et al.* (2003) introduced a constant variable P_0 to the hyperbolic precipitation component in the Rs model. However, this variable introduces another constant parameter, which causes the loss of a degree of freedom of the model, a serious problem when the sample size is small. Another modified model by Hashimoto et al. (2015) introduced precipitation from the previous month (P_{m-1}) to represent P_0 to resolve the "zero precipitation, zero respiration" problem. However, this approach cannot totally resolve the problem because some places could have multiple continuous months without precipitation (especially at arid regions). In this situation, Rs will be estimated to be zero by the model developed by Hashimoto et al. (2015) because both Pm and P_{m-1} are zero. Under global climate change, extreme weather, including persistent drought, may become more frequent in the future (Dai 2011), and thus it is important to improve our ability to predict Rs in the conditions when there is no precipitation.

Global scale high-frequency, high-resolution Ts and SWC data are still not available. As a result, Ta and precipitation data are used to explain Rs spatial and temporal variance (Ben Bond-Lamberty and Thomson 2010; Hashimoto et al. 2015; Raich and Schlesinger 1992; Reichstein et al. 2003). Ta and precipitation will keep playing a key role in future soil carbon dynamics research, as well as determine how soil carbon responds to global warming. Thus, it is important to test whether Ta and precipitation are good surrogates of Ts and SWC in Rs models.

The objective of this research was to test whether Ta and precipitation perform as well as Ts and SWC globally and in each climate region. We also tested whether other precipitation parameters better predict Rs, especially for extreme weather conditions, such as no precipitation within a month, and whether snowpack plays an important role on Ta versus Ts relationship and thus further affects Rs modeling when using Ta as surrogate of Ts.

2.2 METHODS AND MATERIALS

2.2.1 Data sources and processing

Monthly time-scale Rs and related ancillary factors were obtained from a monthly global Rs database (MGRsD, Figure 2-1). The details about MGRsD can be found in (https://data.lib.vt.edu/collections/ns0646000). In MGRsD, there are 9962 measurements out of 13482 that have Rs, Ts and Ta measurements. Daily Ts, Ta, and precipitation data for calculating the snowpack were collected from a global network of micrometeorological flux measurement sites (Fluxnet,147 sites, Figure 2-1) (Baldocchi et al. 2001). The initial measurement interval of Fluxnet data is half an hour. Fluxnet data contains multiple missing data values, which were first checked and handled before analysis. To avoid the bias of missing values, we filtered and excluded records with less than 43 records within a day, or less than 25 records within a month. In other words, we excluded a day with more than five missing records or a month with more than five days missing data.

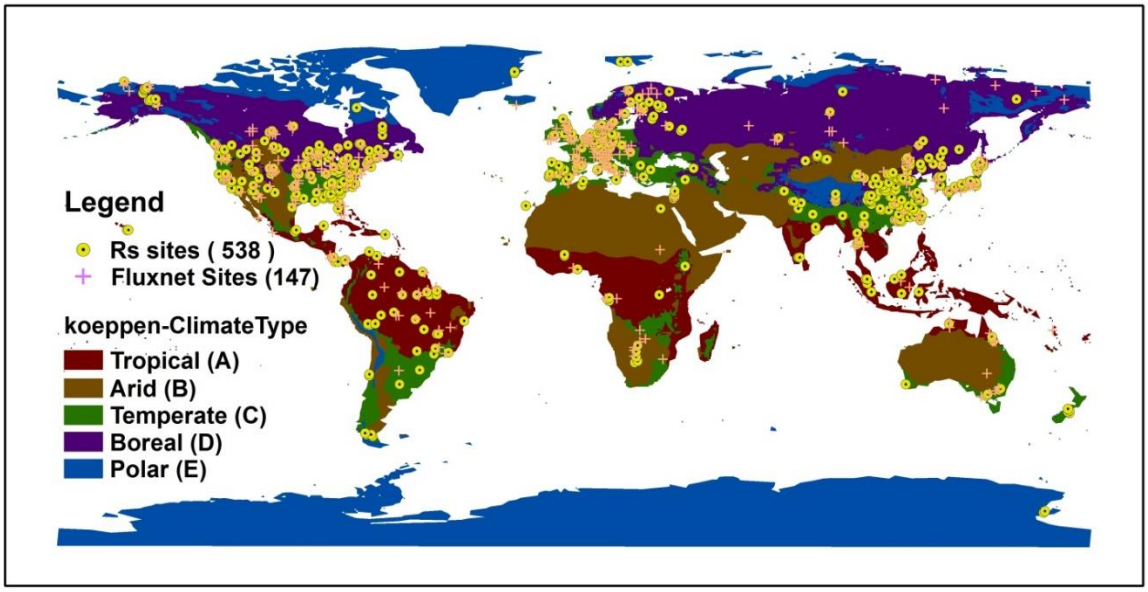

Figure 2-1. The sites of the global monthly soil respiration database (MGRsD) dispersed in five climate regions (based on Köppen Geiger classification), including tropical (A), arid (B), temperate (C), boreal (D) and polar (E) regions. Rs sites indicate 538 sites collected from 724 publications. Fluxnet sites are 147 sites from Fluxnet, daily air temperature, and precipitation data were collected from these sites.

2.2.2 Snowpack calculation

Publications from the MGRsD reported soil temperature at different soil depth, many publications does not reported soil temperature; moreover, most of publications from the MGRsD do not report snowpack information. We thus cannot analyze the relationship between soil temperature and air temperature as well as how the relationship affected by the existing of snowpack. We thus used the soil temperature and air temperature data from the global Fluxnet. The snowmelt Runoff Model (SRM) was used to estimate daily snowpack for all 147 Fluxnet sites based on Ta, precipitation, and vegetation types (Martinec, Rango, and Roberts 2008; Rango and Martinec 1995). Snowpack for each site was calculated with the precipitation and Ta data based on the following principles:

1) To avoid the bias caused by missing values, the whole year's data was discarded if the number of either Ta records or precipitation records was less than 350 days.

2) The data of the initial 244 days before winter of the first given year were excluded from the calculation. Additionally, the initial amount of the snowpack on day 245 was set as zero, assuming snowpack melted during the summer of the first year.
3) The amount of the snowfall on each day was defined as the amount of precipitation when Ta was below 0°C. The snowpack was set as zero when Ta was above 0°C.
4) The amount of the snowmelt was calculated based on the degree melt method when the Ta was above 0°C. The amount of the snowmelt was set as zero when Ta was below 0°C (Martinec et al. 2008; Rango and Martinec 1995).
5) The amount of the snowpack on day *k* was calculated by equation (2-1):

$$Snowpack_k = Snowfall_k - Snowmelt_k + Snowpack_{k-1} \quad (2\text{-}1)$$

where $Snowpack_k$ stands for snowpack on a specific day, $Snowfall_k$ stands for snowfall amount on a specific day, $Snowmelt_k$ stands for snowmelt amount on a specific day, and $Snowpack_{k-1}$ stands for snowpack from the previous day. After snowpack were calculated, Ts, Ta, and snowpack data were aggregated to monthly time-scale before analysis.

2.2.3 Rs response to temperature, precipitation, and soil water content

To characterize the nature of the Ta to Ts relationship, we used simple linear regression (SLR) and piecewise regression to analyze the relationship between Ts and Ta for different climate types. To identify whether snowpack affect the relationship between Ta and Ts, we compared two regression models, with and without snow. Within a specific climate region, we hypothesized that snowpack explains the presence of breakpoint, if the regression below the breakpoint coincided with the regression for data snow present, and if the piecewise regression above the breakpoint coincided with the regression for data with no snow. By using data from

Fluxnet, regression analysis was used to describe relationships between monthly average SWC and monthly precipitation, and the relationship between Rs and precipitation across different climate regions. An α-level of 0.05 was used for determining statistical significance.

To explore how Rs responds to temperature, we evaluated multiple function forms, including Rs not transformed, square root transformed, log transformed, non-curve fitting (linear), and curve fitting (quadratic). Log transformed Rs with curve fitting function was selected because it was the best model for all climate regions (Equation 2-2, where T is Ta or Ts). This equation was applied to test whether Rs response differed between Ta and Ts.

$$Log\ (Rs) = \beta_0 + \beta_1 T + \beta_2 T^2 \qquad (2\text{-}2)$$

Within each climate region, we compared the intercept (β_0) of Ta model with intercept of Ts model to evaluate whether the magnitude of Rs when Ta equals zero differed from the magnitude of Rs when Ts equals zero. We compared the β_1 and β_2 values of Ta function with β_1 and β_2 values of Ts function to evaluate whether the sensitivity of Rs response to Ta differed from Rs response to Ts.

Moreover, there is a potential "zero precipitation, zero respiration" problem when using monthly precipitation to predict Rs (Raich and Potter 1995; Raich et al. 2002; Reichstein et al. 2003). Therefore, we tested whether other precipitation-related factors could explain more Rs variability, including mean annual precipitation (MAP) from 1961 to 2014, annual precipitation (P_{Annual}), average monthly precipitation from 1961 to 2014 (AP_m) and precipitation from the previous month (P_{m-1}). By using a best subset analysis approach (Minitab, version 17), we compared all possible regression models. Goodness of fit was assessed by comparing R^2_{adj} and Mallows Cp values. The Mallows Cp value compares the precision and bias of the full model to

models with a subset of the predictors. We chose models where Mallows' Cp was small and closer to the number of predictors plus the constant in the model.

2.2.4 Soil respiration models

An exponential relationship was widely used to explain how Rs responds to temperature, and a hyperbolic exponential function was widely used to describe how Rs responds to precipitation in previous global Rs modeling (Hashimoto et al. 2015; Raich and Potter 1995). To examine how Rs responds to Ta and precipitation in this study, a base model was developed based on Raich and Potter (1995) and Hashimoto *et al.* (2015). The base model has a potential "zero precipitation, zero respiration" problem. Therefore, we developed a modified model which replaced monthly precipitation with the average monthly precipitation and precipitation from the previous month. We compared the modified model with base model to test whether the "zero precipitation, zero respiration" problem could be resolved, and whether other precipitation factors better explain Rs variability. We used a second-order exponential model to describe how Rs responds to temperature as it better explain how Rs responds to temperature change in the monthly global Rs data (Jian et al. in prep). We used the same Ta function in both the base model and the modified model for better evaluating whether the modified precipitation component in the model helps resolve the "zero precipitation, zero respiration" problem.

$$Rs = F \times e^{(Q \times \mathrm{Ta} - a \times \mathrm{Ta}^2)} \times \frac{p_m}{k + p_m} \qquad \text{(base model)}$$

$$Rs = F \times e^{(Q \times \mathrm{Ta} - a \times \mathrm{Ta}^2)} \times \frac{AP_m + P_{(m-1)}}{k + AP_m + P_{(m-1)}} \qquad \text{(modified model)}$$

In both base model and modified model, Rs is monthly average Rs rate (g C m^{-2} day^{-1}); Ta denotes monthly Ta; Pm is monthly precipitation; P_{m-1} is previous month's precipitation; AP_m

is average monthly precipitation from 1961 to 2014. *F*, *Q*, *a* and *k* are constant parameters. The $e^{(Q\times Ta - a\times Ta^2)}$ describes a second order exponential growth of Rs on Ta, in which the term (-a $\times T_a^2$) allows for a threshold where Rs increases with Ta when below the threshold, but decreases when above the threshold (when $a > 0$).

To determine whether Rs responds to Ta differently from how Rs responds to Ts, we calculated the temperature sensitivity of Rs (Q_{10}) of every site in MGRsD (538 sites in total) based on both Ta and Ts. We used first order exponential rather than second order exponential model to quantify Q_{10} value for each site for two reasons: first, at most sites, we did not detected significant curve fitting. Second, Q_{10} value varies with temperature under second order exponential model, making Q_{10} values in different site do not comparable. We parameterized the first order exponential function [$Rs = F \times e^{(Q\times Ta)}$] based on the Rs, Ts, and Ta data in each site. If the p value for Q > 0.05 in the first-order exponential model, Q_{10} values of those sites will not be used. To ensure accuracy, we only calculated Q_{10} values for sites which had more than 12 Rs measurements. When Q values in all sites were parameterized, Q_{10} values could be calculated based on equation (2-3).

$$Q_{10} = \frac{\exp(Q\times(T+10))}{\exp(Q\times T)} \qquad (2\text{-}3)$$

Where T stands for air temperature or soil temperature. For each climate region, we resampled the median of Q_{10} 10,000 times and used a paired t-test to identify whether Q_{10} based on Ta significantly differed from Q_{10} based on Ts.

To test whether the modified model better predicts Rs, especially for the months with no precipitation, we randomly separated the MGRsD into 2 subsets, one to build the model (subset 1, contained 70% of data from MGRsD, 9437 records), and another for testing the model

performance (subset 2, contained 30% of data from MGRsD, 4045 records). The average squared prediction error (MSE_t, a smaller MSE_t value indicates a better model) of the base model and the modified model were calculated based on the test dataset to evaluate the model performance. Where n_t was the number of observations in the testing dataset, MSE_t can be calculated based on formula (2-4):

$$MSE_t = \frac{1}{n_t}\sum_{i=1}^{n_t}(y_i - \hat{y}_i)^2 \qquad (2\text{-}4)$$

The nonlinear (weighted) least-squares estimates approach (nls function) was used in R, version 3.1.1 (R Core Team, 2014) to estimate the parameters and calculate the R^2, MSE, and AIC values. The maximum number of iterations was set to 50, the parameterization results were listed in Table 2-2, and the "segmented" package was used to execute the piecewise regression.

2.3 RESULTS

2.3.1 Air temperature as a surrogate of soil temperature

Ta is a good surrogate of Ts in global and regional Rs modeling as Ta highly correlated with Ts in all regions (R^2 range from 84% to 94%, Figure 2-2) except tropical (R^2 = 36%, Figure 2-2). Likewise, Ta almost explained the same amount of Rs variability as Ts (41.53% versus 41.87%, Table 2-1). However, the relationships between Ts and Ta were greatly affected by climate types. For tropical region, the Ta explained the least amount of Ts variability among the four climate types (Table 2-1, R^2 = 0.36 and Figure 2-2 panel b1). In the arid region, Ts was highly related with Ta (Figure 2-2 panel c1, R^2 = 0.94). However, for both tropical and arid, Ta and Ts explained limited Rs variation (5.35% and 15.0% for tropical, 18.01% and 8.74% for arid, Table 2-1 and Figure 2-2 panel c2), indicating that neither Ta nor Ts was a good predictor

of Rs in these two regions. Other factors such as soil properties, SWC, and leaf area index should be tested for better predicting Rs.

In temperate and boreal regions, Ts highly correlated with Ta; Ta and Ts explained similar amounts of Rs variation (34.44% and 37.35% for temperate, 60.32% and 58.95% for boreal, respectively, Table 2-1). The piecewise model was a better fit (R^2 = 84%, Figure 2-2 panel d1 and Table 2-1) for Ts versus Ta regression compared to the linear model (data not shown), with a significant breakpoint at Ta of 1.329 ℃ and 0.72 ℃ in temperate and boreal, respectively (Figure 2-2, left panels). To identify whether snowpack explained the transition in the relationship between air and soil temperature, we compared the piecewise relationship between Ts and Ta above and below the breakpoint with the individual linear regression models for data with and without snow. The results showed that within a specific region, the linear regression model for "no snow" data was closer to the piecewise model above the breakpoint, and the linear regression model for "snow" data was similar to the piecewise model under the breakpoint (Table 2-2). These results indicated that snowpack does affect the relationship between Rs and temperature (Table 2-2). Even though no significant breakpoint was detected between the relationship between Rs and temperature (both Ta and Ts), the presence of snowpack likely affected this relationship. The residual plot of simple linear regression of Rs versus Ta showed a clear trend (data not shown), with more residual above zero below the breakpoint, which indicated the linear regression without change point underestimated Rs when Ta below the breakpoint. In addition, Log(Rs) versus temperature (Ta or Ts) below 0.72 ℃ (the breakpoint for Ts vs. Ta regression) were significantly different from the relationship between Log(Rs) and temperature above 0.72 ℃ (Table 2-2). This indicated that seasonal snowpack affected Rs, and the effect of snowpack should take into account in global Rs modeling.

Although Ta and Ts explained the same amount of Rs variation, the nature of the Rs response to temperature (Ta and Ts) varied by climate types because of the non-linear relationship between Rs and temperature (p-value for quadratic term < 0.0001, Table 2-1 and Figure 2-2, middle panels). The parameters (β_0, β_1 and β_2) for Rs predicted by Ta significantly differ from the parameters predicted by Ts in all regions (Table 2-1). The Ta versus Rs regression models had a larger intercept (β_0, except tropical), likely due to the insulating effect of the snow cover.

The response of Rs to changes in Ts were described by the first derivative of equation 3 (Carey, Tang, Templer, Kroeger, Crowther, Burton, Dukes, Emmett, Frey, and Heskel 2016). The results showed that Rs was less sensitive to Ta compared to Ts (Figure 2-2, right panels). For both Ta and Ts, the sensitivity of Rs decreased as temperature increased, except for boreal (Figure 2-2 panel e3, black line). The Q_{10} values of all sites for Rs calculated based on Ta (Figure 2-3 panel a) and Ts (Figure 2-3 panel b) supported these results. The paired t test showed that Rs was more sensitive to Ts change than Ta change ($p < 0.05$, Figure 2-3 panel c). The mean (2.006) and median (1.83) of Q_{10} calculated based on Ta were smaller than the mean (2.325) and median (2.01) of Q_{10} calculated based on the Ts (Figure 2-3 panel a and b).

Table 2-1. Model parameters of soil respiration (log transformed, unit: g C m^{-2} day^{-1}) as a function of temperature (T, air temperature or soil temperature), evaluating air temperature as surrogate of soil temperature. Note that $p < 0.001$ for all parameters.

Model by region	Parameters for model: $\log(Rs) = \beta_0 + \beta_1 T + \beta_2 T^2$				
	$\beta_0 \pm SE$	$\beta_1 \pm SE$	$\beta_2 \pm SE$	n	R^2
All data					
Log(Rs) vs. Ta	-0.266 ± 0.012	0.077 ± 0.001	-8.5e-4 ± 5.1e-5	9962	41.53%
Log(Rs) vs. Ts	-0.61 ± 0.015	0.139 ± 0.002	-2.9e-3 ± 6.6e-5	9962	41.87%
Tropical					
Log(Rs) vs. Ta	-6.24 ± 1.58	0.58 ± 0.13	-0.01 ± 0.003	579	5.35%
Log(Rs) vs. Ts	-1.56 ± 0.54	0.25± 0.04	-0.005 ± 0.0007	579	15.0%
Arid					
Log(Rs) vs. Ta	-0.99 ± 0.15	0.08 ± 0.018	-0.001 ± 0.0006	361	18.01%
Log(Rs) vs. Ts	-0.98 ± 0.19	0.12 ± 0.02	-0.003 ± 0.0006	361	8.74%
Temperate					
Log(Rs) vs. Ta	-0.52 ± 0.02	0.12 ± 0.003	-0.002 ± 0.0001	6086	34.44%
Log(Rs) vs. Ts	-0.90 ± 0.03	0.17 ± 0.003	-0.004 ± 0.0001	6086	37.35%
Boreal & polar					
Log(Rs) vs. Ta	-0.28 ± 0.019	0.078 ± 0.001	0.0003 ± 0.00001	2936	60.32%
Log(Rs) vs. Ts	-0.54 ± 0.019	0.126 ± 0.003	-0.001 ± 0.0001	2936	58.95%

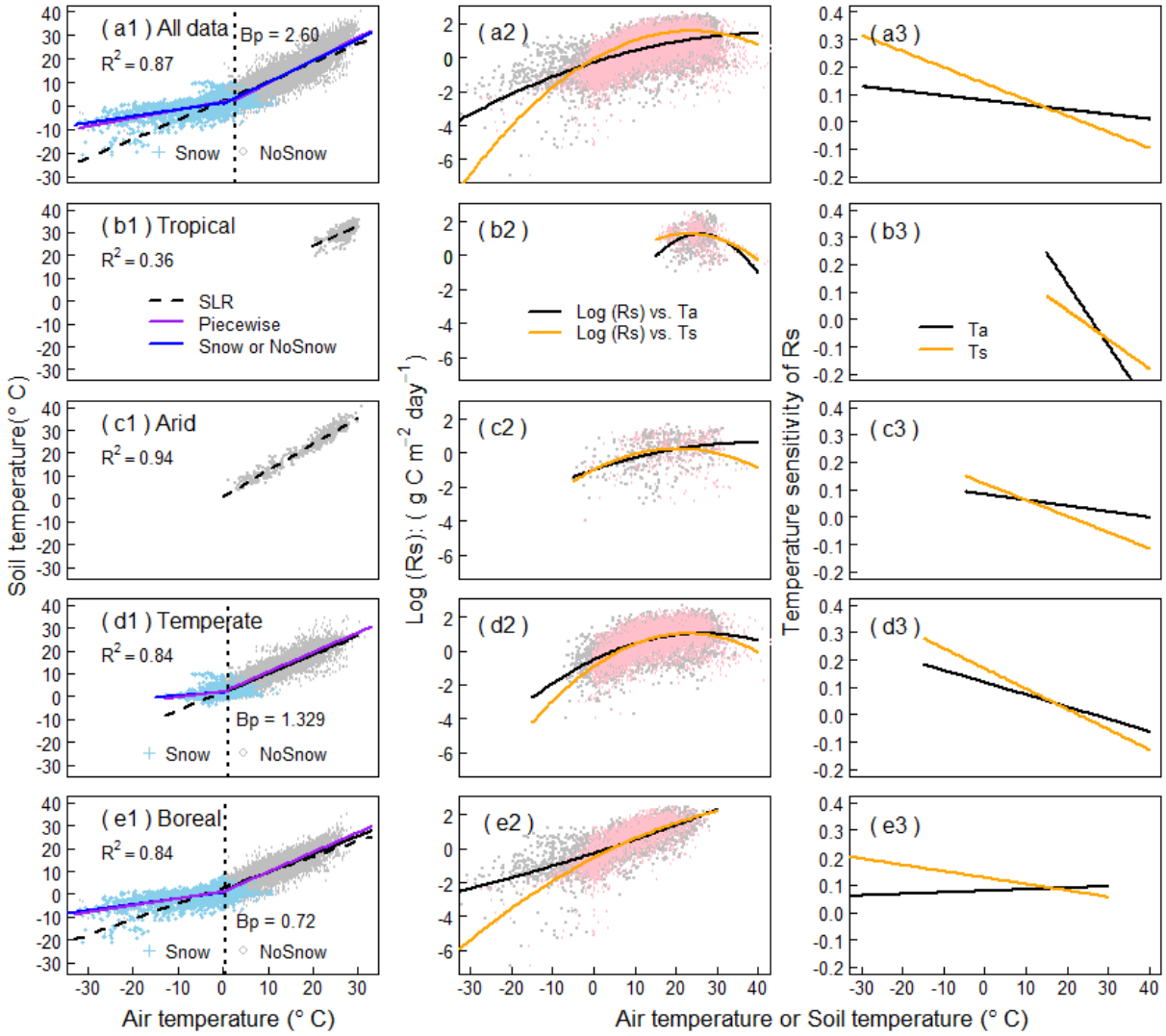

Figure 2-2. Relationship between air temperature (Ta) and soil temperature (Ts) (left panels); Rs response to Ta or Ts (middle panels); Temperature sensitivity of Rs as temperature increase (right panel). Left panel: the black dashed lines indicate simple linear trend. Piecewise regression was applied to identify the change point for Ts versus Ta regression (purple lines at panel a1, d1 and e1, piecewise regression was applied at all relationship at Figure 2-2, but only temperate and boreal regions tested a significant breakpoint) and a breakpoint was detected at 1.329 ℃ in temperate region and 0.72 ℃ at boreal region (vertical black dot lines). Solid blue lines (panel a1, d1 and e1) indicate specific regression trend for data with snow or without snow. Middle panel: Ta versus Rs (gray dots) and Ts versus Rs (pink dots) across different climates showed that Rs response to Ts differ from Rs response to Ta. Right panel: Temperature sensitivity of Rs for all data and in different region. Note that all R^2 values in left panel indicate how much Ts was explained by Ta under simple linear model (b1 and c1) and piecewise model (a1, d1 and e1).

Table 2-2. Model parameters of soil temperature (Ts) versus air temperature (Ta), soil respiration (log transformed, Log(Rs), unit: g C m^{-2} day^{-1}) versus Ta, and Log(Rs) versus Ts regression for data with snow, no snow, and piecewise regression. Note that $p < 0.001$ for all parameters, N/A means data not available.

Model by region	Parameters for model: $y = \beta_0 + \beta_1 x$								
	Ts ~ Ta regression			Log(Rs) ~ Ta regression			Log(Rs) ~ Ts regression		
	$\beta_0 \pm$ SE	$\beta_1 \pm$ SE	n	$\beta_0 \pm$ SE	$\beta_1 \pm$ SE	n	$\beta_0 \pm$ SE	$\beta_1 \pm$ SE	n
All data									
Snow	1.19 ± 0.036	0.28 ± 0.006	5436	N/A	N/A	N/A	N/A	N/A	N/A
Below breakpoint	1.69 ± 0.034	0.35 ± 0.006	35610	-0.47 ± 0.026	0.057 ± 0.004	1495	-0.78 ± 0.022	0.098 ± 0.005	1495
No snow	0.84 ± 0.033	0.92 ± 0.002	30174	N/A	N/A	N/A	N/A	N/A	N/A
Above breakpoint	1.69 ± 0.034	0.62 ± 0.007	35610	-0.55 ± 0.018	0.048 ± 0.001	8467	0.14 ± 0.018	0.036 ± 0.001	8467
Temperate									
Snow	1.72 ± 0.04	0.14 ± 0.014	2026	N/A	N/A	N/A	N/A	N/A	N/A
Below breakpoint	2.04 ± 0.06	0.25 ± 0.022	18829	-0.44 ± 0.045	0.099 ± 0.021	358	-0.15 ± 0.02	0.05 ± 0.001	358
No snow	1.46 ± 0.04	0.85 ± 0.003	16801	N/A	N/A	N/A	N/A	N/A	N/A
Above breakpoint	2.04 ± 0.06	0.62 ± 0.022	18829	-0.83 ± 0.059	0.11 ± 0.016	5728	-0.086 ± 0.02	0.045 ± 0.001	5728
Boreal									
Snow	0.65 ± 0.052	0.26 ± 0.007	3047	N/A	N/A	N/A	N/A	N/A	N/A
Below breakpoint	1.05 ± 0.064	0.30 ± 0.008	13648	-0.486 ± 0.048	0.05 ± 0.005	817	-0.22 ± 0.029	0.08 ± 0.002	817
No snow	1.64 ± 0.055	0.79 ± 0.004	10241	N/A	N/A	N/A	N/A	N/A	N/A
Above breakpoint	1.05 ± 0.064	0.56 ± 0.009	13648	-0.8 ± 0.03	0.096 ± 0.007	2936	-0.129 ± 0.029	0.081 ± 0.002	2936

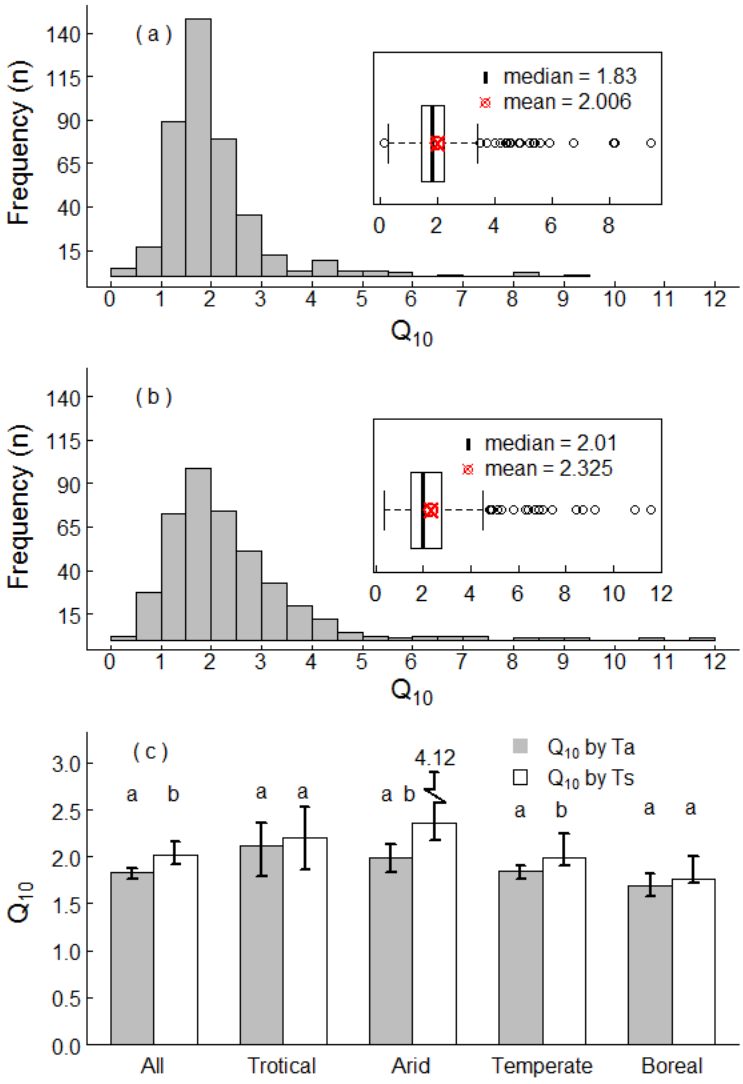

Figure 2-3. Q_{10} of 409 sites (those sites have more than 12 Rs measurements) calculated based on air temperature (a) and soil temperature (b). We resampled the mean Q_{10} value 10000 times for all data and data within different climate region, mean and 95% confidence interval (error bars) were calculated. Paired t test was used to test the difference between Q_{10} calculated based on Ta and calculated based on soil temperature across specific region, different letters in panel c mean significant difference.

2.3.2 Precipitation and soil water content

Precipitation was a very poor predictor of SWC for any of the climate types, where Rs was less strongly related to precipitation in warm climates than in cold climates (Figure 2-4). We detected very weak relationships between SWC and monthly precipitation in the temperate

and boreal climates, and no relationship in the tropical and dry climates. Unexpectedly, we also detected no relationship between Rs and SWC (statistics analysis not shown).

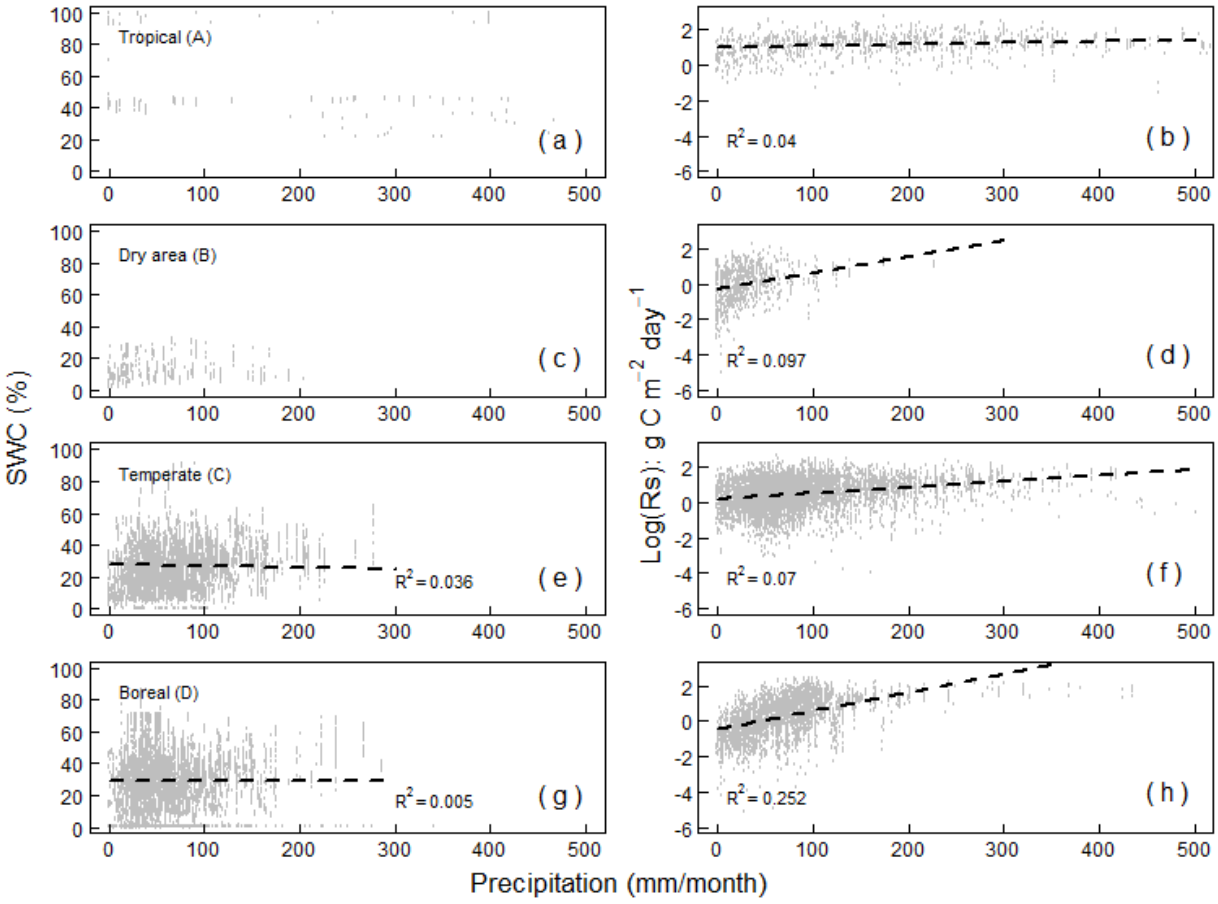

Figure 2-4. Simple linear regression showed that soil water content poorly related with monthly precipitation in all climate regions (left panel) ; however, monthly precipitation can explain certain amount of Rs variability, but Rs more closely related with monthly precipitation in cold region (panel h) than in tropical region (b), arid (d) and temperate (f).

Of the other precipitation factors we tested [mean annual precipitation (MAP), average monthly precipitation (APm) and previous month's precipitation (P_{m-1})], we found that Pm (R^2_{adj} = 10.5%, Mallows Cp = 496.9, Table 2-3) was not the best single predictor to explain Rs. Instead, APm was the best single predictor (R^2_{adj} = 13.4%, Mallows Cp = 38.3, Table 2-3). APm and P_{m-1} were the best combined variables to explain Rs, and adding other precipitation variables

did not increase (or slightly increase) the ability to explain Rs variability (Table 2-3). Replacing P_m by AP_m could resolve the "zero precipitation, zero soil respiration" problem since usually AP_m will never equal zero.

Table 2-3. Best subset analysis of precipitation factors versus Rs showed that average monthly precipitation from 1961 to 2014 (APm) was the best single predictor of respiration rather than monthly precipitation (Pm); APm and previous month's precipitation (P_{m-1}) significantly decrease the Mallows' Cp value of the model (Mallows' Cp is a statistic indicator which compares the full model to models with a subset of the predictors, usually, we look for models where Mallows' Cp is small and close to the number of predictors plus the constant in the model). While include mean annual precipitation (MAP) from 1961 to 2014 and annual precipitation (P_{Annual}) just slightly increase Adj R^2 value of the model.

No. of factors	$R^2_{(adj)}$	Mallows Cp	Pm	MAP	P_{Annual}	APm	P_{m-1}
1	13.4	38.3				x	
1	10.5	496.9	x				
2	13.6	11.7				x	x
2	13.5	27.9	x			x	
3	13.7	2.6	x			x	x
3	13.6	13.0		x		x	x
4	13.7	4.0	x	x		x	x
4	13.7	4.1	x		x	x	x
5	13.7	6.0	x	x	x	x	x

2.3.3 Global soil respiration modeling and validation

We parameterized both the base model and modified model based on subset 1, and the results showed that the modified model was a better fit with lower AIC and MSE values than the base model (Table 2-4). When the two models were tested with the remaining half of the data, the simple linear regression showed that the modified model explained more Rs variability than the base model as well (Figure 2-5). The modified model has the smaller MSE_t value which indicated that the modified model predicts Rs better than the base model (Figure 2-5). When compared to the base model, the modified model improved the overall performance (R^2=0.36 vs. R^2=0.32).

Table 2-4. Summary of model parameters (F, Q, a, k) and model validation results for the base model and the modified model. Comparing Akaike information criterion (AIC) and mean squared error (MSE) suggested that the modified model performs better than the base model in explaining the variation of Rs. Note that $p < 0.001$ for all parameters.

Term	F	Q	a	k	AIC	MSE
Base model	0.831±0.063	0.112±0.008	0.002±0.0002	4.468±0.745	34023	2.152
Modified model	0.933±0.07	0.112±0.008	0.002±0.0002	24.55±3.379	33557	2.048

To identify whether the "zero precipitation, zero soil respiration" problem was resolved by replacing P_m by AP_m, we separated the residuals of the base model and the modified model into two groups (Figure 2-5): monthly precipitation $\neq 0$ and monthly precipitation = 0. Results showed that the base model had a "zero precipitation, zero respiration" problem, where all residuals distributed above 0 when $P_m = 0$ (Figure 2-5 panel c). But this problem was resolved in the modified model (Figure 2-5 panel d), where residuals were distributed equally on both sides of 0 line when $P_m = 0$. Moreover, the modified model significantly improved the Rs simulation accuracy during months with no precipitation (Figure 2-5 panel c and d). The base model predicted no Rs whenever there was no precipitation. But the field-measured data from MGRsD showed that the mean Rs rate during months with no precipitation still maintain at a certain level (1.71 g C m^{-2} day^{-1}), even though it is lower than the mean Rs rate during the months with precipitation (2.27 g C m^{-2} day^{-1}). A plausible reason to explain this phenomenon is soil can still maintain a certain level of soil moisture even after a long-term drought (Luo and Zhou 2006). The modified model replaced the Pm factor by APm and P_{m-1}, where APm is the long-term (1961 to 2014) average of monthly precipitation; it removed the effect of accidental events (some months with no precipitation), thus better simulating the relationship between Rs and precipitation.

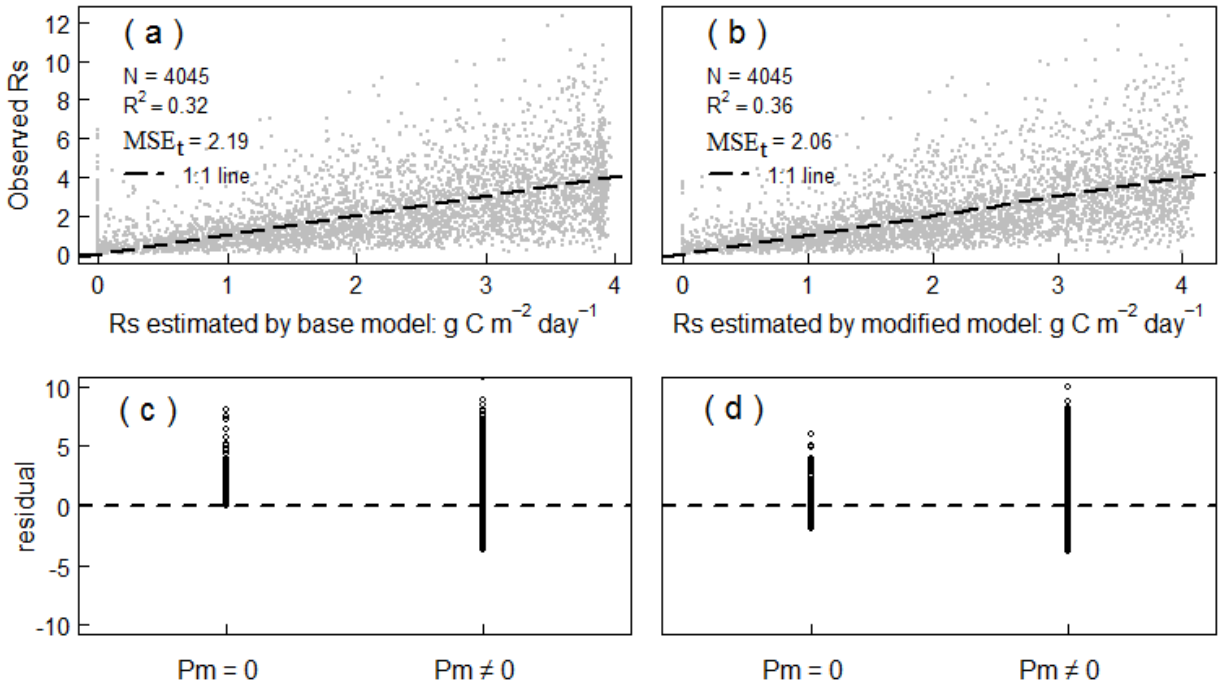

Figure 2-5. Simple linear regression of observed Rs versus estimated Rs indicates that the improved model better explains Rs variability (higher adj R^2 value at panel b than panel a); the modified model resolved the "zero precipitation, zero respiration" problem (panel d), which is a problem in the base model (panel c).

2.4 DISCUSSION

The results demonstrated that Ta explained almost the same amount of Rs variation as Ts. Precipitation, however, was not a good surrogate of SWC in all climate regions; however, replacing Pm with APm improved the accuracy to predict Rs in the model, especially when no precipitation happened in those months. Improved model performance on no-precipitation conditions improves our ability to simulate soil carbon dynamic and its response to global climate change as long-term drought becomes more and more common under global climate change. These results provided insight into using air temperature and precipitation as surrogates to simulate Rs .

We detected clear regional heterogeneity in relationships between Ts and Ta, Log(Rs) and temperature, among different climates. More specifically, Ts in the tropical region was much less correlated with Ta than in other regions. In addition, temperature explained less variation in Rs in tropical and arid regions than in temperate and boreal regions. The possible reason for this result is that the range of Ta (20 to 30 ℃) in these regions was much narrower than for other climates regions. Temperature may not be a limiting factor in tropical and arid regions, but it significantly limits Rs in cold regions. Another possibility is vegetation cover, which is very high under the tropical area and may prevent the Ts from changing with Ta. The heterogeneity of relationships between surrogates may complicate the prediction of Rs at regional scales using a single global model. Climate-specific models could better capture the unique relationship between Rs and its controlling factors.

Unlike temperature, SWC and precipitation were less strongly related to each other and Rs. We detected no relationship between Rs and SWC. One possible reason is the SWC data we collected were from 724 different publications, which used different methods and equipment for measuring SWC, which adds heterogeneity to SWC variance. Another possibility is different researchers used different soil-moisture-measure metrics to describe Rs variation. The relationship between Rs and soil moisture has been expressed as water potential (Orchard and Cook 1983), gravimetric water content (Wildung, Garland, and Buschbom 1975), water holding capacity (Howard and Howard 1993), water-filled pore space (Doran, Mielke, and Power 1990), volumetric water content (Hanson et al. 1993), and depth to water table (Oberhauer et al. 1992). This makes comparison between different research difficult or impossible. Worse still, same soil-moisture-measure metrics are not compariable across different soils. For instance, the volumetric soil water content was used at this study to describe Rs variation. However, soils with different

textures but with the same volumetric soil water content, available soil water to plant and microbial could be very different, because soil texture significantly affects soil water availability (Wu, Huang, and Gallichand 2011). Fine-textured soil has more micro-pores than do coarse-textured soils; water in a fine texture soil is more tightly held by the soil and has a higher wilting point, and thus less water will be available in the fine textures-soils than coarse-textured soils if both soils have the same volumetric soil water content. It is thus possible that SWC can explain site scale Rs variation, but cannot explain Rs variation at the global scale. Future studies should be conducted to test whether soil-available water or water potential explains more Rs variability than water content at global scale.

Temperature sensitivity of Rs is one crucial determinant of quantifying the feedback mechanisms between terrestrial ecosystem and climate. The temperature sensitivity of Rs can be quantified as the Q_{10} value, which describes the Rs rate increase as temperature increases by 10 °C (Qi, Xu, and Wu 2002). We found that global Q_{10} estimated by Ta (median=1.83), which was about 9% lower than Q_{10} estimated by Ts (median = 2.01); this indicated that Rs responds to Ta is less sensitive than Rs responds to Ts. The difference between Q_{10} estimated by Ta and Ts at this study, however, is smaller than that found by other studies. Based on Rs data from a temperate forest, Kicklighter et al. (1994) concluded that Q_{10} estimated by Ta was 1.983, 36% smaller than Q_{10} estimated based on Ts (3.083). Another study using data from different ecosystems in China, found Q_{10} calculated based on Ta was 1.63, 46% lower than Q_{10} estimated based on Ts at 20 cm (3.02) (Peng et al. 2009). The results from previous studies all showed that Q_{10} based on Ta was smaller than Q_{10} value estimated based on Ts. On the other hand, a rule of thumb widely accepted by the biological and global climate-carbon cycle modeling community is constant Q_{10} value of 2 (Sitch et al. 2003), which is very close to our global Q_{10} estimated by

Ts (2.01, median), but significantly higher than Q_{10} estimated by Ta (1.83, median). The difference in Q_{10} raises a question that needs further exploration: should Q_{10} values based on Ts or opon Ta be used to reliably predict future climate change? Several studies re-quantified the ecosystem level Q_{10} value and global carbon-climate feedback. For instance, one study reported that a Q_{10} value smaller than 2 was required for the global carbon cycle to be modeled (Randerson et al. 2009). The earth system models depend on the relationship between Rs and Ts to predict future climate change and how soil carbon responds to global warming; however, results in this study show that how Rs responds to Ta differs from how Rs responds to Ts. This difference may affect future soil carbon and climate warming feedback predictions.

The zero precipitation problem can be solved by replacing Pm by average monthly precipitation (AP_m). Results in this study support that Pm is not the best single predictor of Rs; instead, APm is the best single predictor and AP_m & P_{m-1} are the best two predictors of Rs. We also compared our modified model with models developed by Reichstein et al. (2003) and by Hashimoto et al. (2015). Our modified model performs better than their models as well (with smaller AIC and MSE_t values, statistic result not shown). Solving the zero precipitation problem is critical because it affects how Rs will be predicted under drought conditions. Extreme climate events, including extreme droughts, are more sensitive to climate change (Yan et al. 2015). Warming has led to more frequent droughts in many regions (IPCC 2007). By using global satellite data, Zhao and Running (2010) verified that large-scale droughts have reduced the regional Net Primary Production (NPP). Future climate change is likely to increase frequency and severity of extreme droughts (Allen et al. 2010). Better prediction of Rs under extreme drought (e.g. no precipitation month) conditions becomes more critical for better understanding global carbon cycling under climate change.

2.5 CONCLUSION

This study indicated that Ta explains the similar amount of Rs variation, but Rs responds to Ts change more sensitively than Rs responds to Ta. Monthly precipitation was a uniformly poor indicator of SWC; however, precipitation explains a certain amount of Rs variability across different climate regions. Moreover, average monthly precipitation (APm) is the best single parameter, and average monthly precipitation & previous month's precipitation (P_{m-1}) are the best combined factors to predict Rs. The "Zero precipitation, zero respiration" problem was resolved with replacing monthly precipitation by average monthly precipitation. Our work provides the evidence that Ta is a good surrogate of Ts in global Rs modeling, and using average monthly precipitation as a predictor improves our ability to accurately simulate Rs, especially for months without precipitation.

REFERENCE

Allen, Craig D. et al. 2010. "A Global Overview of Drought and Heat-Induced Tree Mortality Reveals Emerging Climate Change Risks for Forests." *Forest Ecology and Management* 259(4):660–84.

Awe, G. O., J. M. Reichert, and O. O. Wendroth. 2015. "Temporal Variability and Covariance Structures of Soil Temperature in a Sugarcane Field under Different Management Practices in Southern Brazil." *Soil and Tillage Research* 150:93–106.

Baldocchi, Dennis et al. 2001. "Fluxnet: A New Tool to Study the Temporal and Spatial Variability of Ecosystem-Scale Carbon Dioxide, Water Vapor, and Energy Flux Densities." *Bulletin of the American Meteorological Society* 82(11): 2415-34.

Bond-Lamberty, Ben and Allison Thomson. 2010. "Temperature-Associated Increases in the Global Soil Respiration Record." *Nature* 464(7288):579–82.

Brooks, Paul D., Diane McKnight, and Kelly Elder. 2005. "Carbon Limitation of Soil Respiration under Winter Snowpacks: Potential Feedbacks between Growing Season and Winter Carbon Fluxes." *Global Change Biology* 11(2):231–38.

Carey, Joanna C. et al. 2016. "Temperature Response of Soil Respiration Largely Unaltered with Experimental Warming." *Proceedings of the National Academy of Sciences* 113(48):13793–802.

Chen, Shutao et al. 2010. "Modeling Interannual Variability of Global Soil Respiration from Climate and Soil Properties." *Agricultural and Forest Meteorology* 150(4):590–605.

Dai, Aiguo. 2011. "Drought under Global Warming : A Review." *Climate Change* 2 (1):45–65.

Davidson, Eric A., Elizabeth Belk, and Richard D. Boone. 1998. "Soil Water Content and Temperature as Independent or Confounded Factors Controlling Soil Respiration in a Temperate Mixed Hardwood Forest." *Global Change Biology* 4(2):217–27.

Doran, J. W., L. N. Mielke, and J. F. Power. 1990. Microbial Activity as Regulated by Soil Water-Filled Pore Space." In Transactions 14th International Congress of Soil Science, Kyoto, Japan, August 1990, Volume III: 94–99.

Fang, C., John B. Moncrieff, Henry L. Gholz, and Kenneth L. Clark. 1998. "Soil CO_2 Efflux and Its Spatial Variation in a Florida Slash Pine Plantation." *Plant and Soil* 205:135–46.

Feng, Huihui and Yuanbo Liu. 2015. "Combined Effects of Precipitation and Air Temperature on Soil Moisture in Different Land Covers in a Humid Basin." *Journal of Hydrology* 531:1129–40.

Gaur, Nandita and Binayak P. Mohanty. 2013. "Evolution of Physical Controls for Soil Moisture in Humid and Subhumid Watersheds." *Water Resources Research* 49(3):1244–58.

Gehrig-Fasel, Jacqueline, Antoine Guisan, and Niklaus E. Zimmermann. 2008. "Evaluating Thermal Treeline Indicators Based on Air and Soil Temperature Using an Air-to-Soil Temperature Transfer Model." *Ecological Modelling* 213(3–4):345–55.

Haddeland, Ingjerd et al. 2014. "Global Water Resources Affected by Human Interventions and Climate Change." *Proceedings of the National Academy of Sciences of the United States of America* 111(9):3251–56.

Hanson, P. J., S. D. Wullschleger, S. a. Bohlman, and D. E. Todd. 1993. "Seasonal and Topographic Patterns of Forest Floor CO_2 Efflux from an Upland Oak Forest." *Tree Physiology* 13(1):1–15.

Hashimoto, S. et al. 2015. "Global Spatiotemporal Distribution of Soil Respiration Modeled Using a Global Database." *Biogeosciences Discussions* 12(5):4331–64.

Hohenegger, Cathy et al. 2009. "The Soil Moisture-Precipitation Feedback in Simulations with Explicit and Parameterized Convection." *Journal of Climate* 22(19):5003–20.

Holsten, Anne, Tobias Vetter, Katrin Vohland, and Valentina Krysanova. 2009. "Impact of Climate Change on Soil Moisture Dynamics in Brandenburg with a Focus on Nature Conservation Areas." *Ecological Modelling* 220(17):2076–87.

Hongxiang Yan, Hamid Moradkhani. 2016. “Combined Assimilation of Streamflow and Satellite Soil Moisture with the Particle Filter and Geostatistical Modeling.” *Advances in Water Resources* 94:364–78.

Howard, D. M. and P. J. A. Howard. 1993. “Relationships between CO_2 Evolution, Moisture Content and Temperature for a Range of Soil Types.” *Soil Biology and Biochemistry* 25(11):1537–46.

IPCC. 2007. *Climate Change 2007: The Physical Science Basis. Contribution of Working Group I to the Fourth Assessment Report of the Intergovernmental Panel on Climate Change.* Cambridge, United Kingdom: Cambridge University Press.

Jensen, L. S. et al. 1996. “Soil Surface CO_2 Flux as an Index of Soil Respiration in Situ: A Comparison of Two Chamber Methods.” *Soil Biology and Biochemistry* 28(10–11):1297–1306.

Kang, Sinkyu, Sungwoo Kim, and Dowon Lee. 2000. “Spatial and Temporal Patterns of Solar Radiation Based on Topography and Air Temperature.” *Canadian Journal of Forest Research* 136:173–84.

Kicklighter, David W. et al. 1994. “Aspects of Spatial and Temporal Aggregation in Estimatingregional Carbon Dioxide Fluxes from Temperate Forest Soils.” *Journal of Geophysical Research* 99(93):1303–15.

Koster, Randal D. et al. 2004. “Regions of Strong Coupling between Soil Moisture and Precipitation.” *Science* 305(5687):1138–40.

Li, Zhi, Wen-zhao Liu, Xun-chang Zhang, and Fen-li Zheng. 2009. “Impacts of Land Use Change and Climate Variability on Hydrology in an Agricultural Catchment on the Loess Plateau of China.” *Journal of Hydrology* 377(1–2):35–42.

Liang, L. L., D. A. Riveros-Iregui, R. E. Emanuel, and B. L. McGlynn. 2014. “A Simple Framework to Estimate Distributed Soil Temperature from Discrete Air Temperature

Measurements in Data-Scarce Regions." *Journal of Geophysical Research : Atmospheres* 119:407–17.

Luo, Yiqi and Xuhui Zhou. 2006. *Soil Respiration and the Environment*. San Diego, California, Elsevier Academic Press.

Mackiewicz, Michael C. 2012. "A New Approach to Quantifying Soil Temperature Responses to Changing Air Temperature and Snow Cover." *Polar Science* 6(3–4):226–36.

Mariko, Shigeru et al. 2000. "Winter CO_2 Flux from Soil and Snow Surfaces in a Cool-Temperate Deciduous Forest, Japan." *Ecological Research* 15(4):363–72.

Martinec, Jaroslav, Albert Rango, and Ralph Roberts. 2008. *Snowmelt Runoff Model (SRM) User's Manual*. Las Cruces, NM 88003, USA: University of Berne, Department of Geography.

Oberhauer, S. F. et al. 1992. "Environmental Effects on CO_2 Efflux from Riparian Tundra in the Northern Foothills of the Brooks Range, Alaska, USA." *Oecologia* 92(4):568–77.

Orchard, Valerie a. and F. J. Cook. 1983. "Relationship between Soil Respiration and Soil Moisture." *Soil Biology and Biochemistry* 15(4):447–53.

Peng, Shushi, Shilong Piao, Tao Wang, Jinyu Sun, and Zehao Shen. 2009. "Temperature Sensitivity of Soil Respiration in Different Ecosystems in China." *Soil Biology and Biochemistry* 41(5):1008–14.

Qi, Ye, Ming Xu, and Jianguo Wu. 2002. "Temperature Sensitivity of Soil Respiration and Its Effects on Ecosystem Carbon Budget: Nonlinearity Begets Surprises." *Ecological Modelling* 153:131–42.

R Core Team. 2014. *R: A Language and Environment for Statistical Computing. R Foundation for Statistical Computing*. Vienna, Austria.

Raich, J. W. and W. H. Schlesinger. 1992. "The Global Carbon Dioxide Flux in Soil Respiration and Its Relationship to Vegetation and Climate." *Tellus* 44 B(2):81–99.

Raich, James W. and Christopher S. Potter. 1995. “Global Patterns of Carbon Dioxide Emissions from Soils.” *Global Biogeochemical Cycles* 9(1):23–36.

Raich, James W., Christopher S. Potter, and Dwipen Bhagawati. 2002. “Interannual Variability in Global Soil Respiration, 1980–94.” *Global Change Biology* 8(8):800–812.

Randerson, James T. et al. 2009. “Systematic Assessment of Terrestrial Biogeochemistry in Coupled Climate-Carbon Models.” *Global Change Biology* 15(10):2462–84.

Rango, A. and J. Martinec. 1995. “Revisiting the Degree-Day Method for Snowmelt Computations.” *Water Resources Bulletin* 31(4):657–69.

Reichstein, Markus et al. 2003. “Modeling Temporal and Large-Scale Spatial Variability of Soil Respiration from Soil Water Availability, Temperature and Vegetation Productivity Indices.” *Global Biogeochemical Cycles* 17(4):1104.

Schimel, D. S. et al. 2001. “Recent Patterns and Mechanisms of Carbon Exchange by Terrestrial Ecosystems.” *Nature* 414(6860):169–72.

Sitch, Stephen et al. 2003. “Evaluation of Ecosystem Dynamics, Plant Geography and Terrestrial Carbon Cycling in the LPJ Dynamic Global Vegetation Model.” *Global Change Biology* 9(2):161–85.

Sterling, Shannon M., Agnès Ducharne, and Jan Polcher. 2012. “The Impact of Global Land-Cover Change on the Terrestrial Water Cycle.” *Nature Climate Change* 2(10):1–6.

Sun, Shaobo, Baozhang Chen, Jing Chen, Mingliang Che, and Huifang Zhang. 2016. “Comparison of Remotely-Sensed and Modeled Soil Moisture Using CLM4.0 with in Situ Measurements in the Central Tibetan Plateau Area.” *Cold Regions Science and Technology* 129:31–44.

Thunholm, Bo. 1990. “A Comparison of Measured and Simulated Soil Temperature Using Air Temperature and Soil Surface Energy Balance as Boundary Conditions.” *Agricultural and Forest Meteorology* 53(1–2):59–72.

Toy, Terrence J., Andrew J. Kuhaida Jr, and Brian E. Munson. 1978. “The Prediction of Mean Monthly Soil Temperature from Mean Monthly Air Temperature.” *Soil Science* 126(3):181–89.

Wang, Chuankuan, Jinyan Yang, and Quanzhi Zhang. 2006. “Soil Respiration in Six Temperate Forests in China.” *Global Change Biology* 12(11):2103–14.

Wang, Wei, Weile Chen, and Shaopeng Wang. 2010. “Forest Soil Respiration and Its Heterotrophic and Autotrophic Components: Global Patterns and Responses to Temperature and Precipitation.” *Soil Biology and Biochemistry* 42(8):1236–44.

Wang, Wei and Jingyun Fang. 2009. “Soil Respiration and Human Effects on Global Grasslands.” *Global and Planetary Change* 67(1–2):20–28.

Wildung, R. E., T. R. Garland, and R. L. Buschbom. 1975. “The Interdependent Effects of Soil Temperature and Water Content on Soil Respiration Rate and Plant Root Decomposition in Arid Grassland Soils.” *Soil Biology and Biochemistry* 7(6):373–78.

Wohl, Ellen et al. 2012. “The Hydrology of the Humid Tropics.” *Nature Climate Change* 2(9):655–62.

Wu, Yuanzhi, Mingbin Huang, and Jacques Gallichand. 2011. “Transpirational Response to Water Availability for Winter Wheat as Affected by Soil Textures.” *Agricultural Water Management* 98(4):569–76.

Yan, Gao et al. 2015. “Changes of Daily Climate Extremes in Loess Plateau during 1960-2013.” *Quaternary International* 371:5–21.

Yang, Lei, Wei Wei, Liding Chen, and Baoru Mo. 2012. “Response of Deep Soil Moisture to Land Use and Afforestation in the Semi-Arid Loess Plateau, China.” *Journal of Hydrology* 475:111–22.

Yazaki, Tomotsugu et al. 2013. “Influences of Winter Climatic Conditions on the Relation between Annual Mean Soil and Air Temperatures from Central to Northern Japan.” *Cold Regions Science and Technology* 85:217–24.

Yebra, Marta et al. 2015. “Global Vegetation Gross Primary Production Estimation Using Satellite-Derived Light-Use Efficiency and Canopy Conductance.” *Remote Sensing of Environment* 163:206–16.

Zhang, Yu, Wenjun Chen, and Josef Cihlar. 2003. “A Process-Based Model for Quantifying the Impact of Climate Change on Permafrost Thermal Regimes.” *Journal of Geophysical Research* 108(D22):1–15.

Zhao, Maosheng and Steven W. Running. 2010. “Drought-Induced Reduction in Global Terrestrial Net Primary Production from 2000 Through 2009.” *Science* 329(6046):940–43.

Zheng, Daolan, E.Raymond Hunt, and Steven W. Running. 1993. “A Daily Soil Temperature Model Based on Air Temperature and Precipitation for Continental Applications.” *Climate Research* 2:183–91.

CHAPTER 3. Constraining estimates of global soil respiration by quantifying sources of uncertainty

ABSTRACT

Quantifying global soil respiration (Rs_G) and its response to temperature change are critical for predicting the turnover of terrestrial carbon stocks and their feedbacks to climate change. Currently, global estimates of Rs range from 68 to 98 Pg C yr^{-1}, causing considerable uncertainty in the global carbon budget. We argue the source of this variability lies in the assumptions regarding sensitivity of Rs to temperature (Q_{10}), differing and mismatched time-scales, and inclusion of precipitation. To quantify these uncertainties and constrain Rs_G, we developed three climate-driven models [first-order exponential (FKT), second-order exponential (SKT), and second-order exponential with a hyperbolic precipitation function (SKT_HYP)], and used two time-scales (monthly and annual) of climate and Rs data to predict Rs_G. From the resulting Rs_G estimates, we calculated uncertainty associated with constant and variable Q_{10}, mixed-time-scale climate data (Jensen's inequality), different time-scales, and the precipitation function. Our Rs_G estimates ranged from 66.62 Pg (monthly SKT_HYP) to 100.72 Pg (FKT model). The time-scale of the data altered which model best fit Rs, where SKT better fit monthly and FTK better fit annual data. The constant Q_{10} model, Jensen's inequality (Precipitation), and using annual Rs data all increased Rs_G estimates by 12.35, 4.85, and 7.93 Pg respectively; however, Jensen's inequality (Temperature) and the precipitation function decreased estimates by 4.36 and 9.85 Pg. The Rs_G estimated by SKT and SKT_HYP model parameterized from monthly Rs data (70.85 to 80.99 Pg C yr^{-1}) was closest to Rs_G estimated by partitioning the components of global carbon cycle (69.84 to 81.65 Pg C yr^{-1}). In sum, the time-scale of data and identified uncertainty indicated Rs_G is lower than the current benchmark for land models (98 Pg

C yr^{-1}), which may change the predicted rates of terrestrial carbon turnover and the carbon to climate feedback as global temperatures rise.

3.1 INTRODUCTION

Soil respiration (Rs), the release of CO_2 from plant roots, soil microbes, and fauna, is a major flux in the terrestrial carbon cycle, second only to gross primary productivity (GPP). Despite the important role of Rs in regulating terrestrial and atmospheric carbon pools, the global annual Rs flux and its feedback to the climate remains poorly understood (Ben Bond-Lamberty and Thomson 2010). At the global scale, Rs cannot be measured directly, only estimated by up-scaling field Rs measurements through models and environmental factors (e.g. air temperature, precipitation) (Ben Bond-Lamberty and Thomson 2010; Hashimoto et al. 2015; Raich and Potter 1995; Raich et al. 2002; Raich and Schlesinger 1992), through process based models (Exbrayat et al. 2014), or by partitioning Rs from global carbon cycling (Raich & Schlesinger, 1992; Hashimoto *et al.*, 2015). Currently, the number of global Rs estimates are quite limited compared to estimates of other terrestrial carbon fluxes, such as GPP and net primary production (NPP) (Hashimoto et al. 2015). Among the estimates there is a large degree of uncertainty, even though most used a similar climate-driven approach, i.e. estimating global Rs by modeling the response of Rs to climate factors such as air temperature and precipitation (Hashimoto et al. 2015). A gap of 30 Pg C yr^{-1} separates the highest estimate (Bond-Lamberty and Thomson 2010 a, 98 Pg) from the lowest estimate (Raich & Schlesinger. 1992, 68 Pg). The large uncertainty in Rs leads to low confidence in the overall carbon budget and our understanding of soil carbon feedbacks to climate warming (Bradford et al. 2016).

Global Rs models depend on reliable, globally distributed datasets that, ideally, provide co-located site measurements of air temperature, precipitation, and Rs for a period of at least one year. When combined, these large datasets capture global variability in the known temperature, precipitation, and Rs values, and are used to define the coefficients within various empirical model equations which provide the best fit of the independent variables (temperature or temperature and precipitation), and the dependent variable (Rs). Spatially discrete, averaged weather data is then used as inputs to the parameterized equations to generate estimates of Rs for each discrete area, and the total for all areas summed to estimate global Rs (Ben Bond-Lamberty and Thomson 2010; Hashimoto et al. 2015; Raich and Potter 1995; Raich and Schlesinger 1992). Within this processes multiple factors cause uncertainty in global Rs estimates. First, the time-scale of Rs data used to parameterize the coefficients of predictive models may contribute to the wide range of Rs estimates. Site Rs measurements have been aggregated over space and time to estimate global annual mean Rs (Ben Bond-Lamberty and Thomson 2010; Hashimoto et al. 2015; Raich and Potter 1995; Raich and Schlesinger 1992). The most recent and highest global Rs estimate utilized a database that averaged Rs measures over an annual time-scale (Ben Bond-Lamberty and Thomson 2010). Daily mean Rs measurements typically involve capture of CO_2 from the soil surface during a discrete time interval (e.g. between 09:00 and 9:05). Annual average site Rs estimates may be derived from daily mean measurement taken at a frequency of once per week, once per month, or even once every three month (Chen et al. 2014; E. a Davidson, Belk, and Boone 1998; Sheng et al. 2010b). However, often Rs measurements do not span a whole year, as measurements are made more frequently during the growing season. Rs measurements obtained during the growing season are generally larger than annual average Rs rates. Unfortunately, some growing season-only Rs rates have been reported as annual site mean

estimates (Soegaard and Nordstroem 1999), and thus may contribute to overestimation of global annual mean Rs rates when global Rs model was parameterized based on annual time-scale Rs data. Some earlier global mean Rs estimates were based on monthly averaged data (Raich and Potter 1995; Raich et al. 2002), a practice which could better eliminate this source of error.

Another source of uncertainty in global Rs estimates results from parameterizing global modeling coefficients using site-based temperature, precipitation, and Rs datasets with mismatching temporal resolutions. The most recent global Rs estimates and predicted responses to global climate change were generated from monthly time-scale Rs models calibrated using monthly long-term site temperature and precipitation data but regressed against site Rs values at an annual, rather than monthly time-scale (Hashimoto et al. 2015). The use of independent and dependent datasets with differing time-scales requires the underlying condition that both Rs and air temperature, and Rs and precipitation are linearly related. However, Raich et al. (2002) demonstrated non-linearity in these key relationships. When these relationships are non-linear, the annual Rs obtained by averaging the monthly values of Rs estimated from monthly air temperature, $\overline{f(x)}$, does not equal the annual Rs calculated by using the average air temperatures to estimate Rs, $f(\overline{x})$. The difference between $f(\overline{x})$ and $\overline{f(x)}$ is known as Jensen's inequality. We currently have no estimate of uncertainty generated by this common ecological modeling issue (Ruel and Ayres 1999).

In addition, source of uncertainty in global Rs models involves key assumptions regarding the temperature sensitivity of Rs. Rs is influenced by a wide range of climate factors including temperature, soil water content, precipitation, and plant coverage (Fang et al. 1998). Of these, temperature is the most important environmental factor influencing Rs (Davidson and Janssens 2006; Janssens et al. 2001; Trumbore 2006). The temperature sensitivity of Rs can be

quantified by $Q_{10,}$ a measure of the change in Rs over a 10℃ temperature increase (Lloyd and Taylor 1994). Modelers must assume that Q_{10} is either constant or variable across the temperature range of their datasets, and this assumption is reflected in their choice of models. For example, predictive models using a first-order exponential model equation assume a constant Q_{10} across the temperature range. Alternatively, a second-order exponential model equation assumes variable Q_{10} response increasing temperatures. Although models that assume a constant Q_{10} are widely used (Conant, Ryan, Agren, et al. 2011), many studies demonstrate that Q_{10} varies with temperature, with the rate of increase depending on the baseline temperature (Lloyd and Taylor 1994). For instance, a recent meta-analysis found that Q_{10} values had a large range, but when temperature was greater than 25.0℃, the Q_{10} values became negatively correlated to soil temperature (Hamdi et al. 2013). Whether or not Q_{10} is assumed to be constant or variable depends, in part, on the time-scale of Rs and temperature data to parameterize the model. Averaging Rs and temperature data to annual time-scales diminishes the influence of air temperature extremes on Rs, making it difficult to detect Q_{10} variability and promotes the assumption of a constant Q_{10}. Currently, no study has compared and quantified the uncertainty in global Rs estimates resulting from models assuming constant Q_{10} and variable Q_{10}.

Assumptions regarding the effect of soil water content (SWC) on Rs and using precipitation as proxy of SWC in global Rs models also injects uncertainty in global Rs estimates (Jassal et al. 2007; Kirschbaum 1995; Zhang et al. 2006). SWC is another important environmental factor that affects Rs; however, the relationship between SWC and Rs is much more complex than the relationship between Rs and temperature. In previous studies, numerous equations, including linear (Wildung et al. 1975), logarithmic (Orchard and Cook 1983), piecewise (E. a Davidson et al. 1998), and polynomial (Adachi et al. 2009) functions were used

to describe the effect of SWC on Rs. Even worse, an opposite conclusion may be reached by different studies using same model form. For instance, in a temperate mixed hardwood forest, Massachusetts, USA, Rs had a negative linear relationship with SWC (E. a Davidson et al. 1998); however, in central Washington state, Rs had a positive linear relationship with SWC (Wildung et al. 1975). The multifarious relationship between Rs and SWC is caused by the multiple ways SWC can affect Rs. At low SWC, the availability of soluble substrates is limited and increasing SWC promotes carbon availability and accelerates microbial activities (Davidson, Janssens, and Lou 2006), while high at SWC the water in the soil pores decreases the oxygen availability thus limiting Rs (Skopp, Jawson, and Doran 1990). Moreover, seasonal variation of SWC is often correlated with temperature (Feng and Liu 2015), making the relationship between SWC and Rs more unpredictable. As a result, Rs measured under different SWC conditions may show different relationships. To compound the problem, at the global and regional scales there is insufficient long-term, high-frequency SWC data; therefore, global Rs models use precipitation to approximate SWC (Ben Bond-Lamberty and Thomson 2010; Chen et al. 2010; Hibbard et al. 2005; Raich et al. 2002; Wang et al. 2010). Studies commonly use a hyperbolic precipitation function to describe the relationship between precipitation and Rs (Hashimoto et al., 2015 ; Raich and Potter, 1995; Raich et al., 2002; Reichstein et al., 2003), which assumes the hyperbolic function is able to detect the declining Rs at site with limited precipitation (proxy for SWC). One potential issue with this approach is that the value of the hyperbolic precipitation function can approach, but never equal one, causing even optimum precipitation to limit Rs which does not reflect the complicated relationship between Rs and SWC. In addition, rainfall events after dry periods can stimulate high pulses of Rs (Yan et al. 2014), which directly

contradicts the assumption of precipitation-limited Rs. Including or omitting the hyperbolic precipitation function generates an unknown amount of uncertainty in global Rs estimates.

The purpose of this study was to quantify the magnitude of Rs flux associated with these uncertainties in current methods for estimating global Rs by using model forms with different underlying assumptions regarding temperature sensitivity of Q_{10} and the effects of SWC on Rs. In addition, we consider the uncertainty associated with using different time-scales of Rs data (monthly vs. annual) and differences in the time-scale between Rs and the climate data used to estimate global Rs. The specific objectives were to: (1) compare the fit of first- and second-order climate-driven exponential models (with and without precipitation included) to available site monthly and annual time-scale data, (2) estimate global Rs based on four variations of these climate-driven models and two time-scales of data inputs (monthly vs. annual mean), and (3) use Rs estimates to quantify and map at a finer scale, the regional uncertainty generated by variable or constant Q_{10}, the time-scale of Rs data, and the hyperbolic precipitation function. We compared these results to previous estimates and Rs estimates generated by partitioning the global carbon cycle from known estimates of the various fluxes, such as NPP (Raich & Schlesinger, 1992; Hashimoto *et al.*, 2015). Agreement between the partitioning technique and the climate-driven modeling approaches would provide a more constrained range for a global annual average Rs estimate, which serves as a benchmark for earth system models (ESMs).

3.2 MATERIALS AND METHODS

3.2.1 Site Rs, temperature, and precipitation data Sources

The annual site-level Rs measurements for this study were obtained from the Global Soil Respiration Database (Bond-Lamberty and Thomsom 2014) (SRDB. Version 3.0). The SRDB

contains more than 5000 Rs records digitized from historical papers. According to Bond-Lamberty & Thomson (2010b), annual Rs records could be included in SRDB if: (1) Annual Rs rate was reported directly in the paper (Rs was measured discretely or continuously for a period of at least one year); (2) Mean seasonal Rs measurements were reported, thus allowing calculation of annual Rs as the average of four seasons; (3) Annual or seasonal partitioning of Rs was reported; (4) Q_{10} and associated temperature range were reported, allowing Rs to be calculated from this relationship; (5) Rs at 10 ℃ (R_{10}) was reported allowing annual Rs rate to be estimated based on R_{10} and annual mean temperature. For this study, we used a subset of SRDB, S1, to avoid modeling biases that result from data quality issues such as duplicate records, records that depended on multiple assumptions to calculate the annual Rs rate, and measurement methods that overestimate or underestimate Rs rate (Bond-Lamberty & Thomson, 2010a; Hashimoto *et al.*, 2015).

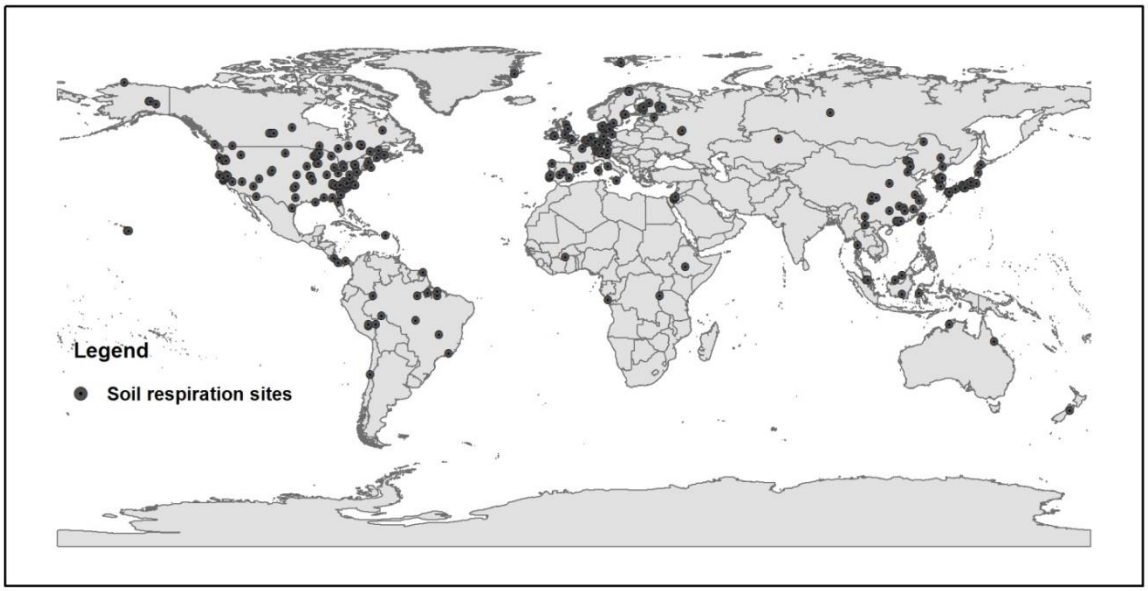

Figure 3-1. Combined site distribution of the yearly global soil respiration dataset (S1), and the monthly global soil respiration dataset (MS1) used in this study.

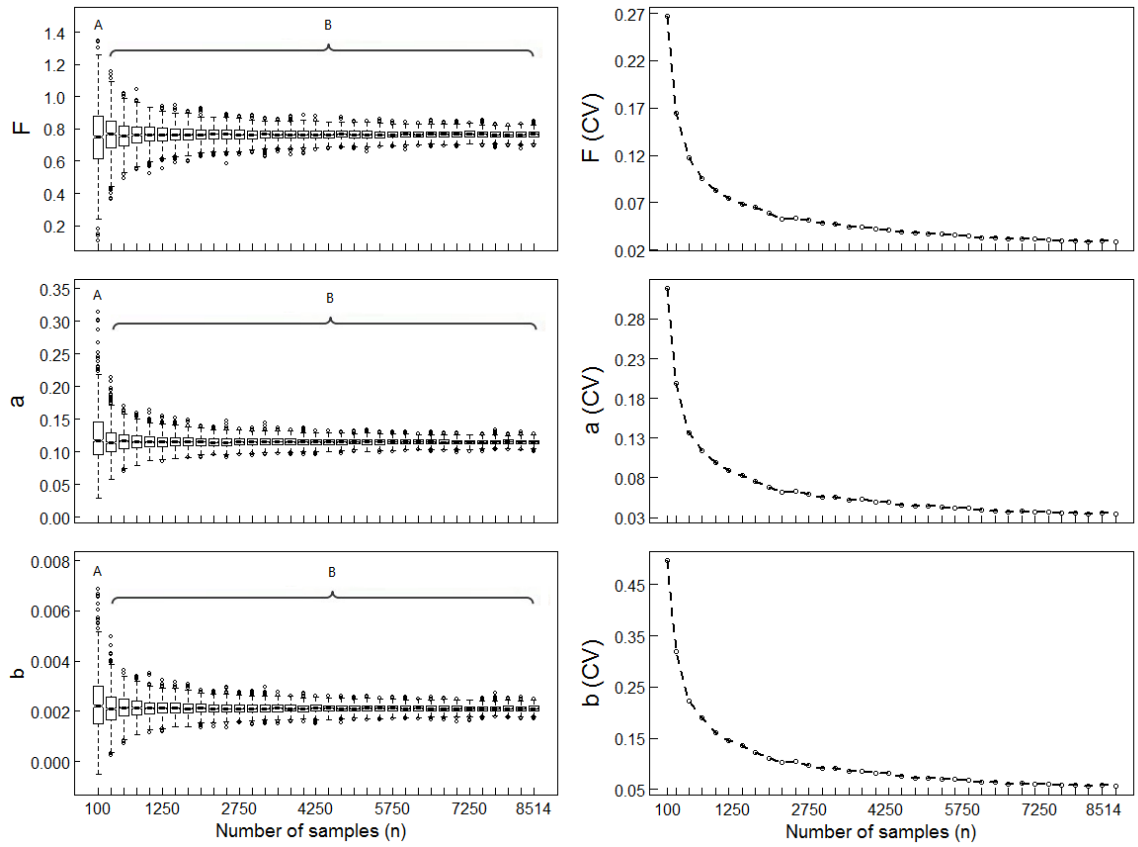

Figure 3-2. Bootstrapped estimates of the second kinetic theory model parameters (F, a and b) as Rs sample size increases from 100 to 8514. Under each step, Rs samples were randomly selected from MS1, and this process was repeated 1,000 times. The left column shows parameters (F, a, b), upper case letters represent significant differences among different Rs sample sizes. Right column shows coefficient of variability (CV) for 1000 simulated parameters.

To generate monthly time-scale data, we digitized the data from all of the original publications in the S1 dataset. The S1 subset contains 371 sites across the globe; however, we could digitize only 243 sites at a monthly time-scale because some publications only report the annual mean Rs rate. To eliminate the bias caused by from sites with only one time-scale, we used only soil respiration data from those 243 sites that included both time-scales (Figure 3-1). The digitized data from the 243 sites generated 8514 measurements of monthly Rs, hereafter referred to as MS1 (https://data.lib.vt.edu/collections/ns0646000, DOI pending), which is a subset of the monthly global soil respiration database. Because the sample size of MS1 (8514)

was much larger than S1 (1308), we used a bootstrapping approach to test whether Rs sample size caused significant variation in the model parameters. The results from the bootstrapping analysis (Figure 3-2) showed that Rs sample size affects Rs model parameters, but only for sample size < 100 (Figure 3-2). Since the sample sizes of S1 (n=1308) and MS1 (n=8514) are both much larger than 100, we were confident that Rs sample size had a negligible effect on global Rs modeling.

3.2.2 Soil respiration models

To determine the nature of Q_{10} relationships (constant or variable) on the uncertainty of global Rs estimates, we tested for goodness of fit with our Rs, air temperature and precipitation datasets (S1 and MS1), using both first-order exponential (FKT) and a second-order exponential (SKT) models,

$$\mathrm{Rs} = \mathrm{F} \times exp^{(a \times \mathrm{Tm})} \qquad \text{FKT}$$

$$\mathrm{Rs} = \mathrm{F} \times exp^{(a \times \mathrm{Tm} - \mathrm{b} \times Tm^2)} \qquad \text{SKT}$$

where F, a and b are constants, Rs is the monthly average Rs rate (g C m^{-2} day^{-1}); Tm denotes the monthly air temperature; $exp^{(a \times \mathrm{Tm} - \mathrm{b} \times Tm^2)}$ describes a second-order exponential relationship of Tm with Rs; and the term (-b × Tm^2) defines a second-order function that includes a Tm threshold in the relationship between Tm and Rs.

To test how the hyperbolic precipitation function contributes to the uncertainty of global annual mean Rs estimates, we developed a second-order exponential equation with a hyperbolic precipitation function model (SKT_HYP). The format was adapted from the model developed by Hashimoto *et al.* (2015) and Reichstein *et al.* (2003),

$$\mathrm{Rs} = \mathrm{F} \times exp^{(a \times \mathrm{Tm} - \mathrm{b} \times Tm^2) \times \frac{Pm+P_0}{k+Pm+P_0}} \qquad \text{SKT\_HYP}$$

where Rs, *Tm*, *a* and *b* are the same as in previous models, *Pm* denotes monthly precipitation, and P_0 is a constant value, which was introduced to resolve the "zero precipitation, zero Rs problem" (Reichstein et al. 2003).

We parameterized the coefficients of FKT, SKT, and SKT_HYP models using both MS1 and S1 training datasets. When using the annual time-scale Rs data (S1), inclusion of the second order term ($-b \times Tm^2$) in the models did not result in a significant improvement in the fit of the model (p-values > 0.05). Therefore, we only used the S1 data to parameterize coefficients in the FKT model, hereafter named FKT_S1. We used MS1 data to parameterize coefficients for all model types (FKT, SKT, and SKT_HYP), hereafter named FKT_MS1, SKT_MS1, and SKT_HYP_MS1. We used the nonlinear (weighted) least-squares estimates approach (nls function) in R, version 3.1.1 (R Core Team, 2014) to estimate the model coefficients, and to calculate the R^2, mean squared error (MSE), and the Akaike information criterion (AIC, for a given set of data, AIC measures the relative quality of statistical models, a smaller value indicates a better fit of the data) values for each model.

3.2.3 Estimating Global Soil Respiration

To generate estimates of global Rs using our three global soil respiration models, we obtained global monthly air temperature and precipitation data from the Center for Climate Research at the University of Delaware (Willmott, Matsuura, and Legates 2001). We used this climate dataset because of its quality (Willmott *et al.*, 2001), high spatial resolution across the whole globe (0.5 °latitude × 0.5 °longitude, totaling 85,794 cells), and coverage of the whole study period, 1961 to 2014 (Lawrimore *et al.*, 2011; Willmott *et al.*, 2001). First, we used the

monthly air temperature and precipitation data to calculate Rs for each cell using each of the three models described above, including every month from 1961 to 2014. This process generated several (54 × 12) monthly estimates for each cell. Then we calculated the mean global annual Rs for each model by summing the monthly estimates for each year for all cells in the study and taking the average across the study period. We refer to this result as $\overline{f(x)}$. Second, we recalculated Rs for each cell by inputting the mean *annual* air temperature and precipitation data into the models and again aggregated all cells Rs values to estimate global annual Rs, named as $f(\bar{x})$.

3.2.4 Calculating Uncertainty

The FKT model is a first-order exponential model, which assumes a constant Q_{10} relationship between Rs and Tm. Both SKT and SKT_HYP are second-order exponential models, which assume a variable Q_{10} relationship between Rs and Tm (Q_{10} negatively related with Tm if coefficient *b* in the models is positive). The SKT_HYP including a precipitation factor, which assume the hyperbolic function serves as a means to detect the trend of declining Rs at marginal site precipitation, even under optimum precipitation or over optimum precipitation condition. FKT and SKT model do not include precipitation, which can be treated as the precipitation function always equals one, and thus assume precipitation not limit Rs under any condition, and temperature is the dominant factor driving Rs variability. Based on the model assumptions and using the global Rs estimates generated by the different model types and different Rs and climate data time-scales, we calculated the uncertainty generated by four sources: constant vs. variable Q_{10}, Jensen's inequality, time-scale, and the hyperbolic precipitation function.

Constant vs. variable Q_{10}: To estimate the uncertainty generated by using a constant Q_{10} (first order) or variable Q_{10} (second order) model, we compared Rs estimated by the SKT model to Rs estimated by the FKT model, named as U (Q_{10}) (Equation 3-1).

$$U\ (Q_{10}) = FKT - SKT \quad (3\text{-}1)$$

The global Rs estimated by the FKT model should be larger than the Rs estimated by the SKT model because the SKT model assumes a variable Q_{10} with a threshold that limits Rs when air temperature is higher than the threshold.

Jensen's inequality: Using the logic of Ruel & Ayres (1999), the difference between the global Rs estimated from annual mean climate data, $f(\bar{x})$, and monthly climate data, $\overline{f(x)}$ is the uncertainty caused by Jensen's inequality, named as U (Jensen's) (Equation 3-2).

$$U\ (\text{Jensen's}) = \text{model}\ [f(\bar{x})] - \text{model}\ [\overline{f(x)}\ ]. \quad (3\text{-}2)$$

Since we developed multiple models, we estimated multiple measures of Jensen's inequality using the difference between Rs estimated from the monthly and annual climate data from each model type. The SKT_HYP model has two independent predictors (temperature and precipitation); therefore, we estimated Jensen's inequality caused by both temperature and precipitation.

Time-scale of site datasets to parameterize the model: We estimated the parameters of FKT model from both the annual time-scale Rs data (S1) and monthly time-scale Rs data (MS1) and calculated the global mean annual Rs from each. The difference between the Rs estimates calculated using the same type of models (FKT) but parameterized from Rs data with different time-scales (MS1 vs. Sl) provided an estimate of the uncertainty caused by differing time-scales of Rs data, hereafter named U (Time-scale) (Equation 3-3).

$$U\ (\text{Time-scale}) = FKT\_S1 - FKT\_MS1 \quad (3\text{-}3)$$

By using the same model type (FKT) and climate data, this estimate excludes uncertainty generated by the threshold or Jensen's inequality.

Hyperbolic precipitation function: To estimate the uncertainty generated by including or omitting a hyperbolic precipitation function, we calculated the differences between global Rs estimated by the SKT_MS1 and SKT_HYP_MS1 models, hereafter named U (HYP) (Equation 3-4).

$$U\ (HYP) = SKT\_MS1 - SKT\_HYP\_MS1 \quad (3\text{-}4)$$

We estimated the four types of uncertainty by applying equations 1 to 4 to each 0.5 ° latitude × 0.5 ° longitude cell across the globe from 1961 and 2014, averaged the value of each uncertainty for each cell in the full period, and mapped the spatial variation of different types of uncertainty across globe.

3.3 RESULTS

3.3.1 Rs response to temperature

The Rs rate in MGRsD ranged from 0.001 to 16.20 g C m^{-2} day^{-1}, with an overall mean and standard deviation of 2.33 (± 1.78). The annual dataset, S1, ranged from 0.019 to 9.45 g C m^{-2} day^{-1}, with an overall mean of 2.32 (± 1.25 standard deviation). The mean of Rs observations from the MS1 dataset was very close to the mean of the S1 dataset, even though the latter excluded Rs measurements from both extremely high and low temperature conditions (Figure 3-3 panel a, blue bars). Because the monthly data included Rs rates from both colder and hotter months, the lowest Rs rate in the S1 (0.019 g C m^{-2} day^{-1}) was larger than the lowest Rs rate in the MS1 (0.001 g C m^{-2} day^{-1}), and the largest Rs rate in the S1 (9.45 g C m^{-2} day^{-1}) was smaller

than the largest Rs in MS1 (16.20 g C m^{-2} day^{-1}). The monthly Rs data covered a wider air temperature range as well, from -31 to 32 ºC (Figure 3-3 panel a, black bars), compared to -14 to 29 ºC in the annual Rs data (Figure 3-3 panel a, blue bars). The variation of Rs observations in the MS1 was larger than the variation of S1, likely due to the monthly Rs data includes month-to-month variability.

The first-order and second-order exponential models derived from monthly and annual time-scale Rs records were significantly different. The central tendency of the monthly data, as represented by medians of 2ºC bins, clearly showed a decline in Rs at high temperatures (Figure 3-3 panel b). In the second-order exponential model (SKT) adding the the *b* parameter significantly improved model fit ($p < 0.0001$), indicating a threshold in the Rs response to temperature change. However, the annual Rs records showed no similar decline and *b term* in the SKT_S1 model did not improve fit significantly (S1, Figure 3-3 panel c). For the monthly time-scale data, the second-order exponential (SKT_MS1) was the better model as indicated by the higher R^2 (0.34 vs. 0.31), lower MSE (1.45 vs.1.48), and lower AIC (30465 vs. 30855) values than the first-order exponential (FKT_MS1) model. The SKT_HYP_MS1 model performance better than the other two models as SKT_HYP has the highest R^2, lowest AIC and MSE values (Figure 3-3), indicated that precipitation Rs is sensitive to changes in precipitation. Precipitation significantly limit Rs when monthly precipitation less than 5cm (precipitation multiplier less than 1), when monthly precipitation greater than 15cm, precipitation no longer clearly limit Rs (precipitation multiplier close to 1, Figure 3-4 panel e).

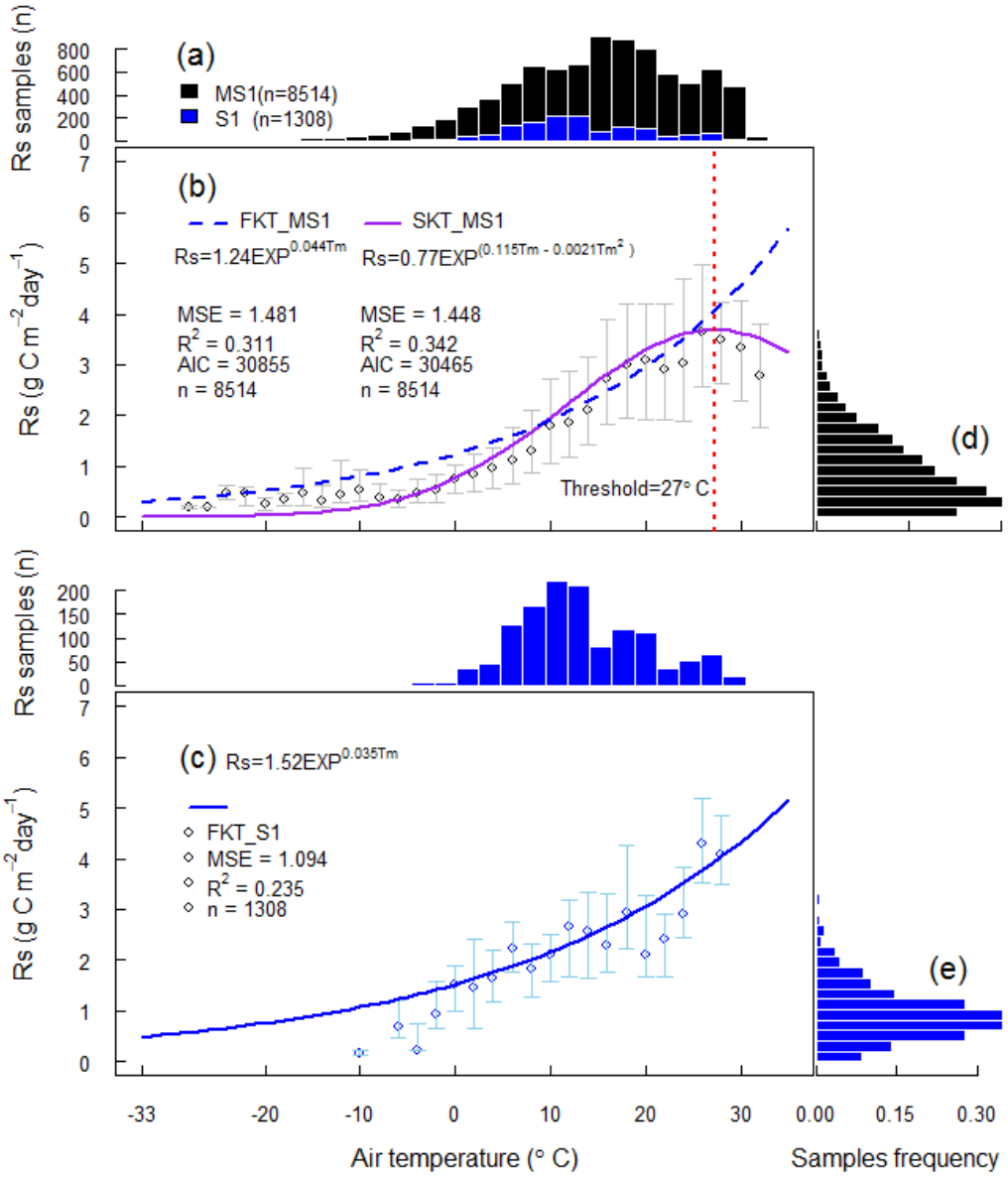

Figure 3-3. Observed soil respiration (Rs) from monthly Rs data (MS1) compared with observed Rs from yearly Rs data (S1), and three models developed based on MS1 and S1. Panel (a) shows the distribution of Rs observations in MS1 (black bar) and S1 (blue bar); Panels (b) and (c) shows Rs response with air temperature from the MS1 and S1 data. Hollow diamonds indicate median Rs and bars indicate first and third quartiles. Panels (d) and (e) showed the frequency of Rs records under different Rs rates from MS1 and S1 data. The hyperbolic model, SKT_HYP_MS1, includes precipitation as a factor, and is not shown. Model parameters for this model, based on the MS1dataset: $Rs = 0.91 \times e^{(0.117 \times Tm - 0.0022 \times Tm^2)} \times \frac{Pm+1.05}{1.26+Pm+1.05}$, MSE = 1.395, R^2 = 0.389, AIC = 29835). Note the error bars in panels (b) and (c) are first and third quantile.

3.3.2 Estimates of global Rs and sources of uncertainty

The ten global mean annual Rs from 1961 to 2014 generated by the four climate-driven models and six climate data input scenarios ranged from 66.62 to 100.72 Pg C yr^{-1} (Table 3-1). Each of the four types of uncertainty contributed to the variation among the ten Rs estimates (Table 3-1). The largest source of uncertainty was caused by the model type (first vs. second-order), and thus the assumption of Q_{10} as constant or variable. Rs from the first-order exponential model, with a constant Q_{10} and no temperature threshold, was 12.35 Pg C yr^{-1} greater than the variable Q_{10}, second-order model.

The precipitation components and data time-scale were the next largest contributors to uncertainty. Including the hyperbolic precipitation function in the second-order exponential model generated 9.56 to 10.14 Pg (mean = 9.85) of uncertainty (Table 3-1). Including the precipitation component decreased the estimate relative to the estimate from the model with no precipitation function. Varying the time-scale of Rs data also generated a sizable amount of uncertainty in global Rs estimates. Parameterizing the first-order exponential model using different time-scales Rs data (MS1 vs. S1) caused 7.93 Pg of uncertainty (Table 3-1).

Table 3-1. Summary of estimated global annual mean soil respiration (Rs) and sources of uncertainty. Models used were: a second-order exponential model parameterized by monthly Rs data (SKT_MS1), a first-order exponential model parameterized by monthly Rs data (FKT_MS1), a first-order exponential model parameterized by annual Rs data (SKT_S1), and a second-order exponential model parameterized by monthly Rs data with a hyperbolic precipitation function (SKT_HYP_MS1). The two types of climate data input to each model were monthly temperature (Tm) and precipitation (Pm), or the annual mean Tm or Pm. Estimates of uncertainty caused by model type and Q_{10}, Jensen's inequality, the precipitation hyperbolic function, and differences in Rs data time-scale were calculated based on the differences between model or input scenarios.

Models	Climate Data Input	Scenario ID	Rs Estimate (Pg C Yr^{-1})	Uncertainty Source	Uncertainty Calculation (Scenario X – Scenario Y)	Uncertainty Estimate (Pg C Yr^{-1})
SKT_HYP_MS1	Monthly Tm + Monthly Pm	I	70.85	*(n/a: baseline)*	*(n/a: baseline)*	*(n/a: baseline)*
	Annual mean Tm + Monthly Pm	II	66.62	Jensen's (Tm)	II - I	-4.23
	Monthly Tm + Annual mean Pm	III	75.75	Jensen's (Pm)	III - I	4.90
	Annual mean Tm + Annual mean Pm	IV	71.41	Jensen's (Pm)	IV - II	4.79
				Jensen's (Tm)	IV - III	-4.34
SKT_MS1	Monthly Tm	V	80.99	Hyperbolic	V - I	10.14
	Annual mean Tm	VI	76.18	Hyperbolic	VI - II	9.56
				Jensen's (Tm)	VI - V	-4.81
FKT_MS1	Monthly Tm	VII	93.29	Q_{10}	VII - V	12.30
	Annual mean Tm	VIII	88.58	Q_{10}	VIII - VI	12.40
				Jensen's (Tm)	VIII - VII	-4.71
FKT_S1	Monthly Tm	IX	100.72	Time-scale	IX - VII	7.43
	Annual mean Tm	X	97.01	Time-scale	X - VIII	8.43
				Jensen's (Tm)	X - IX	-3.71

The difference between global Rs estimated from the annual climate data (air temperature and precipitation) and monthly climate data was smaller in magnitude than the other sources of uncertainty we calculated, and annual climate data could overestimate or underestimate global Rs comparing with monthly climate data. The five measures caused by using annual air temperature to calculate monthly Rs resulted in a decrease in Rs relative to using monthly air temperature and ranged from -4.81 to -3.71, with a mean of -4.36 Pg C yr^{-1} Rs (Table 3-1). These measures of Jensen's inequality were negative [$f(\overline{x}) < \overline{f(x)}$], because the relationship between Rs and temperature is an accelerating function. However, when the annual mean precipitation was used to calculate monthly Rs the two estimates of uncertainty associated with Jensen's inequality resulted in an increase in Rs relative to global Rs estimated from monthly precipitation (4.79 and 4.90 with a mean of 4.85 Pg C yr^{-1}), because the relationship between precipitation and Rs was a decelerating function. For the model that included both temperature and precipitation (SKT_HYP_MS1), the uncertainty due to Jensen's inequality attributable to temperature offset the uncertainty attributable to precipitation (Table 3-1).

3.3.3 Spatial distribution of uncertainty

The magnitude of uncertainty in Rs generated by the sources described above varied regionally across the globe. With respect to Q_{10} uncertainty, the first-order model predicted higher Rs rates in cold and hot climates, and lower Rs rates in mesic climates compared to the second-order model (Figure 3-4 panel a and b). Uncertainty associated with time-scale was also regionally heterogeneous. The monthly time-scale Rs model (FKT_MS1) predicted lower Rs during periods of cold temperatures (< 25 °C), but higher Rs in periods of hot temperatures (> 25 °C, Figure 3-4 panel c). Therefore, except for tropical regions, estimates of Rs generated by

using annual Rs data were larger than estimates from monthly data (Figure 3-4 panel c and d). The hyperbolic precipitation function predicts lower Rs estimates for most regions across the globe except in regions with abundant precipitation throughout the year, such as eastern North America, eastern China, and the tropics (Figures 3-4 panel e and f).

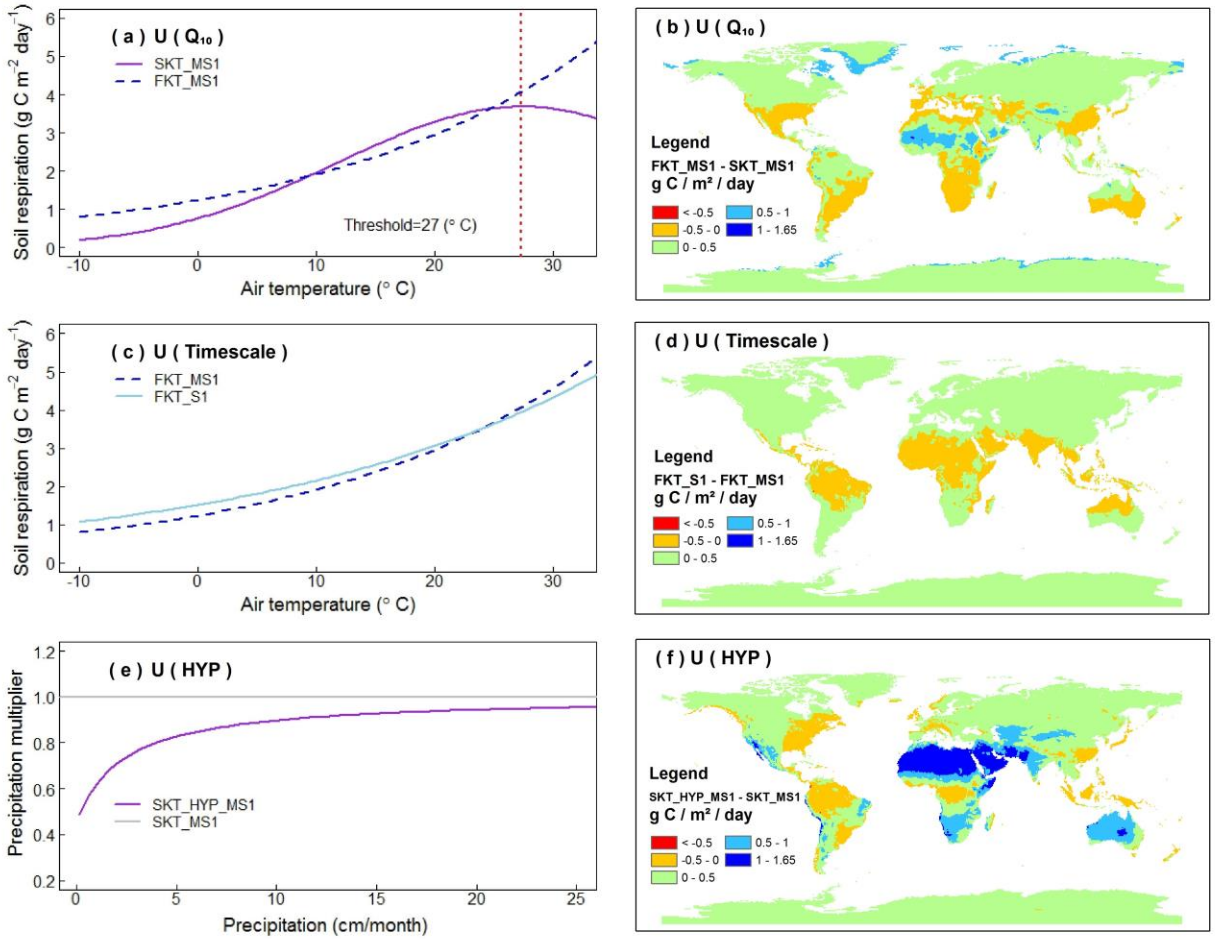

Figure 3-4. Spatial distributions of the uncertainty in soil respiration resulting from Rs models with constant or variable Q_{10} (panels a and b), models parameterized based on different time-scale Rs records (panels c and d) and models with or without hyperbolic precipitation component (panels e and f). The precipitation multiplier of the second-order exponential model without hyperbolic precipitation (SKT_MS1) can be treated to be one (gray line in panel e); however, the precipitation multiplier of SKT_HYP_MS1 model never equals one. Panel f demonstrates that for some regions, Rs estimated from SKT_HYP_MS1 were higher than Rs estimated by SKT_MS1 (green color), that is because the F value of SKT_HYP_MS1 model is larger than SKT _MS1 model (see details in Figure 3-3).

3.4 DISCUSSION

3.4.1 Uncertainty in Global Rs estimates

Our estimates of global mean annual Rs ranged from 66.62 to 100.72 Pg C yr^{-1}, very close to the range of previous estimates (Ben Bond-Lamberty and Thomson 2010; Raich and Potter 1995; Raich and Schlesinger 1992). We documented a sizeable amount of uncertainty embedded within this range of global Rs estimates by comparing estimates generated by multiple modeling assumptions and data inputs with diffing time-scales. These results highlight the importance and provide insights into the uncertainty caused by temporal variance when upscaling from fine temporal scale measurements to coarser temporal scale estimates. The time-scale of the Rs, precipitation, and temperature data both directly (via data time-scale and Jensen's inequality) and indirectly (via Q_{10} and model choice) generated considerable uncertainty in the global Rs estimates. To explore whether uncertainties quantified by this study explained the large range of previous global Rs estimates, we compared our global Rs estimates with previous estimates.

Our global Rs estimates from the first-order exponential model parameterized with annual Rs data [$\overline{f(Tm)}$ 100.72 Pg C yr^{-1} and $f(\overline{Tm})$, 97.01 Pg C yr^{-1}] were close to estimates by Bond-Lamberty & Thomson (2010a) (98 (±12) Pg C yr^{-1}) and Hashimoto et al. (2015) [91(±4) Pg C yr^{-1}], whom both used annual time-scale Rs data. The global Rs models developed by Bond-Lamberty & Thomson (2010a) were linear functions (with Rs square root transformed) and included precipitation, temperature anomalies, precipitation anomalies, leaf area index, nitrogen deposition and biome type in the model. The model developed by Hashimoto et al. (2015) was a second-order exponential model with a hyperbolic precipitation function. The

global Rs estimates from our second-order exponential model with the hyperbolic precipitation function (SKT_HYP_MS1) were smaller (66.62 to 75.75 Pg C yr^{-1}) than estimates by Hashimoto et al. (2015). This difference was not caused by using different climate data, because when we applied our climate data to the model developed by Hashimoto et al. (2015), the difference between our estimate and theirs was only 2.4 Pg C. Furthermore, the difference was not caused by the precipitation hyperbolic function, as the precipitation multiplier of our model was even slightly higher than the precipitation multiplier of the model developed by Hashimoto et al. (2015) (Figure 3-5 panel c). The cause of the larger difference in Rs was the time-scale of Rs data used to parameterize the model. Even though both model formats were second-order, the model by Hashimoto et al. (2015) produced trends similar to our first-order model (FKT_S1) (Figure 3-5 panel a). The Hashimoto et al. (2015) model was parameterized based on annual time-scale Rs data and predicted a threshold of 42.0 ℃, which was much larger than the 27 ℃ predicted by our model parameterized from monthly Rs records. When we subtracted the uncertainty associated with time-scale (7.93 Pg) and Q_{10} (12.35 Pg) from estimate by Hashimoto et al. (2015), the result [70.72 (±4)] fell in the same range as our SKT_HYP_MS1 model estimates. The consistency among those three estimates indicated that regardless of model format or accounting for other biotic/abiotic factors or not, the models parameterized from annual time-scale Rs data provide a higher range of estimates compared to models parameterized by monthly time-scale data.

Even though they used a different model form, the global Rs estimates by Raich et al. (1995) and Raich (2002) (76.5 Pg and 80.4 Pg respectively) were similar to estimates generated by our second-order exponential model parameterized with monthly Rs data (SKT_MS1, 80.99 Pg and 76.18 Pg). Raich *et al.* (1995) and Raich *et al.* (2002) also used monthly Rs data to

parameterize their models, but our Rs data included substantially more Rs records (8514 vs. 977) and records cover longer time period (1961 to 2013 vs. 1963 to 1991). The similarity among these estimates provides further evidence that sample size contributes very little to uncertainty when n > 100 (Figure 3-2). However, an important difference between SKT_MS1 and the models developed by Raich *et al.* (1995) and Raich *et al.* (2002) is that the Raich *et al* estimates included hyperbolic precipitation functions. We found that including a hyperbolic component reduced Rs by 9.85 Pg (Table 3-1). The models developed by Raich *et al.* (1995) and Raich *et al.* (2002) were first-order exponential models (constant Q_{10}), which increases global Rs by around 12.35 Pg (Table 3-1). Thus, the first-order model offset the decrease caused by the hyperbolic precipitation function. This may explain why estimates by Raich et al.(1995) and Raich et al.(2002) were very close to the estimate from the SKT_MS1 model, even though those models used a different model format.

Our results suggest that the error caused by Jensen's inequality (approximately ± 4 Pg) is not negligible and, for comparison, is double the net terrestrial carbon sink (2.1 Pg C yr^{-1}; Le Quéré *et al.,* (2015)). The Jensen's uncertainty related with temperature (-4.36) and precipitation (4.85) are similar magnitude but with different directions. In addition, we observed that the magnitude of uncertainty caused by Jensen's inequality depends upon the parameters in the models, where steeper accelerating or decelerating relationships tend to cause greater error from Jensen's inequality. Historically, though the importance of average environmental conditions has been emphasized by ecologists (Real and Brown 1991), the nature of temporal and environmental variance has received considerable attention and its importance has been extensively discussed (Karban, Agramal, and Mangel 1997; Real and Brown 1991; Ruel and Ayres 1999; Smallwood 1996). These observations highlight the complexity of dealing with

error caused by Jensen's inequality and the need for future studies to consider carefully the benefits of using data averaged to coarser time-scales versus the need for improved accuracy.

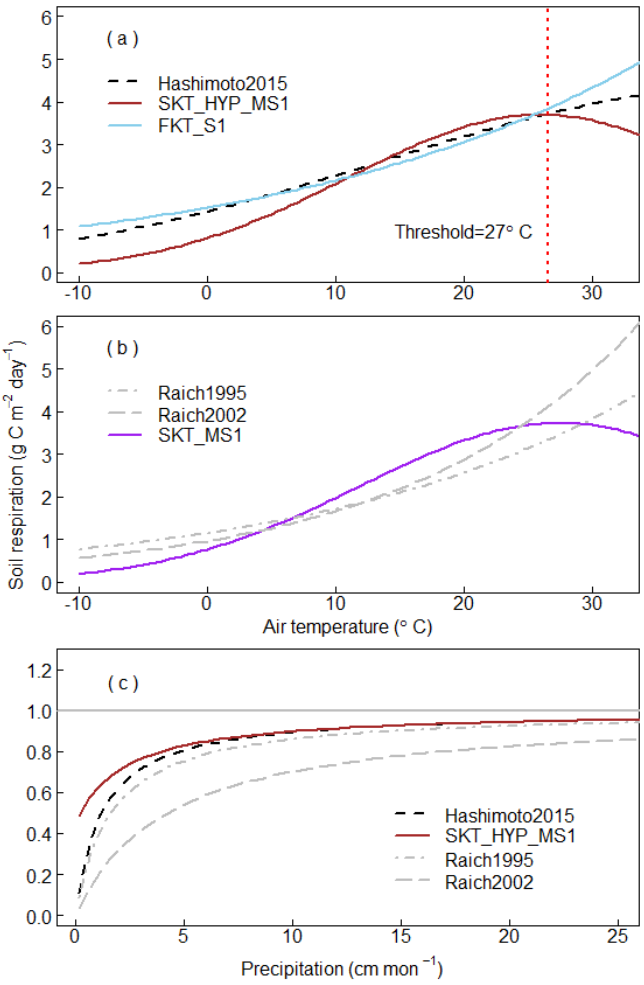

Figure 3-5. Comparison among temperature functions developed at this study with previous studies. (a) Hashimoto (2015)'s model followed the same format as the second-order exponential model with hyperbolic precipitation function model parameterized based on MS1(SKT_HYP_MS1), but is more similar to the first-order exponential model parameterized based on S1 (FKT_S1). (b) Rs estimated by the second-order exponential model parameterized based on MS1 (SKT_MS1) followed the same range of estimates by Raich et al. (1995) and Raich et al. (2002). (c) Precipitation multiplier of Hashimoto2015, SKT_HYP_MS1, Raich1995 and Raich2002 models. Note that in order to make the temperature relationship comparable in panel a and b, we first applied monthly precipitation data to parameters of above models, the average precipitation multiplier: 0.85 (Hashimoto2015), 0.87 (Raich1995), 0.77 (Raich2002) and 0.90 (SKT_HYP_MS1) were used to eliminate the effect of precipitation components.

The choice of time-scale in site Rs and temperature data also affects the degree of uncertainty introduced by assuming a constant Q_{10}. The largest source of uncertainty in our study (constant or variate Q_{10}: 12.35 Pg C), becomes apparent only when using the monthly time-scale temperature and Rs data, which resulted in a model that predicted a decrease in temperature sensitivity above 27 °C. This threshold of 27 °C is consistent with results from prior laboratory and field-scale warming experiments. For example, Hamdi *et al.* (2013) found a threshold of 25 °C in an analysis of 253 unique soils from 63 published laboratory studies. Carey *et al.* (2016) used a meta-analysis to evaluate more than 3800 experimental field-warming measurements and found that Rs rate response to temperature follow a Gaussian response with a threshold of approximately 25.0 °C. At the global scale, however, this threshold is only apparent in our monthly time-scale data. Previous global scale studies either assumed a first-order response or detected a threshold at higher temperatures (Hashimoto et al. 2015). This is the first study to observe this threshold at global scales, thus reconciling previous laboratory and field-scale observations with global scale phenomena.

One source of uncertainty we did not quantify in this study was the uneven spatial distribution of Rs records. In cold regions (such as the arctic), Rs was usually only measured during the growing season because of the extreme difficulty in measuring Rs during cold periods in those regions. Rs observations in cold regions are very important because fewer observations are made in arctic and arid regions than in temperate and tropical regions (B. Bond-Lamberty and Thomson 2010; Raich and Potter 1995; Raich and Schlesinger 1992). More importantly, Rs measured in cold regions expands the Rs records coverage range. Our study suggests that expanding the Rs records scale from annual to monthly helps resolve the geographic distribution problem, because many sites in cold regions can then be included. However, even though the

monthly time-scale increases the data available from arctic and arid regions, the Rs measurements from those regions were still far fewer than measurements from temperate and tropical regions, causing models to be biased toward temperate regions. Aggregating climate-region specific Rs models may help resolve the problem of continued spatial unevenness in Rs sampling.

3.4.2 Constraining global annual mean Rs

The models developed in this study provided quantitative measures of uncertainty that drive the divergence of current Rs estimates; however, constraining the global Rs range requires evaluating the conceptual assumptions and methodology. In some cases, such as Jensen's inequality and mismatching time-scales for climate input data, the source of uncertainty clearly biased estimates and should be excluded; however, other sources of uncertainty are conceptual issues that still need to be resolved. The first conceptual issue is whether to include variability in Q_{10}. In this study, the monthly time-scale data had a clear temperature threshold and the variable Q_{10} model better explained how Rs responded to temperature change. In the annual data, Rs was continuously accelerating. We argue that the variable Q_{10} model parameterized by the finer time-scale data best describes how Rs responds to temperature at global scales, because one, it includes a larger number of measurements representing a wider temperature range, and two, is conceptually consistent with a large number of laboratory incubation (Hamdi et al. 2013) and field warming experiments (Carey *et al.* 2016). The second conceptual issue is the hyperbolic precipitation function. In large-scale studies, precipitation is a surrogate for soil moisture due to the lack of extensive soil moisture data (Hashimoto et al. 2015). The SKT_HYP model was the best performing model and multiple studies observed large increases in Rs with increased

precipitation (S. Chen et al. 2014; Wang and Fang 2009); however, because the hyperbolic function always limits Rs, it cannot account for the pulse responses of Rs to increased soil moisture and thus may underestimate Rs. On the other hand, the SKT model assumes precipitation never limits Rs, thus will tend to overestimate Rs. Based on these conceptual considerations, we argue that the best estimate of global annual mean Rs lies between the estimate from the SKT_HYP model (70.85 Pg C yr^{-1}) and the estimate from the SKT model (80.99 Pg C yr^{-1}).

This conclusion is supported by the Rs estimate that emerges from quantifying Rs from global flux estimates of other components of the terrestrial carbon cycle. To make this comparison, we evaluated two approaches to partitioning the global carbon cycle from known estimates of the various fluxes and calculated the unknowns (Figure 3-6, Table 3-2, and Table 3-3). Both gross primary production (GPP, the atmospheric carbon that is synthesized into carbohydrates by plants) and net primary production [NPP, the remainder of C after portions are respired by plants (Ra)] are more constrained quantities, where GPP is 120 Pg C yr^{-1} (Prentice *et al.* 2007) and NPP is 56.2 Pg C yr^{-1} (Ito, 2011). In the first approach, from NPP we substracted carbon stored in the land sink (2.10 ±0.28 Pg C; Le Quéré *et al.* (2015)), burned by fire (3.53 Pg), drained and released to the atmosphere by fresh water (1.9 Pg), and consumed by forest and grassland herbivores (2.2 Pg C) (Figure 3-6 panel a and Table 3-2). The remainder was the carbon consumed by soil dwelling hetrotrophic respiration [Rh, 46.47 (±2.06) Pg C yr^{-1}](Figure 3-6 panel a). Based on a global analysis of the relationship between the Rh and belowground autotrophic (Rba) components of soil respiration (Bond-Lamberty, Wang, and Gower 2004), we used the ratio Rba/Rh = 0.75 (±0.16) to estimate Rba (35.18 ±8.98 Pg C yr^{-1}) (Figure 3-6 panel a and Table 3-2). The sum of Rh and Rba equaled an Rs of 81.86±10.55 Pg C yr^{-1}, close to the

SKT_MS1 estimate for global Rs (80.99 Pg C yr^{-1}). In the second approach to estimating Rs from the carbon cycle, we substracted the Rh calculated above from GPP to estiamte autrotrophic respiration (Ra), which equaled to 63.80 (± 1.78) Pg C yr^{-1}(Figure 3-6 panel b). Based on known fractions, we estimated C respired by roots (Rroots = 23.37±3.58 Pg C yr^{-1}), stems (Rstem = 16.01±2.91 Pg C yr^{-1}), and leaves (Rleaf = 24.42±3.71 Pg C yr^{-1}) (Figure 3-6 panel b). The sum of Rroot and Rh was 69.54 (±5.36) Pg C yr^{-1}, close to the global annual Rs estimats from the SKT_HYP_MS1 model (66.62 to 75.75 Pg C yr^{-1}). In sum, global annual mean Rs estimated by partitioning from global carbon flux ranged from 69.54 (±5.36) Pg C yr^{-1} to 81.65 (±10.55) Pg C yr^{-1}.

Table 3-2. Summary of published values on global carbon consumed by fire, herbivores animals and carbon sink by terrestrial ecosystem. Mean (± 95% confidence interval, if available) for each item was obtained or calculated based on data from the paper. N/A means data not available. Rba stands for belowground autotrophic respiration, Rh stands for heterotrophic respiration.

Item	Period	Amount (Pg)	Reference
NPP (56.20)	1862-2011	56.20 (± 1.78)	(Ito 2011)
Herbivores consumed (2.20)	N/A	1.40 (± 0.20)	(Doughty and Field 2010)
	N/A	3.00	(Whittaker and Likens 1973)
	1997-2009	2.00	(van der Werf et al. 2010)
	1960s	3.50 (± 1.50)	(Crutzen and Andreae 1990)
	N/A	7.30	(Gerber, Joos, and Prentice 2004)
Fire consumed carbon (3.53)	1901-2002	4.00	(Piao et al. 2009)
	1980-2000	5.10	(Zaehle et al. 2005)
	1920-1970	2.02	(Mieville et al. 2010)
	1970-2010	2.71	(Mieville et al. 2010)
	1900-2000	3.02 (± 0.30)	(Mouillot et al. 2006)
	1960-2000	2.08	(Schultz et al. 2008)
Land sink carbon (2.10)	1959-2014	(2.10± 0.28)	(Le Quéré et al. 2015)
Carbon washed away by fresh water (1.90)	N/A	1.90	(Cole et al. 2007)
	N/A	1.70	(Bastviken et al. 2011)
	N/A	2.10	(Deemer et al. 2016)
Rba / Rh	1983-2004	0.75 (± 0.16)	(Bond-Lamberty et al. 2004)

Table 3-3. Summary of papers separate leaf respiration fraction (Fl), stem respiration fraction (Fs) and root respiration fraction (Fr). N/A means data not available.

Fl (%)	Fs (%)	Fr (%)	Vegetation type	Reference
50.00	N/A	N/A	Tropical forest	(Allen and Lemon 1976)
53.00	35.00	12.00	Tropical forest	(Yoda 1983)
55.00	N/A	N/A	Warm-temperate forest	(Yoda 1978)
28.00	26.00	46.00	Temperate deciduous forest	(Edwards et al. 1981)
33.50	39.40	29.00	Pinus radiata trees	(Ryan et al. 1996)
31.60	39.40	29.00	Forest in northern Manitob, Canada	(Ryan, Lavigne, and Gower 1997)
43.17	34.53	22.30	Forest in Central Saskatchewa, Canada	(Ryan et al. 1997)
32.92	13.60	53.48†	Pine forest	(Law, Ryan, and Anthoni 1999)
75.08 (Fl + Fs)		24.92	Crop	(Suleau et al. 2011)
53.30 (Fl + Fs)		46.70	Young Beech forest	(Granier et al. 2000)
23.30	6.70	70.00	Tropical savanna	(Chen, Hutley, and Eamus 2003)
24.40	18.28	57.32†	Deciduous forest	(Bolstad et al. 2004)
31.27	26.01	42.72	Hardwood forest	(Curtis et al. 2005)
70.99 (Fl + Fs)		29.01	Spruce-dominated forest	(Davidson, Richardson, et al. 2006)
65.22 (Fl + Fs)		34.78	Temperate forest	(Nagy et al. 2006)
50.96 (Fl + Fs)		49.04	Rain forest	(Zhang et al. 2006)
63.57 (Fl + Fs)		36.43†	Douglas Fir	(Jassal et al. 2007)
46.22	17.07	36.71†	Scots Pine	(Zha et al. 2007)
38.10	26.33	35.57	Eucalyptus forest	(Keith et al. 2009)
41.49	12.04	46.47†	Scots pine forest	(Kolari et al. 2009)
50.51	21.21	28.28	Amazonian forests	(Malhi et al. 2009)
24.86	25.15	49.99	Pine forest	(Wieser et al. 2009)
63.79 (Fl + Fs)		36.21	Alpine meadow	(Zhang et al. 2009)
50.00	15.45	34.55	Black spruce forest	(Hermle et al. 2010)
22.96	34.31	42.73†	Brazil Eucalyptus	(Ryan et al. 2010)
55.52	19.42	25.06	Rain forest	(Tan et al. 2010)
76.45 (Fl + Fs)		23.55	Maize	(Jans et al. 2010)
30.70	43.15	26.15†	Eucalyptus plantation	(Campoe et al. 2012)
76.00 (Fl + Fs)		24.00†	Mediterranean pine forest	(Matteucci et al. 2015)
38.27(±2.54)	25.10(±2.49)	36.63(±2.48)	Average	

Label † means that root respiration was estimated from model: $R_A^{0.5} = -7.97 + 0.93Rs^{0.5}$ (units: g c m^{-2} yr^{-1}). (Bond-Lamberty et al. 2004).

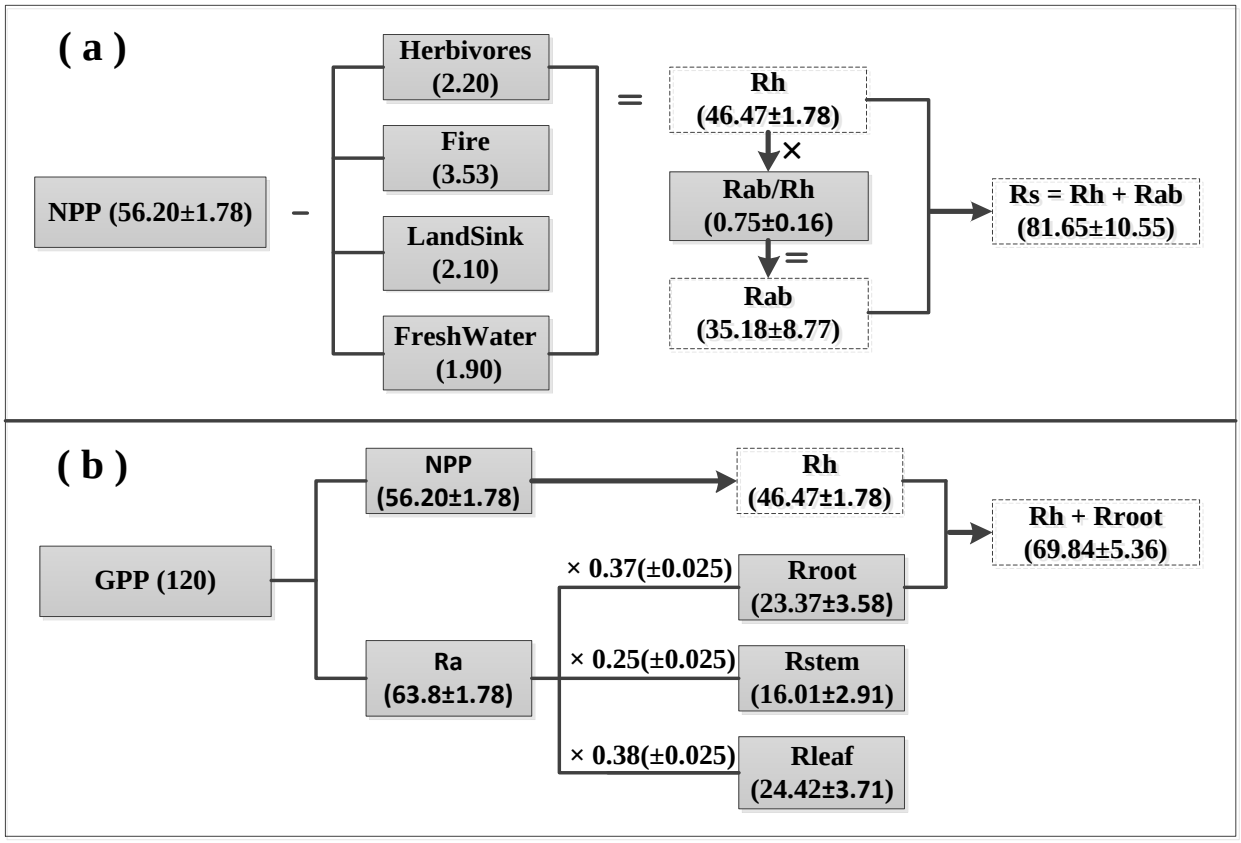

Figure 3-6. Inferring the global soil respiration from the global carbon terrestrial carbon budget. Solid filled boxes denote the values are mean (± 95% confidence interval) of data collected from the literature. The dashed boxes denote calculated values. All units are Pg C yr^{-1}. Abbreviations used are as follows: Gross Primary Production (GPP) was from (Prentice et al. 2007), Net Primary Production (NPP), autotrophic respiration (Ra), belowground autotrophic respiration (Rba), root respiration (Rroot), stem respiration (Rstem), leaf respiration (Rleaf), belowground heterotrophic respiration (Rh), and Soil respiration (Rs). Calculation in panel (a): Rh = NPP - Herbivores - Land Sink - Fire - Freshwater. Calculation in panel (b): Ra = GPP - NPP, Rroot = Ra × proportion of Rroot to Ra (0.37), Rstem = Ra × proportion of Rstem to Ra (0.25), Rleaf = Ra × proportion of Rleaf to Ra (0.38). For details and references about each carbon component, please see supplemental material Table 3-2 and Table 3-3.

The results of this study have significant implications for both our understanding of global carbon cycling and predictions made by land models. In the past few decades, land models have been developed to predict future climate and to understand the mechanisms that control the land carbon cycling. Their performance must be evaluated against benchmarks that verify the models are accurately simulating ecosystem responses and feedback to climate change

(Luo et al. 2012). The International Land Model Benchmark (ILAMB) specified the sources of benchmarks including: direct observations, experimental results, data-model products, and functional relationships or patterns (Luo et al. 2012). For Rs in land models, the annual time-scale global soil respiration database (Ben Bond-Lamberty and Thomson 2010) and data-model products (Ben Bond-Lamberty and Thomson 2010; Hashimoto et al. 2015) have acted as benchmark (Luo et al. 2012). Our global monthly Rs database and models may provide useful tools for benchmarking and development of Rs estimates in future land models. The monthly data extended the Rs range at both low and high temperature conditions and the overall number of observations, thus increasing the ability to detect the relationship between Rs and temperature.

3.5 CONCLUSIONS

Accurately estimating global Rs and how it responds to temperature change is important to determining global soil carbon dynamics under global warming. Rs data-oriented empirical models serve as benchmarks and help to constrain ESMs (Hashimoto et al. 2015). Quantifying the different sources of uncertainty in global Rs estimates helped to constrain the uncertainty in Rs projections. The results of this study also provide evidence for variable Rs-Q_{10} relationships in response to increasing temperatures. We found consensus between different conceptual approaches that the global annual mean Rs is closer to 70-80 Pg C yr^{-1}. Assuming a lower global Rs and decreasing temperature sensitive of Rs as temperature increase could substantially change the predicted rates of carbon turnover, the terrestrial carbon sink, and the feedback carbon-climate under global warming.

REFERENCES

Adachi, Minaco, Atsushi Ishida, Sarayudh Bunyavejchewin, Toshinori Okuda, and Hiroshi Koizumi. 2009. "Spatial and Temporal Variation in Soil Respiration in a Seasonally Dry Tropical Forest, Thailand." *Journal of Tropical Ecology* 25(5):531.

Allen, L. H. and E. R. Lemon. 1976. "Carbon Dioxide Exchange and Turbulence in a Costa Rican Tropical Rain Forest." *Vegetation and the atmosphere*, Lendon, Academic Press: 265–308.

Bastviken, David et al. 2011. "Freshwater Methane Emissions Offset the Continental Carbon Sink." *Science* 331(6013):50.

Bolstad, P. V, K. J. Davis, J. Martin, B. D. Cook, and W. Wang. 2004. "Component and Whole-System Respiration Fluxes in Northern Deciduous Forests." *Tree Physiology* 24(5):493–504.

Bond-Lamberty, B. P. and A. M. Thomsom. 2014. "A Global Database of Soil Respiration Data, Version 3.0." *Oak Ridge National Laboratory Distributed Active Archive Center, Oak Ridge, Tennessee, U.S.A.* http://dx.doi.org/10.3334/ORNLDAAC/1235.

Bond-Lamberty, B. and A. Thomson. 2010. "A Global Database of Soil Respiration Data." *Biogeosciences* 7(6):1915–26.

Bond-Lamberty, Ben and Allison Thomson. 2010. "Temperature-Associated Increases in the Global Soil Respiration Record." *Nature* 464(7288):579–82.

Bond-Lamberty, Ben, Chuankuan Wang, and Stith T. Gower. 2004. "A Global Relationship between the Heterotrophic and Autotrophic Components of Soil Respiration?" *Global Change Biology* 10(10):1756–66.

Bradford, M. A., W. R. Wieder, G. B. Bonan, P. A. Fierer, N. Raymond, and T. W. Crowther. 2016. "Managing Uncertainty in Soil Carbon Feedbacks to Climate Change." *Nature Climate Change* 6(8):751–58.

Campoe, Otavio C., Jose Luiz Stape, Jean Paul Laclau, Claire Marsden, and Yann Nouvellon. 2012. “Stand-Level Patterns of Carbon Fluxes and Partitioning in a Eucalyptus Grandis Plantation across a Gradient of Productivity, in Sao Paulo State, Brazil.” *Tree Physiology* 32(6):696–706.

Carey, Joanna C. et al. 2016. “Temperature Response of Soil Respiration Largely Unaltered with Experimental Warming.” *Proceedings of the National Academy of Sciences* 113(48):13793–802.

Chen, Shutao et al. 2010. “Modeling Interannual Variability of Global Soil Respiration from Climate and Soil Properties.” *Agricultural and Forest Meteorology* 150(4):590–605.

Chen, Shutao, Jianwen Zou, Zhenghua Hu, Haishan Chen, and Yanyu Lu. 2014. “Global Annual Soil Respiration in Relation to Climate, Soil Properties and Vegetation Characteristics: Summary of Available Data.” *Agricultural and Forest Meteorology* 198:335–46.

Chen, Xiaoyong, Lindsay B. Hutley, and Derek Eamus. 2003. “Carbon Balance of a Tropical Savanna of Northern Australia.” *Oecologia* 137(3):405–16.

Chen, Yujuan et al. 2014. “Influence of Urban Land Development and Soil Rehabilitation on Soil–atmosphere Greenhouse Gas Fluxes.” *Geoderma* 226–227:348–53.

Cole, J. J. et al. 2007. “Plumbing the Global Carbon Cycle: Integrating Inland Waters into the Terrestrial Carbon Budget.” *Ecosystems* 10(1):171–84.

Conant, Richard T. et al. 2011. “Temperature and Soil Organic Matter Decomposition Rates - Synthesis of Current Knowledge and a Way Forward.” *Global Change Biology* 17(11):3392–3404.

Crutzen, P. and M. O. Andreae. 1990. “Biomass Burning in the Tropics: Impact on Atmospheric Chemistry and Biogeochemical Cycles.” *Science* 250(4988):1669–78.

Curtis, P. S. et al. 2005. “Respiratory Carbon Losses and the Carbon-Use Efficiency of a Northern Hardwood Forest, 1999-2003.” *New Phytologist* 167(2):437–56.

Davidson, E. A. and Ivan A. Janssens. 2006. “Temperature Sensitivity of Soil Carbon Decomposition and Feedbacks to Climate Change.” *Nature* 440(7081):165–73.

Davidson, E. a, E. Belk, and R. D. Boone. 1998. “Soil Water Content and Temperature as Independent or Confounded Factors Controlling Soil Respiration in a Temperate Mixed Hardwood Forest.” *Global Change Biology*. 4(2):217–27.

Davidson, Eric A., Ivan A. Janssens, and Yiqi Lou. 2006. “On the Variability of Respiration in Terrestrial Ecosystems: Moving beyond Q10.” *Global Change Biology* 12(2):154–64.

Davidson, Eric A., A. D. Richardson, K. E. Savage, and D. Y. Hollinger. 2006. “A Distinct Seasonal Pattern of the Ratio of Soil Respiration to Total Ecosystem Respiration in a Spruce-Dominated Forest.” *Global Change Biology* 12(2):230–39.

Deemer, Bridget R. et al. 2016. “Greenhouse Gas Emissions from Reservoir Water Surfaces: A New Global Synthesis.” *BioScience* 66(11): 949-964.

Doughty, Christopher E. and Christopher B. Field. 2010. “Agricultural Net Primary Production in Relation to That Liberated by the Extinction of Pleistocene Mega-Herbivores: An Estimate of Agricultural Carrying Capacity?” *Environmental Research Letters* 5(4):44001.

Edwards, N. T. et al. 1981. “Carbon Metabolism in Terrestrial Ecosystems.” *Dynamic Properties of Forest Ecosystems*. Cambridge: Cambridge University Press.

Exbrayat, J. F., A. J. Pitman, and G. Abramowitz. 2014. “Response of Microbial Decomposition to Spin-up Explains CMIP5 Soil Carbon Range until 2100.” *Geoscientific Model Development* 7(6):2683–92.

Fang, C., John B. Moncrieff, Henry L. Gholz, and Kenneth L. Clark. 1998. “Soil CO_2 Efflux and Its Spatial Variation in a Florida Slash Pine Plantation.” *Plant and Soil* 205:135–46.

Feng, Huihui and Yuanbo Liu. 2015. “Combined Effects of Precipitation and Air Temperature on Soil Moisture in Different Land Covers in a Humid Basin.” *Journal of Hydrology* 531:1129–40.

Gerber, Stefan, Fortunat Joos, and Colin Prentice. 2004. “Sensitivity of a Dynamic Global Vegetation Model to Climate and Atmospheric CO_2.” *Global Change Biology* 10:1223–39.

Granier, A. et al. 2000. “The Carbon Balance of a Young Beech Forest.” *Functional Ecology* 14(3):2000.

Hamdi, Salwa, Fernando Moyano, Saidou Sall, Martial Bernoux, and Tiphaine Chevallier. 2013. “Synthesis Analysis of the Temperature Sensitivity of Soil Respiration from Laboratory Studies in Relation to Incubation Methods and Soil Conditions.” *Soil Biology and Biochemistry* 58:115–26.

Hashimoto, S. et al. 2015. “Global Spatiotemporal Distribution of Soil Respiration Modeled Using a Global Database.” *Biogeosciences Discussions* 12(5):4331–64.

Hermle, Sandra, Michael B. Lavigne, Pierre Y. Bernier, Onil Bergeron, and David Paré. 2010. “Component Respiration, Ecosystem Respiration and Net Primary Production of a Mature Black Spruce Forest in Northern Quebec.” *Tree Physiology* 30(4):527–40.

Hibbard, K. A., B. E. Law, M. Reichstein, and J. Sulzman. 2005. “An Analysis of Soil Respiration across Northern Hemisphere Temperate Ecosystems.” *Biogeochemistry* 73(1):29–70.

Ito, AKIHIKO. 2011. “A Historical Meta-Analysis of Global Terrestrial Net Primary Productivity: Are Estimates Converging?” *Global Change Biology* 17(10):3161–75.

Jans, W. W. P. et al. 2010. “Carbon Exchange of a Maize (Zea Mays L.) Crop: Influence of Phenology.” Agriculture, *Ecosystems and Environment* 139(3):316–24.

Janssens, I. A. et al. 2001. “Productivity Overshadows Temperature in Determining Soil and Ecosystem Respiration across European Forests.” *Global Change Biology* 7(3):269–78.

Jassal, Rachhpal S. et al. 2007. “Components of Ecosystem Respiration and an Estimate of Net Primary Productivity of an Intermediate-Aged Douglas-Fir Stand.” *Agricultural and Forest Meteorology* 144(1–2):44–57.

Karban, R., a a Agramal, and M. Mangel. 1997. “The Benefits of Induced Defense against Herbivores.” *Ecology* 78(5):1351–55.

Keith, H. et al. 2009. “Multiple Measurements Constrain Estimates of Net Carbon Exchange by a Eucalyptus Forest.” *Agricultural and Forest Meteorology* 149(3–4):535–58.

Kirschbaum, Miko U. F. 1995. “The Temperature Dependence of Soil Organic Matter Decomposition, and the Effect of Global Warming on Soil Organic C Storage.” *Soil Biology and Biochemistry* 27(6):753–60.

Kolari, Pasi et al. 2009. “CO_2 Exchange and Component CO_2 Fluxes of a Boreal Scots Pine Forest.” *Boreal Environment Research* 14(4):761–83.

Law, B. E., M. G. Ryan, and P. M. Anthoni. 1999. “Seasonal and Annual Respiration of a Ponderosa Pin Ecosystem.” *Global Change Biology* 5(2):169–82.

Lawrimore, Jay H. et al. 2011. “An Overview of the Global Historical Climatology Network Monthly Mean Temperature Data Set, Version 3.” *Journal of Geophysical Research Atmospheres* 116(19):1–18.

Lloyd, J. and J. A. Taylor. 1994. “On the Temperature Dependence of Soil Respiration.” *Functional Ecology* 8(3):315–23.

Luo, Y. Q. et al. 2012. “A Framework for Benchmarking Land Models.” *Biogeosciences* 9(10):3857–74.

Malhi, Yadvinder et al. 2009. “Comprehensive Assessment of Carbon Productivity, Allocation and Storage in Three Amazonian Forests.” *Global Change Biology* 15(5):1255–74.

Matteucci, Marco, Carsten Gruening, Ignacio Goded Ballarin, Guenther Seufert, and Alessandro Cescatti. 2015. “Components, Drivers and Temporal Dynamics of Ecosystem Respiration in a Mediterranean Pine Forest.” *Soil Biology and Biochemistry* 88:224–35.

Mieville, A. et al. 2010. “Emissions of Gases and Particles from Biomass Burning during the 20th Century Using Satellite Data and an Historical Reconstruction.” *Atmospheric Environment* 44(11):1469–77.

Mouillot, Florent, Ajay Narasimha, Yves Balkanski, Jean-François Lamarque, and Christopher B. Field. 2006. “Global Carbon Emissions from Biomass Burning in the 20th Century.” *Geophysical Research Letters* 33(1):2–5.

Nagy, Miklos T., Ivan A. Janssens, Jorge Curiel Yuste, Arnaud Carrara, and Reinhart Ceulemans. 2006. “Footprint-Adjusted Net Ecosystem CO_2 Exchange and Carbon Balance Components of a Temperate Forest.” *Agricultural and Forest Meteorology* 139(3):344–60.

Orchard, Valerie a. and F. J. Cook. 1983. “Relationship between Soil Respiration and Soil Moisture.” *Soil Biology and Biochemistry* 15(4):447–53.

Piao, Shilong et al. 2009. “Spatiotemporal Patterns of Terrestrial Carbon Cycle during the 20th Century.” *Global Biogeochemical Cycles* 23(4):1–16.

Prentice, I. C. et al. 2007. “The Carbon Cycle and Atmospheric Carbon Dioxide.” *Contribution of Working Group I to the Fourth Assessment Report of the Intergovernmental Panel on Climate Change*. Cambridge, United Kingdom: Cambridge University Press.

Le Quéré, Corinne et al. 2015. “Global Carbon Budget 2015.” *Earth System Science Data* 7(2):349–96.

R Core Team. 2014. *R: A Language and Environment for Statistical Computing. R Foundation for Statistical Computing*. Vienna, Austria.

Raich, J. W. and W. H. Schlesinger. 1992. “The Global Carbon Dioxide Flux in Soil Respiration and Its Relationship to Vegetation and Climate.” T*ellus* 44 B(2):81–99.

Raich, James W. and Christopher S. Potter. 1995. “Global Patterns of Carbon Dioxide Emissions from Soils.” *Global Biogeochemical Cycles* 9(1):23–36.

Raich, James W., Christopher S. Potter, and Dwipen Bhagawati. 2002. “Interannual Variability in Global Soil Respiration, 1980–94.” *Global Change Biology* 8(8):800–812.

Real, L. A. and J. H. Brown. 1991. *Foundations of Ecology*. Chicago, IL 60637： University of Chicago Press.

Reichstein, Markus et al. 2003. “Modeling Temporal and Large-Scale Spatial Variability of Soil Respiration from Soil Water Availability, Temperature and Vegetation Productivity Indices.” *Global Biogeochemical Cycles* 17(4):1104.

Ruel, Jonathan J. and Matthew P. Ayres. 1999. “Jensen’s Inequality Predicts Effects of Environmental Variation.” *Tree* 5347(99):361–66.

Ryan, M. G., M. B. Lavigne, and S. T. Gower. 1997. “Annual Carbon Cost of Autotrophic Respiration in Boreal Forest Ecosystems in Relation to Species and Climate.” *Journal of Geophysical Research* 102(D24):28871–83.

Ryan, Michael G. et al. 2010. “Factors Controlling Eucalyptus Productivity: How Water Availability and Stand Structure Alter Production and Carbon Allocation.” *Forest Ecology and Management* 259(9):1695–1703.

Ryan, Michael G., Robert M. Hubbard, Silvia Pongracic, R. J. Raison, and Ross E. M. C. Murtrie. 1996. “Foliage, Fine-Root, Woody-Tissue and Stand Respiration in Relation To Nitrogen Status.” *Tree Physiology* 16:333–43.

Schultz, Martin G. et al. 2008. “Global Wildland Fire Emissions from 1960 to 2000.” *Global Biogeochemical Cycle*s 22(2):1–17.

Sheng, Hao et al. 2010. “The Dynamic Response of Soil Respiration to Land-Use Changes in Subtropical China.” *Global Change Biology* 16(3):1107–21.

Skopp, J., M. D. Jawson, and J. W. Doran. 1990. “Steady-State Aerobic Microbial Activity as a Function of Soil Water Content.” *Soil Science Society of America Journal* 54(6):1619–25.

Smallwood, Peter D. 1996. “An Introduction to Risk Sensitivity: The Use of Jensen’s Inequality to Clarify Evolutionary Arguments of Adaptation and Constraint.” *American Zoologist* 36(4):392–401.

Soegaard, Henrik and Claus Nordstroem. 1999. “Carbon Dioxide Exchange in a High-Arctic Fen Estimated by Eddy Covariance Measurements and Modeling.” *Global Change Biology* 5(5):547–62.

Suleau, Marie et al. 2011. “Respiration of Three Belgian Crops: Partitioning of Total Ecosystem Respiration in Its Heterotrophic, above- and below-Ground Autotrophic Components.” *Agricultural and Forest Meteorology* 151(5):633–43.

Tan, Zhenghong et al. 2010. “Carbon Balance of a Primary Tropical Seasonal Rain Forest.” *Journal of Geophysical Research Atmospheres* 115(13):1–17.

Trumbore, Susan. 2006. “Carbon Respired by Terrestrial Ecosystems–recent Progress and Challenges.” *Global Change Biology* 2:141–53.

Wang, Wei, Weile Chen, and Shaopeng Wang. 2010. “Forest Soil Respiration and Its Heterotrophic and Autotrophic Components: Global Patterns and Responses to Temperature and Precipitation.” *Soil Biology and Biochemistry* 42(8):1236–44.

Wang, Wei and Jingyun Fang. 2009. “Soil Respiration and Human Effects on Global Grasslands.” *Global and Planetary Change* 67(1–2):20–28.

van der Werf, G. R. et al. 2010. “Global Fire Emissions and the Contribution of Deforestation, Savanna, Forest, Agricultural, and Peat Fires (1997–2009).” *Atmospheric Chemistry and Physics* 10(23):11707–35.

Whittaker, R. H. and G. E. Likens. 1973. “Carbon in the Biota.” *Carbon and biosphere*, U.S.A: National Technical Information Service.

Wieser, Gerhard et al. 2009. “Respiratory Fluxes in a Canary Islands Pine Forest.” *Tree Physiology* 29(3):457–66.

Wildung, R. E., T. R. Garland, and R. L. Buschbom. 1975. “The Interdependent Effects of Soil Temperature and Water Content on Soil Respiration Rate and Plant Root Decomposition in Arid Grassland Soils.” *Soil Biology and Biochemistry* 7(6):373–78.

Willmott, Cort J., Kenji Matsuura, and D. R. Legates. 2001. “Terrestrial Air Temperature and Precipitation: Monthly and Annual Time Series (1950-1999).” *Center for Climate Research*.

Yan, Liming, Shiping Chen, Jianyang Xia, and Yiqi Luo. 2014. “Precipitation Regime Shift Enhanced the Rain Pulse Effect on Soil Respiration in a Semi-Arid Steppe.” *PloS One* 9(8):e104217.

Yoda, K. 1978. “Estimation of Community Respiration.” *Biological Production in a Warm Temperate Evergreen Oak Forest of Japan.* Tokyo: University of Tokyo Press.

Yoda, K. 1983. “Community Respiration in a Lowland Rain Forest in Pasoh, Peninsular Malaysia.” *Japanese Journal of Ecology* 33(2):183–97.

Zaehle, S., S. Sitch, B. Smith, and F. Hatterman. 2005. “Effects of Parameter Uncertainties on the Modeling of Terrestrial Biosphere Dynamics.” *Global Biogeochemical Cycles* 19(3):1–16.

Zha, Tianshan, Zisheng Xing, Kai Yun Wang, Seppo Kellomaki, and Alan G. Barr. 2007. “Total and Component Carbon Fluxes of a Scots Pine Ecosystem from Chamber Measurements and Eddy Covariance.” *Annals of Botany* 99(2):345–53.

Zhang, Pengcheng, Yanhong Tang, Mitsuru Hirota, Akinori Yamamoto, and Shigeru Mariko. 2009. “Use of a Regression Method to Partition Sources of Ecosystem Respiration in an Alpine Meadow.” *Soil Biology and Biochemistry* 41(4):663–70.

Zhang, Yiping et al. 2006. “Annual Variation of Carbon Flux and Impact Factors in the Tropical Seasonal Rain Forest of Xishuangbanna, SW China.” *Science in China, Series D: Earth Sciences* 49(SUPPL. 2):150–62.

CHAPTER 4. Regional decreases with warming will not prevent increasing trends in global soil respiration.

ABSTRACT

Between 1960 and 2014, the global soil respiration (Rs) flux accelerated at a rate of 0.05 Pg C yr^{-1}; however, future acceleration is uncertain. Differences in the sensitivity of Rs to temperature change may alter the regional acceleration rates of Rs, where the Rs rates of some regions may decelerate while others continue to rise. Here, using monthly global Rs data, we modeled the relationship between Rs and temperature for the globe and eight climate regions, and estimated annual Rs for two time periods (1961-2014 and 2015-2100) using historical temperature data and two future temperature scenarios (RCP 2.6 and 8.5). We found that historical acceleration of global annual Rs (0.05 Pg C yr^{-1}) was similar to previous historical estimates; however, under the RCP8.5 scenario, which estimates approximately 3ºC of warming globally, the forecasted acceleration of Rs increased from 0.05 to 0.11 and 0.13 Pg C yr^{-1}. Under this scenario, we observed a declining temperature sensitivity of Rs in the arid, winter-dry temperate and tropical climates; however, these regional decelerations were offset by large Rs accelerations in the boreal and polar regions. In contrast, under the RCP 2.6 scenario (a < 1ºC warming) the global Rs rate decelerated slightly from current rates. If rising greenhouse gas emission remain unmitigated, this work suggests that future acceleration of Rs will be much faster than current and historical rates, thereby enhancing future losses of soil carbon and contributing to positive feedbacks of climate change.

4.1 INTRODUCTION

Soil respiration (Rs), the production of carbon dioxide from the soil when plant roots, microbes and fauna respire, is the second largest carbon flux between the land and atmosphere (Raich and Schlesinger 1992; Zhao et al. 2017). From 1961 to 2011, global Rs rates increased on average by 0.04 to 0.10 Pg C yr^{-1} (Ben Bond-Lamberty and Thomson 2010; Hashimoto et al. 2015; Zhao et al. 2017). While these historical trends provide some insight, the future rate of change in global Rs remains uncertain, the future rate of change of global temperatures and global Rs rise remain uncertain. This uncertainty in global Rs is due, in part, to a lack of knowledge regarding how regional Rs rates will respond to rising temperatures. Globally, average maximum and minimum temperatures over land have both increased by 0.1°C per decade since 1950 (Flato et al. 2013); however, in high-latitude regions, temperature has risen much faster than the global average, 0.6 °C per decade over the last 30 years (Schuur et al. 2015). Temperature is a critical driver of Rs. Assumptions regarding the sensitivity of Rs to temperature change significantly affect predictions of global Rs rates, and how those rates will respond to global warming (Davidson and Janssens 2006; Janssens et al. 2001; Trumbore 2006). When temperatures rise above a certain threshold, Rs rates level off or begin to decline (Lellei-Kovacs et al., 2011; Parker et al., 1983); however, the temperature sensitivity of Rs differs with climates and biomes (Zhao et al. 2017). A recent study found that Rs rates in specific biomes are already less sensitive to temperature increases (Zhao et al. 2017). In warm climates, declining Rs rates might dampen global Rs rates as temperatures increase; however, increasing Rs rates in colder regions may outweight any warm regional declines. This heterogeneity in regional-scale sensitivity of Rs could play an important role in future global Rs fluxes and feedbacks to climate change.

The temperature sensitivity of Rs can be quantified by Q_{10} functions, where Q_{10} is a measure of the change in rate of Rs as temperature increases 10 ℃ (Lloyd and Taylor 1994). In ecosystem models constant Q_{10} functions (a thumb of rule is $Q_{10} = 2$) were widely used (Conant, Ryan, Agren, et al. 2011). Likewise, global scale soil respiration models also assume a linear relationship, or constant Q_{10} relationships between Rs and temperature (Raich and Potter 1995; Raich et al. 2002). Under linear or constant Q_{10} models, as global temperatures rise, so do global Rs fluxes (Ben Bond-Lamberty and Thomson 2010). However, numerous laboratory and warming experiments demonstrate that Rs rates declines when temperatures rise above specific optimums (Bradford et al. 2008; Crowther and Bradford 2013; Frey et al. 2013; Luo et al. 2001; Sistla et al. 2013). For example, a meta-analysis analyzed Rs measurements from 27 experimental field-warming studies and found the Gaussian model best explain how Rs responds to temperature in both control sites and warming sites. Moreover, they detected a threshold of approximately 25.0 °C (Carey *et al.* 2016). Based on soils originating from different ecosystems (including forest, grassland, cultivated, tundra, peat-land and polar), incubated from a few hours to 720 days and from -15℃ to 55℃, , a recent meta-analysis found that Q_{10} values of Rs ranged from 0.5 to 300, and the Q_{10} values negatively correlated to soil temperature when temperature below 25℃ (Hamdi et al. 2013). These studies suggested that warmer regional temperatures should result in a leveling off or decline of Rs rates when temperatures are obove the optimum, which is more likely to occur in the future as temperatures rise.

Differences in regions will likely result in differences in fluxes and temperature sensitivity. The annual Rs rate varies from several g C m^{-2} $year^{-1}$ in the desert and tundra to thousands of g C m^{-2} $year^{-1}$ in biomes such as temperate and tropic forests (Conant et al., 1998; Jin et al., 2010; Christiansen et al., 2012; Chunming, 2010; H. Fang et al., 2012; Lin et al., 2011;

Brito et al., 2009; Panosso et al., 2009; Pendall et al., 2010). Even within similar biomes, annual Rs rate varies with mean annual precipitation (MAP) and mean annual temperature (MAT). For instance, in a previous study, Wang et al. (2010) found that annual Rs rates from naturally-regenerated forests ranged from 220 to 2560 g C m^{-2} yr^{-1} and were positively correlated with MAT. Wang et al. (2010) found that Rs was more sensitive to MAP change (slope = 0.753) when MAP was <813 mm, but less sensitive when MAP was >813 mm (slope = 0.203). In another study on world grasslands, Wang & Fang (2009) found that annual Rs rate ranged from 52.1 g C m^{-2} yr^{-1} to 1004 g C m^{-2} yr^{-1} in different grasslands. The Rs rates were positively correlated with MAT, but again soil respiration changed with annual precipitation followed a polynomial trend (Wang and Fang, 2009). These differing responses of Rs to MAT and MAP create heterogeneity in the temperature sensitivity (Q_{10}) among different biomes. For example, by collecting 173 estimates of the Q_{10} value assembled from 90 published studies across Chinese forest ecosystems, Song et al. (2014) found that Q_{10} values in the forests of China significantly decreased with the MAT but increased with elevation and latitude. Across the global forest biomes, Q_{10} of evergreen broad forest was significantly lower than that of deciduous broad forest and evergreen needle forest (Wang et al. 2010). Regional and biome specific differences in temperature sensitivity will result in regional differences in Rs as temperatures rise.

The heterogeneity of temperature sensitivity of Rs may affect how soil carbon stocks will respond to temperature warming. Numerous studies find that carbon stocks decrease with warming trends, but that decrease is regionally heterogeneous (Cramer et al. 2001; Davidson 2016; Dorrepaal et al. 2009; Frey et al. 2013; Karhu et al. 2014; Lu et al. 2013). For example, between 1978 and 2003 soil carbon was lost at a mean rate of 0.6% yr^{-1} across England and Wales due to climate change (Bellamy et al. 2005). Across North America, Europe and Asia, T.

Crowther et al. (2016) found that the effects of warming on soil carbon loss depend on the initial soil carbon stock, with loss considerable soil carbon at high-latitudes due to its high carbon stocks. Schuur et al. (2015) found that around 20% and 10% of soil carbon will be released after 10 years of incubation from the organic soils and mineral soils, respectively. However, other studies found that soil carbon does not show clear decrease trend or even increased under temperature warming (Liski et al., 1999; Sistla et al., 2013). Some of this heterogeneity may be linked to increases in plant biomass and changing, or may be linked to differences in loss of carbon through Rs (Conant et al., 2011). The regional heterogeneity of Rs rates and sensitivity may partially control carbon cycling and the feedbacks to climate change from regional to global scales (Bahn et al. 2008; Fang et al. 1998; Raich and Schlesinger 1992).

Accurate modeling of Rs and carbon cycling across multiple scales is essential for predicting Rs response to climate change. Early global Rs modeling only included coarse biome classifications. For instance, Raich & Potter (1995) analyzed the heterogeneity of Rs responds to environmental factors within three biomes (moist biomes with no dramatic dry season, biomes with a distinct dry season, and wetlands) and created three biome-specific models to estimate global Rs. A major obstacle that causes uncertainty in regional and global Rs modeling is insufficient annual Rs field records with unequal distribution across localities and biomes (Raich et al. 2002). The number of site Rs measurements increased substantially over the past several decades to explore how soil efflux may respond to climate change. Subsequently, a continuously updated annual time-scale global Rs database (SRDB) was developed (Bond-Lamberty and Thomsom 2014). Based on the SRDB, Ben Bond-Lamberty & Thomson (2010) built boreal, temperate, and tropical specific models to estimate global Rs and analyzed how Rs responds to global warming. In a recent study, by integrating Rs data from SRDB, a new compendium of Rs

data for Africa (Epule 2015), and field Rs records from China (Song et al. 2014), artificial neural network models were developed to estimate Rs for 10 biomes in the globe (Zhao et al. 2017). This study also developed a global Rs model which integrated the most up-to-date and complete global scale Rs dataset available, but some biomes such as desert (n=14), savanna (n=16), shurbland (n=37), tundra (n=19), and wetlands (n=54) still have less than 100 of Rs records to support Rs modeling (Zhao et al. 2017). According to an analysis on how sample size affects Rs model parameterization, at least 100 data points are required to avoid added uncertainty (Jian et al. 2017, Chapter 3). Downscaling the global Rs database from annual time-scale to monthly time-scale helps to resolve the insufficient Rs records problem by increasing sample size (if the measurement frequency larger than once per year) and including measurements that does not cover a whole year. Increasing the number of measurements should help increase the accuracy of regional scale Rs estimates and models.

In this study, our goal was to determine how the future global Rs rates will change with predicted increases temperatures, and if the decreases in the sensitivity of Rs to temperature changes in some regions will offset acceleration in other regions enough to dampen future global fluxes. The specific objectives of this study were to: (1) model the relationships between Rs and air temperature (T_a) for eight climate regions, (2) estimate annual Rs fluxes for each region and aggregated to the global scale, (3) predict annual Rs fluxes from 1961 to 2014 and compared the temporal patterns of single vs. multiple models, and (4) estimate global annual Rs may respond to temperature increase under differing climate changes scenarios from 2015 to 2100. Understanding how the regional-scale dynamics affect global Rs rates under future temperatures enhances our ability to predict changes in carbon stocks and their interaction with climate change (Wieder, Bonan, and Allison 2013).

4.2 DATA AND METHODS

4.2.1 Data

We created a global monthly temperature and soil respiration database to support single and climate-specific Rs modeling. Global 0.5° latitude × 0.5° longitude spatial resolution and monthly air temperature between 1961 and 2014 were collected from the Center for Climate Research at the University of Delaware (Willmott et al. 2001). Global air temperature between 2015 and 2100 were collected from a Geophysical Fluid Dynamics Laboratory ESM2G (GFDL-ESM2G) model (https://www.gfdl.noaa.gov/earth-system-model/), for both the Representative Concentration Pathways with a possible radiative forcing value increase 2.6 W/m^2 (RCP2.6) and 8.5 W/m^2 (RCP8.5). We used air temperature from GFDL-ESM2G model because of its coverage of the whole study period with temporal solution of monthly. We compared air temperature data between 2011 to 2014 from both data sources, and the result showed that air temperature from GFDL-ESM2G model were highly correlated with air temperature from the Center for Climate Research at the University of Delaware (adj $R^2 = 0.84$, data not shown). According to the IPCC AR5 report which compared as much as 42 climate models (Flato et al. 2013) and another study compared 23 climate models from CMIP5 (Forster et al. 2013), air temperature predicted by GFDL-ESM2G model is close but slightly lower than the mean of multiple models. All data used for this study can be found at https://data.lib.vt.edu/collections/ns0646000.

Past estimates of the historical Rs acceleration were based on annual time-scale Rs data (Ben Bond-Lamberty and Thomson 2010; Raich and Potter 1995; Raich and Schlesinger 1992; Zhao et al. 2017), but here we used monthly time-scale data for two reasons. One, the temperature sensitivity of Rs differs with time-scale of data. Short-term increases in temperature

often cause a non-linear response in Rs (Davidson and Janssens 2006; Davidson, Janssens, et al. 2006). Likewise, comparisons of global Rs predicted from annual time-scale and a monthly time-scale data found that only monthly time-scale temperature and Rs data followed a second-order-exponential change, with a threshold at 27 °C (Jian et al. 2017, Chapter 3). Two, it has long been recognized that the uneven spatial distribution of Rs records could bias global Rs estimates (Raich and Schlesinger 1992). To avoid the bias caused by sample size, at least 100 Rs records are required to parameterize the model in each region (Jian et al. 2017, Chapter 3). In arid and polar regions, however, very limited measurements are available and many of those Rs measurements were taken during warm periods rather than throughout the whole year. By using monthly time-scale data, we can incorporate more Rs measurements in these regions. Therefore, in order to increase Rs data measurements to support climate-specific models parameterization and to capture the second-order-exponential relationship between Rs and temperature, in this study, we used a monthly time-scale global soil respiration data.

To develop a Monthly Time-scale Global Soil Respiration Database (MGRsD), we collected 619 English language papers from the global Soil Respiration Database (B. Bond-Lamberty and Thomson 2010). In addition, we collected 50 papers published in Chinese with English abstracts from another meta-analysis (S. Chen et al. 2014). Since these two meta-analyses only provide publications before 2011, additional publications were gathered via a literature search using ISI Web of Science for papers published after 2011. This generated an additional 54 papers published after 2011. We digitized most of the Rs data from figures reported in the original papers using Data Thief (version III, http://datathief.org/).

We used the following criteria to determine if data would be included in the database. (1) The publication reported monthly, daily or sub-daily Rs rate. (2) If experiments exposed soil to

treatments (for example, nitrogen addition, air/soil warming, rain/litter exclude), only Rs measurements from control plot were included. (3) Rs collected with alkaline absorption were included only if the area of absorption was > 6% of the chamber area and the chambers were inserted > 5 cm into the soil. Otherwise alkaline absorption underestimates actual fluxes (Raich and Nadelhoffer 1989). After digitization, all data was aggregated to a monthly time-scale and normalized to g C m^{-2} day^{-1}. If measurements within same location (latitude and longitude is same) and within same month of a year, the measurements were averaged to obtain a mean Rs rate. A number of ancillary data were collected. The date and location (latitude and longitude) of Rs records were directly collected from the papers. Climate classification was based on Koppen climate classification (http://koeppen-geiger.vu-wien.ac.at/).

Quality control was performed to guarantee the quality of the data. When all digitization was finished, we mapped sites by countries in ArcGIS (ESRI v10.2) to identify incorrect latitude or longitude information. After site locations were checked, the climate, air temperatures, monthly precipitation, soil properties information of every site were collected based on latitude and longitude information. In addition, if the papers reported annual Rs and the monthly Rs covered whole year, we summed them to an annual time-scale and compared with the reported annual Rs from paper or from SRDB. We assumed the data was digitized correctly when the gap between the averaged Rs annual mean and paper reported or SRDB reported Rs annual mean was small. We also checked Rs versus air temperature scatter plot by site to inspect the relationship. If the Rs versus air temperature follows relationship rather than a linear increase, a nonlinear first order exponential, or second order exponential growth, we double check the digitized data with original paper.

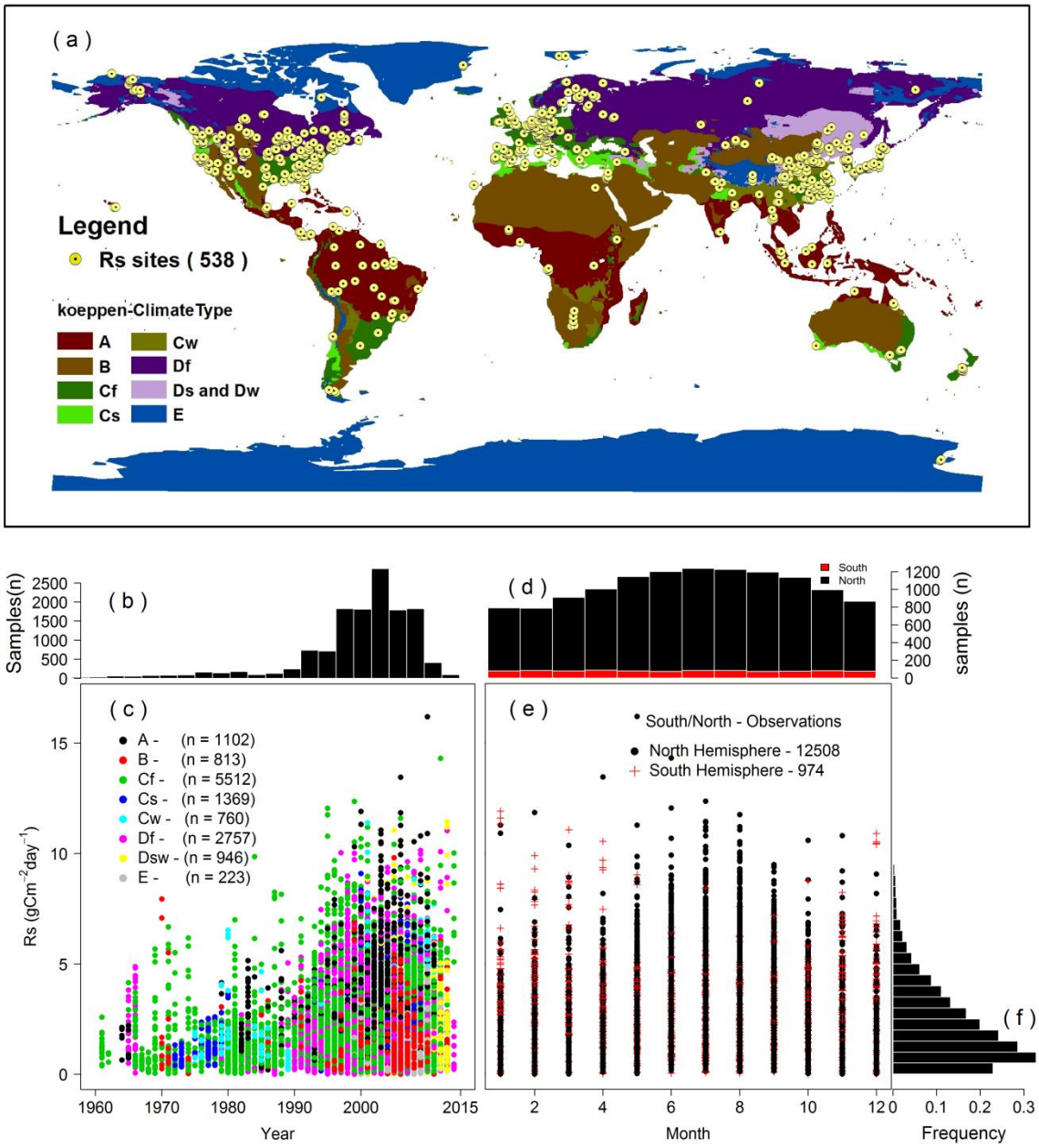

Figure 4-1. Spatial and temporal distribution of the monthly global soil respiration database (MGRsD) in tropical (A), arid (B), temperate humid (Cf), temperate summer dry (Cs), temperate winter dry (Cw), boreal humid (Df), boreal summer dry or winter dry (Dsw) and polar (E) climate regions. a) Sites labeled as "Rs sites" include 538 sites from monthly global soil respiration database (MGRsD). b) The frequency of soil respiration (Rs) records from 1961 to 2014. c) The distribution of soil respiration measurements from 1961 to 2014 by different climate regions, labeled by different colors. d) The frequency of soil respiration observations distribution from January to December. e) The distribution soil respiration records from January to December in the south (red crosses) and north hemispheres (black dots). f) The distribution of soil respiration measurements by soil respiration rate.

After criteria and quality control, the MGRsD included records from 57 countries, including 14 Rs measurements from Antarctica (Figure 4-1 panel a). The collected Rs records at MGRsD were dispersed from 1961 to 2014, with more data available from 1990 to 2010 (Figure 4-1 panel b and c). More data were available from the Northern hemisphere (12508) than Southern hemisphere (974), and from temperate and boreal regions compared to tropical and polar regions (Figure 4-1 panel c, d, and e). In the Northern hemisphere, more Rs measurements were available during the growing season than other months (Figure 4-1 panel d, the black bars), while in the Southern hemisphere, the Rs measurements were evenly distributed among months (Figure 4-1 panel d, the red bars). Rs rate in the MGRsD ranges from 0.001 to 16.201 g C m^{-2} day^{-1}, but showed heavily right skew distribution (tail at high rate), with more data under lower Rs rate range (Figure 4-1 panel f).

4.2.2 Global soil respiration modeling

We tested a simple linear model, first order (equation 4-1) and second order (equation 2) exponential relationships between Rs and air temperature for the global scale and in each climate region. A first-order exponential model, where Q_{10} is a constant value, means that Rs responds positively to temperature increase. A second order exponential model, where Q_{10} negatively is related with air temperature (when parameter b > 0 in equation 4-2).

$$Rs = F \times EXP^{a \times Tm} \quad (4\text{-}1)$$

$$Rs = F \times EXP^{(a \times Tm - b \times Tm^2)} \quad (4\text{-}2)$$

Where F indicates the Rs rate when air temperature (Tm) is zero, *a* indicates the increase rate of Rs with air temperature. In the second order exponential, *b* donates a second order growth of Rs with air temperature, where if $b > 0$, there is a threshold (i.e. optimum air temperature for

Rs) temperature in the relationship, where Rs increases with air temperature below this threshold temperature and decreases with air temperature when greater than this threshold. We parameterized both single global Rs model and climate-specific models using the maximum likelihood estimation approach in R (R 2014). Lastly, we calculated a threshold based on the second order exponential model (equation 4-3).

$$\text{Threshold} = \frac{-a}{2 \times b} \quad (4\text{-}3)$$

4.2.3 Future and historical Rs estimation

For each climate region and the globe, the best performing model was selected to estimate Rs of the study period (Table 4-1). We predicted global Rs from 1961 to 2014 at a spatial resolution of 0.5° longitude × 0.5° latitude and a monthly time-scale. According to a recent analysis of Rs response to temperature under warming versus control temperatures, the reginal (except desert region) and global response of Rs to temperature remained unaltered with warming, in other words, the relationship between Rs and temperature remained not unaltered under soil warming treatment (Carey et al., 2016). Based on the monthly global Rs data, we separated Rs into two groups: Rs measured before 2000 (treat as control), and Rs measured after 2000 (average temperature is about 0.5 ℃ higher than first group, treat as warming condition), we then compared the relationship between Rs and air temperature before 2000 and after 2000, our results showed that how Rs responds to temperature does not significantly differ before or after 2000 (statistis results not shown). We thus assume that it is appropriate to predict the future Rs by the Rs models developed at this study based on historical Rs records. Global Rs from 2015 to 2100 were estimated based on the single global Rs model and climate-specific Rs models using air temperature predictions of the GFDL-ESM2G model under both global warming

scenarios RCP2.6 and RCP8.5. Our models were adjusted to align with the spatial resolution of the GFDL-ESMG2 (2.5 ° longitude × 2.0° latitude) temperature predictions. These three data sets, historical and predicted 2.6 and 8.5 were then aggregated at an annual scale and subjected to further analyses to explore how global annual Rs will change under global warming.

Table 4-1. Parameter summary of soil respiration models for all data and for each climate region. Note that $p < 0.001$ for all parameters except in tropical ($P > 0.05$ for parameter F, labeled by bold italic) and arid ($P < 0.05$ for parameter b, labeled by*).

	F	a	b	Threshold	R^2 (%)	MSE	Records (n)
Single	0.77(±0.024)	0.11(±0.004)	0.002(±0.0001)	27.50	30.53	1.5	13482
Regional							
Tropical	***0.01(±0.02)***	0.43(±0.10)	0.008(±0.002)	26.30	3.72	2.01	1092
Arid	0.68(±0.13)	0.08(±0.02)	0.001(±0.0005)*	28.05	9.51	1.52	813
Temperate							
Humid	0.60(±0.03)	0.13(±0.0.006)	0.002(±0.0.0002)	28.33	34.77	1.35	5512
Summer dry	1.03(±0.08)	0.14(±0.01)	0.004(±0.0004)	14.39	12.22	1.43	1369
Winter dry	0.43(±0.09)	0.15(±0.02)	0.003(±0.0005)	27.12	24.42	1.38	760
Boreal							
Humid	0.86(±0.04)	0.11(±0.006)	0.001(±0.0002)	/	50.72	1.31	2757
Dry	0.83(±0.05)	0.07(±0.003)	/	/	49.19	1.33	946
Polar	1.02(±0.09)	0.10(±0.01)	/	/	42.74	1.03	223

To determine whether temperature sensitivity decrease at the regional and global scales might affect Rs response to temperature warming in the future, we also analyzed three data sets for the Rs anomalies versus temperature anomalies. Rs or temperature anomalies are the difference between Rs or temperature at specific year and the long-term average Rs or temperature, which present a clearer relationship of how Rs responds to temperature warming than Rs or temperature themselves (Ben Bond-Lamberty and Thomson 2010; Hansen et al. 2010; Hashimoto et al. 2015). In order to make the relationship between Rs anomalies and temperature anomalies for three scenarios (historical, RCP2.6 and RCP8.5) centered at a same original point and thus easier to compare, we used mean Rs or temperature within each group as the reference

point. To test for whether reginal and global decrease in temperature sensitivity of Rs lead to Rs deceleration, we analyzed how the Rs anomalies correlated with temperature anomalies for three scenarios: historically from 1961 to 2014 and both future (2015 to 2100) temperature scenarios (RCP2.6 and RCP8.5). Positive correlations indicated increases in Rs with temperature (acceleration), whereas null or negative correlations indicated that Rs does not respond or decreases with temperature (deceleration).

4.3 RESULTS

4.3.1 Regional and Global historical Rs Estimates

The global annual mean Rs from 1961 to 2014 was 78.34 ± 4.4 Pg C yr^{-1} when estimated by the single model, and 72.55 ± 13.97 Pg C yr^{-1} when estimated by the climate-specific models (Table 4-2). The climate-specific Rs models captured the magnitude of Rs for all climate regions with reasonable accuracy, but the single model overestimated Rs in arid region and underestimated Rs in cold regions (Figure 4-2, note only Rs measurements from north hemisphere were used). The difference between Rs estimates from the single and climate-specific models at the regional scale ranged from -2.14 to +9.67 Pg C yr^{-1} (Table 4-2). The single model overestimated Rs rates in arid regions, which lead to a cumulative difference of 9.67 Pg, approximately 55% of the annual flux (Table 4-2), due to the large area of arid region (17.80%). In contrast, the single model underestimated Rs by 0.14 to 2.14 Pg in boreal and polar regions (Table 4-2). The single model underestimated annual Rs by 1.65 Pg C yr^{-1}, approximately 40% of the flux in polar region. For the temperate region, the difference between single model and climate region specific model were very small (Table 4-2).

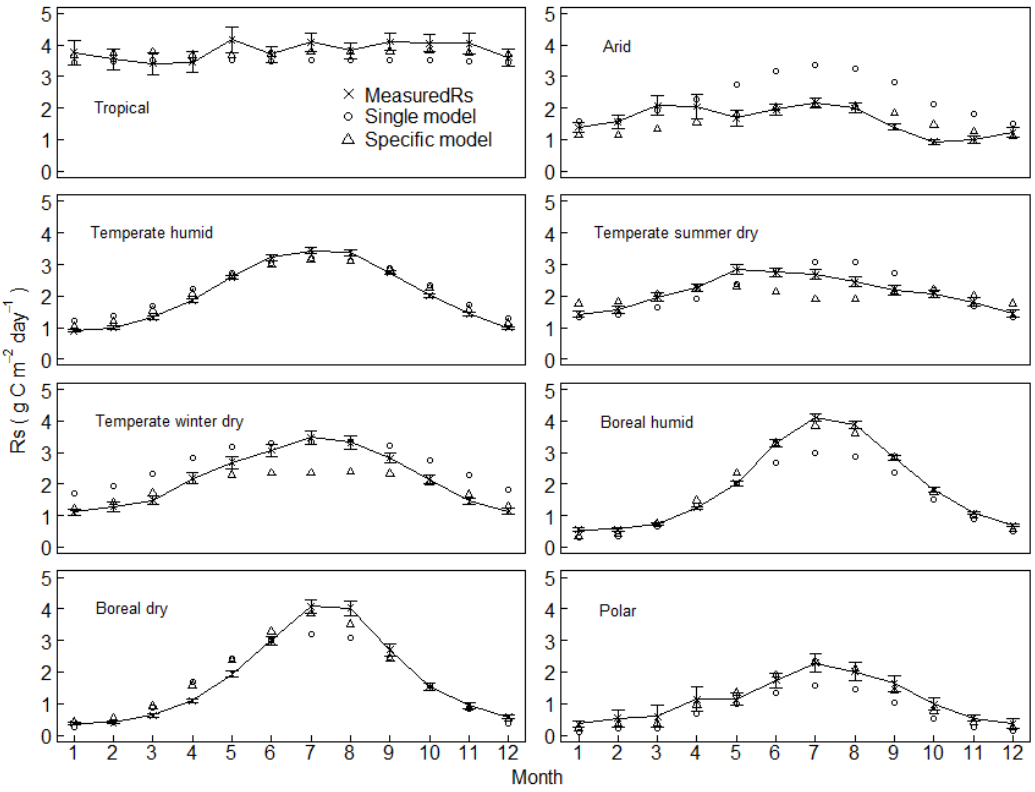

Figure 4-2. Validation plots present the predictive strength of the statistical models across eight climate regions. Black cross dots are the mean of measured soil respiration from MGRsD by climate region, while black bar indicate the 95% confidence interval, black circle dots are the mean of Rs estimated by single model, while the black triangles are the mean of Rs estimated by climate region specific model. Comparing measured Rs with modelled Rs requires awareness that climate specific Rs models have captured the magnitude of Rs for all climate regions with reasonable accuracy, but the single model tend to overestimate Rs in arid region but underestimate Rs in cold regions. Note that only Rs measurements from north hemisphere were used.

Air temperature explained some variation in Rs for all regions; however, air temperature explained more Rs variability in colder regions than in warmer regions (Table 4-1 and Figure 4-3). The nature of the Rs vs. air temperature relationship also differed among regions. In warmer regions, the second-order models best fit temperature responses (Smallest AIC value in Figure 4-3), while a first-order models best fit temperature responses in the polar and boreal regions (Figure 4-3 and Table 4-1). The air temperature thresholds for Rs under warmer regions ranged from 14.4 to 28.3℃ (Figure 4-3, identified by vertical lines). A threshold was also calculated for

the boreal humid region (36.98 ℃); however, the threshold temperature was greater than the highest monthly air temperature records from the climate data in this region and we remain skeptical of accuracy of the threshold in this region.

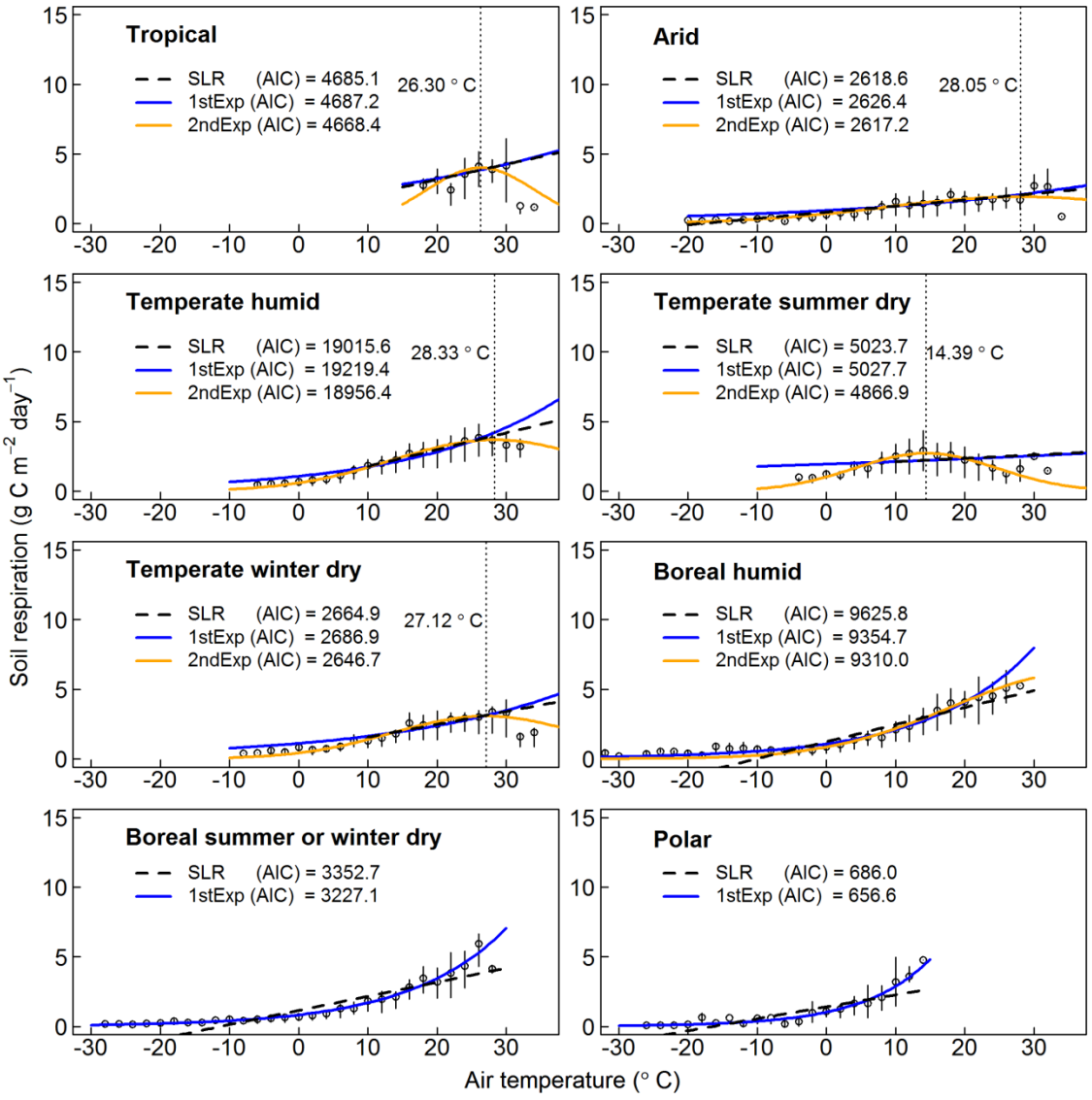

Figure 4-3. Soil respiration versus air temperature scatter plot and regression in different climates. Open circles indicate median Rs and bars indicate first and third quartiles. Akaike information criterion (AIC) values are compared to identify which model better explains soil respiration variability, smaller AIC value indicates a better model. If ploted, regressions are significant at $p < 0.05$. Note the error bars in panels are first and third quantile.

Table 4-2. Area extent and estimated mean annual soil respiration rate (Rs) of globe for eight climate regions classified by Koeppen_Geiger classification. Tropical (A), Arid (B), Temperate humid (Cf), Temperate summer dry (Cs), Temperate winter dry (Cw), Boreal humid (Df), Boreal summer dry or winter dry (Dsw) and Polar (E). Grid cells were 0.5 ° latitude × 0.5 ° longitude; each cell area was calculated as 0.173905×10^4 km^2. The mean Rs was weighted by region area and was averaged for each vegetation coverage from 1961 to 2014.

			Single model		Climate-specific models		
Climate Region	Number of grid cells	Area (10^4 km^2)	Mean Rs rate (g C m^{-2} day^{-1})	Annual mean Rs (Pg C yr^{-1})	Mean Rs rate (g C m^{-2} day^{-1})	Annual mean Rs (Pg C yr^{-1})	Difference (Single model–Specific)
A	9746 (11.36%)	1695	3.47	21.45	3.73	23.11	-1.66 (-7.2%)
B	15273 (17.80%)	2656	2.82	27.31	1.82	17.64	+9.67 (+54.8%)
Cf	4868 (5.67%)	847	2.36	7.29	2.25	6.97	+0.32 (+4.6%)
Cs	1590 (1.85%)	276	2.35	2.37	1.96	1.98	+0.39 (+19.7%)
Cw	2046 (2.38%)	356	2.86	3.71	2.09	2.71	+1.00 (+36.9%)
Df	17047 (19.87%)	2964	1.06	11.49	1.26	13.63	-2.14 (-15.7%)
Dsw	2902 (3.38%)	505	1.21	2.22	1.28	2.36	-0.14 (-5.9%)
E	32322 (37.67%)	5621	0.12	2.50	0.20	4.15	-1.65 (-39.8%)
Global	85794	14920	1.44 (weighted)	78.34 (±4.4)	1.33 (weighted)	72.55 (±13.97)	+5.79 (+8.0%)

4.3.2 Historical and scenario-based future acceleration of global Rs

Historical acceleration of global Rs fluctuated across the decades according to both the single and climate-specific models (Figure 4-4 panel a). Rs was relatively constant from 1961 to 1980, then increased rapidly at a rate of around 0.06 Pg C yr^{-1} from 1981 to 2000. Global Rs then decelerated to 0.025 Pg C yr^{-1} from 2001 to 2014. The damping of global annual Rs increase rate corresponded with the damping of global air temperature increase from 2001 to 2014 (Figure 4-4 panel a). The future acceleration of Rs depended on the warming scenarios. Under the RCP8.5 scenario, an approximately 3ºC warming, the acceleration doubled (single model = 0.11 Pg C year^{-1} and climate-specific model = 0.13 Pg C year^{-1}, Figure 4-4 panel b) compared with

previous decades. However, under the RCP2.6 scenario, Rs rates remained relatively constant (Figure 4-4 panel b). During both the historical and future periods, the acceleration of global Rs estimated by climate-specific models was slightly larger than the rate of increase estimated by the single model (Figure 4-4 panel a and b).

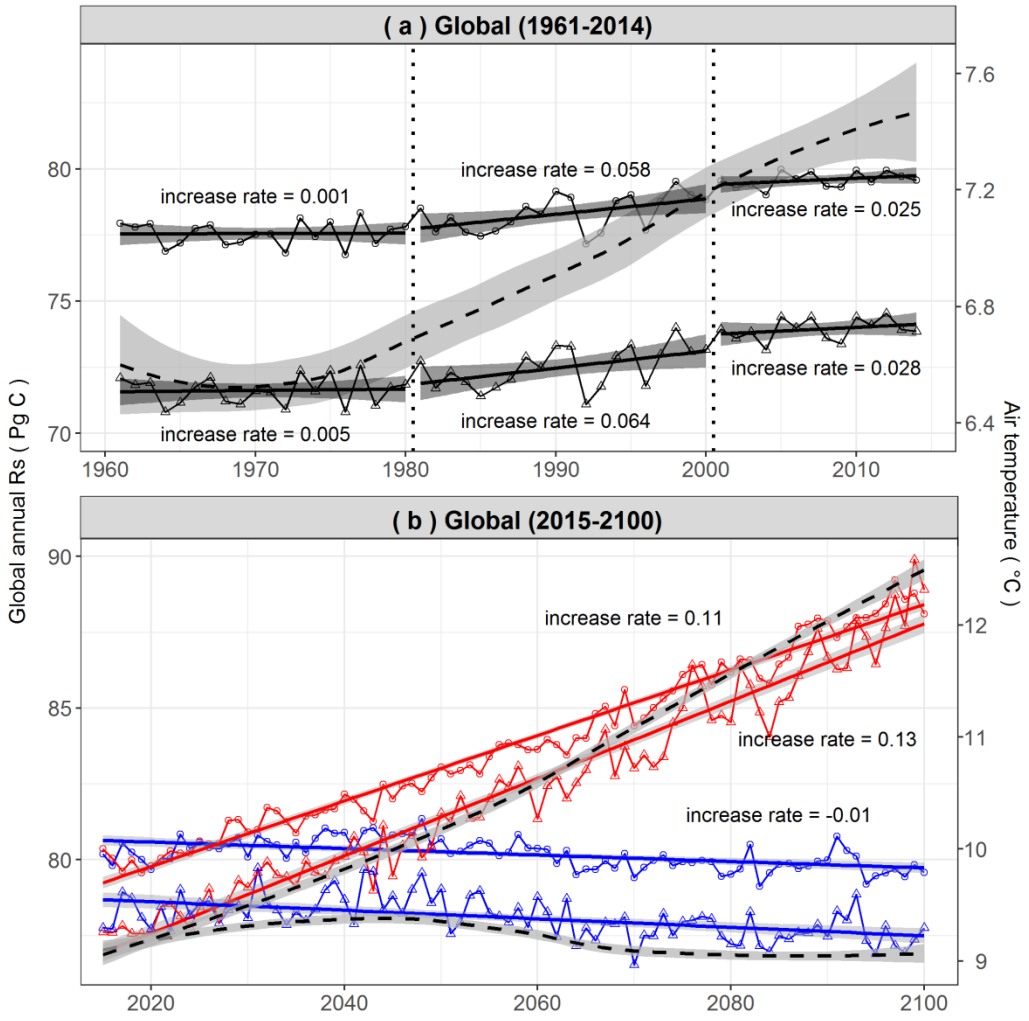

Figure 4-4. Estimated global annual soil respiration (Rs) changes from 1961 to 2014 (upper panel a) and from 2015 to 2100 (lower panel b). Two future warming scenarios suggest that the mitigation of human CO_2 production will halt increased Rs acceleration (RCP2.6, blue dots and lines), while unmitigated human CO_2 production (RCP8.5, red dots and lines) will significantly accelerate future Rs rates. Circles are global annual Rs estimated by single model and triangles are global annual Rs estimates by multiple models. Dashed line with confidence interval range are air temperature change trends fitted by 'loess' method in R.

4.3.3 Regional Rs acceleration and temperature sensitivity

With no CO_2 mitigation (RCP8.5) the future global Rs rates accelerated to twice the current rate; however, the Rs rates of some regions showed reduced sensitivity to rising temperatures (Figure 4-5). Rs predicted by the climate-specific model was less sensitive to increases in temperature in the tropical and temperate summer dry regions, where Rs rates showed either no increase (arid) or a negative correlation with increases in temperature under RCP8.5 global warming scenario (Figure 4-5). No decrease in sensitivity was observed in the RCP2.6 scenario (Figure 4-5). However, the single Rs model did not predict any decline in the sensitivity of Rs (Figure 4-5), as Rs responds to temperature positively within all climate regions and within all time periods (historical, RCP2.6, and RCP8.5). In other climate regions, however, the annual Rs increased substantially as temperature increased, generating a positive relationship between Rs and warming (Figure 4-5).

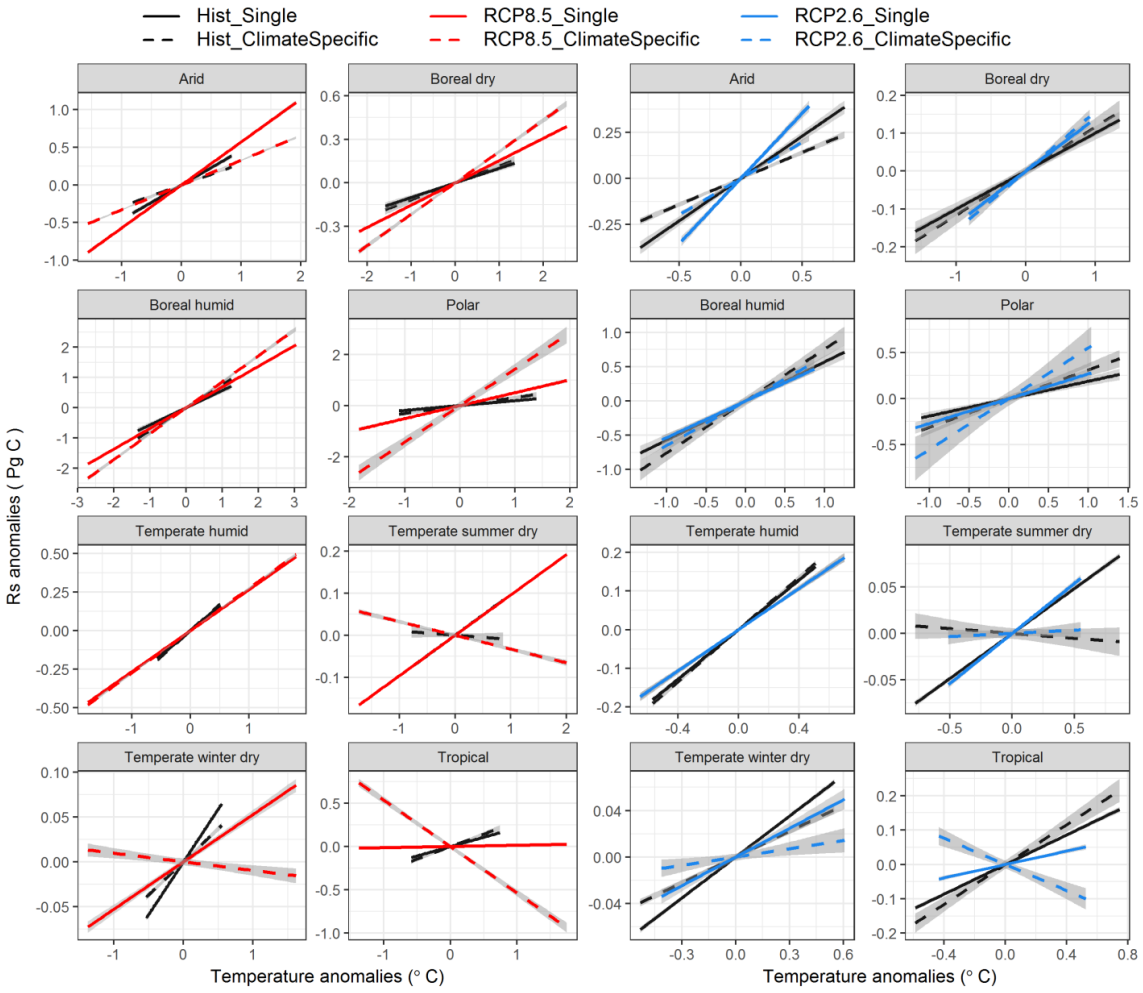

Figure 4-5. Correlation between the estimated annual soil respiration (Rs) anomalies and temperature anomalies from 1961 to 2014 (black lines) and from 2015 to 2100 under unmitigated human CO_2 production scenario (RCP8.5, red lines) and mitigated human CO_2 production (RCP2.6, blue lines). Solid lines represent results from the single model, while dashed lines are results from climate climate-specific models. From 2015 to 2100 under the RCP8.5 scenario, Rs deceleration occurred in tropical, temperate summer-dry and temperate winter-dry climates; however, this Rs deceleration was only detected by the climate-specific models. In Boreal and polar climates, however, Rs responds to warming even more sensitive in future under RCP8.5 than in the historical period. Note that x-axis and y-axis differ from panel to panel.

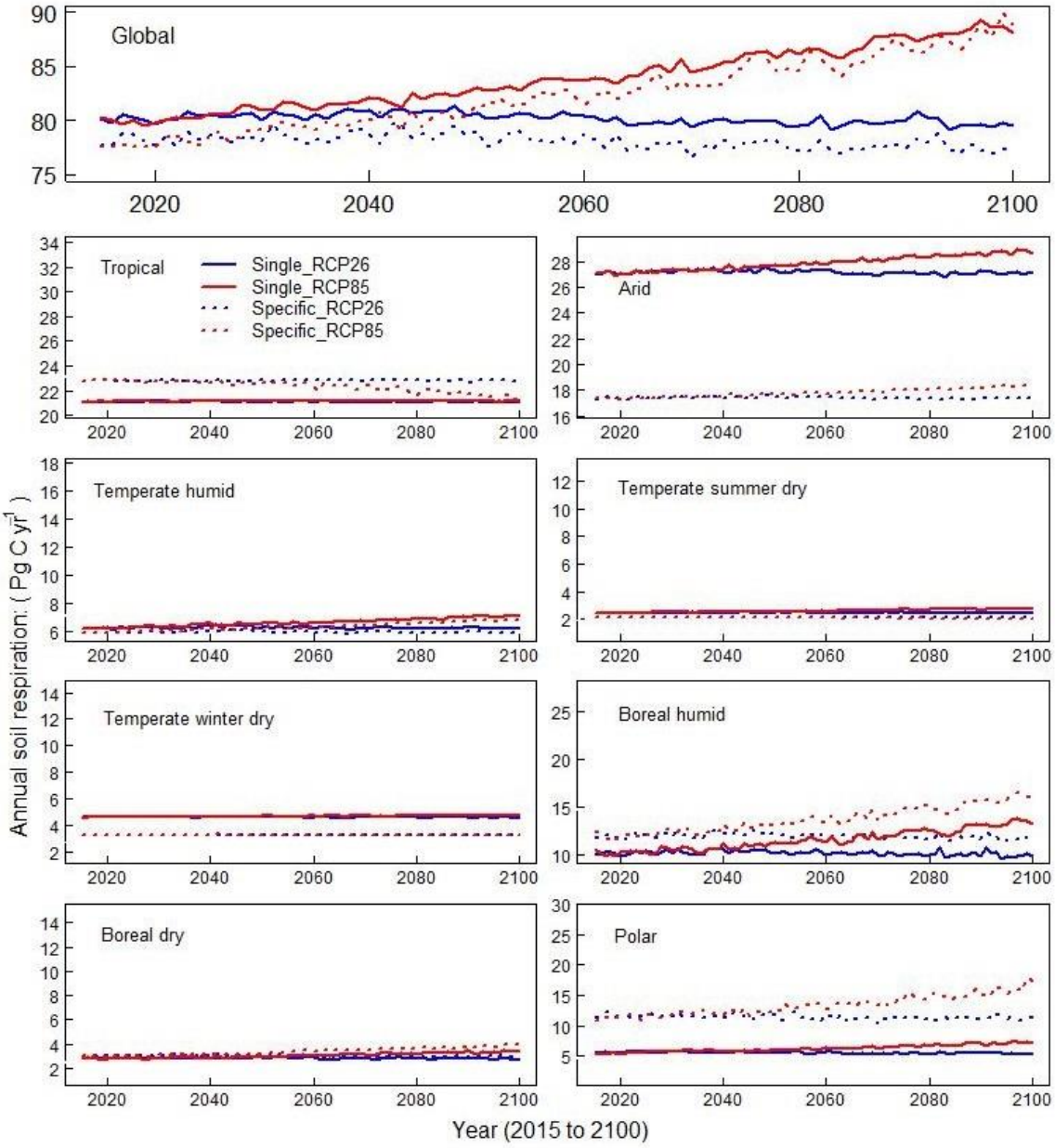

Figure 4-6. Estimated annual soil respiration in global and in each climate region between 2015 and 2100 under substantial mitigation of human CO_2 production global warming scenario, with around 1 ºC warming in 2100 (RCP2.6, blue lines), and business-as-usual global warming scenario with around 3 ºC warming in 2100 (RCP8.5, red lines) by single model (solid lines) and climate-specific models (dashed lines). The single model overestimated Rs rates in arid regions but underestimated Rs in cold regions and tropical regions. For the temperate region, the difference between single model and climate region specific model were very small. Over the study period (2015 to 2100) and under RCP8.5, Rs in tropical maintain at a certain level, Rs in temperate summer dry region slightly decrease, and Rs showed clear increase trend for other climate regions. Under RCP2.6, no increase trend of Rs was generated.

4.4 DISCUSSION

We found that future global Rs rates will accelerate substantially if human activities related CO_2 emissions are not mitigated and global temperatures increase by approximately 3ºC by 2100. Historical acceleration rates were consistent with prior estimates of historical global Rs acceleration (0.04 to 0.10 Pg C yr^{-1}) (Ben Bond-Lamberty and Thomson 2010; Hashimoto et al. 2015; Zhao et al. 2017) and similar among Rs model types (Figure 4-4 panel a). However, if no mitigation of human emissions occurs, the future global Rs rates between 2011 and 2100 increased at an even higher rate, 0.11 and 0.13 Pg C $year^{-1}$ based on the single and climate-specific models respectively (Figure 4-4 panel b). Under these conditions, global Rs will increase from around 72.55 to 88 Pg C yr^{-1}. If, however, significant reductions in emissions limit the increase in global temperatures to < 1ºC, global Rs should decline at a rate of 0.01 Pg C yr^{-1} by 2100 (Figure 4-4 panel b). Likewise, if human CO_2 emissions are mitigated and warming is limited to < 1ºC, regional Rs with decreased sensitivity will be limited to temperate summer-dry regions (Figure 4-5). However, when global temperatures increased by 3 ºC, the climate-specific models predicted Rs will decelerate in the arid, winter-dry and summer-dry temperate, and tropical climates (Figure 4-5).

When comparing the global annual mean Rs estimated by the single model and climate-specific models, we found that global annual mean Rs during the historical period (1961 to 2014) estimated from the single model (mean with 95% confidence interval: 78.34±4.40) was around 6 Pg C larger than that estimated by the region-specific estimate (72.55±13.97 Pg C yr^{-1}). The estimate range was consistent with previous estimates based on monthly Rs data (Raich and Potter 1995; Raich et al. 2002), but lower than previous estimates based on annual Rs data (Ben Bond-Lamberty and Thomson 2010; Hashimoto et al. 2015; Zhao et al. 2017). The differing

results from the single model and the climate-specific models were likely caused by the regional heterogeneity of Rs response to temperature change (Figure 4-3). For instance, a threshold at 14.39 °C was detected in temperate summer-dry region by the climate-specific model, but in the single model, the threshold was 27.50 °C (Figure 4-3). Thus, when temperature is > 14.39 °C, Rs was negatively correlated with temperature increase under climate-specific models, but the single model still predicted positive response in temperate summer dry region until over 27.50 °C. Such difference likely caused the modest increase in global estimates by the single model.

Regional-scale estimates derived from the global single model differed substantially from estimates derived from aggregated climate-specific models. This difference between predictions from the sinlge global model and using region-specific models highlights the need to account for regional heterogeneity in the response of Rs to temperature when studying the effects of warming on soil-carbon dynamics in future. However, climate specific models require sufficient data coverage for model parameterization at a reginal scale. For example, polar and arid regions make up 37.67% and 17.80%, respectively, of total area across globe; however, only 223 and 813 records were available from these region, account for 1.65% and 6.03% of total records from MGRsD. The lack of data in these regions contributes some uncertainty, and more measurements from these regions would be valuable to global Rs estimates (Table 4-2).

Though we observed that a decrease in temperature sensitivity caused Rs deceleration in tropical, temperate summer dry and temperate winter dry regions, the climate-specific models predicted Rs was more sensitive to temperature increases in colder regions (Figure 4-5) and increases Rs in the boreal and polar regions outweights declines, results in accelerating Rs global (Figure 4-5 and Figure 4-6). The predicted increase in Rs in the boreal and polar regions may have substantial effects on losses of carbon stocks in those regions. The temperature of colder

regions is increasing at higher rate compared to the rest of the globe and almost 1,700 Pg of organic carbon is stored in the permafrost (Tarnocai et al. 2009). A recent meta-analysis compared total percentage soil carbon under warming and ambient conditions across Eurasia and North America, and found warming stimulated carbon losses from soil to the atmosphere regardless of how many years (effect-time) the full soil carbon response to warming is realized, but with a very large range of uncertainty (Crowther et al. 2016). Given the larger acceleration rates observed in this study, the loss of soil carbon stocks may be towards the upper end (around 200 Pg C) of the uncertainty bounds if human emissions are not limited (Crowther et al. 2016), mainly driven by carbon losses in colder climates. An increase in primary production carbon may offset losses from soil respiration; however, substantial uncertainty still exists in the response of primary productivity to CO_2 fertilization (Korner et al. 2005; Norby et al. 2005, 2010) and global warming induced drought (Zhao and Running 2010) at regional and global scales. At present, terrestrial ecosystems remove around 1.7 Pg C from atmosphere each year, which help mitigating the global warming (Le Quéré et al. 2013). Whether terrestrial ecosystems can remain as carbon sink depends on how soil respiration responds to global warming. Our results indicate that without human mitigation of CO_2, even though the temperature sensitivity of Rs will decreases in some climates, we can expect even large Rs fluxes at the global scale that may reduce the soil's capacity to act as a carbon sink.

4.5 CONCLUSIONS

In this study, we determined that one, the future global Rs rates will accelerate substantially with predicted increases temperatures if no CO_2 mitigation occurs, and two, a decrease in the temperature sensitivity of Rs of some warm regions will be offset by the acceleration of Rs with increase temperature in colder regions. Each climate type had a distinct relationship between Rs and air temperature that influenced how Rs responded to future warming temperatures and highlighted the importance of accounting for regional heterogeneity in global scale modeling and estimates. This study provides further evidence that Rs deceleration could occur at large spatial scales; unfortunately, this decreasing in temperature sensitivity of Rs will likely not be strong enough to suppress the surge in soil respiration rates if global temperatures are allowed to rise by 3ºC.

REFERENCES

Bahn, Michael et al. 2008. "Soil Respiration in European Grasslands in Relation to Climate and Assimilate Supply." *Ecosystems* 11(8):1352–67.

Bellamy, Pat H., Peter J. Loveland, R.Ian Bradley, R.Murray Lark, and Guy J. D. Kirk. 2005. "Carbon Losses from All Soils across England and Wales 1978–2003." *Nature* 437(7056):245–48.

Bond-Lamberty, B. P. and A. M. Thomsom. 2014. "A Global Database of Soil Respiration Data, Version 3.0." *Oak Ridge National Laboratory Distributed Active Archive Center, Oak Ridge, Tennessee, U.S.A.* http://dx.doi.org/10.3334/ORNLDAAC/1235.

Bond-Lamberty, B. and A. Thomson. 2010. "A Global Database of Soil Respiration Data." *Biogeosciences* 7(6):1915–26.

Bond-Lamberty, Ben and Allison Thomson. 2010. "Temperature-Associated Increases in the Global Soil Respiration Record." *Nature* 464(7288):579–82.

Bradford, Mark A. et al. 2008. "Thermal Adaptation of Soil Microbial Respiration to Elevated Temperature." *Ecology Letters* 11(12):1316–27.

Brito, Liziane De Figueiredo, Gener Tadeu Pereira, and Zigomar Menezes. 2009. "Soil CO_2 Emission of Sugarcane Fields As Affected By Topography." *Scientia Agricola*. 66(1):77–83.

Carey, Joanna C. et al. 2016. "Temperature Response of Soil Respiration Largely Unaltered with Experimental Warming." *Proceedings of the National Academy of Sciences* 113(48):13793–802.

Chen, Shutao et al. 2014. "Global Annual Soil Respiration in Relation to Climate, Soil Properties and Vegetation Characteristics: Summary of Available Data." *Agricultural and Forest Meteorology* 198:335–46.

Christiansen, Casper T. et al. 2012. “High Arctic Heath Soil Respiration and Biogeochemical Dynamics during Summer and Autumn Freeze-in - Effects of Long-Term Enhanced Water and Nutrient Supply.” *Global Change Biology* 18(10):3224–36.

Chunming, Jiang. 2010. “CO_2 Flux Estimation by Different Regression Methods from an Alpine Meadow on the Qinghai-Tibetan Plateau.” *Advances in Atmospheric Sciences*, 27(6):1372–79.

Ciais, Philippe et al. "Carbon and other biogeochemical cycles." 2014. *Climate change 2013: the physical science basis. Contribution of Working Group I to the Fifth Assessment Report of the Intergovernmental Panel on Climate Change*. Cambridge University Press.

Conant, Richard T. et al. 2011. “Temperature and Soil Organic Matter Decomposition Rates - Synthesis of Current Knowledge and a Way Forward.” *Global Change Biology* 17(11):3392–3404.

Conant, Richard T., Jeffrey M. Klopatek, Robert C. Malin, and Carole C. Klopatek. 1998. “Carbon Pools and Fluxes along an Environmental Gradient in Northern Arizona.” *Biogeochemistry* 43(1):43–61.

Cramer, Wolfgang et al. 2001. “Global Response of Terrestrial Ecosystem Structure and Function to CO_2 and Climate Change: Results from Six Dynamic Global Vegetation Models.” *Global Change Biology* 7(4):357–73.

Crowther, Thomas W. and Mark a Bradford. 2013. “Thermal Acclimation in Widespread Heterotrophic Soil Microbes.” *Ecology Letters* 16(4):469–77.

Crowther, TW et al. 2016. “Quantifying Global Soil C Losses in Response to Warming.” *Nature*. 540(7631): 104-08.

Davidson, E. A. and Ivan A. Janssens. 2006. “Temperature Sensitivity of Soil Carbon Decomposition and Feedbacks to Climate Change.” *Nature* 440(7081):165–73.

Davidson, Eric A. 2016. “Biogeochemistry: Projections of the Soil-Carbon Deficit.” *Nature* 540(7631):47–48.

Davidson, Eric A., Ivan A. Janssens, and Yiqi Lou. 2006. “On the Variability of Respiration in Terrestrial Ecosystems: Moving beyond Q10.” *Global Change Biology* 12(2):154–64.

Dorrepaal, Ellen et al. 2009. “Carbon Respiration from Subsurface Peat Accelerated by Climate Warming in the Subarctic.” *Nature* 460(7255):616–19.

Epule, Terence. 2015. “A New Compendium of Soil Respiration Data for Africa.” *Challenges* 6(1):88–97.

Fang, C., John B. Moncrieff, Henry L. Gholz, and Kenneth L. Clark. 1998. “Soil CO_2 Efflux and Its Spatial Variation in a Florida Slash Pine Plantation.” *Plant and Soil* 205(2):135–46.

Fang, Huajun et al. 2012. “Responses of CO_2 Efflux from an Alpine Meadow Soil on the Qinghai Tibetan Plateau to Multi-Form and Low-Level N Addition.” *Plant and Soil* 351(1–2):177–90.

Flato, Gregory, et al. "Evaluation of Climate Models. In: Climate Change 2013: The Physical Science Basis. Contribution of Working Group I to the Fifth Assessment Report of the Intergovernmental Panel on Climate Change." *Climate Change 2013* 5 (2013): 741-866.

Forster, Piers M. et al. 2013. “Evaluating Adjusted Forcing and Model Spread for Historical and Future Scenarios in the CMIP5 Generation of Climate Models.” *Journal of Geophysical Research Atmospheres* 118(3):1139–50.

Frey, Serita D., Juhwan Lee, Jerry M. Melillo, and Johan Six. 2013. “The Temperature Response of Soil Microbial Efficiency and Its Feedback to Climate.” *Nature Climate Change* 3(4):395–98.

Hamdi, Salwa, Fernando Moyano, Saidou Sall, Martial Bernoux, and Tiphaine Chevallier. 2013. “Synthesis Analysis of the Temperature Sensitivity of Soil Respiration from Laboratory Studies in Relation to Incubation Methods and Soil Conditions.” *Soil Biology and Biochemistry* 58:115–26.

Hansen, J., R. Ruedy, M. Sato, and K. Lo. 2010. “Global Surface Temperature Change.” *Reviews of Geophysics*. 48(4):RG4004.

Hashimoto, S. et al. 2015. “Global Spatiotemporal Distribution of Soil Respiration Modeled Using a Global Database.” *Biogeosciences Discussions* 12(5):4331–64.

Janssens, I. A. et al. 2001. “Productivity Overshadows Temperature in Determining Soil and Ecosystem Respiration across European Forests.” *Global Change Biology* 7(3):269–78.

Jin, Z., Y. S. Dong, Y. C. Qi, and Z. S. An. 2010. “Soil Respiration and Net Primary Productivity in Perennial Grass and Desert Shrub Ecosystems at the Ordos Plateau of Inner Mongolia, China.” *Journal of Arid Environments* 74(10):1248–56.

Karhu, Kristiina et al. 2014. “Temperature Sensitivity of Soil Respiration Rates Enhanced by Microbial Community Response.” *Nature* 513(7516):81–84.

Korner, C. et al. 2005. “Carbon Flux and Growth in Mature Deciduous Forest Trees Exposed to Elevated CO_2.” *Science* 309(5739):1360–62.

Lin, Xingwu et al. 2011. “Response of Ecosystem Respiration to Warming and Grazing during the Growing Seasons in the Alpine Meadow on the Tibetan Plateau.” *Agricultural and Forest Meteorology* 151(7):792–802.

Liski, Jari, Hannu Ilvesniemi, and Carl Johan Westman. 1999. “CO_2 Emissions from Soil in Response to Climatic Warming Are Overestimated: The Decomposition of Old Soil Organic Matter Is Tolerant of Temperature.” *Ambio* 28(2):171–74.

Lloyd, J. and J. A. Taylor. 1994. “On the Temperature Dependence of Soil Respiration.” *Functional Ecology* 8(3):315–23.

Lu, Meng et al. 2013. “Responses of Ecosysem Carbon Cycle to Experimental Warming: A Meta-Analysis.” *Ecology* 94(3):726–38.

Luo, Y., S. Wan, D. Hui, and L. L. Wallace. 2001. “Acclimatization of Soil Respiration to Warming in a Tall Grass Prairie.” *Nature* 413(October):622–25.

Norby, Richard J. et al. 2005. “Forest response to elevated CO_2 is conserved across a broad range of productivity.” *Proceedings of the National Academy of Sciences* 102(50):18052–56.

Norby, Richard J., Jeffrey M. Warren, Colleen M. Iversen, Belinda E. Medlyn, and Ross E. McMurtrie. 2010. "CO_2 Enhancement of Forest Productivity Constrained by Limited Nitrogen Availability." *Proceedings of the National Academy of Sciences of the United States of America* 107(45):19368–73.

Panosso, A. R., J. Marques, G. T. Pereira, and N. La Scala. 2009. "Spatial and Temporal Variability of Soil CO_2 Emission in a Sugarcane Area under Green and Slash-and-Burn Managements." *Soil and Tillage Research* 105(2):275–82.

Parker, L. W., J. Miller, Y. Steinberger, and W. G. Whitford. 1983. "Soil Respiration in a Chihuahuan Desert Rangeland." *Soil Biology & Biochemistry* 15(3):303–9.

Pendall, E. et al. 2010. "Land Use and Season Affect Fluxes of CO_2, CH4, CO, N2O and H2 and Isotopic Source Signatures in Panama: Evidence from Nocturnal Boundary Layer Profiles." *Global Change Biology* 16(10):2721–36.

Le Quéré, C. et al. 2013. "The Global Carbon Budget 1959-2011." *Earth System Science Data* 5(1):165–85.

R Core Team. 2014. *R: A Language and Environment for Statistical Computing. R Foundation for Statistical Computing*. Vienna, Austria.

Raich, J. W. and K. J. Nadelhoffer. 1989. "Belowground Carbon Allocation in Forest Ecosystems: Global Trends." *Ecological Society of America* 70(5):1346–54.

Raich, J. W. and W. H. Schlesinger. 1992. "The Global Carbon Dioxide Flux in Soil Respiration and Its Relationship to Vegetation and Climate." *Tellus B* 44(2):81–99.

Raich, James W. and Christopher S. Potter. 1995. "Global Patterns of Carbon Dioxide Emissions from Soils." *Global Biogeochemical Cycles* 9(1):23–36.

Raich, James W., Christopher S. Potter, and Dwipen Bhagawati. 2002. "Interannual Variability in Global Soil Respiration, 1980–94." *Global Change Biology* 8(8):800–812.

Schuur, E. A. G. et al. 2015. “Climate Change and the Permafrost Carbon Feedback.” *Nature* 520(7546):171–79.

Sistla, Seeta a et al. 2013. “Long-Term Warming Restructures Arctic Tundra without Changing Net Soil Carbon Storage.” *Nature* 497(7451):615–18.

Song, Xinzhang et al. 2014. “Quantification of Soil Respiration in Forest Ecosystems across China.” *Atmospheric Environment* 94:546–51.

Tarnocai, C. et al. 2009. “Soil Organic Carbon Pools in the Northern Circumpolar Permafrost Region.” *Global Biogeochemical Cycles* 23(2):1–11.

Trumbore, Susan. 2006. “Carbon Respired by Terrestrial Ecosystems–recent Progress and Challenges.” *Global Change Biology* 12(2):141–53.

Wang, Wei, Weile Chen, and Shaopeng Wang. 2010. “Forest Soil Respiration and Its Heterotrophic and Autotrophic Components: Global Patterns and Responses to Temperature and Precipitation.” *Soil Biology and Biochemistry* 42(8):1236–44.

Wang, Wei and Jingyun Fang. 2009. “Soil Respiration and Human Effects on Global Grasslands.” *Global and Planetary Change* 67(1–2):20–28.

Wieder, William R., Gordon B. Bonan, and Steven D. Allison. 2013. “Global Soil Carbon Projections Are Improved by Modelling Microbial Processes.” *Nature Climate Change* 3(10):909–12.

Willmott, Cort J., Kenji Matsuura, and D. R. Legates. 2001. “Terrestrial Air Temperature and Precipitation: Monthly and Annual Time Series (1950-1999).” *Center for Climate Research*.

Zhao, Maosheng and Steven W. Running. 2010. “Drought-Induced Reduction in Global Terrestrial Net Primary Production from 2000 Through 2009.” *Science* 329(6046):940–43.

Zhao, Zhengyong et al. 2017. “Model Prediction of Biome-Specific Global Soil Respiration from 1960 to 2012.” *Earth’s Future* 5(7):715–29.

CHAPTER 5. Soil CO_2 flux from urban parks in Blacksburg, Virginia: vegetation, spatial and temporal variability, and model estimation

ABSTRACT

Belowground CO_2 flux is an important component of the carbon cycle that determines surface-atmosphere carbon exchange; however, dynamics of CO_2 fluxes from urban landscapes remain understudied compared to other ecosystems. Here, we investigated 1) temporal variations in CO_2 flux from turfgrass and wooded areas of five parks in Blacksburg, Virginia, USA, between June 2016 and July 2017; 2) environmental factors affecting that fluxes; 3) the effectiveness of the Denitrification-Decomposition (DNDC) model to predict those CO_2 fluxes. Results show that the annual mean CO_2 flux rate was higher in turfgrass compared to wooded areas, although fluxes were spatially variable among the five parks. Soil bulk density, soil total carbon, soil total nitrogen and soil C/N ratio explained some variation (range from 8% to 75%) in the annual CO_2 flux across the five parks. Diurnal, weekly and seasonal CO_2 fluxes were primarily related to changing soil temperature, but varied between the turf and wooded areas. The DNDC model, although developed for agriculture and undeveloped lands, closely estimated soil temperature, moisture and CO_2 flux across the seasons and therefore could be used to estimate and understand CO_2 fluxes from urban ecosystems in future studies. These results contribute to improving our understanding of CO_2 flux spatial and temporal variation and how it interacts with environmental conditions in turfgrass and wooded areas in urban systems. In addition, these results indicated that the DNDC model can be used to estimate CO_2 fluxes whthin urban areas which improve accuracy of future flux estimates.

5.1 INTRODUCTION

Cities are expanding globally, by 2030, urban land could increase by 1.2 million km^2, triple the urban land in 2000 (Seto, Guneralp, and Hutyra 2012). With the expansion of cities, urban greenspaces, such as urban parks' forests, golf courses and lawns also expanded significantly (Lubowski et al. 2006). In the United States, there were 3.8 billion urban trees in 2002, which corresponds to 27% of canopy in urban lands (Nowak et al. 2001). Turfgrasses also occupy a large percentage of urban landscapes. Using mapping and modeling methods, Milesi et al. (2005) calculated that there were potentially 163,800 km^2 (±35,850 km^2) of land covered by turfgrasses in the continental USA, triple the areal coverage of any irrigated crop. In Singapore, managed vegetation, a large proportion of which is turfgrass, makes up 27% of total land area (Ng et al. 2015). In Beijing and Shanghai, China, about 115 km^2 of land is converted to urban lawn each year (Zhou et al. 2012). Such rapid land-use change in cities has important effects on urban ecosystem functions, soil carbon pools, and greenhouse fluxes such as belowground CO_2 flux. Considerable numbers of studies focus on carbon dynamics in undeveloped and agricultural ecosystems; however, very few studies investigate urban soil carbon dynamics and urban CO_2 flux (Chen et al. 2014; Kaye, McCulley, and Burke 2005). Without the ability to understand and predict the carbon dynamics of these soils, it is difficult to estimate impacts of green spaces in urban areas at the city, regional, or global scales.

Urbanization is often associated with disturbance and land-cover changes, such as vegetation clearing, impervious surfaces, and compaction that could threaten biodiversity and reduces ecosystem productivity and reduce soil CO_2 flux emission (Seto et al. 2012). Compaction and increasing of impervious surface area in cities may cause oxygen deficiency

belowground, change urban soil aggregate size distribution, and thus altering soil carbon decomposition rates in urban soil (Drew 1983). In addition, urbanization can decrease soil hydraulic conductivity, leading to reduced soil water content and thus decreased urban soil CO_2 efflux (Chen et al. 2014). On the other hand, soils previously subjected to grading and compaction through land development practices may have a higher potential to enhance their carbon storage through post-development soil management strategies (Chen et al. 2013). Well-managed urban greenspaces can sequestrate carbon, help mitigating and adapting to urban heat island affect and global climate change (Chen et al. 2013). However, intensive management and disturbance associated with land development may also cause urban greenspaces could be a sources of greenhouse gases (Chen et al. 2014; Ng et al. 2015). Urbanization could affect CO_2 flux through deposition of nitrogen (Hu et al. 2010; Li et al. 2010; Zhang et al. 2014), and introduction of microbial, underground small animal, and plant species into the urban environment (McKinney 2008). Decina et al (2016) found that during the growing season, soil respiration (Rs) emitted from urban greenspaces was as much as 72% of fossil fuel emitted CO_2. In southwestern part of Seoul, a high-density urban area, the annual soil respiration budget in an urban forest accounted for approximately one third of annual CO_2 emissions (Park, Joo, and Park 2014). Thus disturbance, landcover change, and management patterns are all important features of the urban environment that influence soil carbon dynamics.

CO_2 flux rate is closely related to soil physical and chemical properties, and carbon pools, which may be greatly altered by human management in urban ecosystems. In Fort Collins, Colorado, Kaye et al (2005) found that due to higher surface soil organic carbon and total nitrogen, and higher water contents from irrigation in the urban soil, soil respiration from urban ecosystems was 2.5 to 5 times greater than native land, corn, and wheat land-use. Previous

studies in New York City detected increased invertebrate and fungal densities (Pouyat, Parmelee, and Carreiro 1994), larger carbon (C) pools and CO_2 fluxes (Pouyat et al. 2002) in the urban soils than rural soils along an urban-rural gradient. In the greater Boston area, Decina et al (2016) found that soil respiration from urban landscapes was 2.2 times greater than soil respiration rates found in nearby rural ecosystems. The urban heat island, a prominent characteristic of the urban climate, may contribute to increases in CO_2 fluxes, as it affects the plant physiology and as well as the respiration of carbon from soil and plants (Hansen et al. 2010). Many model results and field measurements predicted that autotrophic respiration will increase as temperatures increase (Cramer et al. 2001; Davidson 2016; Dorrepaal et al. 2009; Frey et al. 2013; Karhu et al. 2014). In warm regions, where the city might be cooler and more humid than the surrounding desert (Hall et al. 2016), CO_2 fluxes remain high. In the Phoenix, Arizona metropolitan region, Koerner and Klopatek (2002) compared soil CO_2 efflux from native desert with human-maintained lands including golf courses, landfills, mesic and xeric landscapes, and agricultural sites. Not surprisingly, their results showed that the desert canopy and interspace showed the lowest rate of CO_2 evolution, while mesic landscaping (grass lawns), golf courses and all agricultural land uses resulted in higher rates of CO_2 evolution, and landfills exhibited the highest rates of CO_2 evolution (Koerner and Klopatek 2002). Soil CO_2 flux is the consequence of interaction between environmental conditions and human activities, making the spatial and temporal variation of urban soil CO_2 flux even more complex compared to natural soils.

Accurate monitoring and assessments of changes in CO_2 fluxes between underground and atmosphere is critical to estimate the role of greenspaces played in mitigating climate change (Bae and Ryu 2017; Chen et al. 2013; Zhou et al. 2012). Measuring soil carbon dynamics across broad scales is difficult, however, because measuring CO_2 flux is labor-intensive, costly, and

time consuming. Thus flux models can be useful tools for studying carbon dynamics and greenhouse gas emissions in such systems. However, some widely used process-based models are not designed or tested in urban ecosystems. Models developed for undeveloped and agricultural lands, such as the Denitrification-Decomposition Model (DNDC), may be adaptable to urban ecosystems. DNDC is a process-base model which was originally developed for assessing carbon and nitrogen emissions from the US agricultural soils (Li, Frolking, and Froking 1992). This model has been adapted to pasture ecosystems (Saggar et al. 2004), wetland ecosystems (Cui, Li, and Trettin 2005; Zhang and Li 2002), grasslands (Surinder Saggar et al. 2007), and forest ecosystems (Mo et al. 2005). To date, however, no research has evaluated the DNDC model for stimulating carbon dynamics and estimating CO_2 flux in urban ecosystems.

While the differences between urban and undeveloped land have been previously explored (Pouyat et al. 1994), the variability of CO_2 fluxes from urban greenspaces remain poorly understood and our ability to model those fluxes is limited. The objectives of this study were to: 1) examine the CO_2 flux spatial and temporal variation from urban greenspaces (wooded areas and urban turfgrass), 2) identify the factors that that contribute to CO_2 flux spatiotemporal variance in urban greenspaces, and 3) test the ability of the DNDC model to predict CO_2 flux in this urban setting. Determining the variability of CO_2 fluxes from urban green spaces and being able to model those fluxes will help to better understand and predict the role of urban greenspace and its management in the local and global carbon cycles.

5.2 METHODS

5.2.1 Site information

Five parks [Dehart Road Park (DRP); Heritage Community Park (HCP); Nellies Cave Park (NCP); Owen Street Park (OSP); and Tom's Creek Park (TCP)] (37.2106°N to 37.2530°N, 80.4594°W to 80.3925°W, Figure 5-1) were selected in Blacksburg, Montgomery County, Virginia. Criteria for selecting parks included its neaeness to the town center, the presence of both turfgrass and wooded areas within the park, and accessibility. We selected a 10m×10m area of turfgrass and 10m×10m of wooded area in each park. Soil taxonomic information was obtained from the UC Davis "SoilWeb" (https://casoilresource.lawr.ucdavis.edu/gmap/) (Table 5-1). The turfgrass vegetation was similar among the five parks, while the tree species in urban wooded areas were much more heterogeneous among the five parks (Table 5-1). DRP, OSP, and TCP were built during the 1970s, NCP was developed in the 1980s, while HCP was developed most recently, in the late 1990s (Table 5-1).

Table 5-1. The characteristics of the five study parks in Blacksburg, VA, USA, including: year built, soil series and order, and the plant species present.

Parks (built time)	Soil Series	Plant species	
		Turfgrass	Wooded area
Dehart Road Park - DRP (1970s)	Groseclose (Ultisols, 97%) Purdy (Ultisols, 3%)	The turfgrass vegetation was similar among the five parks, dominated by white clover (*Trifolium repens* L.), Narrow leaf plantain (*Plantago lanceolata* L.), Dandelion [*Taraxacum officinale* (L.)], Bermudas grass (*Cynodon* spp.), plantain (*Plantago major* L.), perennial ryegrass (*Lolium perenne* L.), and fescue (*Festuca* spp.).	Serviceberry (Amelanchier spp., A. arborea) with grapevine (Vitis spp., probably V. riparia or V. rotundifolia) climbing on trees.
Heritage Community Park - HCP (1999)	Groseclose (Ultisols, 50%) Poplimento, (Alfisols, 50%)		White Pine (Pinus strobus L.).
Nellies Cave Park - NCP (1980s)	Groseclose, (Ultisols, 97%) Purdy (Ultisols, (3%)		White pine (Pinus strobus L.) and Pitch pine (Pinus rigida Mill.).
Owen Street Park - OSP (1970s)	Groseclose (Ultisols, 97%) Purdy (Ultisols, 3%)		sugar maple (*Acer saccharum* Marsh.), black walnut (*Juglans nigra* L.), Blackberry (*Rubus* spp.) , goldenrod (*Solidago* spp.), black locust (*Robinia pseudoacacia* L.), and Amur honeysuckle [*Lonicera maackii* (Rupr.) Herder].
Tom's Creek Park - TCP (1970s)	Groseclose (Ultisols, 50%) Poplimento (Alfisols, 50%)		boxelder maple (*Acer negundo* L.), black walnut (*Juglans nigra* L.), and tree of heaven [*Ailanthus altissima* (Mill.) Swingle].

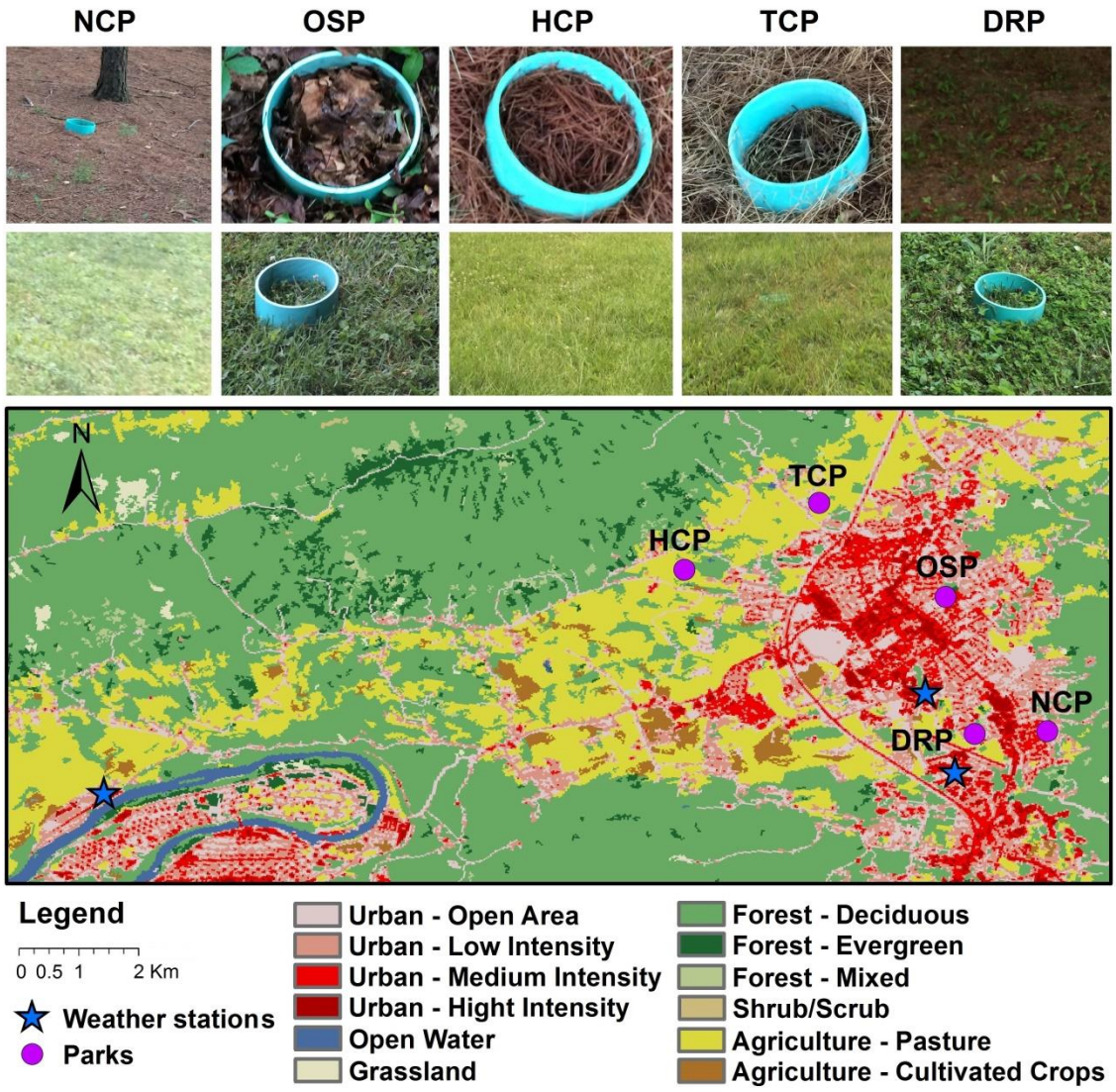

Figure 5-1. Location of selected parks [Tom's Creek park (TCP); Heritage Community Park (HCP); Dehart Road Park (DRP); Nellies Cave Park (NCP); and Owen Street Park (OSP)] and landscape of urban turfgrass vs. urban wooded area in selected parks.

Weather data were collected from Virginia Agricultural Experiment Station at Kentland Farm (37.201°N, 80.567°W, http://vaes.vt.edu/college-farm/weather/2017weather.html), Virginia Tech Turfgrass Research Center (37.219°N, 80.415°W), and a local weather station from National Oceanic and Atmospheric Administration (NOAA, 37.204°N, 80.410°W) (Figure 5-1), which provide hourly time-scale near surface air temperature, soil temperature, ground

radiation, wind speed, wind direction, and precipitation data. On average, there are 214 sunny days per year in Montgomery County. The average air temperature is 11.78 ℃, the highest air temperature appears in July (28.33 ℃), and the lowest air temperature appears in January (-5.00 ℃). The annual average rainfall is 1034 mm, annual average snowfall is 558.8 mm.

5.2.2 CO_2 flux sampling

The Closed Dynamic Chamber technique (CDC, LI-COR 8100, Nebraska, USA) and a flux chamber consisting of a Polyvinyl chloride (PVC) collar (20cm diameter × 13cm height) was used to measure CO_2 flux. We did not remove near-surface plants before or during measurements, thus the CO_2 flux measured in this study included both autotrophic respiration from near-surface plant and soil respiration. The CDC technique uses a closed chamber to cover a ground surface area (20cm diameter circle area at this study) for a period (usually between 1 and 3 minutes, was set up as 2 minutes in this study). The LI-COR was calibrated regularly in the laboratory using calibration tanks with a standard of CO_2 concentration (0, 200, and 2000 ppm) at controlled temperature.

PVC collars were set up at each park (both urban turfgrass and wooded area) 24 hours before CO_2 flux sampling, in order to avoid PVC collars being broken by mowing, we removed all collars after gas sampling. Setting up PVC collars disturbs soil structure, and thus influences CO_2 flux. To avoid the bias caused by PVC collar set up, we analyzed the CO_2 flux rate weekly variation after PVC collars were set up 1 day after until 7 days after to identify how many days the collars should be left to equilibrate and avoid the pulse of CO_2 flux associated with severed roots caused by installation. The results indicated that the daily CO_2 flux rate did not shown a clear trend within one week, but was affected by air temperature and soil moisture (Data not

shown) suggesting that waiting 24 hours was long enough for CO_2 flux to equilibrate. Therefore, PVC collars were set up at least 24 hours before CO_2 flux sampling, same as the minimum waiting time by previous studies (Luo and Zhou 2006).

CO_2 flux was measured every two weeks using LI-COR 8100 from June 2016 to July 2017. CO_2 fluxes were measured from a consistent time window (8:00 to 12:00) to limit the effect of diurnal CO_2 fluxes variations, the order of the sites and landscape (turfgrass vs. wooded area) was changed randomly every time and all the measurements finished in the same day during each sampling event. Soil water content at 10 cm depth was measured near by the collars using Portable Soil Moisture Meter (Model No: MO750, Manufacturer: Extech, Melrose, MA, USA) and soil temperature at 10 cm was measured using Digital Pocket Thermometer (Model No: PDT550, Manufacturer: UEI, Melrose, MA, USA) after CO_2 flux measurement.

Constraints of labour and time often limited the number of subsamples that are feasible. We used three PVC collars (three subsamples) within the selected 10m × 10m study area per experimental unit when we start the experiment at June 18th, 2016. Spatial heterogeneity of CO_2 flux exists even though that landscape appears mostly homogeneous (Davidson et al. 2002). An important consideration is determing how many collars are required to capture the CO_2 flux spatial variability within certain accuracy. To determine the accuracy of using three collars, we set up 7 collars in the turfgrass, and 8 collars in the wooded area in the NCP between August 12 and August 18, 2016. CO_2 flux rates were measured between 8:00 and 9:00 am for one week. Based on those measurements, we adapted the method developed by Davidson et al. (2002) to determine the measurement accuracy of three collars according to equation (5-1),

$$n = \left[\frac{t \cdot s}{rang/2}\right]^2 \qquad (5\text{-}1)$$

where *n* is the number of collars, *t* is the two-way t statistical value for a given confidence level (95%, 90%, and 80%, respectively) and degrees of freedom (43 measurements for the turfgrass and 47 measurements for the wooded area), *s* is the standard deviation of the all measurements of turfgrass (all 43 measurements) and wooded area (all 47 measurements), and range is the width of the overall mean ×10%, 20%, or 30%. We found that with three collars in each experimental unit, we have a 95% confidence interval that the measured CO_2 flux follows ± 30% of the overall mean, or a 80% confidence interval that the measured CO_2 flux follows ± 20% of the overall mean (Table 5-2), which would reasonably capture the spatial CO_2 flux variation in both turfgrass and wooded area.

Table 5-2. Number of collars required for various degrees of precision (within ± 10 to ± 50 of the overall mean) and at various confidence (80-90%) based on a total of 47 measurements (for woodland) and 43 measurements (for grassland) at the Nellies Cave park from August 12th to 18th, 2016.

Interval about the full population mean (%)	99% Confidence ($\alpha = 0.01$)	95% Confidence ($\alpha = 0.05$)	90% Confidence ($\alpha = 0.1$)	80% Confidence ($\alpha = 0.2$)
		Turfgrass		
± 10	60	28	18	10
± 20	15	7	5	***3***
± 30	7	4	***2***	2
± 40	4	***2***	2	1
± 50	***3***	2	1	1
		Wooded area		
± 10	57	27	18	10
± 20	14	7	5	***3***
± 30	7	***3***	***2***	2
± 40	4	2	2	1
± 50	***3***	2	1	1

CO_2 flux diurnal variability is another measure uncertainty which affects measurement accuracy. Diurnal variability affects the ability to capture the daily mean CO_2 flux rate, making it difficult to scale up to annual CO_2 flux rate based on daily measured CO_2 flux rate (Luo and Zhou 2006). We measured CO_2 flux once per hour (but once per three hours from 0:00 to 5:00) on August 16th/2016 (representing summer), October 23rd/2016 (representing autumn), and March 6th/2017 (representing spring) to identify the CO_2 flux diurnal variation in summer, autumn and spring, and to test whether CO_2 flux measured from 8:00 to 12:00 can capture daily mean CO_2 flux rate in urban turfgrass and wooded area. Notice that we did not measure CO_2 flux diurnal variation in winter because winter CO_2 flux diurnal variation is negligible (Jian and Steele 2017, Chapter I).

Collar-insert depth to soil is an important factor that affects CO_2 flux measurement accuracy. A collar insert too deep likely leads to sever surface roots thus weakening autotrophic respiration. On the other hand, a collar insert too shallow may lead to gas leakage problems (Heinemeyer et al. 2011). Total CO_2 flux measurements (n = 762) in this study shown that our collars were inserted into soil (including litter and organic layers) from 2 to 10 cm, with a mean of 5.05 cm in turfgrasss (median = 5.00, Figure 5-2 panel a), with a mean of 5.77 cm in wooded areas (median = 5.70, Figure 5-2 panel b), very close to the mean of a synthesized studies in forest ecosystem (4.6 cm), but deeper than the mean of nine studies in turfgrass (2.7 cm) (Heinemeyer et al. 2011). The collar-insert depth in this study was within a reasonable range, thus unlikely contributing botable bias to measurement accuracy.

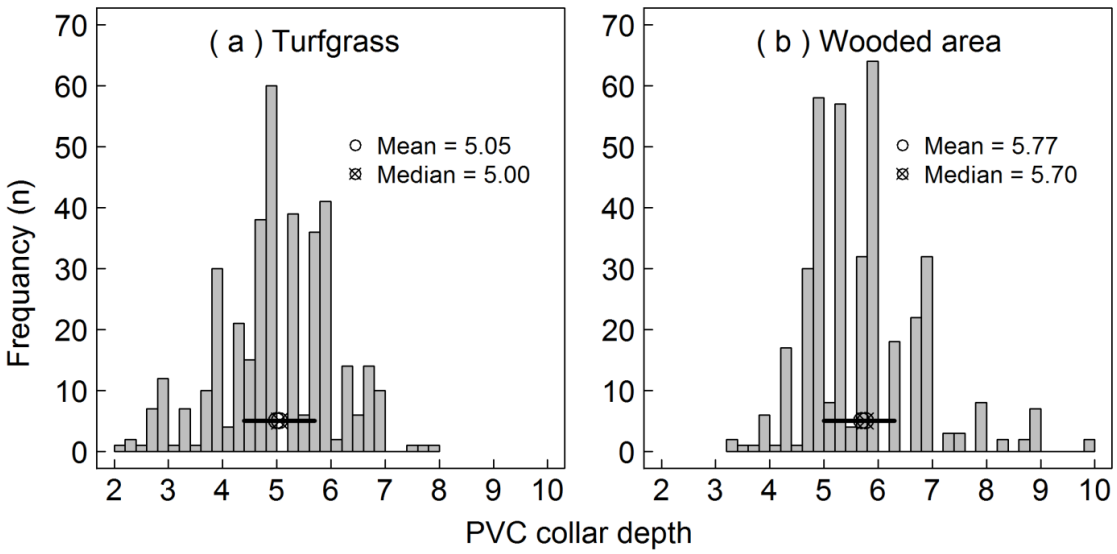

Figure 5-2. Histogram of collar-insertion depth. The collar-insertion depth range from 2.0 cm to 10.0 cm at this study, the black lines shown 25% to 75% quantile (Total measurements *n* = 381 for turfgrass and *n* = 381 for wooded area).

5.2.3 Soil sampling and plant sampling

Soil samples were taken on 22-March-2017 to measure the soil texture, pH, soil bulk density, soil porosity, soil total nitrogen (TN), total carbon (TC), and carbon to nitrogen ratio (C/N). Soil samples from each park were air dried, and then sieved to pass a 2 mm sieve. A 1 g subsample was used for TC, TN, and C/N test using a High Temperature Combustion Analyzer (Elementar, VarioMax). Another 1 g subsample was used to measure the soil texture by the Particle Size Analyzer (Cilas Particle Size 1190, Madison, Wisconsin). Soil bulk density was measured by drying samples to a constant weight at 103° C. Plant species for turfgrass and wooeded area of each park were identified by expert. Mowing frequency and grass cut length in each park was identified by interviewing park mowing workers, the park manager, and on site measurements.

5.2.4 Denitrification-Decomposition Model

The DNDC model is a process-base model that contains two components (Li et al. 1992). The first is a physio-chemical component, which consists of soil climate, crop growth and decomposition sub-models. The physio-chemical component predicts soil temperature, moisture, pH, redox potential (Eh) and substrate concentration profiles which respond to ecological drivers (e.g., climate, soil, vegetation and anthropogenic activity). The biochemical component consists of nitrification, denitrification, and fermentation sub-models, and predicts CO_2, CH_4, NH_3, NO, N_2O and dinitrogen (N_2) emissions for plant-soil systems using soil environmental factors calculated based on the physio-chemical data (Li et al. 2004, 1992; Saggar et al. 2004; Zhang et al. 2002). The DNDC model can run at field or regional scales. In this study, the field-scale mode was used in this study (version 9.5, http://www.dndc.sr.unh.edu/).

Daily weather data were collected from the nearby weather stations; soil samples were collected and analyzed to obtain soil properties required in the DNDC model. For the plant properties (grain production, biomass fraction and thermal degree days for maturity, please see details in Table 5-3), we first narrow down the values to a appropriate range for all required plant input parameters through literature review and synthsize analysis, we then ran the model and manually comparing simulating results with measurements until the MSE of the simulated CO_2 flux, soil temperature, and soil water content can not be decreased; and urban grass management practices were obtain through interviews of mowers (please see the final results in Table 5-3). Other soil parameters (e.g., field capacity, wilting point, conductivity, and SOC partitioning) were set to the default values based on soil texture. Based on the collected input data, input files were created for the urban turfgrass and wooded area. In order to reduce residual effects of initial conditions, DNDC simulations were conducted consecutively from January 2015 to January

2018 and the simulation results for the study period (June 2016 to July 2017) were extracted and compared with field measurements. Due to variation among parks, we separated parks into two groups (group one: parks on the urban fringe, group two: interior urban parks) and the measured Ts, SWC and CO_2 flux within each group were compared with model results from DNDC to identify whether DNDC can simulate the dynamics of Ts, SWC and CO_2 flux in urban greenspaces.

Table 5-3. Plant properties' input values for both turfgrass and wooded area of the DNDC model and sources of citation. Note that the values are averaged from difference plant species in all parks and same values were used in the DNDC simulation.

Parameter		Turfgrass	References	Wooded area	References
Max. biomass production (kg C/ha/yr)	Grain	256	(Abdalla et al. 2010; Beheydt et al. 2007; Coleman et al. 1997; Gopalakrishnan, Cristina Negri, and Salas 2012; Kayatz 2014; S. Saggar et al. 2007; Saggar et al. 2004; Surinder Saggar et al. 2007)	380	(Aber et al. 1995; Aber, Reich, and Goulden 1996; Aber and Federer 1992; Butterbach-Bahl et al. 2009; Kiese et al. 2011; Kurbatova et al. 2008; Lamers, Ingwersen, and Streck 2007; Lu and Cheng 2009; Miehle et al. 2006)
	Leaf	5775		7189	
	Stem	1925		1232	
	Root	4877		1469	
Annual N demand (kg N/ha/yr)		129		9	
Thermal degree days for maturity		4400		4500	
Water demand (g water / g dry biomass)		250		50	
N fixation index		1.5		1.0	
Optimum temperature (℃)		20		20	
Valscularity		0		0	
Maturity age		NA		50	
Current age		NA		20	

5.2.5 Statistics analysis

A two-way ANOVA was used to test whether CO_2 flux from turfgrass or wooded areas were significantly differing from park to park. Simple linear regression (SLR) and non-linear regression (exponential, equation 5-2) were used to test the response of CO_2 flux to temperature. SLR was used to test the response of CO_2 flux soil moisture. Based on the parameters in equation

5-2, temperature sensitivity of CO_2 flux was evaluated by the Q_{10} function (equation 5-3) in turfgrass and wooded area. In addition, the paired-t test was used to test for significant differences between simulated and measured CO_2 flux rates. The relationship between the simulated and measured CO_2 flux rates was fitted by SLR to evaluate model performance. The slope of the SLR indicates the extent of a systematic bias and the significance of the intercepts and the correlation coefficients were also calculated and tested. All statistical analyses were performed in R (version 3.2), and all significant differences were based on $p<0.05$.

$$CO_2\ flux = F \times\ exp^{(a \times \mathrm{Ts})} \tag{5-2}$$

$$Q_{10} = \frac{\exp(F \times (Ts + 10) - a \times (Ts + 10))}{\exp(F \times \mathrm{Ts} - a \times Ts^2)} \tag{5-3}$$

Where F is a constant value, Ts stands for soil temperature at 10 cm.

For the evaluation of DNDC model performance, we used five model evaluation statistics (Table 5-4) including mean error (*E*), root mean square error (*RMSE*), normalized RMSE (*nRMSE*), index of agreement (*d*) and modeling efficiency (*EF*). Features of each deviation statistic was described in detail in Table 5-4 based on previous publications (Li et al. 2017; Yang et al. 2014). Each deviation statistic addresses only a specific aspect of a model performance, but the combination of five indexes would help quantify the overall model performance. The five deviation statistics were calculated using the equations (5-4) to (5-8):

Table 5-4. DNDC model evaluation deviation statistic, their advantage, disadvantage, and criteria for model evaluation based on Yang et al. (2014); Li et al. (2017).

Deviation statistic	Features	Criteria
E	E > 0: Simulated values overestimate the observed data; E < 0: Simulated values underestimate the observed data. Paried t test was used to test the significant differ between simulated and measured values.	P < 0.05: simulated values significant differ from measured values. P > 0.05: simulated values do not significant differ from measured values.
RMSE	Summarizes the average difference between observed and predicted values. Advantage: resolved the issue related with E statistic (the positive and negative errors can negate each other).	RMSE is a positive value, smaller value indicates good model performance.
nRMSE	nRMSE is used as a relative measure for inter-comparisons of different variables or different models.	nRMSE ≤ 15% indicates good agreement. 15% ≤ nRMSE ≤ 30% indicates moderate agreement. nRMSE ≥ 30% indicates poor agreement between measured and predicted values.
d	It is a dimensionless and bounded measure, thus allows cross-comparisons between simulated and observed data.	d ≥ 0.9: excellent agreement between measured and predicted values. 0.8 ≤ d < 0.9: good agreement between measured and predicted values. 0.7 ≤ d < 0.8: moderate agreement between measured and predicted values. d < 0.7: poor agreement between measured and predicted values.
EF	Similar to d, EF statistic is a sum of squares-based, dimensionless statistics, mainly used to depict the degree to which the deviation toward zero.	EF = 1: perfect match between measured and predicted values. EF < 0: the model predicted values are worse than simply using the observed mean to replace the simulated values. EF > 0 is a critical condition to conclude "goodness of match" between the simulated and the observed.

$$E = \frac{\sum_{i=1}^{n}(S_i - M_i)}{n} \quad (5\text{-}4)$$

$$RMSE = \sqrt{\frac{\sum_{i=1}^{n}(S_i - M_i)^2}{n}} \quad (5\text{-}5)$$

$$\text{nRSME} = \frac{RSME}{\bar{M}} \times 100\% \quad (5\text{-}6)$$

$$\text{d} = 1 - \frac{\sum_{i=1}^{n}(S_i - M_i)^2}{\sum_{i=1}^{n}(|S_i - \bar{M}| + |M_i - \bar{M}|)^2} \quad (5\text{-}7)$$

$$\text{EF} = 1 - \frac{\sum_{i=1}^{n}(S_i - M_i)^2}{\sum_{i=1}^{n}(M_i - \bar{M})^2} \quad (5\text{-}8)$$

where S_i is the simulated value, M_i is the measured value, n is the number of measured values, and $\bar{M}$ is the average of the measured values.

5.3 RESULTS

We detected significant CO_2 flux variation in both turfgrass and wooded areas in five parks, which ranged from 4.89 to 7.73 g C m^{-2} day^{-1} in turfgrass, and 4.07 to 5.09 g C m^{-2} day^{-1} in wooded areas. There was significant difference in CO_2 flux from park to park. In the turfgrass, CO_2 flux from parks closest to the centre of town (DRP and NCP) were significantly lower than parks (HCP and DCP) on the edge of town (Figure 5-3 panel a). In the wooded areas, CO_2 flux was much more consistent across parks, where only one (NCP) was significantly lower than the others (Figure 5-3 panel b).

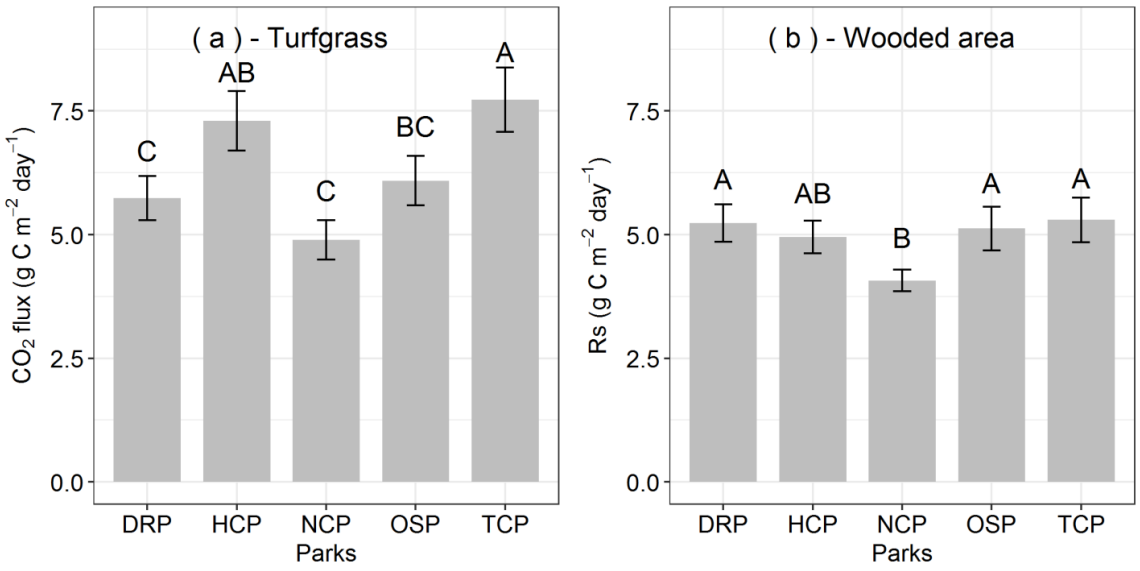

Figure 5-3. Mean annual soil CO_2 flux of five parks for grass (a) and woods (b) over the study period. Vertical bars represent standard error of the mean (*n*=75 for turfgrass and *n*= 78 for wooded area). Different letters above the vertical bars denotes significant difference.

The CO_2 flux difference among parks can be partially explained by differences in soil properties: bulk density (Figure 5-4 panel a and b), soil total carbon (Figure 5-4 panel c and d), and soil total nitrogen (Figure 5-4 panel e and f). Soil carbon to nitrogen ratio explains a limit amount (8%) of CO_2 efflux variation among turfgrasss (data not shown) but not for wooded areas (data not shown). CO_2 flux negatively correlated with soil bulk density, but positively related to soil total carbon, soil total nitrogen and soil carbon to nitrogen ratio (Figure 5-4).

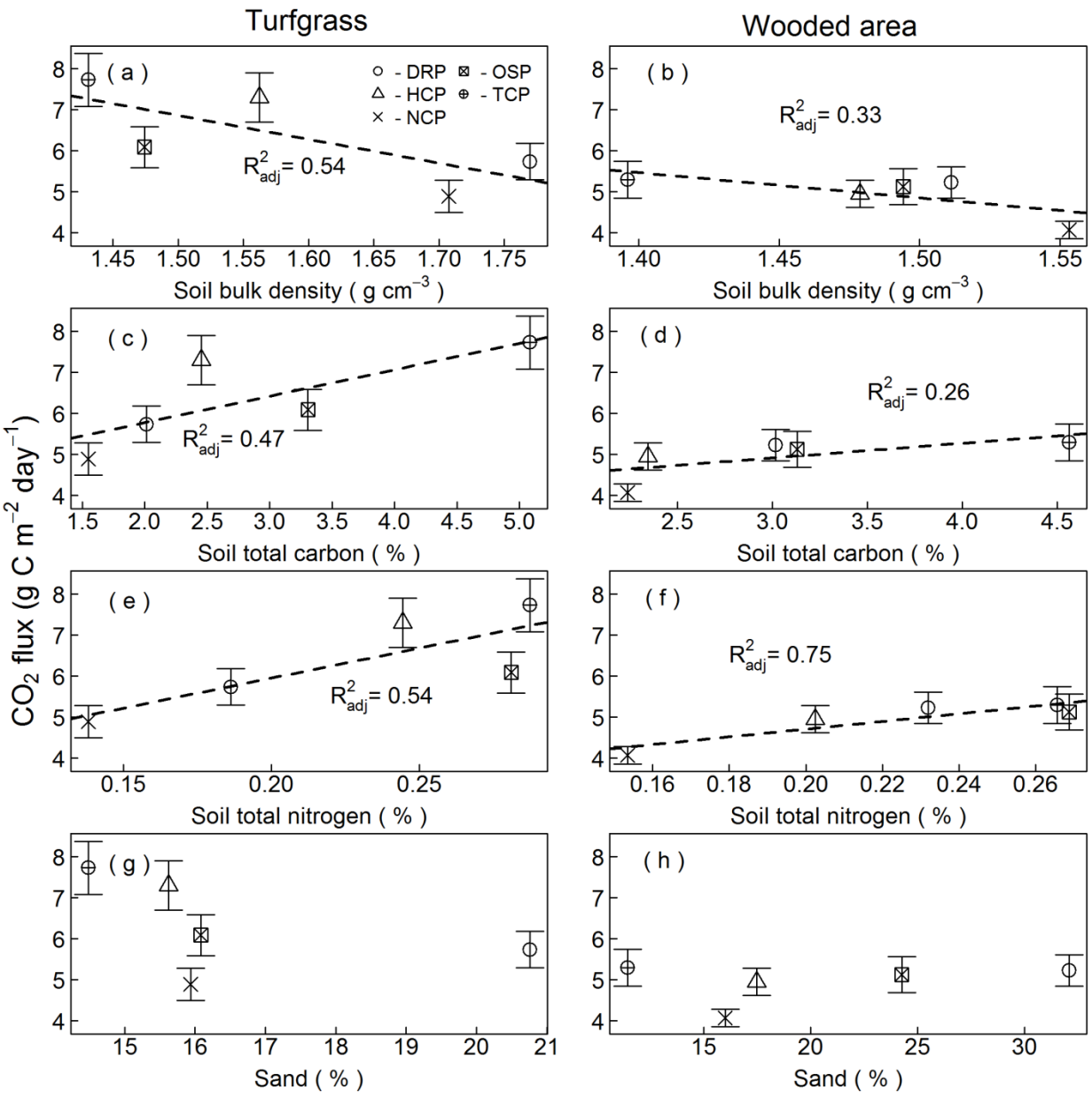

Figure 5-4. The relationship between annual soil CO_2 flux and soil bulk density (a and b), (c and d) soil total carbon (TC) storage at 0–10 cm, (e and f) soil total nitrogen (TN) storage at 0–10 cm, and (g and h) Sand content (%) at 0–10 cm. The error bars are standard error (n=3), regression lines only plotted if p value < 0.05.

5.3.1 Temporal variation of CO_2 flux

A strong diurnal variation in CO_2 flux was observed in the turfgrass (Figure 5-5 panel a, c and e); however, the diurnal variation in the wooded area was smaller (Figure 5-5 panel b, d and

f). Within the turfgrass, there was considerable CO_2 diurnal flux variation in summer (Figure 5-5 panel c), moderate CO_2 flux variation in fall (Figure 5-5 panel e), and minimal in spring (Figure 5-5 panel a). Soil temperature and soil moisture explained some of the diurnal variation of CO_2 flux in turfgrass and wooded area (Figure 5-5). Temperature was more strongly correlated with CO_2 fluxes during the spring and fall, than in the summer (Figure 5-5). For soil CO_2 flux diurnal variation, we detected a positive relationship between CO_2 flux and soil temperature in turfgrass for all three seasons (Figure 5-6, panel a).

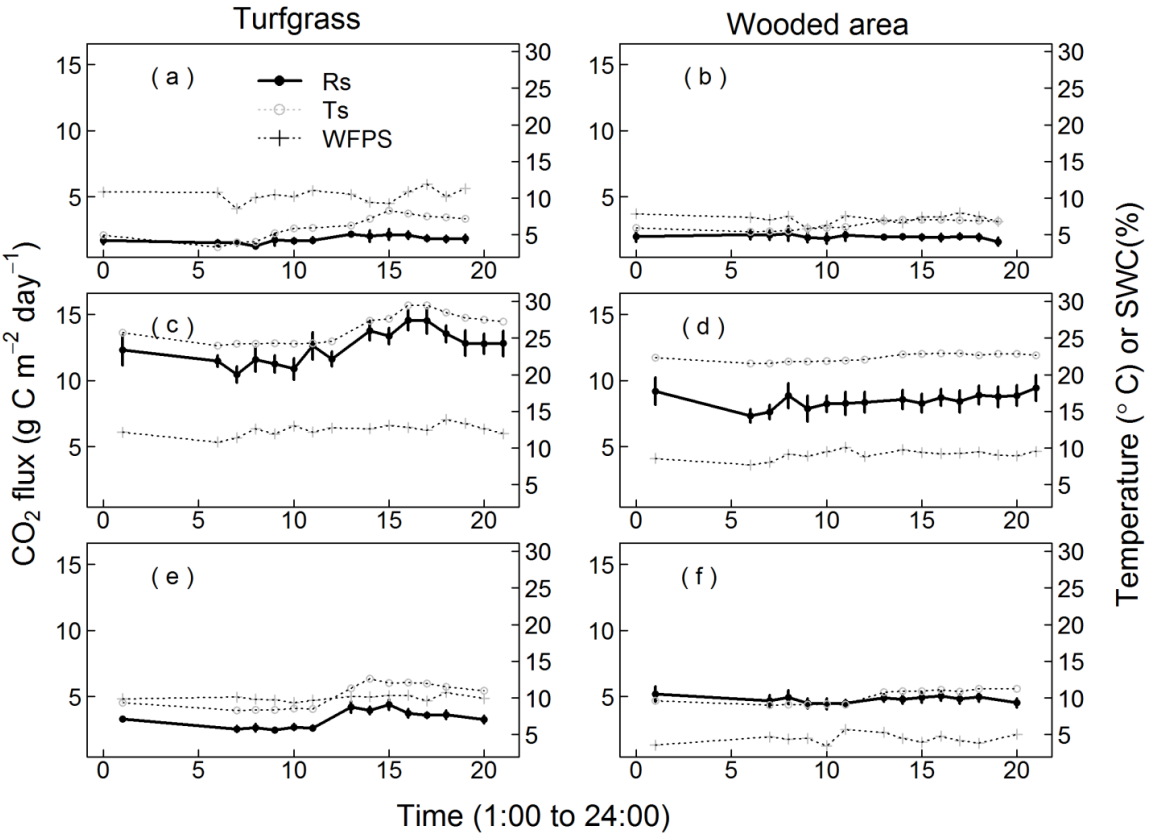

Figure 5-5. Diurnal variation in soil CO_2 flux rates, air temperature, and soil water content for turfgrass (left panels) and wooded area (right panels) in August 2016 (a, b), October 2016 (c, d), and March 2017 (e, f), stand for CO_2 flux diurnal variation in spring, summer, and autumn, respectively. Vertical bars represent standard error (n=5 to 8).

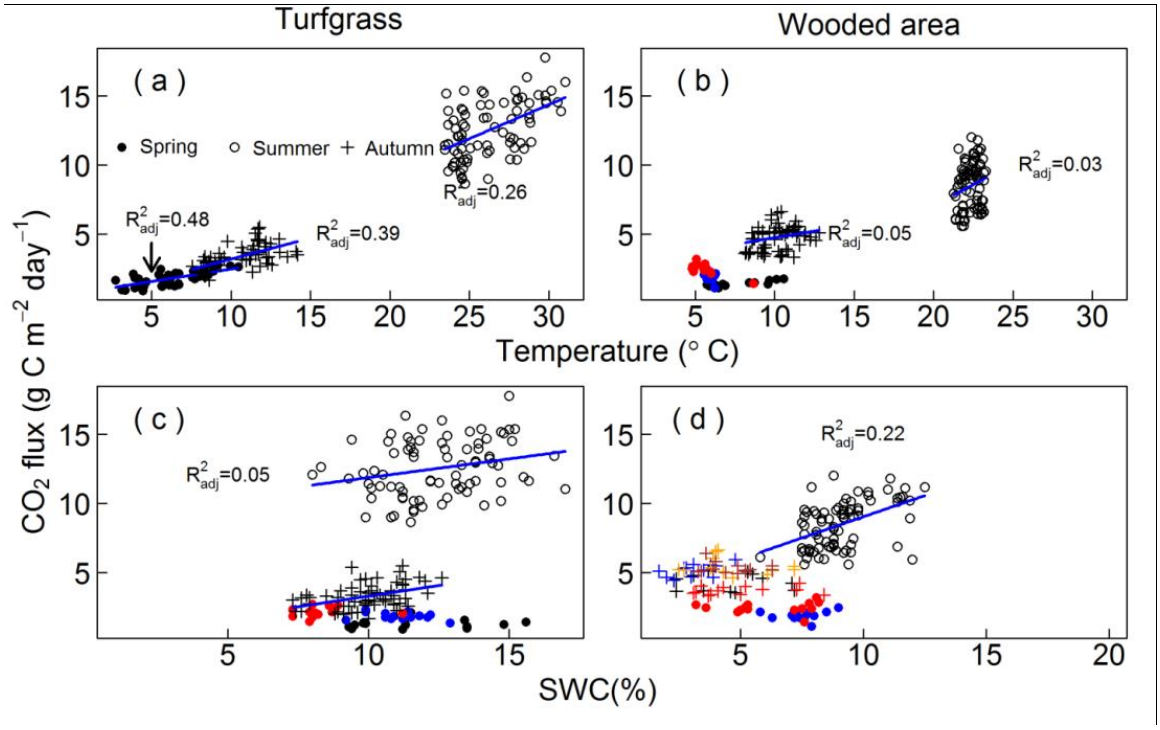

Figure 5-6. Diurnal variation of CO_2 flux response to soil temperature at 10 cm (a and b), and diurnal variation of CO_2 flux response to soil water content change at 10 cm (c and d). In wooded areas, CO_2 flux was negatively correlated with soil temperature at spring, but when down-scaled to each collar (dots in different colors in panel b), CO_2 flux either positively correlates with soil temperate or showed no correlation. We detected negative relationships between CO_2 flux and soil water content in spring for turfgrass (dots in different colors in panel c); and detected a negative relationship between CO_2 flux and soil water content in spring [dots in different colors in panel (d) and autumn crosses in different colors in panel (d)] for wooded area. When grouped by collars, either no relationship or a positive relationship was detected.

In wooded areas, CO_2 flux diurnal variations were positively related with soil temperature at summer and autumn, but correlate negatively with soil temperature at spring. We grouped the CO_2 flux data in spring by collars (different colors in Figure 5-6 panel b), and found that the air temperature measured from one of the collars spanned a relatively large range, and CO_2 flux measured at this collar positively related with air temperature change. For other two collars, we detected no significant relationship between CO_2 flux and air temperature. Similarly, in turfgrass, we detected negative relationships between CO_2 flux and SWC in spring. In the

wooded area, we detected negative relationships between CO_2 flux and SWC in spring and autumn. However, when grouped by collars, either no relationship, or a positive relationship, was detected (Figure 5-6 panels c and d). These results indicated that when CO_2 flux, soil temperature, and SWC diurnal fluctuation is very small, the collar to collar variation is bigger than the diurnal fluctuation, and thus data must be carefully analyzed.

Seasonal variation of CO_2 flux from all parks followed a clear pattern which paralleled soil temperature, but the soil water content did not shown a similar pattern in either the turfgrass nor in wooded areas (Figure 5-7 panels a and b). The CO_2 flux peaked in summer (June, July, and August) and then gradually fell into its lowest values in winter (December and January). Our results exhibited a strongly exponential positive correlation of CO_2 flux with soil temperature for both turfgrass and wooded area (Figure 5-7 panels c and d), suggesting that soil temperature was a good predictor for seasonal CO_2 flux at these individual sites. Soil water content, however, was a very poor predictor, only accounting for 4% of the variability in CO_2 flux in turfgrass and none in wooded areas.

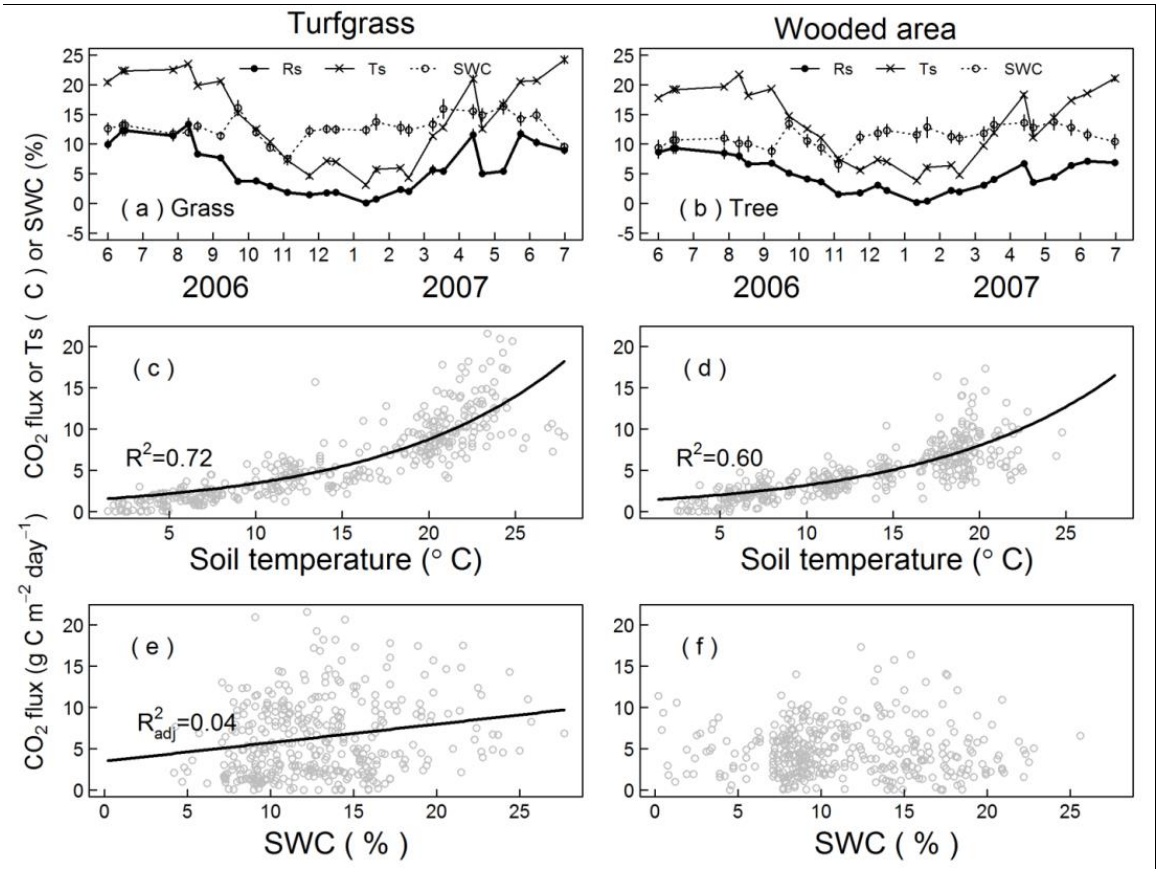

Figure 5-7. CO_2 flux seasonal variation. (panels a and b): Seasonal change of soil CO_2 flux [black solid dots with mean ± standard error; n = 15 (3 collars in each park)], soil temperature at 10 cm (crosses with solid lines), and soil water content at 10 cm (dots with dashed lines). (panels c and d): Relationships between soil CO_2 flux and air temperature for grasses and woods, respectively. (panels e and f): Relationships between soil CO_2 flux and soil moisture for turfgrass and wooded area, respectively. All depicted regressions are significant at $p< 0.05$.

5.3.2 DNDC simulation results

The simulated dynamics in soil temperature, SWC and CO_2 flux by DNDC agreed well with seasonal measurements between June 2016 and July 2017 for both urban turfgrass and wooded areas (Figure 5-8 and 5-9). Over the whole study period, the d-values ranged from 0.62 to 0.98, and EF values ranged from 0.12 to 0.89 (Table 5-5, all data). The DNDC model performs best in simulating soil temperature (d = 0.98 and 0.96, EF = 0.89 and 0.86 for turfgrass and wooded areas, respectively, Table 5-5) and CO_2 flux (d = 0.88 and 0.91, EF = 0.51 and 0.75

for turfgrass and wooded areas, respectively, Table 5-5, all data); however, it does not perform well in simulating soil water content (d = 0.64 and 0.62, EF = 0.12 and 0.28 for turfgrass and wooded areas, respectively, Table 5-5, all data) in this study.

Simulated dynamics in soil temperature, which was primarily driven by air temperature, agreed well with the seasonal measurements for both urban turfgrass (Figure 5-8 panel a and 5-9 panel a) and wooded areas (Figure 5-8 panel b and Figure 5-9 panel b). The calculated E of soil temperature for the turfgrass (0.29, Table 5-5) and wooded area (1.61, Table 5-5) were larger than zero, indicated that DNDC model overestimated soil temperature compared with measured soil temperature at 10 cm depth. The t-test showed that there were no significant differences between Ts estimated by DNDC model and measured data for turfgrass (p-value = 0.32), however, DNDC model significantly overestimate Ts in wooded areas (p-value < 0.001, Table 5-5), similar results were found when down-scaled to each season (Table 5-5).

The seasonal dynamic of SWC simulated by DNDC was primarily determined by rainfall. Simulated results showed that the DNDC can simulate soil moisture seasonal variation in both urban and turfgrass (Figure 5-8 panels c, d and Figure 5-9 panels c and d). The calculated E of SWC for the turfgrass (2.10, Table 5-5) and wooded area (2.05, Table 5-5) were larger than 0, indicated that the DNDC model overestimated soil moisture at 10 cm depth compared with measured soil moisture. The t-test showed that there were significant differences between SWC estimated by DNDC model and measured data for both turfgrass and wooded areas (p-value < 0.001). When downscaled to the season, the results showed that DNDC could obtain the fluctuation well in autumn in turfgrass, and summer and autumn in wooded areas (P > 0.05, Table 5-5), but significantly overestimated in other periods (P < 0.05).

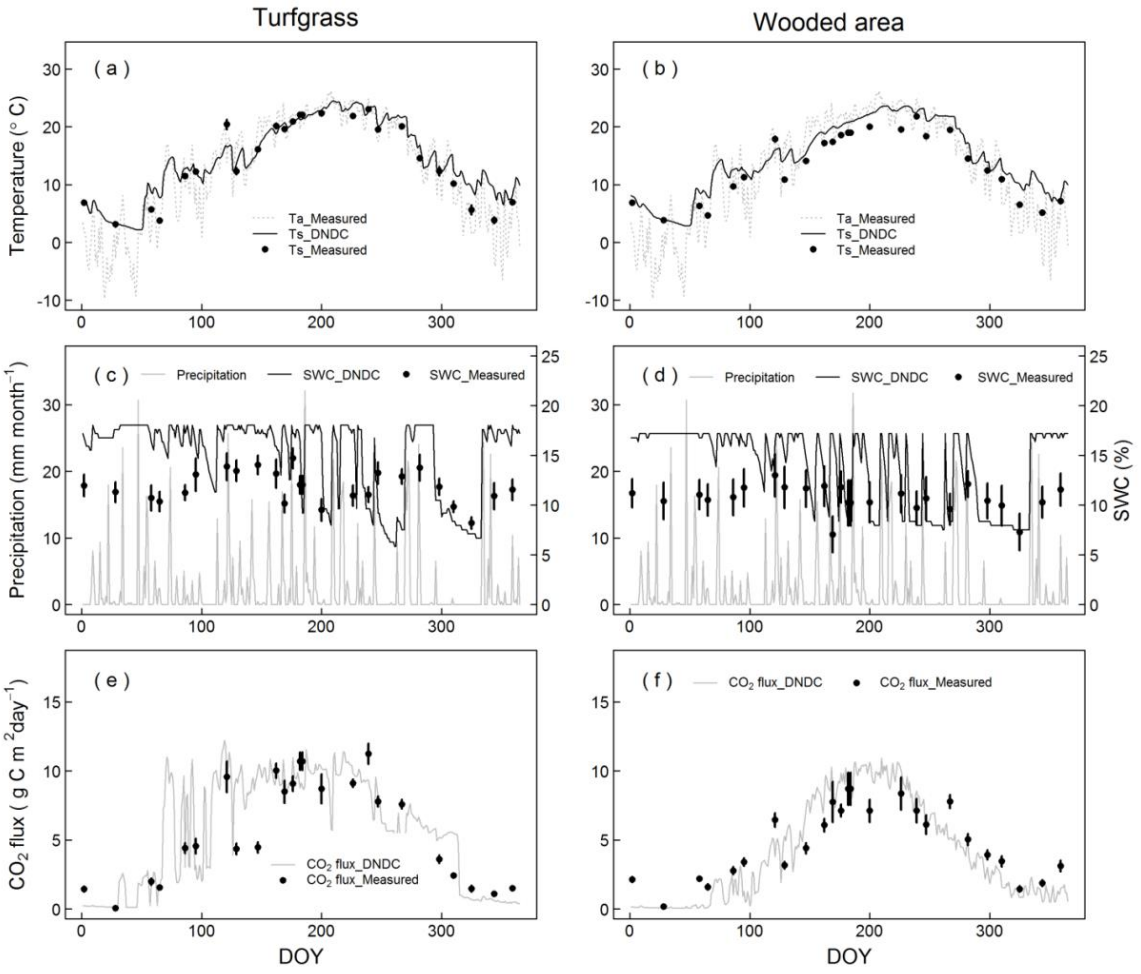

Figure 5-8. Comparison between the DNDC model simulated and field measured air temperature, soil temperature (in the 0–10 cm depth), soil water content (SWC) (in the 0–10 cm depth), and soil CO_2 flux for urban park turfgrass (left panel), and wooded areas (right panel) from June 2016 to July 2017 in DRP, OSP, and NCP.

Simulated dynamics in CO_2 flux agreed well with seasonal measurements of CO_2 flux for both turfgrass and wooded areas (Figure 5-8 panel e, f and Figure 5-9 panel e, f) during our study period. The calculated E of CO_2 flux for the turfgrass (-0.66, Table 5-5) and wooded areas (-0.34, Table 5-5) were lower than 0, indicated that DNDC model underestimated CO_2 flux compared with measured CO_2 flux. The t-test showed that there were no significant differences between Ts estimated by DNDC model and measured data for both turfgrass (p-value = 0.09)

and wooded areas (p-value = 0.20), however, DNDC model significantly underestimated CO_2 flux in summer, winter in turfgrass, summer, autumn and winter in wooded areas ($P<0.05$, Table 5-5).

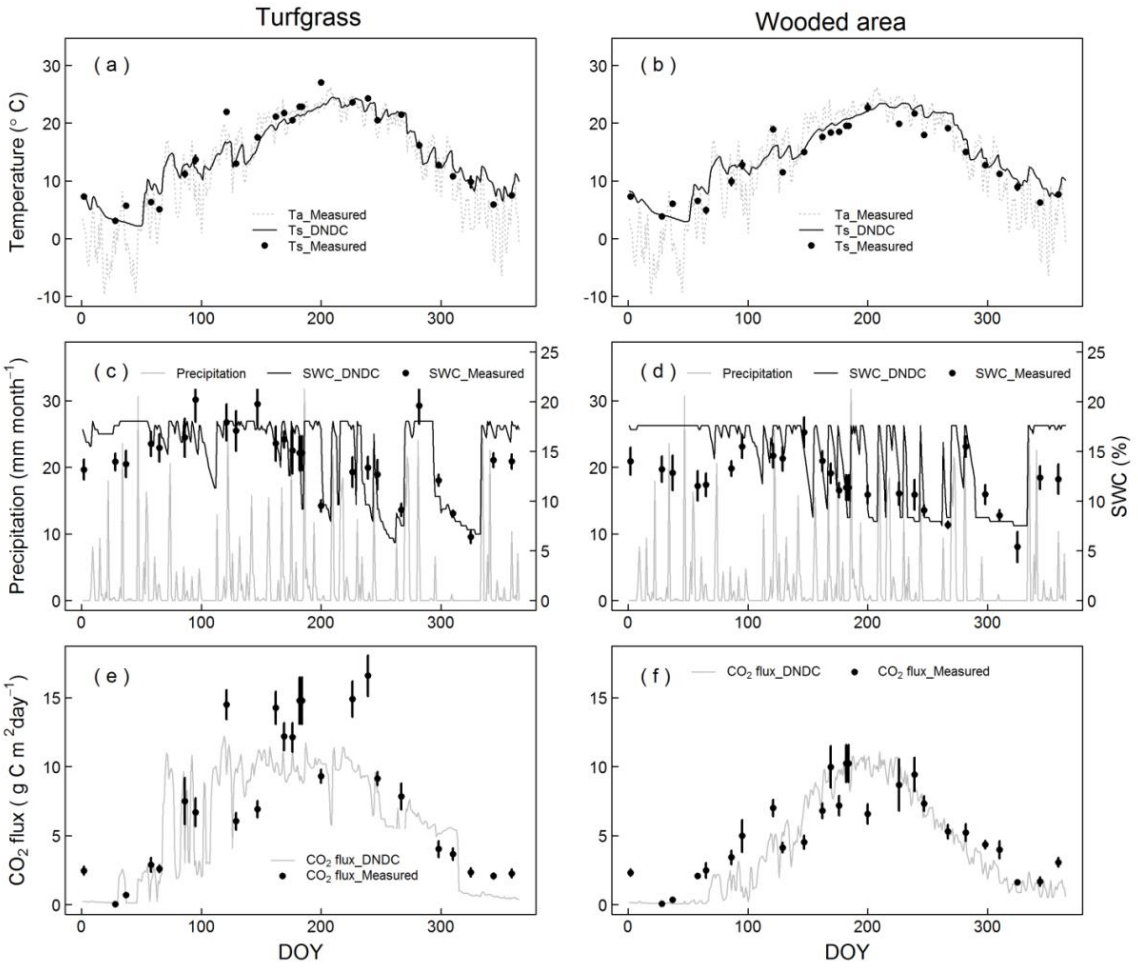

Figure 5-9. Comparison between the DNDC model simulated and field measured air temperature, soil temperature (in the 0–10 cm depth), soil water content (SWC) (in the 0–10 cm depth), and soil CO_2 flux for urban park turfgrass (left panel), and wooded areas (right panel) from June 2016 to July 2017 in HCP and TCP.

Table 5-5. Statistical evaluations of simulated daily CO_2 flux, soil temperature (Ts), and soil water content (SWC) compared with measured values in five parks from June 2016 to July 2017.

Landscape	Variables	Measured	Simulated	N	E	RMSE	nRMSE (%)	d	EF	t-test (p)
				Turfgrass						
All	Ts	14.73	15.02	51	0.29	2.03	14	0.98	0.89	0.32
	SWC	13.13	15.23	51	2.10	4.18	32	0.64	0.12	<0.001
	CO_2 flux	6.56	5.90	51	-0.66	2.79	42	0.88	0.51	0.09
Spring	Ts	13.26	13.15	12	-0.11	2.52	19	0.90	0.24	0.89
	SWC	15.25	17.68	12	2.43	3.82	25	0.46	-1.27	0.02
	CO_2 flux	6.11	6.23	12	0.12	3.57	58	0.70	0.07	0.91
Summer	Ts	22.25	21.6	16	-0.65	1.57	7	0.74	0.08	0.10
	SWC	12.91	15.45	16	2.54	4.78	37	0.42	-0.25	0.03
	CO_2 flux	11.69	9.79	16	-1.91	3.39	29	0.40	-1.77	0.02
Autumn	Ts	14.49	15.55	12	1.06	1.61	11	0.97	0.87	0.01
	SWC	11.55	10.34	12	-1.21	2.63	23	0.86	0.56	0.11
	CO_2 flux	4.81	5.26	12	0.44	1.95	40	0.82	0.29	0.45
Winter	Ts	5.67	6.91	11	1.23	2.39	42	0.64	0.21	0.08
	SWC	12.85	17.56	11	4.71	4.93	38	0.36	-0.07	<0.001
	CO_2 flux	1.51	0.60	11	-0.91	1.16	77	0.62	-0.17	0.003
				Wooded areas						
All	Ts	13.47	15.08	51	1.61	2.23	17	0.96	0.86	<0.001
	SWC	11.36	13.40	51	2.05	3.85	34	0.62	0.28	<0.001
	CO_2 flux	4.97	4.63	51	-0.34	1.89	38	0.91	0.75	0.20
Spring	Ts	11.81	13.17	12	1.31	2.44	21	0.88	0.32	0.06
	SWC	12.99	16.23	12	3.24	3.93	30	0.40	-0.31	<0.001
	CO_2 flux	4.04	3.14	12	-0.89	2.48	61	0.58	0.17	0.23
Summer	Ts	19.41	21.03	16	1.62	1.90	9.8	0.68	0.20	<0.001
	SWC	10.96	11.60	16	0.64	3.59	33	0.43	-0.02	0.49
	CO_2 flux	8.14	9.33	16	1.19	1.99	24	0.36	-1.02	0.01
Autumn	Ts	13.95	16.23	11	2.28	2.40	17	0.92	0.75	<0.001
	SWC	9.75	9.56	11	-0.19	2.16	22	0.86	0.61	0.77
	CO_2 flux	4.64	3.69	11	-0.95	1.30	28	0.89	0.67	0.004
Winter	Ts	6.10	7.32	12	1.22	2.24	37	0.59	0.22	0.07
	SWC	11.90	17.13	12	5.23	5.30	45	0.28	-0.01	<0.001
	CO_2 flux	1.74	0.45	12	-1.29	1.51	87	0.55	-0.17	<0.001

5.4 DISCUSSION

In this study, we found that the CO_2 flux from urban turfgrass differed from wooded areas of parks and were spatially and temporally variable. Despite this variability, the DNDC model successfully predicted CO_2 fluxes. The higher CO_2 fluxes from turfgrass in the five selected urban parks is not surprising because we did not remove near-surface plants during gas sampling, thus CO_2 fluxes from urban turfgrass including both soil respiration and grass stem and leaf respiration, but CO_2 fluxes from wooded areas was primarily contributed by soil respiration.

One intriguing result was the variability among parks. Parks on edges of urban development (HCP and TCP) had larger annual CO_2 efflux comparing with parks near downtown (DRP, NCP, and OSP). Several other studies observed similar patterns in other cities across the US, but causes remain unclear (W. Chen et al. 2013; Decina et al. 2016; Groffman et al. 1995; Kaye et al. 2005; Koerner and Klopatek 2010). Soils from the edges of parks tended to have more carbon and nitrogen and lower bulk densities (Figure 5-4); however, the soil properties alone could not explain the variation among parks. Lower CO_2 fluxes from interior greenspaces may be caused by differences in soil physical and chemical characteristics not measured here, such as higher concentrations of metals or reduced aggregation. Urban activities such as topsoil stripping, grading, and compacting greatly destroy soil aggregate structures, alter soil hydraulic conductivity, and thus may also decrease soil carbon pools and greenhouse gas fluxes (Chen, et al. 2014).

The CO_2 fluxes from these urban greenspaces fell in a similar range of previous urban measurements across the globe. The average annual mean CO_2 flux from wooded areas in the

five parks (4.72 g C day^{-1} m^{-2}) was similar to CO_2 flux rates (4.01 g C day^{-1} m^{-2}) in a temperate urban forest in Beijing, China (Wu et al. 2015); and similar to CO_2 flux rate (3.97 g C day^{-1} m^{-2}) from a mixed forest in an urban park from in temperate climate, South Korea (Bae and Ryu 2017). However, our measurements were higher than the CO_2 flux rate (2.62 g C day^{-1} m^{-2}) from an urban forest in Boston, USA (Decina et al. 2016) and an urban forest in Hefei, China (2.60 g C day^{-1} m^{-2}) (Tao et al. 2016). The average annual mean CO_2 flux from urban turfgrass in the five parks (6.17 g C day^{-1} m^{-2}) was higher than the CO_2 flux rate (3.34 g C day^{-1} m^{-2}) from urban lawns in an park from temperate climates, South Korea (Bae and Ryu 2017), and from an urban lawn in Boston, USA (4.49 g C day^{-1} m^{-2}) (Decina et al. 2016). However, we observed lower CO_2 flux rates than from urban lawns in drier climates, including Fort Collins, CO (7.61 g C day^{-1} m^{-2}) and Phoenix, AZ (8.18 g C day^{-1} m^{-2}) (Koerner and Klopatek 2002); and lower CO_2 flux rate than from urban tropical grassland, Singapore (8.19 g C day^{-1} m^{-2}) (Ng et al. 2015). Previous analyses have synthesized research results from forests and grassland ecosystems across the globe to explore the heterogeneity of CO_2 fluxes and its causal factors (such as precipitation, temperature, and soil properties) in forests and grassland ecosystems (Wang et al. 2010; Wang and Fang 2009). However, we do not have enough published data to support such synthesize analyses in urban ecosystems. Human interactives with environmental conditions may lead to more complex spatial and temporal variation of CO_2 flux in urban soils compared to natural soils. Macro-scale (cross ecosystem or continental) experimental designs under appropriate analytical framework (Polsky et al. 2014) for assessing the homogenization of urban CO_2 flux could help clarify spatial and temporal variation of urban CO_2 flux.

CO_2 fluxes from urban greenspaces in this study were strongly correlated with temperature. The strong temperature dependence of CO_2 flux has been supported in many studies

on temperate ecosystems (Davidson, Richardson, et al. 2006) and urban ecosystems (Zhou et al. 2012). However, the correlation of CO_2 flux with soil moisture was relatively poor (Figure 5-7 panel e and f). A possible reason is due to the plentiful rainfall, the soils seldom underwent long-term saturation or frequent prolonged drought (SWC maintain at 5-10% all year around, Figure 5-7 panels a and b), thus seasonal variation of soil moisture was relatively small and may not limit activities of microbe in most months. In addition, during wet or normal years in temperate regions, root respiration from trees and grasses may not respond to seasonal variation of soil moisture because the root activity is seldom limited by soil water availability (Yang et al. 2007). Generally, our results indicated that the major driver of CO_2 flux seasonal variation was soil temperature rather than soil moisture (Figure 5-7) in both urban turfgrasss and urban wooded areas in our chosen parks.

For soil CO_2 flux diurnal variation, we detected a positive relationship between CO_2 flux and soil temperature in turfgrass for all three seasons. In wooded areas however, CO_2 flux diurnal variation was positively related with soil temperature in summer and autumn, but negatively correlate with soil temperature at spring. Temperature is the most important environmental factor affecting carbon decomposition processes and CO_2 flux. Studies demonstrated that CO_2 flux increases exponentially with increasing temperature in its low range, reaches its maximum at an optimum temperature, and then declines in extreme high temperature conditions as enzymes may degrade and respiratory activity decreases (Luo and Zhou 2006). However, this curve response between CO_2 flux and soil temperature unlikely explains the negative relationship between CO_2 flux and soil temperature observed in the spring because we detected positive relationships between CO_2 flux and soil temperature during summer when temperature is high. We analysed the relationship between soil temperature and soil water

content in spring from the wooded area to test whether the interaction between soil temperatures and soil water content cause the negative relationship between CO_2 flux and soil temperature. We did not detect any significant relationship between soil temperature and soil water content at diurnal scales (statistical results not shown), thus it is unlikely that soil temperature and soil water content interaction cause negative relationships between CO_2 flux and soil temperature in spring. We thus grouped CO_2 flux measurements in spring by collars (different colors in Figure 5-6), we found that within each collar, the Rs either positively related with soil temperature change or show no relationship to soil temperature (Figure 5-6). Similarly, in turfgrass, we detected negative relationships between CO_2 flux and SWC in spring (Figure 5-6 panel c). In wooded area, we detected a negative relationship between CO_2 flux and SWC in spring and autumn (Figure 5-6 panel d); however, when grouped by collars, either no relationship or positive relationship was detected (different colors in Figure 5-6 panels c and d). The results indicated that in spring, when CO_2 flux, soil temperature, and SWC diurnal fluctuation is very small, collar-to-collar variation is larger than the diurnal fluctuation. Thus, caution should be taken if unusual relationships between CO_2 flux and environmental factors occur.

The DNDC model performed moderately well for soil temperature, soil water content, and CO_2 flux in both turfgrass and wooded areas; however, sometimes the indicator by one statistic conflicted with another. For instance, the nRMSE value of SWC% in turfgrass = 27%, which indicates a moderate agreement between simulated values and measured values (Table 5-1), but d value = 0.65, which indicates a poor agreement between measured and predicted values (Table 5-1). Similar situation were detected by other studies, in the Loess Plateau of Northwestern China, Li et al. (2015) used the Decision Support System for Agrotechnology Transfer (DSSAT) model to simulate yield and soil organic carbon and nitrogen, the results

indicated that model evaluate statistic E value did not agree with the results indicated by nRMSE and d values. Thus, caution should be taken to consider all statistics together with graphic evaluation to draw final conclusion on the model performance in soil temperature, soil water content and CO_2 flux by DNDC model.

Our results showed that the DNDC model has potential to derive large-scale estimates of CO_2 flux from urban soils. The parameters, input variables, and calibration are key elements to increase use of the DNDC model in future. The DNDC model needs a certain number of parameters and input variables, including: climate, soil, plants, and human management. Climate data usually can be collected from local weather stations. Soil parameters and management can be collected through soil physical and chemical properties analyses and surveys, if available. Moreover, when soil texture characteristics was determined, DNDC model will provide default soil physical and chemical input variables. But land disturbance in urban areas may result in unexpected soil conditions (i.e., that are not typical for a given texture).

However, plant parameters used for the plant growth sub-module of the DNDC model are very difficult to obtain. In this study, we reviewed literature to collect appropriate values for all required plant input parameters. When all necessary parameters were prepared, model calibration is an important step to improve the simulation. We ran the model and comparing simulating results with measurements, and the calibration was done manually. However, the procedure of manual model calibration is very time consuming, and the manual calibration does not necessarily yield optimal parameter estimates. To resolve disadvantages related with manual calibration, Lamers et al. (2007) developed an automatic calibration of the Forest-DNDC model, results showed that the software linkage between Forest-DNDC and a computer code for universal inverse modelling (UCODE) yields a useful procedure for automatic calibration of the

DNDC model, the calibration significantly improved agreement between model results and measured data. However, the linking of Forest-DNDC with UCODE requires the source code of DNDC model, but the DNDC model is not an open source, thus the automatic calibration cannot be applied at this study. An "open-source code" philosophy would tremendously increase the more extensive and creative usage of DNDC model and facilitate any calibration effort of the DNDC model in future.

5.5 CONCLUSION

Urban carbon fluxes play crucial role for informing sustainable urban planning in climate-friendly cities, but to date, there is little information about their spatial and temporal variation. In this study, we investigated spatial and temporal variations in CO_2 flux in five parks in Blacksburg, VA, USA, between June 2016 and July 2017. Temperature, and soil water content were the main environmental factors control CO_2 flux diurnal, weekly and seasonal variation. Spatially, we observed a significant difference in CO_2 flux among the five parks in this study. Soil bulk density, soil total carbon and soil total nitrogen can explain a certain amount of CO_2 flux variation in different parks. The DNDC model was used to simulate daily soil temperature, soil water content and CO_2 flux from turfgrass and wooded areas in five parks from June 2016 to July 2017. The DNDC model performaed best in simulating soil temperatures (0-10 cm layer), performaing well in simulating CO_2 flux, but relatively poor in simulating soil water content in both turfgrass and wooded areas. These results contribute to our understanding of carbon cycles in different urban land cover types.These results indicated that DNDC model can be used to estimate CO_2 fluxes from urban areas, which may help attain more accurate estimates of carbon cycling from urban areas.

REFERENCE

Abdalla, M. et al. 2010. "Testing DayCent and DNDC Model Simulations of N2O Fluxes and Assessing the Impacts of Climate Change on the Gas Flux and Biomass Production from a Humid Pasture." *Atmospheric Environment* 44(25):2961–70.

Aber, John D. et al. 1995. "Predicting the Effects of Climate Change on Water Yield and Forest Production in the Northeastern United States." *Climate Research* 207–22.

Aber, John D. and C.Anthony Federer. 1992. "A Generalized, Lumped-Parameter Model of Photosynthesis,evapotranspirationand Net Primary Productionintemperate and Boreal Forestecosystems." *Oecologia* 92:463–74.

Aber, John D., Peter B. Reich, and Michael L. Goulden. 1996. "Extrapolating Leaf CO2 Exchange to the Canopy: A Generalized Model of Forest Photosynthesis Compared with Measurements by Eddy Correlation." *Oecologia* 106(2):257–65.

Bae, Jeehwan and Youngryel Ryu. 2017. "Spatial and Temporal Variations in Soil Respiration among Different Land Cover Types under Wet and Dry Years in an Urban Park." *Landscape and Urban Planning* 167:378–85.

Beheydt, Daan, Pascal Boeckx, Steven Sleutel, Changsheng Li, and Oswald Van Cleemput. 2007. "Validation of DNDC for 22 Long-Term N2O Field Emission Measurements." *Atmospheric Environment* 41(29):6196–6211.

Butterbach-Bahl, K. et al. 2009. "A European-Wide Inventory of Soil NO Emissions Using the Biogeochemical Models DNDC/Forest-DNDC." *Atmospheric Environment* 43(7):1392–1402.

Chen, Wenjing et al. 2013. "Soil Respiration in a Mixed Urban Forest in China in Relation to Soil Temperature and Water Content." *European Journal of Soil Biology* 54:63–68.

Chen, Yujuan et al. 2013. "Changes in Soil Carbon Pools and Microbial Biomass from Urban Land Development and Subsequent Post-Development Soil Rehabilitation." *Soil Biology and Biochemistry* 66:38–44.

Chen, Yujuan et al. 2014. “Influence of Urban Land Development and Soil Rehabilitation on Soil–atmosphere Greenhouse Gas Fluxes.” *Geoderma* 226–227:348–53.

Chen, Yujuan, Susan D. Day, Abbey F. Wick, and Kevin J. McGuire. 2014. “Influence of Urban Land Development and Subsequent Soil Rehabilitation on Soil Aggregates, Carbon, and Hydraulic Conductivity.” *Science of the Total Environment* 494:329–36.

Coleman, K. et al. 1997. “Simulating Trends in Soil Organic Carbon in Long-Term Experiments Using the Verberne / MOTOR Model.” *Geoderma* 81:29–44.

Cramer, Wolfgang et al. 2001. “Global Response of Terrestrial Ecosystem Structure and Function to CO_2 and Climate Change: Results from Six Dynamic Global Vegetation Models.” *Global Change Biology* 7(4):357–73.

Cui, Jianbo, Changsheng Li, and Carl Trettin. 2005. “Modeling Biogeochemistry and Forest Management Practices for Assessing GHGs Mitigation Strategies in Forested Wetlands.” *Environmental Modeling and Assessment* 10(1):43–53.

Davidson, E. a, K. Savage, L. V Verchot, and R. Navarro. 2002. “Minimising Artifacts and Biases in 20 Chamber-Based Measurements of Soil Respiration.” *Agriculture, Ecosystems & Environment. Forest Meteorology* 113(1):21–37.

Davidson, Eric A. 2016. “Biogeochemistry: Projections of the Soil-Carbon Deficit.” *Nature* 540(7631):47–48.

Davidson, Eric A., A. D. Richardson, K. E. Savage, and D. Y. Hollinger. 2006. “A Distinct Seasonal Pattern of the Ratio of Soil Respiration to Total Ecosystem Respiration in a Spruce-Dominated Forest.” *Global Change Biology* 12(2):230–39.

Decina, Stephen M. et al. 2016. “Soil Respiration Contributes Substantially to Urban Carbon Fluxes in the Greater Boston Area.” *Environmental Pollution* 212:433–39.

Dorrepaal, Ellen et al. 2009. “Carbon Respiration from Subsurface Peat Accelerated by Climate Warming in the Subarctic.” *Nature* 460(7255):616–19.

Drew, M. C. (1983). Plant injury and adaptation to oxygen deficiency in the root environment: a review. *Plant and soil*, 75(2), 179-199.

Frey, Serita D., Juhwan Lee, Jerry M. Melillo, and Johan Six. 2013. "The Temperature Response of Soil Microbial Efficiency and Its Feedback to Climate." *Nature Climate Change* 3(4):395–98.

Goldman, Meadow B., Peter M. Groffman, Richard V Pouyat, Mark J. McDonnell, and Steward T. A. Pickett. 1995. "CH_4 Uptake and N Availability in Forest Soils along an Urban to Rural Gradient." *Soil Biology and Biochemistry* 27(3):281–86.

Gopalakrishnan, Gayathri, Maria Cristina Negri, and William Salas. 2012. "Modeling Biogeochemical Impacts of Bioenergy Buffers with Perennial Grasses for a Row-Crop Field in Illinois." *Global Change Biology Bioenergy* 4(6):739–50.

Groffman, Peter M. et al. 1995. "Carbon Pools and Trace Gas Fluxes in Urban Forest Soils." *Soil management and greenhouse effect*. London: Lewis Publishers.

Hall, Sharon J. et al. 2016. "Convergence of Microclimate in Residential Landscapes across Diverse Cities in the United States." *Landscape Ecology* 31(1):101–17.

Hansen, J., R. Ruedy, M. Sato, and K. Lo. 2010. "Global Surface Temperature Change." *Reviews of Geophysics*. 48(4):RG4004.

Heinemeyer, A. et al. 2011. "Soil Respiration: Implications of the Plant-Soil Continuum and Respiration Chamber Collar-Insertion Depth on Measurement and Modelling of Soil CO_2 Efflux Rates in Three Ecosystems." *European Journal of Soil Science* 62(1):82–94.

Hu, Zhenghua et al. 2010. "Effects of Simulated Nitrogen Deposition on Soil Respiration in Northern Subtropical Deciduous Broad-Leaved Forest." *Environmental Science* 31(8):1726–32.

Karhu, Kristiina et al. 2014. "Temperature Sensitivity of Soil Respiration Rates Enhanced by Microbial Community Response." *Nature* 513(7516):81–84.

Kayatz, Benjamin. 2014. “Modelling of Nitrous Oxide Emissions from Clover Grass Ley: Wheat Crop Rotations in Central Eastern Germany: An Application of DNDC.” *Student Thesis Series INES*.

Kaye, J. P., R. L. McCulley, and I. C. Burke. 2005. “Carbon Fluxes, Nitrogen Cycling, and Soil Microbial Communities in Adjacent Urban, Native and Agricultural Ecosystems.” *Global Change Biology* 11(4):575–87.

Kiese, Ralf et al. 2011. “Quantification of Nitrate Leaching from German Forest Ecosystems by Use of a Process Oriented Biogeochemical Model.” *Environmental Pollution* 159(11):3204–14.

Koerner, B. and J. Klopatek. 2002. “Anthropogenic and Natural CO_2 Emission Sources in an Arid Urban Environment.” *Environmental Pollution* 116:45–51.

Koerner, Brenda A. and Jeffrey M. Klopatek. 2010. “Carbon Fluxes and Nitrogen Availability along an Urban-Rural Gradient in a Desert Landscape.” *Urban Ecosystems* 13(1):1–21.

Kurbatova, J., C. Li, A. Varlagin, X. Xiao, and N. Vygodskaya. 2008. “Modeling Carbon Dynamics in Two Adjacent Spruce Forests with Different Soil Conditions in Russia.” *Biogeosciences* 5(4):969–80.

Lamers, Marc, Joachim Ingwersen, and Thilo Streck. 2007. “Modelling N2O Emission from a Forest Upland Soil: A Procedure for an Automatic Calibration of the Biogeochemical Model Forest-DNDC.” *Ecological Modelling* 205(1–2):52–58.

Li, Changsheng, Jianbo Cui, Ge Sun, and Carl Trettin. 2004. “Modeling Impacts of Management on Carbon Sequestration and Trace Gas Emissions in Forested Wetland Ecosystems.” *Environmental Management* 33(SUPPL. 1):176–86.

Li, Changsheng, Steve Frolking, and Tod A. Froking. 1992. “A Model of Nitrous Oxide Evolution from Soil Driven by Rainfall Events: 1. Model Structure and Sensitivity.” *Journal of Geophysical Research* 97(D9):9759–76.

Li, Renhong et al. 2010. “Effects of Simulated Nitrogen Deposition on Soil Respiration in a Neosinocalamus Affinis Plantation in Rainy Area of West China.” *Chinese Journal of Applied Ecology* 21(7):1649–55.

Li, Zhuo Ting, J. Y. Yang, C. F. Drury, and G. Hoogenboom. 2015. “Evaluation of the DSSAT-CSM for Simulating Yield and Soil Organic C and N of a Long-Term Maize and Wheat Rotation Experiment in the Loess Plateau of Northwestern China.” *Agricultural Systems* 135:90–104.

Li, Zhuoting et al. 2017. “Evaluation of the DNDC Model for Simulating Soil Temperature, Moisture and Respiration from Monoculture and Rotational Corn, Soybean and Winter Wheat in Canada.” *Ecological Modelling* 360:230–43.

Lu, Xuyang and Genwei Cheng. 2009. “Climate Change Effects on Soil Carbon Dynamics and Greenhouse Gas Emissions in Abies Fabri Forest of Subalpine, Southwest China.” *Soil Biology and Biochemistry* 41(5):1015–21.

Lubowski, R. N., Marlow Vesterby, Shawn Bucholtz, Alaba Baez, and Michael J. Roberts. 2006. *Major Uses of Land in The United States, 2002*. United States Department of Agriculture, Economic Research Service, Washington, D.C., USA.

Luo, Yiqi and Xuhui Zhou. 2006. *Soil Respiration and the Environment*. San Diego, California, Elsevier Academic Press.

McKinney, Michael L. 2008. “Effects of Urbanization on Species Richness: A Review of Plants and Animals.” *Urban Ecosystems* 11(2):161–76.

Miehle, P., S. J. Livesley, P. M. Feikema, C. Li, and S. K. Arndt. 2006. “Assessing Productivity and Carbon Sequestration Capacity of Eucalyptus Globulus Plantations Using the Process Model Forest-DNDC: Calibration and Validation.” *Ecological Modelling* 192(1–2):83–94.

Mo, Wenhong et al. 2005. “Seasonal and Annual Variations in Soil Respiration in a Cool-Temperate Deciduous Broad-Leaved Forest in Japan.” *Agricultural and Forest Meteorology* 134(1–4):81–94.

Ng, B. J. .. et al. 2015. “Carbon FLuxes from an Urban Tropical Grasslan.” *Environmental Pollution* 203:227–34.

Nowak, Dj, Mh Noble, Sm Sissini, and Jf Dwyer. 2001. “Assessing the US Urban Forest Resource.” *Journal of Forestry* 99(3):37–42.

Park, Moon-Soo, Seung Jin Joo, and Soon-Ung Park. 2014. “Carbon Dioxide Concentration and Flux in an Urban Residential Area in Seoul, Korea.” *Advances in Atmospheric Sciences* 31(5):1101–12.

Polsky, C. et al. 2014. “Assessing the Homogenization of Urban Land Management with an Application to US Residential Lawn Care.” *Proceedings of the National Academy of Sciences* 111(12):4432–37.

Pouyat, R., P. Groffman, I. Yesilonis, and L. Hernandez. 2002. “Soil Carbon Pools and Fluxes in Urban Ecosystems.” *Environmental Pollution* 116:S107–18.

Pouyat, Richard V, Mark J. McDonnell, and S. T. A. Pickett. 1995. “Soil Characteristics of Oak Stands along an Urban-Rural Land-Use Gradient.” *Journal of Environmental Quality* 24(3):516–26.

Pouyat, Richard V, R. W. Parmelee, and M. M. Carreiro. 1994. “Environmental Effects of Forest Soil-Invertebrate and Fungal Densities in Oak Stands along an Urban-Rural Land Use Gradient.” *Pedobiologia*.

Saggar, S. et al. 2004. “Modelling Nitrous Oxide Emissions from Dairy-Grazed Pastures.” *Nutrient Cycling in Agroecosystems* 68(3):243–55.

Saggar, S., C. B. Hedley, D. L. Giltrap, and S. M. Lambie. 2007. “Measured and Modelled Estimates of Nitrous Oxide Emission and Methane Consumption from a Sheep-Grazed Pasture.” Agriculture, *Ecosystems & Environment* 122(3):357–65.

Saggar, Surinder, D. L. Giltrap, C. Li, and K. R. Tate. 2007. “Modelling Nitrous Oxide Emissions from Grazed Grasslands in New Zealand.” *Agriculture, Ecosystems & Environment* 119(1–2):205–16.

Seto, K. C., B. Guneralp, and L. R. Hutyra. 2012. “Global Forecasts of Urban Expansion to 2030 and Direct Impacts on Biodiversity and Carbon Pools.” *Proceedings of the National Academy of Sciences* 109(40):16083–88.

Tao, Xiao, Jun Cui, Yunze Dai, Zefu Wang, and Xiaoniu Xu. 2016. “Soil Respiration Responses to Soil Physiochemical Properties in Urban Different Green-Lands: A Case Study in Hefei, China.” *International Soil and Water Conservation Research* 4(3):224–29.

Wang, Wei, Weile Chen, and Shaopeng Wang. 2010. “Forest Soil Respiration and Its Heterotrophic and Autotrophic Components: Global Patterns and Responses to Temperature and Precipitation.” *Soil Biology and Biochemistry* 42(8):1236–44.

Wang, Wei and Jingyun Fang. 2009. “Soil Respiration and Human Effects on Global Grasslands.” *Global and Planetary Change* 67(1–2):20–28.

Wu, Xiaogang et al. 2015. “Seasonal Spatial Pattern of Soil Respiration in a Temperate Urban Forest in Beijing.” *Urban Forestry and Urban Greening* 14(4):1122–30.

Yang, J. M., J. Y. Yang, S. Liu, and G. Hoogenboom. 2014. “An Evaluation of the Statistical Methods for Testing the Performance of Crop Models with Observed Data.” *Agricultural Systems* 127:81–89.

Yang, Yu Sheng, Guang Shui Chen, Jian Fen Guo, Jin Sheng Xie, and Xiao Guo Wang. 2007. “Soil Respiration and Carbon Balance in a Subtropical Native Forest and Two Managed Plantations.” *Plant Ecology* 193(1):71–84.

Zhang, Chunping et al. 2014. “Effects of Simulated Nitrogen Deposition on Soil Respiration Components and Their Temperature Sensitivities in a Semiarid Grassland.” *Soil Biology and Biochemistry* 75:113–23.

Zhang, Yu and Changsheng Li. 2002. “An Integrated Model of Soil, Hydrology, and Vegetation for Carbon Dynamics in Wetland Ecosystems.” *Global Biogeochemical Cycles* 16(4):1061.

Zhang, Yu, Changsheng Li, Xiuji Zhou, and Moore III Berrien. 2002. "A Simulation Model Linking Crop Growth and Soil Biogeochemistry for Sustainable Agriculture." *Ecological Modelling* 151(1):75–108.

Zhou, Xiaoping et al. 2012. "Soil Warming Effect on Net Ecosystem Exchange of Carbon Dioxide during the Transition from Winter Carbon Source to Spring Carbon Sink in a Temperate Urban Lawn." *Journal of Environmental Sciences (China)* 24(12):2104–12.

SUMMARY AND PERSPECTIVES

Soil respiration (Rs) is the second largest carbon exchange between the land and atmosphere, how global Rs responds to global warming will largely affect future climate change. The studies in this dissertation analyze the processes of estimating global Rs based on site-scale and short-time-scale Rs measurements. Despite the great advances that this research has achieved in global Rs modeling, there are still many remaining challenges to be addressed in future studies.

First, our results comprehensively analyze Rs diurnal pattern across global and macro scales, and our findings provide data and statistical support for generating field Rs measurements using the manual chamber method in future studies. In order to improve Rs measurement accuracy at the site scale and across the globe, this work raises other questions related to sampling schemes and measurements that should be carefully considered. For example: how can we 1) improve instrument measurements and thus decrease systematic and random errors, 2) select an appropriate minimum sample size to capture the Rs spatial variability, 3) determine the appropriate depth for inserting the collar into the soil, and 4) determine how often Rs should be measured in order to capture the Rs seasonality variability. Based on the answers to these questions, a Rs measurement protocol needs to be created in order to guide field Rs measurement in future studies.

Secondly, many site scale studies have demonstrated that soil temperature and soil water content are the most important environmental conditions influencing Rs; consequently, soil temperature and soil water content are the most frequently reported factors in previous studies. But different scientists report soil temperature and soil water content measured at different soil depths, making comparison and synthesis analysis difficult. According to the results from

MGRsD, our results showed that soil temperature and soil water content measured at 10 cm were most frequently reported in previous studies. Thus, we suggest that future field Rs experiments should also report soil temperature and soil water contents measured at a depth of 10 cm even though soil temperature and soil water contents at other depths will be reported.

Thirdly, for the soil water content, there is no consensus on which soil water content metric should be reported. In fact, soil-moisture-measure metrics, such as water potential, gravimetric water content, water holding capacity, water-filled pore space, volumetric water content, and depth to water table, have been reported by different researchers. Future studies should be conducted to test which soil water content metric is comparable among different soils and thus should be reported in future field Rs measurements.

Fourth, many other biotic and abiotic factors such as soil organic carbon content, soil nitrogen content, soil bulk density, above ground biomass, and leaf area index are also reported to significantly influence Rs, but not many filed Rs experiments measure these factors. We argue that future Rs field measurements should report such factors whenever it is possible, and a field Rs measure protocol is urgently needed to clarify which factors should be measured and reported together with Rs.

Lastly, currently it is hard to separate Rh and Ra in the field Rs measuremnts, more handy equipment and methods should be developed to separate Rh and Ra from Rs in future studies. Global Rs data is very important to evaluate the performance of climate models. However, the climate models' soil sub-model simulates heterotrophic respiration (Rh), but usually the field Rs measurement do not separate Rs into Rh and autotrophic respiration (Ra). It is important to highlight the importance of "experimenters with modeling in mind," that is, future

field soil respiration measurement should separate heterotrophic and autotrophic respiration whenever possible.